

**UCSF**

**UC San Francisco Electronic Theses and Dissertations**

**Title**

Optimization of anti-tuberculosis treatment in children

**Permalink**

<https://escholarship.org/uc/item/3v63b1pj>

**Author**

Radtke, Kendra Kae

**Publication Date**

2021

Peer reviewed|Thesis/dissertation

Optimization of anti-tuberculosis treatment in children

by  
Kendra K. Radtke

DISSERTATION  
Submitted in partial satisfaction of the requirements for degree of  
DOCTOR OF PHILOSOPHY

in  
Pharmaceutical Sciences and Pharmacogenomics

in the  
GRADUATE DIVISION  
of the  
UNIVERSITY OF CALIFORNIA, SAN FRANCISCO

Approved:

DocuSigned by:  
*Deanna Kroetz* \_\_\_\_\_ Deanna Kroetz  
0611A116B51E4AA... \_\_\_\_\_ Chair

DocuSigned by:  
*Radojka Savic* \_\_\_\_\_ Radojka Savic

DocuSigned by:  
*Anthony Garcia-Prats, MD* \_\_\_\_\_ Anthony Garcia-Prats, MD  
7E3013040228414... \_\_\_\_\_

\_\_\_\_\_  
\_\_\_\_\_  
Committee Members



## Acknowledgements

I have many people to thank.

First, thank you to all the study participants, volunteers, and their parents/guardians for contributing data that served as the foundation of many pieces of work in this dissertation. Thank you as well as to all the personnel involved in establishing and running the clinical trials. Without your contributions, the analyses and resulting conclusions would not have been possible.

To my mentor and advisor, Dr. Rada Savic – I am incredibly grateful for all the support, guidance, and encouragement you have given me. I have learned so much from you—not only a multitude of skills in pharmacology and modeling and clinical trial design but also, how to be a confident investigator, believe in myself, and dream big. You provided me with many opportunities I had never dreamed of. You trusted me, even when I didn't trust myself. You believed in me. You challenged me. Your fearless leadership and optimism inspire me. I am honored to have had the opportunity to learn from you.

Thank you to Dr. Deanna Kroetz, my thesis committee Chair and academic advisor. You have been a part of my journey since early on in my PharmD training. Your wisdom, assistance, and encouragement in my pursuit of dual PharmD-PhD degrees was unprecedented. I likely would not be here if it were not for your support. Also, I appreciated your thoughtful perspectives and curiosities on my dissertation research. Your contributions undoubtedly strengthened the work.

Thank you to Dr. Anthony Garcia-Prats for your many valuable contributions to this dissertation, including as a member of my thesis committee. I am grateful to have had the chance to work with and learn from you on several projects. Your involvement and insight elevated the impact of this work, and for that, I am sincerely grateful. On top of that, you are a joy to work with! I have really appreciated your kindness and mentorship on my profession and career.

Thank you to every member of the Savic Lab—your unconditional support, as a collective but also as individuals, throughout my graduate training means so much to me. Thank you to the Pediatric TB Team for your support in problem solving, idea generations, and overall, the community we cultivated over the last 1.5 years (mostly while remote no less!). My research mentors Maria and Belen, I cannot thank you enough for your guidance and friendship. I learned most everything I know about NONMEM and population approaches from you both. Importantly, you brought so much joy to my every day in the lab. I will forever miss “coffee time” and “Spanish lunch” and seeing your smiling faces each day. Thank you to Emma for your friendship and partnership. I learned so much from you about modelling, PSPG life, and the Savic Lab, and together we accomplished a lot (I am proud of us!). Vincent and Jackie – I am so grateful for your friendship inside and outside of the lab and for all I’ve learned from you through working with you on projects and your lab meeting presentations. Thank you to Irene and Sandy for giving me the priceless gift of mentorship. I learned so much from working with each of you. And to Craig, thank you for the many one-on-one conversations and the guidance and support you have given me. I developed my interprofessional skills/relations immensely as a result. You have been a great asset to me and this work!

Thank you to Meghan Whalen for paving a path for PharmDs to pursue PhDs at UCSF, for being my biggest cheerleading, for your friendship, and for your wisdom. Your passion, perseverance, and intelligence inspire me to keep going. Thank you to PSPG cohorts 2017 and

2018 for each welcoming me with open arms. Your diverse research interests and inquisitive nature have kept me on my toes and opened my mind. I am grateful for the PSPG program and community for being flexible to my interests, clinical background, and training trajectory. The opportunity to complete lab rotations and PSPG course requirements while in the PharmD program contributed to my overall success in completing this dissertation.

I am grateful to our many collaborators: the Tuberculosis Trials Consortium (TBTC), International Maternal Pediatric Adolescent AIDS Clinical Trials Network (IMPAACT), Stellenbosch University and the Desmond Tutu TB Centre. Thank you for inviting me to your calls and the opportunities to collaborate and make an impact together. A special thanks to Anneke Hesseling, Kelly Dooley, Nicole Salazar-Austin, and Christy Beneri – thank you for your support and encouragement and the knowledge you shared through our collaboration.

Thank you to my many friends for being my cheerleaders and for providing me with a stimulating social outlet. The countless ski trips, girl's trips, backpacking trips, and board game nights contributed immensely to my overall health and wellbeing. I am grateful to be surrounded by such strong, independent women (and men). Thank you to my SF triathlon/cycling community - Anthony, Megan, Aileen, Mollie, and more - for introducing me to sunrise Hawk Hill rides (occasionally in costume!) and inspiring me to stay active, accomplish non-research goals, and most importantly – have fun! This friendship and community brought so much joy to my everyday life. I am grateful for your unwavering support and having a safe space to talk through tough times.

To my family – thank you for your unconditional love, support, and guidance. Mom and dad, thank you for always believing in me, encouraging my academics, and teaching me a hard work ethic. I am grateful to my dad who taught me responsibility and independence. I thank my mom

for giving me the gift of compassion and desire to make the world a better place. Thank you to my grandparents and aunts and uncles; you have always been there when I needed extra support, and I am forever grateful to be surrounded by such a loving and close-knit family. You all have trusted me and encouraged me throughout my journey, even when you didn't understand it. I can now say, "Yes, I am finally done with school," but I will forever be a learner.



And finally, to my partner, Adam – words cannot describe how much gratitude I have for you. You have been my confidant through my first doctorate, my decision to pursue a second doctorate, and through the completion of this dissertation. You were there to listen when things weren't going well, when I was frustrated or afraid, when I doubted myself or felt inadequate. You were there to celebrate all my accomplishments, big and small, even when I didn't feel worthy of being celebrated. You made me feel like a superstar. I am grateful for all that I have learned from you watching you progress and navigate through your own career with confidence in your abilities and your worth. Thank you for being an incredible adventure partner. You have helped me live a balanced life, full of joy and adventures and relaxation, that helped me not feel like a student. The memories we have created together will last a lifetime.

## Contributions

Several chapters in this dissertation contain material that has been published previously or is currently under consideration/review. They do not necessarily represent the final published form and in all cases have been edited slightly.

Chapter 2 is a shortened version of a report submitted to the World Health Organization: Solans B.P., Béranger A, Radtke K.K., Mohamed A, Nahid P, Savic R. (2021) “Pharmacokinetics of first-line drugs (rifampicin, isoniazid, ethambutol and pyrazinamide) among children (<18 years old) treated for drug-susceptible tuberculosis: systematic review and meta-analysis.” B.P.S., K.R., R.S., and P.N. designed the research, B.P.S., K.R., A.M., and A.B. performed the research and wrote the manuscript, all authors reviewed the manuscript.

Chapter 3 is modified from the publication: Radtke KK, Dooley KE, Dodd PJ, Garcia-Prats AJ, McKenna L, Hesselning AC, Savic RM (2019). “Alternative dosing guidelines to improve outcomes for childhood tuberculosis: a mathematical modeling study.” *Lancet Child and Adolescent Health*. 3(9):636-645. K.D., A.G.P., L.M., A.H., and R.S. conceived the study. K.R., P.D., and R.S. performed the study. K.R. drafted the manuscript and all authors reviewed and approved the study results and manuscript.

Chapter 4 is modified from an accepted manuscript: Radtke KK, Hesselning AC, Winckler JL, Draper HR, Solans BP, Thee S, Wiesner L, van der Laan LE, Fourie B, Nielsen J, Schaaf HS, Savic RM, Garcia-Prats AJ. “Moxifloxacin pharmacokinetics, cardiac safety, and dosing for the treatment of rifampicin-resistant tuberculosis in children.” *Clin Infectious Dis*. R.S, A.G.P, and A.H. designed the study. R.S, A.G.P, A.H., H.S., L.W, B.F., L.V.D.L., and J.W. collected the



data. K.R., H.D., S.T., B.S., A.G.P, R.S., and J.N. performed or contributed to the data analysis. K.R. wrote the manuscript. All authors reviewed and approved the manuscript.

Chapter 5 is modified from the publication: Hibma JE and Radtke KK, Dorman SE, Jindani A, Dooley KE, Weiner M, McIlleron HM, Savic RM (2020). "Rifapentine Population Pharmacokinetics and Dosing Recommendations for Latent Tuberculosis Infection." *Am J Respir Crit Care Med.* 202(6):866-877. All authors contributed to the intellectual content of the manuscript and approved the manuscript version submitted for publication. Data was acquired by S.E.D., A.J., K.E.D., M.W., and H.M.M. Data analysis was performed by J.E.H., K.K.R., and R.M.S. J.E.H., K.K.R., and R.M.S. made substantial contributions to the study concept and design.

Chapter 6 is modified from the publication: Radtke KK, Hibma JE, Hesselring AC, Savic RM (2020). "Pragmatic global dosing recommendations for the 3-month, once-weekly rifapentine and isoniazid preventive TB regimen in children." *Eur Respir J.* 57(1):2001756. R.S. and A.C.H contributed to the study concept and design. K.R. and J.H. performed the analysis. K.R. wrote the manuscript and J.H., A.C.H, and R.S. reviewed and approved the manuscript.

# Optimization of anti-tuberculosis treatment in children

Kendra K. Radtke

## Abstract

Childhood tuberculosis (TB) affects one million children annually, and in 2019, 194,000 children under 15 years of age died from TB. Malnourished, HIV-positive, and young children have an increased risk of TB disease progression, severe forms of TB, and poor treatment outcomes. Historically, children with TB have been treated as small adults. This may contribute to poorer outcomes due to pharmacokinetic differences between adults and children that result in suboptimal drug exposure. The aims of this work were to apply modeling and simulation to optimize pediatric dosing of important drugs/regimens for drug-susceptible TB, drug-resistant TB, and latent TB infection.

Current treatment guidelines for drug-susceptible TB endorsed by the World Health Organization (WHO) recommend dosing children by body weight alone, which may lead to systematic underdosing and worse treatment outcomes in underweight children. A systematic review and meta-analysis were performed to assess rifampicin pharmacokinetics in children. At the current WHO recommendations, rifampicin exposures were much lower in children compared to adults. Younger and HIV-positive children trended toward lower exposures compared to older and HIV-negative children, respectively, but data reporting by these groups were too sparse to draw definitive conclusions. In a separate study, an integrated pharmacologic-epidemiologic model was developed to predict childhood TB outcomes in a real-world population of children under 5 years of age from high burden TB countries. An alternative dosing method, which dosed children by ideal body weight instead of actual body weight, was

predicted to reduce unfavorable child outcomes by at least 33%, with major improvements in the youngest children and those who were malnourished. The findings from both analyses support higher doses of rifampicin than currently recommended.

Moxifloxacin is a high-priority drug for drug-resistant TB treatment per WHO guidelines. However, doses are not optimized for children due to a lack of pharmacokinetic and safety data, especially in young children. To address this need, the population pharmacokinetics and relationship with QT-interval prolongation were characterized in a cohort of 85 children with TB (median age 4.6 years). Optimal moxifloxacin doses were found to be 10-50% higher than current WHO recommendations, depending on child weight. The risk of QT-interval prolongation was low during the study, but requires further assessment at higher doses, especially with coadministration of other QT-prolonging anti-TB agents such as clofazimine and bedaquiline.

Tuberculosis disease can be prevented in those with latent infection with anti-tuberculosis therapy. Novel short-course rifapentine-based therapies are an appealing, non-inferior alternative to the standard 9-months of isoniazid. However, rifapentine pharmacokinetic data in children are lacking. To inform on optimal rifapentine dosing in children, the pharmacokinetics and autoinduction profile were first characterized in adults. The adult model informed the model structure for pediatric simulations as well as pharmacokinetic targets for different regimens. Then, optimized and pragmatic weight band dosing was proposed for the 3-month once weekly regimen (3HP) for labelled use and for the experimental regimens being evaluated in pediatric clinical trials. Lastly, prior knowledge of rifapentine (and rifamycins, in general) pharmacokinetics was leveraged to inform the design of a pediatric PK study evaluating daily rifapentine for TB prevention.

Collectively, this dissertation research contributes to the prevention and treatment of TB in children by applying model-based approaches to optimize the dosing of key drugs in current and novel regimens. There is a focus on vulnerable child populations that are typically

underrepresented in clinical trials and underserved by standard weight-based dosing practices but represent a large burden of the mortality (e.g., malnourished, HIV-coinfected, young).

# Table of Contents

<b>Chapter 1. Introduction.....</b>	<b>1</b>
Thesis aims.....	6
References .....	8
<b>Chapter 2. Systematic review and meta-analysis of rifampicin</b>	
<b>pharmacokinetics.....</b>	<b>13</b>
Introduction .....	13
Methods .....	14
Results.....	19
Discussion .....	35
Conclusion.....	37
Supplementary Information .....	38
References .....	40
<b>Chapter 3. Alternative dosing regimens to improve outcomes for children</b>	
<b>with tuberculosis .....</b>	<b>45</b>
Abstract.....	45
Background.....	46
Methods .....	48
Results.....	62
Discussion .....	73
Supplemental Table 3.1 Pharmacokinetic models from literature.....	78
Supplemental Table 3.2 Pharmacokinetic parameter estimates from literature. ....	79
References .....	80

<b>Chapter 4. Moxifloxacin pharmacokinetics, cardiac safety, and dosing for the treatment of rifampicin-resistant tuberculosis in children .....</b>	<b>87</b>
Abstract.....	87
Introduction .....	88
Methods.....	89
Results.....	93
Discussion .....	105
Supplemental Table 4.1. Moxifloxacin weight banded dosing used in MDR-PK2 .....	109
Supplemental Table 4.2. Demographics of child population with TB used for pharmacokinetic simulations. ....	109
References .....	110
 <b>Chapter 5. Rifapentine population pharmacokinetics and dosing recommendations for latent tuberculosis infection .....</b>	 <b>116</b>
Abstract.....	116
Introduction .....	117
Methods.....	119
Results.....	123
Discussion .....	139
References .....	145
 <b>Chapter 6. Pragmatic global dosing recommendations for the 3-month, once-weekly rifapentine and isoniazid preventive TB regimen in children .....</b>	 <b>150</b>
Introduction .....	150
Methods.....	151
Results.....	152
Discussion .....	153

References .....	156
<b>Chapter 7. Prediction of optimal opening doses of rifapentine-based tuberculosis preventive therapy for evaluation in novel pediatric clinical trials .....</b>	<b>158</b>
Introduction .....	158
Methods .....	159
Results .....	162
Discussion .....	166
References .....	169
<b>Chapter 8. Stochastic simulation and estimation to support pediatric clinical design: a case study with rifapentine for preventive tuberculosis treatment .....</b>	<b>172</b>
Introduction .....	172
Methods .....	173
Results .....	177
Discussion .....	182
References .....	185
<b>Chapter 9. Conclusions and future directions .....</b>	<b>188</b>
References .....	192

## List of Figures

<b>Figure 2.1</b> PRISMA flow diagram of systematic review .....	20
<b>Figure 2.2</b> Rifampicin AUC by weight band.....	28
<b>Figure 2.3</b> Forest plot displaying estimated rifampicin AUC (a) and $C_{max}$ (b).....	30
<b>Figure 2.4</b> Forest plot displaying estimated rifampicin AUC (a) and $C_{max}$ (b) by HIV status.....	32
<b>Figure 2.5</b> Forest plot displaying estimated rifampicin AUC (a) and $C_{max}$ (b) by age group.....	34
<b>Figure 3.1</b> Integrative model schematic.....	49
<b>Figure 3.2</b> Childhood tuberculosis dosing schematic.....	53
<b>Figure 3.3</b> Proposed dosing chart for boys. ....	56
<b>Figure 3.4</b> Proposed dosing chart for girls. ....	57
<b>Figure 3.5</b> Pharmacokinetic model selection flowchart.....	59
<b>Figure 3.6</b> Underdosing prevalence with current WHO treatment guidelines. ....	63
<b>Figure 3.7</b> Simulated $AUC_{ss}$ of rifampicin (a), isoniazid (b), and pyrazinamide (c) for current (red), proposed (blue), and individualized (yellow) dosing algorithms.....	64
<b>Figure 3.8</b> Simulated average daily concentration of rifampicin (a), isoniazid (b), and pyrazinamide (c) versus minimum inhibitory concentration (MIC; yellow dashed line).....	65



<b>Figure 3.9</b> Impact of malnutrition on rifampicin exposure target outcomes.....	66
<b>Figure 3.10</b> Rifampicin target exposure outcomes in high-burden tuberculosis countries.....	67
<b>Figure 3.11</b> Impact of malnutrition on isoniazid exposure target outcomes. ....	68
<b>Figure 3.12</b> Impact of malnutrition on pyrazinamide exposure target outcomes.....	69
<b>Figure 3.13</b> Predicted probability of unfavorable outcome ( $P_{\text{unf}}$ ) for each dosing method. ....	70
<b>Figure 4.1</b> MDR-PK2 Study Design.....	90
<b>Figure 4.2</b> Moxifloxacin pharmacokinetic profiles in children treated for rifampicin-resistant tuberculosis.....	95
<b>Figure 4.3</b> Pharmacokinetic profiles in 8 subjects that received two formulations in MDRPK2.....	98
<b>Figure 4.4</b> Visual predictive check of the final (a) pharmacokinetic model and (b) pharmacokinetic-QTcF model. ....	99
<b>Figure 4.5</b> Moxifloxacin $AUC_{24}$ (a,c) and apparent clearance (b,d) by nutritional status and body weight.....	100
<b>Figure 4.6</b> QTcF profiles in children treated with moxifloxacin for rifampicin-resistant tuberculosis as (a) QTcF interval over time and (b) maximum change in QTcF during the dosing interval in children receiving clofazimine (n= 29) and not (n=27).....	102
<b>Figure 4.7</b> Simulated moxifloxacin (a) $AUC_{24}$ and (b) maximum concentration at steady state with weight band dosing according to current WHO recommendations (blue) and model-informed optimized doses (yellow).....	104

<b>Figure 5.1</b> PRISMA Flow Diagram. ....	124
<b>Figure 5.2</b> Final rifapentine pharmacokinetic-enzyme model. ....	127
<b>Figure 5.3</b> Rifapentine autoinduction profile. ....	129
<b>Figure 5.4.</b> Validation of the structural rifapentine population pharmacokinetic model. ....	130
<b>Figure 5.5</b> Final visual predictive check (VPC) of full rifapentine population pharmacokinetic model, stratified by study. ....	131
<b>Figure 5.6</b> Visual predictive check (VPC) of 25-desacetyl-rifapentine (i.e., metabolite) pharmacokinetic model. ....	132
<b>Figure 5.7</b> Relationship between weight and rifapentine clearance. ....	133
<b>Figure 5.8</b> Individuals influencing the relationship between weight and clearance. ....	134
<b>Figure 5.9</b> Effect of dose and dosing frequency on rifapentine exposure. ....	135
<b>Figure 5.10</b> Pharmacokinetic profiles of rifapentine following (A) 1HP and (B) 3HP regimens. ....	137
<b>Figure 5.11</b> Predicted rifapentine exposures with different dosing methods for (A) 1HP and (B) 3HP regimens. ....	138
<b>Figure 5.12</b> Predictors of month 2 culture conversion. ....	139
<b>Figure 7.1</b> Typical value of rifapentine clearance (TVCL) in children 0-15 years based on assumed functions. ....	160

<b>Figure 7.2</b> Simulated rifapentine AUC with opening 3HP doses in children under 2 years. ....	163
<b>Figure 7.3</b> Simulated rifapentine AUC with opening 1HP doses. ....	166
<b>Figure 8.1</b> Stochastic simulation and estimation schematic. ....	175
<b>Figure 8.2</b> Distribution of age in each simulated clinical trial population. ....	176
<b>Figure 8.3</b> Relative bias (A) and RMSE (B) of rifapentine clearance under different study designs.....	178
<b>Figure 8.4</b> Relative bias (A) and RMSE (B) of rifapentine volume of distribution under different study designs.....	179
<b>Figure 8.5</b> Power to detect relevant factors influencing rifapentine clearance with 40% interindividual variability.....	181

## LIST OF TABLES

<b>Table 1.1</b> Current and historical doses of first-line anti-tuberculosis drugs recommended in WHO guidance in children under 25 kg* .....	3
<b>Table 2.1</b> Systematic review search strategy .....	16
<b>Table 2.2</b> Summary of included studies.....	21
<b>Table 2.3</b> Number of children contributing rifampicin pharmacokinetic data by study and covariates as reported in the original study .....	25
<b>Table 2.4</b> Rifampicin AUC and $C_{max}$ as reported in the original studies.....	26
<b>Table 3.1</b> Study Population.....	51
<b>Table 3.2</b> Age or expected weight-based dosing for underweight children. ....	55
<b>Table 3.3</b> Probability of disease progression.....	61
<b>Table 3.4</b> Estimated number of treatment failures or deaths from tuberculosis per year in children under five years of age. ....	72
<b>Table 4.1.</b> Demographic and clinical characteristics of children treated for rifampicin-resistant tuberculosis in the MDR-PK1 and MDR-PK2 studies. ....	94
<b>Table 4.2.</b> Population pharmacokinetic and QTcF parameter estimates in children treated for moxifloxacin for rifampicin-resistant tuberculosis.....	97

<b>Table 4.3.</b> Currently recommended and optimized pediatric weight band dosing for moxifloxacin .....	103
<b>Table 5.1</b> Baseline characteristics of the study participants in the pooled datasets.....	125
<b>Table 5.2.</b> Final parameter estimates for the rifapentine population pharmacokinetic model .....	128
<b>Table 5.3</b> Change in rifapentine clearance by dose and dosing frequency. Values reflect the percent change from first dose to last dose of a one-month treatment course.....	135
<b>Table 6.1.</b> Revised dosing recommendations for 3-month, once-weekly rifapentine and isoniazid (3HP) preventive treatment regimen.....	153
<b>Table 7.1</b> Opening doses for 3HP in children under 2 years of age .....	163
<b>Table 7.2</b> Opening doses for 1HP in children 0-15 years of age .....	165
<b>Table 8.1</b> Overview of tested sampling designs .....	176

## Chapter 1. Introduction

Tuberculosis (TB) was the leading cause of mortality by infectious diseases in 2019 with an estimated 10.0 million cases (range 8.9 – 11.0 million) and 1.4 million deaths (range 1.1 – 1.6 million) worldwide.<sup>1</sup> Children less than 15 years of age accounted for 12% of the people who developed TB and approximately 20% of the deaths. People living with HIV accounted for 8.2% of TB cases and 14% of TB deaths. Young children under 5 years of age are disproportionately affected by TB.<sup>1,2</sup> The global burden of TB is presented in **Figure 1.1**.

### Estimated TB incidence (all forms) per 100 000 population, 2019

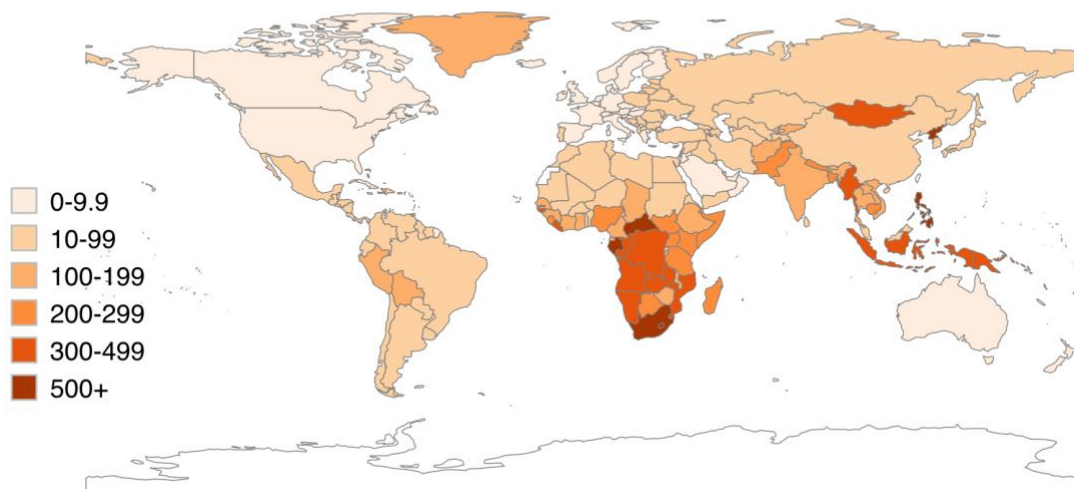


**Figure 1.1** Estimated global TB incidence adapted from 2019 WHO Global TB report.

Drug-resistant TB has remained a threat globally. Of the 10.0 million people who developed TB in 2019, 0.5 million (5%) developed rifampicin-resistant TB with the majority (78%) having multidrug-resistant TB (i.e., TB resistant to both isoniazid and rifampicin, the two most effective anti-TB drugs).<sup>1</sup> The global percentage of new TB cases with multidrug resistance was 3.3% in 2019, which remains stable from previous years. India, China, and the Russian Federation share 49% of the global burden of drug-resistant TB. Of even greater concern is extensively drug-resistant TB defined until recently as TB infection with additional resistance to fluoroquinolone antibiotics and second-line injectable agents such as aminoglycosides. The estimated global incidence of extensively drug-resistant TB is 12,350 cases per year.<sup>1</sup>

The World Health Organization (WHO) and United Nations (UN) have put forth several targets to support the fight against TB. The WHO End TB Strategy targets an 80% reduction in the TB incidence rate and a 90% reduction in annual TB deaths by 2030 (versus 2015).<sup>3</sup> In order to reach these targets, the WHO projects that treatment coverage, treatment success, and preventive treatment coverage need to be 90% or higher.<sup>3</sup> The UN high-level meeting on TB has proposed a target of 40 million individuals treated for TB and 30 million individuals receiving TB preventive therapy between 2018 and 2022.<sup>1</sup> This proposal includes specific targets for children, people living with HIV, and people who develop drug-resistant TB. The most recent data from 2019 show that the global progress is lagging behind what is needed to reach these targets.<sup>1</sup>

Unfortunately, the COVID-19 pandemic is expected to have a devastating impact on the global burden of TB disease and threatens to reverse much of recent progress.<sup>1,4</sup> GeneXpert machines, typically used for TB diagnosis, are being used for COVID-19 in 43 countries including 13 high TB burden countries.<sup>1</sup> Staff have been reassigned from national TB programmes to COVID-19 related duties in 85 countries including 20 high TB burden countries,

and 14 high TB burden countries have reallocated budgets away from TB services. Data collection and TB reporting have also been affected. Modelling studies predict that only a short disruption in TB services (e.g., 3-6 months) could increase TB incidence by thousands to millions over 5 years in major high burden countries even with significantly reduced person-to-person contact as would be expected in lockdown situations.<sup>5,6</sup> The impact on TB-related deaths could be an increase of 200,000 to 400,000 deaths in 2020, reversing five years of progress in TB elimination.<sup>1</sup> Optimizing the treatment and prevention of TB is more critical than ever.

The standard of care for drug-susceptible TB treatment is six months of daily rifampicin, isoniazid, pyrazinamide, and ethambutol. In children, ethambutol is optional but recommended for children living with HIV or in regions with high HIV prevalence.<sup>7</sup> The recommended pediatric dosages of first-line treatment have undergone some changes in the last decade, increasing from the same mg/kg dosage as adults in 2010 and formalized in 2014 (**Table 1.1**).<sup>7,8</sup> However, the resulting recommendations were based on a few small studies in children. Experts in the field, including the WHO, have questioned whether these doses are optimal.<sup>9,10</sup>

**Table 1.1** Current and historical doses of first-line anti-tuberculosis drugs recommended in WHO guidance in children under 25 kg\*

<b>Drug</b>	<b>Daily dose prior to 2010 (mg/kg)</b>	<b>Daily dose in 2010 (mg/kg)</b>	<b>Daily dose in 2014 (mg/kg)</b>
Rifampicin	10 (range 8-12)	10-20	15 (range 10-20)
Isoniazid	5 (range 4-6)	10-15	10 (range 7-15)
Pyrazinamide	25 (range 20-30)	30-40	35 (range 30-40)
Ethambutol	20 (range 15-25)	15-25	20 (range 15-25)
<i>RIF, rifampicin; INH, isoniazid; PZA, pyrazinamide; ETH, ethambutol</i> <i>*As children approach a body weight of 25 kg, adult dosages can be used</i>			



Among a 2018 cohort of 13,185 children with TB 0-14 years of age for whom treatment outcomes were available and reported to the WHO, 84% experienced a successful treatment outcome.<sup>1</sup> Country-specific treatment success ranged from 73% to 97% in this cohort,<sup>1</sup> which is similar to observational studies.<sup>11-15</sup> In the novel SHINE study, a randomized clinical trial that evaluated four versus six months of the four-drug first-line regimen with currently recommended doses, only 34 of 1204 (3%) children experienced an unfavorable outcome.<sup>16</sup> The study was limited to children with non-severe TB disease. While these findings are encouraging, the treatment successes reported by many national TB programs still fall below the WHO target of 90%. Together these data might suggest that currently recommended first-line therapy may be sufficient for easy-to-treat child populations in controlled settings (such as those in SHINE) but fail to adequately treat some children.

Young, malnourished, and HIV-infected children are more vulnerable to death and unfavorable treatment outcomes.<sup>17-19</sup> For example, one study found that children under 5 years of age were 6.1 times more likely to die, and underweight children were 2.1 times more likely to die following TB treatment.<sup>17</sup> Children living with HIV were 2.6 times more likely to die.<sup>19</sup> Children under five years of age account for half of all child TB cases (0-14 years).<sup>2</sup> TB and undernutrition are complexly linked—poor nutritional status increases the risk of TB progression and TB disease further worsens the nutritional state.<sup>20</sup> Child undernutrition is highly prevalent in high-burden TB countries: >20% of children under five years of age are stunted (low height for age) in 26 of 30 high-burden countries and >5% are wasted (low weight for height) in 18 countries.<sup>21</sup> HIV is similarly prevalent especially in African regions, where up to 50% of children with TB are co-infected with HIV.<sup>18</sup> Despite these well-known risk factors for treatment failure/death and their high prevalence in high TB burden countries, all children are treated with the same uniform

weight-based doses (**Table 1.1**). Assessing the dosing needs of high-risk child populations such as these would likely increase the odds of treatment success and improve overall outcomes.

Treatment success rates for drug-resistant forms of TB are generally worse than drug-susceptible TB. The most recent global estimate of treatment success for rifampicin-resistant TB was 57%.<sup>1</sup> Rifampicin-resistant TB outcomes in children tend to be better than adults.<sup>22</sup> Drug-resistant TB treatment is complicated by longer treatment durations (typically 9 to 24 months), the use of more agents (typically 5+) including injectable drugs, narrow therapeutic windows, and significant adverse effects.<sup>23,24</sup> Second-line injectable agents, formerly the backbone of rifampicin-resistant TB treatment, have less activity against TB and poor penetration into tissues where TB resides (e.g., lesions).<sup>25,26</sup> Additionally, most second-line agents have less *in vitro* potency and bactericidal activity against *Mycobacterium tuberculosis* than rifampicin.<sup>27</sup>

Recent research has identified new compounds with good antimycobacterial activity.<sup>23</sup> These include new agents (e.g., bedaquiline, pretomanid) and repurposed agents previously not used in TB treatment (e.g., moxifloxacin, linezolid, clofazimine). A recent meta-analysis of drug-resistant treatment outcomes found that these drugs were associated with improved treatment success and lower mortality.<sup>28</sup> Regimens including these agents may offer additional benefit of reducing treatment duration to 6-9 months.<sup>29,30</sup> However, as with most second-line agents, there are significant dose-limiting toxicities that need to be considered. Moxifloxacin, clofazimine, pretomanid, and bedaquiline prolong the QT interval, and linezolid induces peripheral neuropathy and bone marrow suppression that may manifest as neutropenia, thrombocytopenia, and/or anemia.<sup>23</sup> Their optimal use (i.e., dose, frequency, duration, and drug combination) in people with TB is an active area of research. In children, there is very limited knowledge of the safety and efficacy of these newly recommended agents; several pharmacokinetic and safety studies are underway or planned.<sup>31</sup> Access to child-friendly

formulations that are palatable is also lacking and critical to safe and effective treatment of drug-resistant TB in children.<sup>31,32</sup>

Another critical component to eliminating TB is prevention. Approximately ¼ of the world's population is estimated to be infected by TB (i.e., latent TB infection).<sup>33</sup> While these individuals do not experience TB symptoms and do not contribute to the spread of TB, they are at risk of progressing to active disease.<sup>34</sup> Children younger than five years of age, individuals living with HIV or other immunocompromised conditions, and poorly nourished individuals have an increased risk of progressing to TB disease.<sup>18,34</sup> TB preventive therapy is the most available and effective form of TB prevention.<sup>1,35</sup> Currently recommended TB preventive regimens include isoniazid or rifampicin monotherapy and isoniazid in combination with rifampicin or rifapentine (new).<sup>36</sup> Compliance to isoniazid monotherapy (historical standard of care) is generally low, resulting in poor programmatic efficacy, and isoniazid-associated hepatitis is a concern.<sup>37-39</sup> Rifapentine-based regimens have demonstrated improved compliance and fewer or similar adverse event profiles with shorter treatment durations and non-inferior efficacy.<sup>40-42</sup> Rifapentine use in children is limited to those 2 years and older and no child-friendly formulation exists.<sup>43</sup>

### **Thesis aims**

This thesis aims to address important and policy-driven questions around dose and treatment optimization for anti-TB drugs in the pediatric population. This work is focused on the most important drugs used in TB treatment today where significant gaps in knowledge in the pediatric population exist. As such, the findings will have important implications on pediatric TB policy and dosing guidance.

Chapters 2 and 3 are focused on evaluating first-line anti-TB drug exposures and outcomes in children with the goal of ensuring successful treatment outcomes in all children. These chapters are primarily focused on optimal rifampicin use, which is thought to be the main driver of response. Chapter 2 reviews current evidence of rifampicin pharmacokinetics and re-evaluates currently recommended doses. Chapter 3 re-evaluates the algorithm by which doses are prescribed to children, which currently are based on weight alone, with special focus on malnourished children.

Chapter 4 addresses an important gap in knowledge for optimizing drug-resistant TB treatment. Moxifloxacin pharmacokinetics and the relationship with QT prolongation are characterized in a young pediatric population with TB for the first time. The research evaluates current moxifloxacin doses in the context of drug exposure and safety and proposes optimal dosing given currently available formulations.

Chapters 5-8 are related to the optimization of rifapentine-based regimens for TB prevention. Rifapentine pharmacokinetics and autoinduction are first characterized in adults (Chapter 5), and the resulting model is used for pharmacokinetic targets and parameters in subsequent analyses to recommend pediatric dosing for approved (Chapter 6) and experimental (Chapter 7) regimens. In Chapter 8, knowledge of rifapentine pharmacokinetics is leveraged along with modeling and simulation tools to inform the optimal trial characteristics for assessing rifapentine pharmacokinetics in children.

Together, this dissertation encompasses research that is novel and important for pediatric TB policy in the areas of drug-susceptible TB, drug-resistant TB, and latent TB infection.

## References

1. Global Tuberculosis Report. WHO, 2020. (Accessed February 25, 2021, 2021, at <https://www.who.int/publications/i/item/9789240013131>.)
2. Dodd PJ, Gardiner E, Coghlan R, Seddon JA. Burden of childhood tuberculosis in 22 high-burden countries: a mathematical modelling study. *Lancet Glob Health* 2014;2:e453-9.
3. WHO End TB Strategy: Global strategy and targets for tuberculosis prevention, care and control after 2015. (Accessed March 1, 2020, at [https://www.who.int/tb/post2015\\_strategy/en/](https://www.who.int/tb/post2015_strategy/en/).)
4. COVID-19: Considerations for tuberculosis (TB) care. (Accessed May 12, 2020, at [https://www.who.int/tb/COVID\\_19considerations\\_tuberculosis\\_services.pdf](https://www.who.int/tb/COVID_19considerations_tuberculosis_services.pdf).)
5. McQuaid CF, McCreesh N, Read JM, et al. The potential impact of COVID-19-related disruption on tuberculosis burden. *Eur Respir J* 2020;56.
6. Cilloni L, Fu H, Vesga JF, et al. The potential impact of the COVID-19 pandemic on the tuberculosis epidemic a modelling analysis. *EClinicalMedicine* 2020;28:100603.
7. Guidance for national tuberculosis programmes on the management of tuberculosis in children. (Accessed May 4, 2020, 2020, at [https://www.who.int/tb/publications/childtb\\_guidelines/en/](https://www.who.int/tb/publications/childtb_guidelines/en/).)
8. World Health Organization. Rapid Advice: Treatment of tuberculosis in children. Geneva, Switzerland: WHO Press; 2010.
9. Call for expressions of interest: Systematic reviews on dose optimization of the first-line TB medicines. 2020. (Accessed August 1, 2020, at <https://www.who.int/news-room/articles-detail/call-for-expressions-of-interest-systematic-reviews-on-dose-optimization-of-the-first-line-tb-medicines>.)
10. GAP-f Portfolio: Tuberculosis. 2021. (Accessed July 20, 2021, at <https://www.who.int/initiatives/gap-f/our-portfolio/tuberculosis>.)

11. Mukherjee A, Velpandian T, Singla M, Kanhiya K, Kabra SK, Lodha R. Pharmacokinetics of isoniazid, rifampicin, pyrazinamide and ethambutol in Indian children. *BMC Infect Dis* 2015;15:126.
12. Ranjalkar J, Mathew SK, Verghese VP, et al. Isoniazid and rifampicin concentrations in children with tuberculosis with either a daily or intermittent regimen: implications for the revised RNTCP 2012 doses in India. *Int J Antimicrob Agents* 2018;51:663-9.
13. Bekker A, Schaaf HS, Draper HR, et al. Pharmacokinetics of Rifampin, Isoniazid, Pyrazinamide, and Ethambutol in Infants Dosed According to Revised WHO-Recommended Treatment Guidelines. *Antimicrob Agents Chemother* 2016;60:2171-9.
14. Nansumba M, Kumbakumba E, Orikiriza P, et al. Treatment outcomes and tolerability of the revised WHO anti-tuberculosis drug dosages for children. *Int J Tuberc Lung Dis* 2018;22:151-7.
15. Arya A, Roy V, Lomash A, Kapoor S, Khanna A, Rangari G. Rifampicin pharmacokinetics in children under the Revised National Tuberculosis Control Programme, India, 2009. *Int J Tuberc Lung Dis* 2015;19:440-5.
16. E. Wobudeya CC, A.C Hesseling, V. Mave, S. Hissar, A. Turkova, A.M Crook, D.M Gibb; , Team obotST. Shorter treatment for minimal tuberculosis in children: main findings from the SHINE trial. *Union World Conference 2020. Sevilla, Spain2020.*
17. Drobac PC, Shin SS, Huamani P, et al. Risk Factors for In-Hospital Mortality Among Children With Tuberculosis: The 25-Year Experience in Peru. *Pediatrics* 2012;130:e373-e9.
18. Newton SM, Brent AJ, Anderson S, Whittaker E, Kampmann B. Paediatric tuberculosis. *Lancet Infect Dis* 2008;8:498-510.
19. Russell GK, Merle CS, Cooke GS, Casas EC, Silveira da Fonseca M, du Cros P. Towards the WHO target of zero childhood tuberculosis deaths: an analysis of mortality in 13 locations in Africa and Asia. *Int J Tuberc Lung Dis* 2013;17:1518-23.

20. Jaganath D, Mupere E. Childhood tuberculosis and malnutrition. *J Infect Dis* 2012;206:1809-15.
21. Joint child malnutrition estimates - levels and trends. 2018. (Accessed 22 August, 2018, at <http://www.who.int/nutgrowthdb/estimates/en/>.)
22. Harausz EP, Garcia-Prats AJ, Law S, et al. Treatment and outcomes in children with multidrug-resistant tuberculosis: A systematic review and individual patient data meta-analysis. *PLoS Med* 2018;15:e1002591.
23. Lange C, Dheda K, Chesov D, Mandalakas AM, Udwadia Z, Horsburgh CR, Jr. Management of drug-resistant tuberculosis. *Lancet* 2019;394:953-66.
24. Kim HY, Heysell SK, Mpagama S, Marais BJ, Alffenaar JW. Challenging the management of drug-resistant tuberculosis. *Lancet* 2020;395:783.
25. Strydom N, Gupta SV, Fox WS, et al. Tuberculosis drugs' distribution and emergence of resistance in patient's lung lesions: A mechanistic model and tool for regimen and dose optimization. *PLoS Med* 2019;16:e1002773.
26. Ernest JP, Sarathy J, Wang N, et al. Lesion penetration and activity limit the utility of second-line injectable agents in pulmonary tuberculosis. *Antimicrob Agents Chemother* 2021:AAC0050621.
27. Lakshminarayana SB, Huat TB, Ho PC, et al. Comprehensive physicochemical, pharmacokinetic and activity profiling of anti-TB agents. *J Antimicrob Chemother* 2015;70:857-67.
28. Collaborative Group for the Meta-Analysis of Individual Patient Data in MDR-TB treatment, Ahmad N, Ahuja SD, et al. Treatment correlates of successful outcomes in pulmonary multidrug-resistant tuberculosis: an individual patient data meta-analysis. *Lancet* 2018;392:821-34.

29. treatment-2017; CGftM-AolPDiM-T, Ahmad N, Ahuja SD, et al. Treatment correlates of successful outcomes in pulmonary multidrug-resistant tuberculosis: an individual patient data meta-analysis. *Lancet* 2018;392:821-34.
30. Conradie F, Diacon AH, Ngubane N, et al. Treatment of Highly Drug-Resistant Pulmonary Tuberculosis. *N Engl J Med* 2020;382:893-902.
31. Garcia-Prats AJ, Svensson EM, Weld ED, Schaaf HS, Hesselning AC. Current status of pharmacokinetic and safety studies of multidrug-resistant tuberculosis treatment in children. *Int J Tuberc Lung Dis* 2018;22:15-23.
32. Harausz EP, Garcia-Prats AJ, Seddon JA, et al. New and Repurposed Drugs for Pediatric Multidrug-Resistant Tuberculosis. Practice-based Recommendations. *Am J Respir Crit Care Med* 2017;195:1300-10.
33. Houben RM, Dodd PJ. The Global Burden of Latent Tuberculosis Infection: A Re-estimation Using Mathematical Modelling. *PLoS Med* 2016;13:e1002152.
34. Pai M, Behr MA, Dowdy D, et al. Tuberculosis. *Nat Rev Dis Primers* 2016;2:16076.
35. LoBue PA, Mermin JH. Latent tuberculosis infection: the final frontier of tuberculosis elimination in the USA. *Lancet Infect Dis* 2017;17:e327-e33.
36. WHO operational handbook on tuberculosis. Module 1: Prevention- tuberculosis preventive treatment. 2020.
37. Horsburgh CR, Jr., Goldberg S, Bethel J, et al. Latent TB infection treatment acceptance and completion in the United States and Canada. *Chest* 2010;137:401-9.
38. Snider DE, Jr., Caras GJ. Isoniazid-associated hepatitis deaths: a review of available information. *Am Rev Respir Dis* 1992;145:494-7.
39. Kopanoff DE, Snider DE, Jr., Caras GJ. Isoniazid-related hepatitis: a U.S. Public Health Service cooperative surveillance study. *Am Rev Respir Dis* 1978;117:991-1001.
40. Sterling TR, Villarino ME, Borisov AS, et al. Three months of rifapentine and isoniazid for latent tuberculosis infection. *N Engl J Med* 2011;365:2155-66.



41. Bliven-Sizemore EE, Sterling TR, Shang N, et al. Three months of weekly rifapentine plus isoniazid is less hepatotoxic than nine months of daily isoniazid for LTBI. *Int J Tuberc Lung Dis* 2015;19:1039-44, i-v.
42. Swindells S, Ramchandani R, Gupta A, et al. One Month of Rifapentine plus Isoniazid to Prevent HIV-Related Tuberculosis. *N Engl J Med* 2019;380:1001-11.
43. Prifitin (rifapentine) Product Label. 1998. at [https://www.accessdata.fda.gov/drugsatfda\\_docs/label/2014/021024s011lbl.pdf](https://www.accessdata.fda.gov/drugsatfda_docs/label/2014/021024s011lbl.pdf).)

## **Chapter 2. Systematic review and meta-analysis of rifampicin pharmacokinetics\***

### **Introduction**

Progress has been made in the control of tuberculosis (TB) in the recent decade, however, the annual decline in incidence is less than 2%. Furthermore, treatment success rates are still below targets: 85% of adults and 84% of children treated for drug-susceptible TB had favourable outcomes in 2018.<sup>1</sup> Young age (<5 years old), HIV-coinfection, and malnutrition are risk factors for worse treatment outcomes.<sup>1,2</sup> Extrapulmonary and disseminated disease, which are more common in young children, also result in worse outcomes.<sup>2</sup> Optimizing anti-TB treatment for all individuals and for key high-risk groups could have significant benefits on ending the TB epidemic.

First-line regimens for TB have undergone little change since their introduction more than 40 years ago.<sup>3</sup> The addition of rifampicin (RIF) and pyrazinamide (PZA) to isoniazid (INH) reduced treatment duration to six months and established this trio (HRZ) as the backbone of effective therapy.<sup>4</sup> The addition of a fourth drug served to prevent drug resistance, particularly in people already harbouring INH-resistant strains and at a higher risk of treatment failure. Streptomycin

---

\* adapted from a report submitted to the World Health Organization: Solans B.P., Béranger A, Radtke K.K., Mohamed A, Nahid P, Savic R. (2021) Pharmacokinetics of first-line drugs (rifampicin, isoniazid, ethambutol and pyrazinamide) among children (<18 years old) treated for drug-susceptible tuberculosis: systematic review and meta-analysis.

was initially used for this purpose but was replaced by the oral agent ethambutol (EMB) resulting in the current standard four-drug first-line regimen.<sup>5</sup> Recently, accepted doses of the four drugs in children under 25 kg (see **Table 1.1**) have undergone re-evaluation based on modern preclinical and clinical pharmacokinetic-pharmacodynamic (PK-PD) data, and new early phase clinical trials are establishing proof-of-concept that higher doses of RIF may improve efficacy and/or shorten treatment duration.<sup>6-9</sup> However, whether these possible benefits can improve treatment outcomes and be achieved without additional toxicity, has not been established.

Pharmacokinetic (PK) and safety studies are the mainstay in pediatric drug development when the same exposure-response relationship can be assumed between adults and children.<sup>10</sup> Therefore, ensuring PK targets are achieved for first-line anti-TB drugs could improve relapse-free treatment success. Furthermore, intensification of treatment with higher doses could be important for people with severe or disseminated disease or in vulnerable populations. Unfortunately, no efficacy studies have been conducted in children assessing higher than recommended doses. Therefore, the objective of this review was to assess the PK of first-line anti-TB drugs in children treated for drug-susceptible TB with current and higher than currently recommended doses used as part of a 3- or 4-drug combination regimen. This report will focus specifically on RIF.

## **Methods**

### **Search Strategy and Selection Criteria**

Studies were identified in accordance with the Preferred Reporting Items for Systematic Reviews and Meta-Analyses (PRISMA) guidelines.<sup>11</sup> We searched for all clinical studies, including observational and descriptive studies, and randomized controlled trials. Case reports

were excluded. We identified studies involving children and adolescents under 18 years of age being treated for confirmed or suspected TB in which pharmacokinetic data were collected. All forms of TB (pulmonary, extrapulmonary or disseminated) were considered. Studies that included patients with confirmed or presumed resistance to RIF, INH, PZA or ETH were excluded from the analysis.

Pubmed, EMBASE, CENTRAL (Cochrane central register of controlled trials), Cochrane Infectious diseases Group Clinical trials register, WHO International Clinical Trials Registry and Clinicaltrials.gov electronic databases were searched. All the databases were searched using the terms reported in **Table 2.1**, which employs the Cochrane Highly Sensitive Search Strategies for identification of clinical trials appropriate to those resources. The search was conducted for the period of January 2010 (date of the WHO guideline revisions) to October 2020 (date of search), regardless of language or publication status (published, unpublished, in press and in progress). The search was performed for all first-line TB drugs. Only studies including RIF data were included in this review.

All titles and abstracts were imported into Covidence. Two independent reviewers (A.B. and A.M.A.) screened the titles and abstracts for relevance and appraised full text for using pre-specified selection criteria. Key articles were identified by consensus with a third and fourth reviewer (K.R. and B.P.S.).

**Table 2.1** Systematic review search strategy

Search set	Pubmed	Cochrane	Embase
1	child* OR neonat* OR pediatr*	child* OR neonat* OR pediatr*	child* OR neonat* OR pediatr*
2	Tuberculosis	Tuberculosis	Tuberculosis
3	#1 AND #2	#1 AND #2	#1 AND #2
4	isoniazid OR pyrazinamide OR ethambutol OR rifampicin	isoniazid OR pyrazinamide OR ethambutol OR rifampicin	isoniazid OR pyrazinamide OR ethambutol OR rifampicin
5	#3 AND #4	#3 AND #4	#3 AND #4
6	pharmacokinetic* OR outcome	pharmacokinetic* OR outcome	pharmacokinetic* OR outcome
7	#5 AND #6	#5 AND #6	#5 AND #6
8	prevention* OR latent	prevention* OR latent	prevention* OR latent
9	#7 NOT #8	#7 NOT #8	#7 NOT #8

### **Assessment of quality / bias**

Quality of evidence and bias were assessed for the included studies, using a scoring tool previously published and adapted to our situation (see Supplementary Information).<sup>12,13</sup> Quality was assessed by four researchers (A.M.A., A.B., B.P.S. and K.R.). Disagreements were resolved by consensus.

### **Data extraction**

A standardized extraction form (see Supplementary Information) was developed by four authors in consensus (A.M.A., A.B., B.P.S. and K.R.). Two authors (A.B. and B.P.S.) reviewed the full text and independently extracted data. In case of discrepancy, a consensus was found between A.B. and B.P.S, who also synthesized the data.

The variables of interest included the country where the study took place, year of publication, study design, study sample size, age, form of TB, HIV status, study doses, adverse events, percentage of unfavorable outcomes, PK parameters, and significant associations. PK parameters (i.e., area under the concentration time curve (AUC) and maximum concentration ( $C_{max}$ )) were extracted as available in the included studies. If available in the original report, drug exposures by key subgroups were also extracted, including body weight, age, HIV status, nutritional status (definition based on specific study), and dosing regimen (daily dose or other).

### **Data synthesis**

Data were organized using Excel version 16.46 (Microsoft 2021) and visualized using R version 1.3.1093. Study participant characteristics were summarized as reported in the original article, either as full cohort (preferred) and/or by participant group (e.g., HIV status) if full cohort summary was not available. Malnutrition was summarised by each nutritional status measure separately, if possible, as reported in the original study: height-for-age z-score (HAZ) or stunting

(HAZ < -2), weight-for-age z-score (WAZ) or underweight (WAZ < -2), and weight-for-height z-score (WHZ) or wasting (WHZ < -2). Any Z score below -2 was considered malnutrition to avoid discrepancies in our report. Age was summarized as a continuous variable if possible. For studies that grouped participants by age group, data were summarised as done in the original report.

Drug exposures (i.e.,  $C_{max}$ , AUC) were summarized for the whole cohort, dosing group or study arm, and by each relevant covariate: nutritional status, HIV status, and age. For AUC, the time interval for each study was recorded. AUC from 0 to 4 hours after dose ( $AUC_{0-4}$ ) or greater was considered as representing AUC. Data reported as ' $C_{max}$ ' or concentration at 2 hours after dose ' $C_{2h}$ ' was considered as representing  $C_{max}$ . RIF PK targets were 38.7  $\mu\text{g}\cdot\text{h}/\text{mL}$  and 8-24  $\mu\text{g}/\text{mL}$  for AUC and  $C_{max}$ , respectively.<sup>14</sup>

### **Summary measures**

Summary estimates for AUC and  $C_{max}$  were obtained by meta-analysis with the 'metafor' package version 2.4-0 in R. Mean and standard deviation were used. Where summary statistics were not available in this format, the mean and standard deviation were estimated using the summary statistics provided (e.g., median and interquartile range) using previously described methods.<sup>15</sup> The main objective of the analysis was to collate and summarize available data on the drug exposures derived from subjects taking rifampicin, with special attention to higher than recommended doses. The secondary objective was to summarize drug exposures by key subgroups (i.e., age, HIV status, and nutritional status). A restricted maximum likelihood mixed-effects model was used to perform a meta-analysis of AUC and  $C_{max}$  estimates. DerSimonian–Laird estimator was applied for residual heterogeneity. This approach fits a random-effects model. Heterogeneity was assessed by the  $I^2$  statistic and visual inspection of forest plots. Meta-

regression was performed with key covariates to assess their impact on inter-study heterogeneity.

## **Results**

### **Included Studies**

The PRISMA flow diagram is shown in **Figure 2.1**. There were 18 studies that met the inclusion criteria, of which 14 contained rifampicin PK data and were included in this analysis. One study<sup>16</sup> was assessed as a moderate quality, one study<sup>17</sup> as low quality and all the remaining studies were scored very low quality.

The included studies are summarized in **Table 2.2**. All studies were prospective observational studies. The studies were conducted in the following geographic locations: India (n=6), South Africa (n=4), Malawi (n=1), Ghana (n=1), Vietnam (n=1) and Tanzania (n=1). All the studies included children with an age range from infants to adolescents under 16 years of age. HIV infection was reported in 12 studies, of which 8 included HIV-positive children.



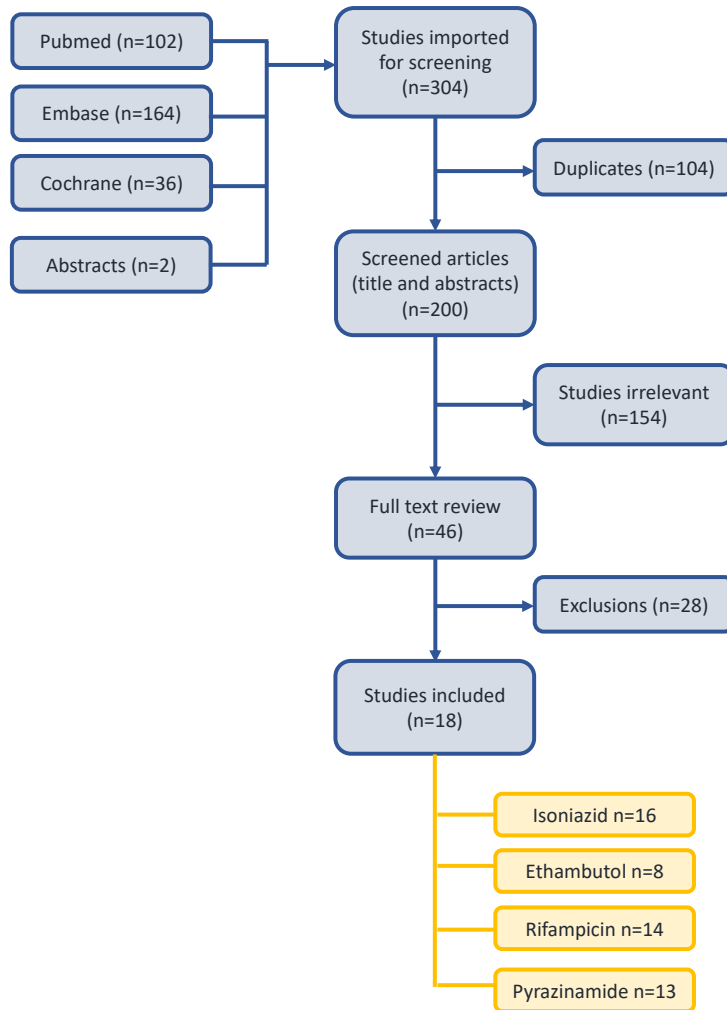


**Figure 2.1** PRISMA flow diagram of systematic review

**Table 2.2** Summary of included studies

Author (year)	Study details	Dosing regimen <sup>1</sup>	Number of subjects	Type of TB	HIV n (%)	Age (years)	Body weight (kg)	Nutritional status	Reported PK measures
Thee <i>et al.</i> (2011)	South Africa Prospective Monocenter	INH: 5 and 10 mg/kg RIF: 10 and 15 mg/kg PZA: 25 and 35 mg/kg	20	PTB, n=11 EPTB, n=1 TBM, n=8	5 (25)	Mean (SD) 1.1 (0.5)	NR	Mean (SD) WAZ -1.74 (1.84)	C <sub>max</sub> AUC <sub>0-5</sub>
Ramachandran <i>et al.</i> (2013)	India Prospective Multicenter	INH: 10 mg/kg RIF: 10 mg/kg PZA: 30-35 mg/kg EMB: 30 mg/kg <i>thrice weekly</i>	84	PTB, n=19 EPTB, n=63 P+EPTB, n=2	0 (0)	Mean (Range) 7.1 (1-12)	Med [IQR] 18 [13-23]	Stunted, n=22 Underweight, n=31 Wasted, n=16  Med [IQR] HAZ -1.2 [-2.1, -0.3] WAZ -1.8 [-2.4, -1.1] WHZ -1.2 [-1.9, -0.3]	C <sub>max</sub> AUC <sub>0-8</sub>
Ramachandran <i>et al.</i> (2015)	India Prospective Multicenter	INH: 10 mg/kg RIF: 10 mg/kg PZA: 30-35 mg/kg EMB: 30 mg/kg <i>thrice weekly</i>	77	PTB, n=49 EPTB, n=28	77 (100)	Median (range) 9 (1-15)	Med [IQR] 17 [14.1-22.5]	Stunted, n=59 Underweight, n=56 Wasted, n=15  Med [IQR] HAZ -3.0 [-4.1, -2.0] WAZ -2.7 [-3.4, -1.9] WHZ -1.1 [-1.7, -0.02]	C <sub>max</sub> AUC <sub>0-8</sub>
Anya <i>et al.</i> (2015)	India Prospective Monocenter	INH: 10 mg/kg RIF PZA: 30-35 mg/kg EMB: 30 mg/kg <i>thrice weekly</i>	20 • G1: 8 • G2: 12	PTB Lymph node TB	NR	Median (Range) • G1: 9 (6-10) • G2: 12 (6-12)	Median (Range) • G1: 20.6 (15-22.4) • G2: 24.2 (15.2-25)	NA	C <sub>max</sub> AUC <sub>0-12</sub>
Mlotha <i>et al.</i> (2015)	Malawi Prospective Monocenter	INH 5 mg/kg RIF 10 mg/kg PZA 25 mg/kg EMB 20 mg/kg	30	PTB, n=21 EPTB, n=9	20 (66)	Median (Range) 7.5 (0.5-15.6)	Median (Range) 18 (4.8-45)	NA	C <sub>max</sub> AUC <sub>0-last</sub> AUC <sub>0-60</sub>
Hiruy <i>et al.</i> (2015)	South Africa Prospective Monocenter	INH 10-15mg/kg RIF 10-15 mg/kg PZA 30-40 mg/kg EMB 15-25 mg/kg	31	PTB, n=22 EPTB, n=9	7 (23)	Median (Range) 2.29 (0.25-10.5)	Median (Range) 11.5 (6.1-19)	Malnourished, n=20	C <sub>max</sub> AUC <sub>0-24</sub> C <sub>2h</sub>

**Table 2.2** (continued)

Author (year)	Study details	Dosing regimen <sup>1</sup>	Number of subjects	Type of TB	HIV n (%)	Age (years)	Body weight (kg)	Nutritional status	Reported PK measures
Mukherjee <i>et al.</i> (2015)	India Prospective Multicenter	INH • G1: 5 (4-6) mg/kg • G2: 10 (7-15) mg/kg RIF • G1: 10 (8-12) mg/kg • G2: 15 (10-12) mg/kg PZA 30-35 mg/kg EMB 20-25 mg/kg	127 • G1, n=64 • G2, n=63	PTB, n=63 EPTB, n=64	0 (0)	Range 0.5-15	NR	Malnourished, n=58	Cmax AUC0-4 C2h
Bekker <i>et al.</i> (2016)	South Africa Prospective Multicenter	INH 14 (9-20) mg/kg RIF 14 (9-20) mg/kg PZA 32 (19-45) mg/kg ETH 20 (13-29) mg/kg	39	PTB, n=36 TBM, n=1 PTB+EPTB, n=2	5 (13)	Mean (range) 0.55 (0-1)	Mean (sd) 6.45 (1.67)	Mean (sd) WAZ: -1.62 (1.53) WHZ: -0.4 (1.26)	Cmax AUC0-8
Mukherjee <i>et al.</i> (2016)	India Prospective Monocenter	INH 4-6 mg/kg RIF 8-12 mg/kg PZA 30-35 mg/kg EMB 20-25 mg/kg	56	PTB, n=52 Pleural TB, n=4 Associated EPTB, n=19	24 (43)	Range 0.5-15	NR	Med [IQR] • HIV+ HAZ -2.5 [-4.2, -1.6] WAZ -3.2 [-4.5, -2.1] • HIV- HAZ -1.4 [-2.3, 0] WAZ -1.4 [-2, -0.7]	Cmax AUC0-4 C2h
Antwi <i>et al.</i> (2017)	Ghana Prospective Monocenter	Median [IQR] INH 11.2 [9.1-12.8] mg/kg RIF 15.8 [13.6-18.8] mg/kg PYR 24.8 [22.6-30] mg/kg EMB 16.9 [15-20.6] mg/kg	113	PTB, n=85 EPTB, n=28	54 (48)	Median [IQR] 5 [2.2-8.3]	Median [IQR] 14.0 [8.8-19.5]	Median [IQR] HAZ: -2.0 [-3.2, -1.1] WAZ: -2.5 [-3.8, -1.4]	Cmax AUC0-8
Ranjalkar <i>et al.</i> (2018)	India Prospective Multicenter	Median [IQR] • G1: Thrice weekly INH 10 [8-12] mg/kg RIF 10 [9-12] mg/kg • G2: daily INH 8 [7-9] mg/kg RIF 11 [10-12] mg/kg	41 • G1, n=27 • G2, n=14	PTB, n=36 G1, n=24 G2, n=13 Lymph node TB, n=5 G1, n=3 G2, n=2	NR	Range 2-16	Median [IQR] • G1: 14.7 [12-24] • G2: 37 [21-41]	Median [IQR] HAZ • G1: -1.412 [-2, -0.56] • G2: -0.316 [-1.15, 0.22]	Cmax AUC0-6 C2h

**Table 2.2** (continued)

Author (year)	Study details	Dosing regimen <sup>1</sup>	Number of subjects	Type of TB	HIV n (%)	Age (years)	Body weight (kg)	Nutritional status	Reported PK measures
Garcia-Prats <i>et al.</i> (2019)	South Africa RIF Prospective Multicenter	INH 5 mg/kg RIF 10 mg/kg PZA 25 mg/kg EMB 15 mg/kg	62	PTB, n=45 EPTB, n=2 P+EPTB, n=15	0 (0)	Median (range) • G1: 2 (1.2-3.4) • G2: 2 (1.1-3.9) • G3: 2.8 (1-5.5)	Median (range) • G1: 10.6 (8.7-14.2) • G2: 10.9 (9.3-14.1) • G3: 12.5 (8-17.4)	Underweight, n=18	Cmax AUC0-24
Panjasawatwong <i>et al.</i> (2020)	Vietnam Prospective Monocenter	INH 5 mg/kg RIF 10 mg/kg PZA 25 mg/kg EMB 15 mg/kg	100	TBM, n=100	4 (4)	Median (range) 3 (0.2-15)	Median (range) 10.9 (4-43)	Median (range) HAZ: -1.64 (-9.17, 2.21) WAZ: -1.93 (-5.52, 2)	Cmax AUC0-24
Justine <i>et al.</i> (2020)	Tanzania Prospective Monocenter	INH 2-10 mg/kg RIF 5-20 mg/kg PZA 10-40 mg/kg EMB 7.5-35 mg/kg	51	PTB, n=18 EPTB, n=17 P+EPTB, n=16	0 (0)	Median (range) 5.3 (0.75-14)	NR	Stunted, n=16/23 Underweight, n=16/23	Cmax

<sup>1</sup>Dosing regimen expressed per day, except if mentioned otherwise

INH: isoniazid, RIF: rifampicin, PZA: pyrazinamide, EMB: ethambutol  
G1: group 1, G2: group 2

n: number of patients

PTB: pulmonary tuberculosis, EPTB: extra pulmonary tuberculosis, TBM: tuberculosis meningitis

HIV+: HIV positive, HIV-: HIV negative

HAZ: Height for age Z score (if  $\leq -2$  SD, stunted), WAZ: Weight for age Z score (if  $\leq -2$  SD, underweight), WHZ: Weight for height Z score (if  $\leq -2$  SD, wasted)

## Overview of PK data

RIF PK data was assessed in a total of 950 patients in the 14 included studies. All studies reported  $C_{max}$  and 13 studies reported AUC:  $AUC_{0-4}$  (n=2),  $AUC_{0-5}$  (n=1),  $AUC_{0-6}$  (n=1),  $AUC_{0-8}$  (n=4),  $AUC_{0-12}$  (n=1),  $AUC_{0-24}$  (n=3), and  $AUC_{0-last}$  (n=1).

PK parameters were reported differently across studies: 11 (73%) studies and 12 (80%) studies reported AUC and  $C_{max}$  parameters for the full cohort, respectively (**Table 2.3**). Only 4 (27%) studies reported AUC parameters by age. There were 3 (21%) studies that reported AUC by malnutrition, but the metrics differed by study. Five studies reported AUC by HIV status and an additional three studies included only HIV-positive or HIV-negative children; therefore, the HIV status for AUC estimates were known for 173 (26%) children in 8 studies. Extracted PK data are summarized in **Table 2.4**.

**Table 2.3** Number of children contributing rifampicin pharmacokinetic data by study and covariates as reported in the original study

Study	N	AUC				Cmax			
		Whole cohort	HIV-positive	Malnutrition	Age	Whole cohort	HIV positive	Malnutrition	Age
Thee 2011 (10mg/kg)	11	11 (100%)	4 (36%)	-	-	11 (55%)	4 (36%)	-	-
Thee 2011 (15mg/kg)	11	11 (100%)	4 (36%)	-	-	11 (55%)	4 (36%)	-	-
Antwi 2017	113	113 (100%)	59 (52%)	-	-	113 (100%)	59 (52%)	-	-
Bekker 2016	39	39 (100%)	5 (13%)	Underweight: 18 (46%)	39 (100%)	5 (13%)	Underweight: 18 (46%)	39 (100%)	56 (100%)
Mukherjee 2016	56	14 (100%)	24 (43%)	-	14 (100%)	24 (43%)	UNK	14 (100%)	14 (100%)
Ranjalkar 2018	14	14 (100%)	0 (0%)	Malnourished: 26 (41%)	-	14 (100%)	Malnourished: 26 (41%)	-	-
Mukherjee 2015	63	63 (100%)	0 (0%)	Underweight: 56 (73%)	-	63 (100%)	Underweight: 56 (73%)	-	-
Ramachandran 2015*	77	-	77 (100%)	Stunted: 59 (77%)	77 (100%)	77 (100%)	Stunted: 59 (77%)	77 (100%)	77 (100%)
Ramachandran 2013*	84	-	0 (0%)	Wasted: 15 (20%)	-	-	Wasted: 15 (20%)	-	84 (100%)
Arya 2015	8	8 (100%)	-	-	8 (100%)	0 (0%)	-	-	-
Hiruy 2015	31	31 (100%)	-	-	31 (100%)	-	-	-	-
Panjasawatwong 2020	100	100 (100%)	-	-	100 (100%)	-	-	-	-
Mlotha 2015	28	28 (100%)	-	-	28 (100%)	-	-	-	-
Garcia-Prats 2019 (15-20 mg/kg)*	20	20 (100%)	0 (0%)	-	20 (100%)	-	-	-	-
Justine 2020	16	-	-	-	-	0 (0%)	-	-	-
Total	671	11 (73%) studies;	8 (57%) studies;	3 (21%) studies;	4 (27%) studies;	12 (80%) studies;	4 (27%) studies;	5 (33%) studies;	5 (33%) studies;
		438 (65%) children	173 (26%) children	26 (4%) patients 'malnourished', 74 (11%) patients 'underweight', 15 (2%) patients 'wasted', 59 patients stunted (8.8%)	214 (33%) children	173 (26%) children	26 (4%) patients 'malnourished', 74 (11%) patients 'underweight', 15 (2%) patients 'wasted'	270 (41%) children	270 (41%) children

\*data was not reported by HIV status but the HIV status for all participants was the same

UNK: unknown number of children associated with group

(-) PK data not reported for that group

Table 2.4 Rifampicin AUC and C<sub>max</sub> as reported in the original studies

Study	Metric	Whole cohort	HIV status		Nutritional status				Age		Significant associations
			HIV-	HIV+	Normal	Stunted	Underweight	Wasted	Younger	Older	
Thee 2011 (10mg/kg)	AUC	17.8 (12.8-22.8)	18.4 (12.8-24.0)	16.7 (0.2-33.1)	-	-	-	-	-	-	-
	Cmax	6.36 (4.5-8.3)	6.9 (4.4-9.3)	5.5 (0.1-10.9)	-	-	-	-	-	-	-
Thee 2011 (15mg/kg)	AUC	36.9 (27.7-46.3)	36.1 (22.7-49.6)	38.4 (15.2-61.6)	-	-	-	-	-	-	-
	Cmax	11.7 (8.7-14.7)	12.5 (7.7-27.4)	10.2 (6.5-14.0)	-	-	-	-	-	-	-
Antwi 2017	AUC	27.3 (20.6-36.3)	30.5 (21.9-38.2)	24.9 (15.9-35.3)	-	-	-	-	-	-	Lower AUC for HIV+ *
	Cmax	6.4 (4.9-8.8)	7.7 (5.2-9.1)	5.8 (3.7-8.3)	-	-	-	-	-	-	Lower Cmax for HIV+ *
Bekker 2016	AUC	12.1 (1.8-33.0)	11.5 (sd=8.7)	16.5 (sd=15.0)	10.6 (sd=8.2)	-	-	13.9 (sd=10.9)	12.8 (sd=9.72)	11.4 (sd=9.63)	-
	Cmax	2.9 (0.6-8.0)	2.8 (sd=2.0)	3.67 (sd=3.3)	2.6 (sd=1.9)	-	-	3.2 (sd=2.4)	2.9 (sd=2.16)	2.9 (sd=2.24)	-
Mukherjee 2016	AUC	-	22.6 (16.7-30.6)	18.5 (13.3-25.7)	-	-	-	-	-	-	-
	Cmax	-	9.2 (6.7-12.5)	7.8 (5.6-10.7)	-	-	-	-	-	-	-
Ranjalkar 2018	AUC	19.4 (11.3-30.4)	-	-	-	-	-	-	13.3	18.4	-
	Cmax	5.9 (3.8-8.8)	-	-	-	-	-	-	5.8	6.2	-
Mukherjee 2015	AUC	30.5 (17.1-58.9)	-	-	26.3 (21.0-27.4)	-	-	32.8 (11.7-66.7)	-	-	-
	Cmax	12.0 (6.1-24.3)	-	-	11.3 (8.1-23.6)	-	-	13.2 (5.3-25.7)	-	-	-
Ramachandran 2015	AUC	-	-	-	9.9 (3.6-22.0)	10.1 (6.1-17.6)	10.9 (6.7-17.7)	11.5 (6.5-19.8)	9.5 (0.8-13.2)	10.9 (6.5-19.8)	-
	Cmax	-	-	-	3.3 (1.1-4.7)	2.4 (1.1-4.4)	2.5 (1.3-4.2)	3.4 (1.9-4.4)	2.4 (1.1-4.1)	2.7 (1.4-4.6)	-

Table 2.4 (continued)

Study	Metric	Whole cohort	HIV status		Nutritional status				Age		Significant associations
			HIV-	HIV+	Normal	Stunted	Underweight	Wasted	Younger	Older	
Ramachan dran 2013	Cmax	-	-	-	3.3 (1.1-4.7)	2.4 (1.1-4.4)	2.5 (1.3-4.2)	3.4 (1.9-4.4)	2.4 (1.1-4.1)	2.7 (1.4-4.6)	-
	AUC	-	-	-	-	-	-	-	15 (9.6-19.2)	31.8 (18.8-38.1)	AUC increased by 2.0 mg.h/L per age year ** and increased by 2.8 mg.h/L per unit of WAZ*
Arya 2015	Cmax	-	-	-	-	-	-	-	3.1 (2.4-4.0)	5.9 (4.1-7.1)	Cmax increased by 0.4 mg/L per age year *** and increased by 0.6 mg/L per unit of WAZ *
	AUC	33.3 (29.7-36.1)	-	-	-	-	-	-	-	-	-
Hiruy 2015	Cmax	6.2 (5.4-7.6)	-	-	-	-	-	-	-	-	-
	AUC	21.2 (1.8 - 67.3)	-	-	-	-	-	-	-	-	-
Justine 2020	Cmax	3.5 (0.6 - 10.2)	-	-	-	-	-	-	-	-	-
	AUC	-	-	-	-	-	-	-	-	-	-
Panjasawat wong 2020	Cmax	2.17 (0.59-4.61)	-	-	-	-	-	-	-	-	-
	AUC	21.5 (14.2-36.5)	-	-	-	-	-	-	-	-	-
Mlotha 2015	Cmax	4.9 (2.5-8.4)	-	-	-	-	-	-	-	-	-
	AUC	7.50 (5.6 - 13.1)	-	-	-	-	-	-	-	-	-
Garcia-Prats 2019 (15-20 mg/kg)	Cmax	2.9 (2.1 - 3.4)	-	-	-	-	-	-	-	-	-
	AUC	39.5 (11.7-76.1)	-	-	-	-	-	-	-	-	-
	Cmax	8.4 (3.1-15.5)	-	-	-	-	-	-	-	-	-

HIV+, HIV positive; \*, p<0.05; \*\*, p<0.01; \*\*\*, p<0.001



None of the studies under evaluation assessed PK parameters by weight. Therefore, raw data from confidential unpublished studies (shorter treatment for minimal tuberculosis in children ('Shine', n=76); optimal dosing of first line antituberculosis and antiretroviral drugs in children, a pharmacokinetic study ('Datic', n=179) and pooled published data<sup>18,19</sup> were used to show the range in exposure by weight band (**Figure 2.2**). Guiastrennec *et al.*<sup>19</sup> reported data by WHO weight bands pooled from two studies<sup>20,21</sup> included in this systematic review. Zvada *et al.*<sup>18</sup> reported pooled data; one study<sup>22</sup> is represented in this systematic review, but the other study<sup>23</sup> did not meet our inclusion criteria.

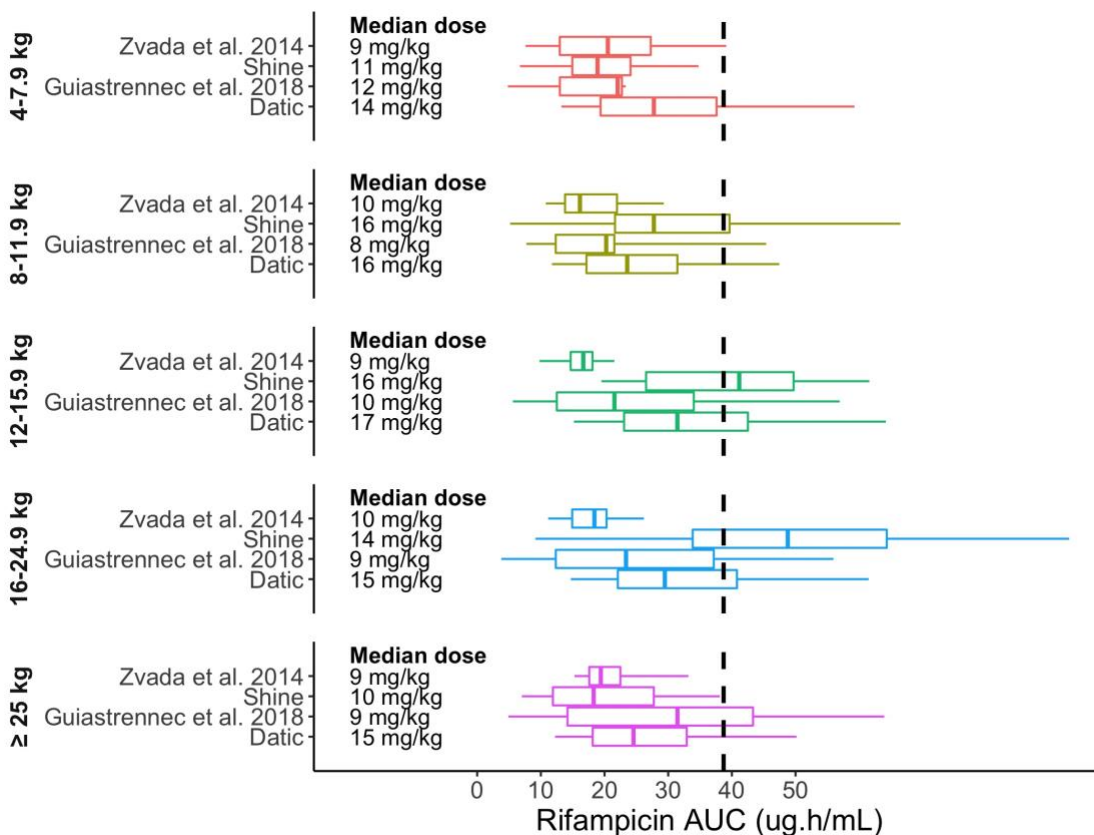


**Figure 2.2** Rifampicin AUC by weight band. Boxplots represent 5th, 25th, 50th, 75th, and 95th percentiles. The number of children included are 76 (Shine), 179 (Datic), 161 (Guiatrennec et al. 2018), and 76 (Zvada et al. 2014). Dashed line represents the target AUC (38.7  $\mu\text{g}\cdot\text{h}/\text{mL}$ ).

### Summary estimates of rifampicin PK

The summary estimate for the 13 studies that reported rifampicin AUC was 23.4  $\mu\text{g}\cdot\text{h}/\text{mL}$  compared to the target of 38.7  $\mu\text{g}\cdot\text{h}/\text{mL}$  (**Figure 2.3**). In one study, the mean estimate achieved the target; in two studies, the 95% CI for one group crossed the target threshold but not the mean; in all remaining studies, the 95% CI was below the target. The summary estimate for the 14 studies that reported rifampicin  $C_{\text{max}}$  was 6  $\mu\text{g}/\text{mL}$  compared to the target of 8  $\mu\text{g}/\text{mL}$  (**Figure 2.3**). The mean estimate was greater than the target in two studies and in one group in two studies. In three studies, the 95% CI of one group crossed the target threshold but the mean was below. All remaining studies were below the target. The heterogeneity in  $C_{\text{max}}$  and AUC between studies was high (AUC  $I^2=98.3\%$ ;  $C_{\text{max}}$   $I^2=96.9\%$ ).

Multivariate meta-regression of full cohort AUC estimates including dose (mg/kg), dosing frequency, rifampicin formulation, and study country variables identified dose (mg/kg) and RIF formulation as significantly impacting AUC ( $p<0.05$ ). Higher mg/kg dose increased AUC while administration of RIF suspension was associated with lower AUC. Of note, the RIF suspension was only used in one study where all children were under one year of age. Inclusion of these variables reduced heterogeneity by 1% ( $I^2=97.4\%$ ). In multivariate meta-regression of  $C_{\text{max}}$  estimates, RIF formulation was the only significant predictor. The  $I^2$  was mostly unaffected.

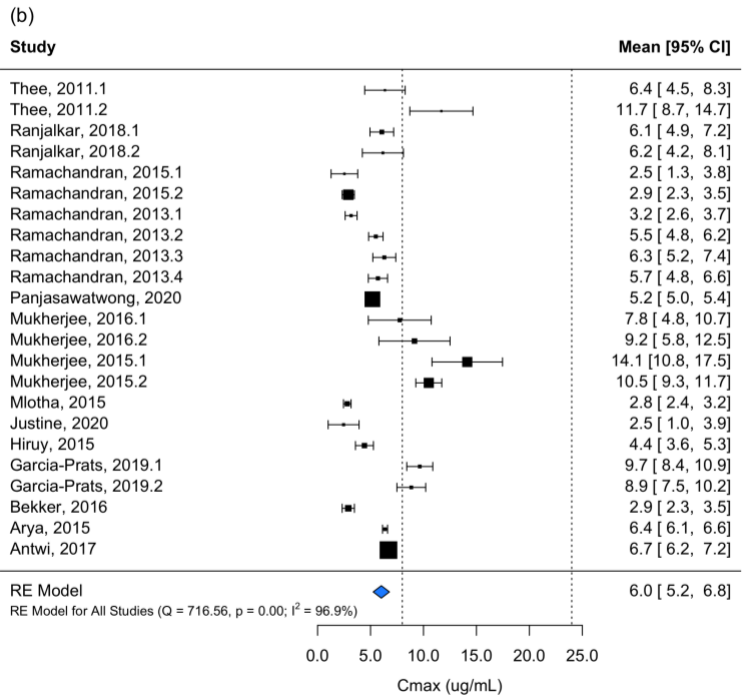
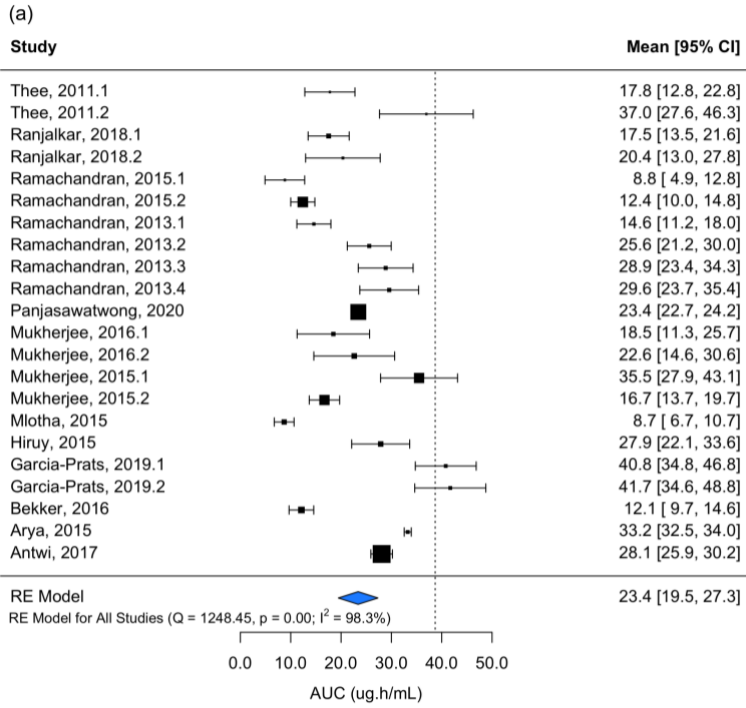


**Figure 2.3** Forest plot displaying estimated rifampicin AUC (a) and C<sub>max</sub> (b). Dashed lines represent the target or target range. Square is proportional to the sample size in each group.

## Subgroup analysis and predictors of rifampicin PK

All RIF exposure values by subgroups as reported in the original studies are in **Table 2.4**.

**Dose.** RIF dose was associated with increased PK levels in four studies.<sup>22,24-26</sup> A median dose of 15 mg/kg was associated with greater RIF AUC ( $p=0.01$ ) and  $C_{max}$  ( $p=0.04$ ) than 10 mg/kg in univariate analysis but not multivariate analysis. Dosing frequency was not a significant modifier. Study-specific dose comparison found  $C_{max}$  and  $AUC_{0-12}$  were higher with >10 mg/kg.<sup>22,26</sup> In separate studies,  $AUC_{0-\infty}$  increased by 0.12  $\mu\text{g}\cdot\text{h}/\text{mL}$  per mg/kg RIF ( $p=0.028$ ),<sup>24</sup> and  $C_{2h}$  increased by 0.2  $\mu\text{g}/\text{mL}$  per mg/kg ( $p=0.005$ ).<sup>25</sup> Only one study assessed doses  $\geq 20$  mg/kg. These data (unpublished) show a wide range in  $C_{max}$  and  $AUC_{0-24}$  among individuals receiving 15 to 60 mg/kg.<sup>27</sup> Steady state median (range)  $AUC_{0-24}$  was 39.5 (11.7-76.1)  $\mu\text{g}\cdot\text{h}/\text{mL}$  with 15-20 mg/kg, 68.4 (18.9 – 169)  $\mu\text{g}\cdot\text{h}/\text{mL}$  with 35 mg/kg, and 192.8 (17.2 – 415.6)  $\mu\text{g}\cdot\text{h}/\text{mL}$  with 60 mg/kg. Steady state median (range)  $C_{max}$  was 8.4 (3.1-15.5)  $\mu\text{g}/\text{mL}$  with 15-20 mg/kg, 13.7 (4.8 – 29.5)  $\mu\text{g}/\text{mL}$  with 35 mg/kg, and 28.4 (3.5 – 47.4)  $\mu\text{g}/\text{mL}$  in the 60 mg/kg group.

**HIV status.** HIV-positive children had significantly lower  $C_{max}$  and AUC in one study.<sup>17</sup>

Univariate analysis did not find a significant effect of HIV status; however, there was a trend toward lower RIF AUC (**Figure 2.4**). The PK variability within a study and between studies was large.

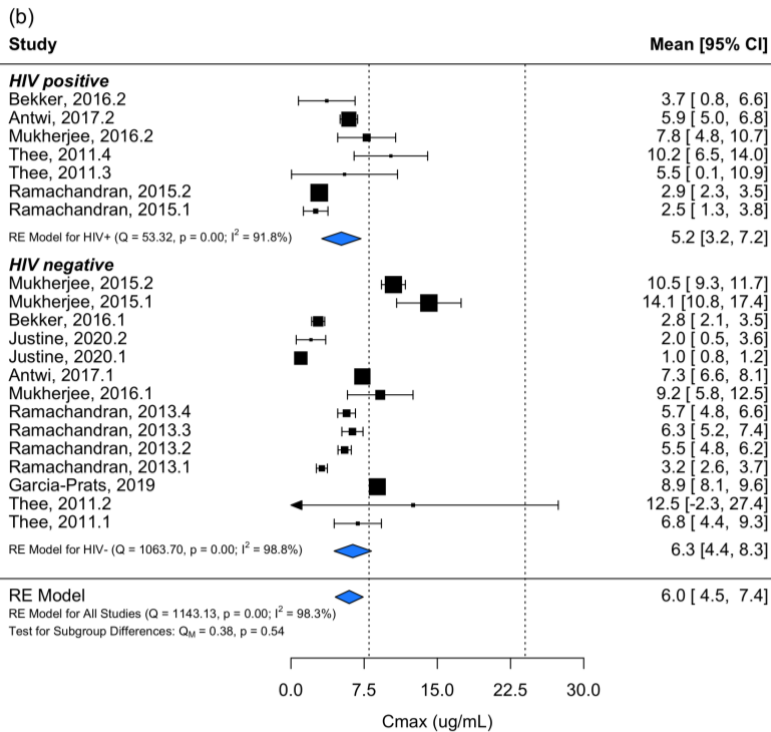
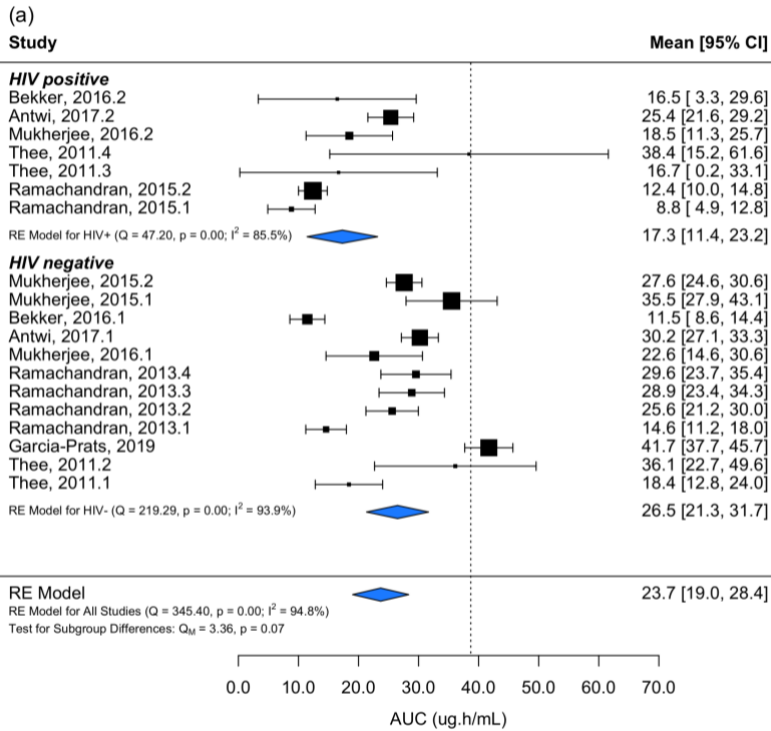


**Figure 2.4** Forest plot displaying estimated rifampicin AUC (a) and C<sub>max</sub> (b) by HIV status. Dashed lines represent the target or target range. Square is proportional to the sample size in each group.

**Age.** Younger age was associated with significantly lower exposures in one study.<sup>21</sup> Summary estimates by age group are shown in **Figure 2.5**. Younger children (0 to <6 years) had lower RIF AUC, estimated as 14.0  $\mu\text{g}\cdot\text{h}/\text{mL}$  versus 22.0  $\mu\text{g}\cdot\text{h}/\text{mL}$  ( $p=0.03$ ). RIF  $C_{\text{max}}$  trended toward lower in younger children but was not significant in the subgroup analysis. Of note, age stratification differed by study; therefore, estimate differences by group need to be interpreted with caution.

**Malnutrition.** Nutritional status was associated with lower RIF exposure in two studies.<sup>21,25</sup> Ramachandran *et al.* reported an increase in AUC of 2.8  $\mu\text{g}\cdot\text{h}/\text{mL}$  per unit WAZ and an increase in  $C_{\text{max}}$  of 0.6  $\mu\text{g}/\text{mL}$  per unit WAZ.<sup>21</sup> Justine *et al.* reported 2.03  $\mu\text{g}/\text{mL}$  lower RIF  $C_{2\text{h}}$  in children with any malnutrition.<sup>25</sup> There were too few studies that reported PK parameters by the same measure of nutritional status to test the association of malnutrition in the meta-analysis.

**Other variables.** In addition to these results, drug formulation significantly influenced AUC and  $C_{\text{max}}$ .<sup>22</sup> In a separate study, low serum albumin was associated with lower  $C_{\text{max}}$ .<sup>20</sup>

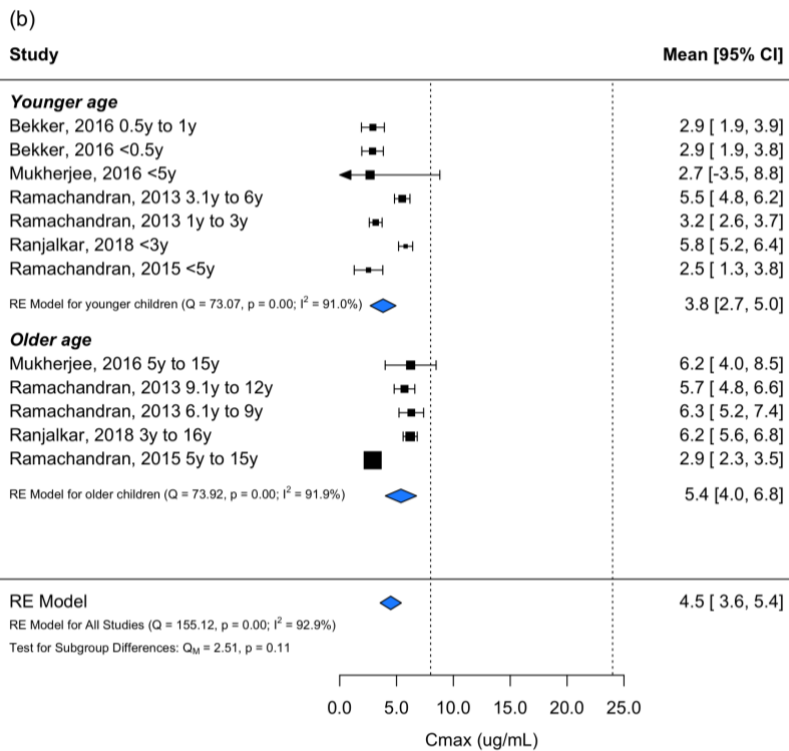
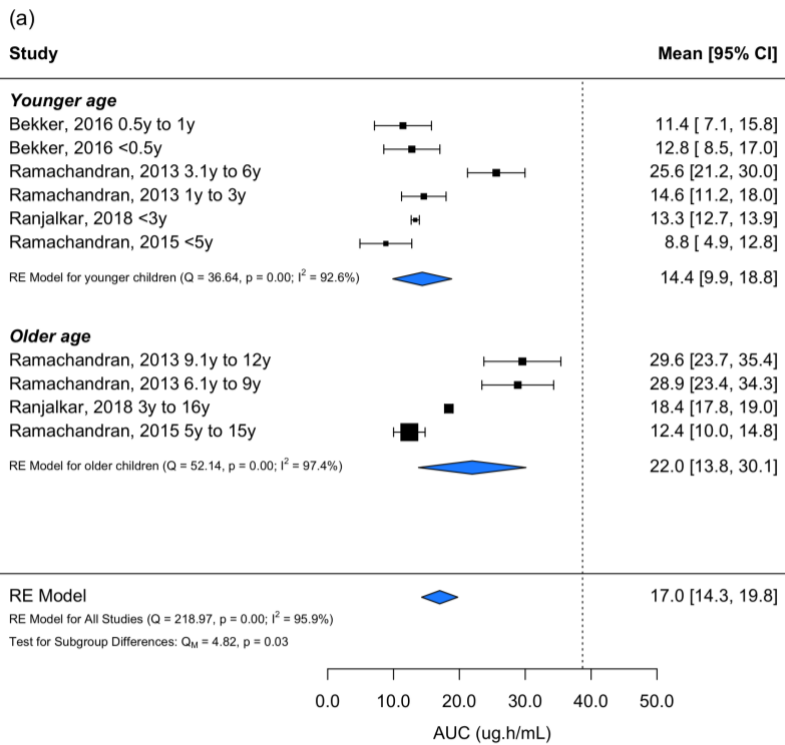


**Figure 2.5** Forest plot displaying estimated rifampicin AUC (a) and C<sub>max</sub> (b) by age group. Dashed lines represent the target or target range. Square is proportional to the sample size in each group.

## Discussion

This is the first time, to our knowledge, that RIF PK at doses higher than those currently recommended by WHO have been systematically reviewed in children. We found a significant lack of research evaluating higher than recommended doses. Only one such study was identified ('OptiRif'); these data are unpublished but findings were presented in 2019 at the Union World Conference.<sup>27</sup> Among studies evaluating current WHO doses, only 'OptiRif' (15-20 mg/kg) achieved AUC target attainment.<sup>27</sup>

Until WHO guideline revisions in 2010, first-line anti-TB drugs were prescribed at the same mg/kg dose in children as in adults.<sup>28</sup> Substantially lower exposures in children compared to adults prompted empirical increases in pediatric doses (e.g., from 10 mg/kg to 15 mg/kg for RIF).<sup>22,29,30</sup> However, these dose increases were based on only a few pharmacokinetic studies including small numbers of children.

The results from this systematic review and meta-analysis demonstrate that current RIF dosing (10-20 mg/kg daily) in children is suboptimal. Within the WHO recommended dose range, higher doses were found to result in higher RIF exposures but remained below the AUC target. More than 15 mg/kg RIF is likely required, at least for some children, to match the typical AUC in adults treated with 10 mg/kg RIF. Modelling and simulation predicted 25 mg/kg is needed to ensure target exposure attainment and favourable outcomes.<sup>19,31</sup> Findings from 'OptiRif' (unpublished) support safe RIF dose increases up to 60 mg/kg in children.<sup>27</sup> However, these doses were only given for two weeks, and long-term safety remains unknown. The published results of 'OptiRif' and future high-dose RIF studies in children are urgently needed to confirm PK and safety.



We found high variability in RIF exposures and large heterogeneity between studies. This could be expected given typically large PK variability in children<sup>32</sup> compounded by heterogenous study populations (e.g., wide age range) and study characteristics. However, multivariate meta-regression of study characteristics only found a significant association with mg/kg dose and/or RIF suspension, which was only used in one study of children under 1 year of age.<sup>33</sup> Thus, the latter may reflect an age or formulation effect. Age was significantly associated with RIF AUC, where younger (<3 to <6 years, depending on study age grouping) had lower exposures. However, these results need to be interpreted with caution due to the small number of studies that reported PK by age and inconsistent age groupings. There was a trend toward lower AUC in HIV-positive children. Some studies also reported significant associations with malnutrition, but these could not be assessed in this meta-analysis due to the limited number of studies and inconsistent nutritional status metrics.

Individual participant data meta-analysis (IPD-MA) should be done to make conclusive recommendations on the appropriate RIF dosing in children. Population-based approaches and nonlinear mixed effects modelling with pooled individual-level data has been successful in determining optimal doses for populations as well as high-risk subgroups.<sup>34-36</sup> With a large PK database that includes diverse child populations, including substantial proportions of malnourished children and children living with HIV of various ages, we can better understand the true drivers of RIF PK. Given the large number of PK studies that have already been conducted, this approach would be feasible and preferred over a new study.

This analysis is limited by the inconsistent reporting of PK parameters between studies, heterogenous populations, and small sample sizes. Mainly, important influencers of RIF PK could not be reliably determined through traditional meta-analysis approaches given the limited number of children, inconsistent or unreported metrics, and inability to correct for correlated

predictors. For example, only 4 of 14 studies reported PK by age but represented the same age distribution (e.g., <5 or  $\geq$  5 years). Similarly, 3 studies reported PK by malnutrition but only 2 studies reported by the same metric (e.g., 'underweight'). IPD-MA would be a more robust approach for assessing important influencers of PK.

Another limitation of this review is regarding assumptions. The reported AUC values varied from 0-4 hours to 0-24 hours, which were considered equivalent in this analysis. Given RIF's short half-life of 3-4 hours, this would be expected to minimally impact results, especially given the inherent variability observed within study. Further, only one study reported PK results as mean and SD; therefore, the parameters from remaining studies utilized estimated statistics. These assumptions would not be needed with methods that utilized raw PK data as in the proposed IPD-MA approach.

## **Conclusion**

In this report, we showed that there is a lack of research studying higher doses than recommended by WHO in children. At currently recommended doses, RIF exposures are consistently lower than adults in the included studies. Our findings suggest that younger children and perhaps those with HIV infection may require higher doses than older children and those uninfected with HIV. However, given this study's limitations and the high heterogeneity observed between studies, more robust methods such as IPD-MA with population PK modelling are needed to inform appropriate RIF doses for optimal treatment of all children, including high-risk child subgroups.

## Supplementary Information

### Quality of Evidence scoring for PK studies

Final scoring: high (1 point), moderate (2 points), low (3 points), or very low (>4 points).

*Study design:*

Randomized trial: 1

Controlled pharmacokinetic study, prospective: 2

Pharmacokinetic study, retrospective: 3

Observational study: 3

Other: 4

*Add one point for the following situations of poor evidence:*

The publication was a conference abstract or not published in a peer-reviewed journal

Sample size < 10 children in each arm or 30 in the whole study

Doses were lower than currently recommended or not specified for any drug used or the formulation used was other than WHO-recommended FDC or not specified

Not all relevant PK parameters were reported or PK outcomes are not well defined (AUC, C<sub>max</sub>)

Inclusion and/or exclusion criteria are not defined (selection bias).

The PK sampling strategy is not defined or only sparse sampling was collected (<3 samples per child)

Demonstration of confirmed drug-sensitive TB or that drug-resistant TB not probable is not described

*Remove one point for significant findings:*

The study investigated doses higher than currently recommended with a comparator arm

The study uses compartmental analyses with at least an internal validation

There was a >50% decrease or >2-fold increase in PK parameters between reference and comparator group.

## Data extraction form

*The data extraction form was an excel spreadsheet for each of the drug. For a better understanding of our methods, here are detailed what we collected for each study and for each drug when appropriate (INH, RIF, PZA and EMB).*

Publication information: Publication ID, title, Author, Year of publication, country, design

Design information: sample size, numbers of HIV positive patients, studied drugs (INH, RIF, PZA, EMB), definition of TB, dosing regimen for each drug, formulation for each drug, PK sample design, PK outcome definitions

Population information: age, body weight, sex, nutritional status (all Z-score with the numbers of patients having Z score < 2 and/or raw data)

For each study: PK outcome for each drug (INH, RIF, PZA and EMB) for the whole cohort for each covariate when available (HIV, nutritional status, age and NAT2 genotype for INH). Each covariate was separated in different columns when appropriate (e.g. HIV positive and HIV negative, details for all the different ages). We reported the PK outcomes as follow: C<sub>max</sub>: mean or median, range, IQR or SD; AUC: mean or median, range, IQR or SD

Other reported associations with PK outcomes in free comments

For each study: Clinical outcome (favourable or unfavourable) when reported.

PK target attainment: Number of patients attaining the PK target (AUC and/or C<sub>max</sub>) for each drug (INH, RIF, PZA and EMB)

Adverse events in free comments

## References

1. Global Tuberculosis Report. WHO, 2020. (Accessed February 25, 2021, 2021, at <https://www.who.int/publications/i/item/9789240013131>.)
2. Drobac PC, Shin SS, Huamani P, et al. Risk factors for in-hospital mortality among children with tuberculosis: the 25-year experience in Peru. *Pediatrics* 2012;130:e373-9.
3. Thwaites G, Nahid P. Triumph and Tragedy of 21st Century Tuberculosis Drug Development. *N Engl J Med* 2020;382:959-60.
4. Fox W, Ellard GA, Mitchison DA. Studies on the treatment of tuberculosis undertaken by the British Medical Research Council tuberculosis units, 1946-1986, with relevant subsequent publications. *Int J Tuberc Lung Dis* 1999;3:S231-79.
5. Short-course chemotherapy in pulmonary tuberculosis. A controlled trial by the British Thoracic and Tuberculosis Association. *Lancet* 1976;2:1102-4.
6. Technical report on the pharmacokinetics and pharmacodynamics (PK/PD) of medicines used in the treatment of drug-resistant tuberculosis. WHO, 2018. (Accessed February 25, 2021, 2021, at <https://apps.who.int/iris/handle/10665/260440>.)
7. Svensson RJ, Svensson EM, Aarnoutse RE, et al. Greater Early Bactericidal Activity at Higher Rifampicin Doses Revealed by Modeling and Clinical Trial Simulations. *J Infect Dis* 2018;218:991-9.
8. Boeree MJ, Diacon AH, Dawson R, et al. A dose-ranging trial to optimize the dose of rifampin in the treatment of tuberculosis. *Am J Respir Crit Care Med* 2015;191:1058-65.
9. Aarnoutse RE, Kibiki GS, Reither K, et al. Pharmacokinetics, Tolerability, and Bacteriological Response of Rifampin Administered at 600, 900, and 1,200 Milligrams Daily in Patients with Pulmonary Tuberculosis. *Antimicrob Agents Chemother* 2017;61.

10. Draft Guidance for Industry: General Clinical Pharmacology Considerations for Pediatric Studies for Drugs and Biological Products. (Accessed June 1, 2021, at <http://www.fda.gov/downloads/Drugs/GuidanceComplianceRegulatoryInformation/Guidances/UCM425885.pdf>.)
11. Moher D, Liberati A, Tetzlaff J, Altman DG, Group P. Preferred reporting items for systematic reviews and meta-analyses: the PRISMA statement. *Ann Intern Med* 2009;151:264-9, W64.
12. Jacobs TG, Svensson EM, Musiime V, et al. Pharmacokinetics of antiretroviral and tuberculosis drugs in children with HIV/TB co-infection: a systematic review. *J Antimicrob Chemother* 2020;75:3433-57.
13. Seden K, Gibbons S, Marzolini C, et al. Development of an evidence evaluation and synthesis system for drug-drug interactions, and its application to a systematic review of HIV and malaria co-infection. *PLoS One* 2017;12:e0173509.
14. Stott KE, Pertinez H, Sturkenboom MGG, et al. Pharmacokinetics of rifampicin in adult TB patients and healthy volunteers: a systematic review and meta-analysis. *J Antimicrob Chemother* 2018;73:2305-13.
15. Wan X, Wang W, Liu J, Tong T. Estimating the sample mean and standard deviation from the sample size, median, range and/or interquartile range. *BMC Med Res Methodol* 2014;14:135.
16. Mukherjee A, Velpandian T, Singla M, Kanhiya K, Kabra SK, Lodha R. Pharmacokinetics of isoniazid, rifampicin, pyrazinamide and ethambutol in Indian children. *BMC Infect Dis* 2015;15:126.
17. Antwi S, Yang H, Enimil A, et al. Pharmacokinetics of the First-Line Antituberculosis Drugs in Ghanaian Children with Tuberculosis with or without HIV Coinfection. *Antimicrob Agents Chemother* 2017;61.

18. Zvada SP, Denti P, Donald PR, et al. Population pharmacokinetics of rifampicin, pyrazinamide and isoniazid in children with tuberculosis: in silico evaluation of currently recommended doses. *J Antimicrob Chemother* 2014;69:1339-49.
19. Guiastrennec B, Ramachandran G, Karlsson MO, et al. Suboptimal Antituberculosis Drug Concentrations and Outcomes in Small and HIV-Coinfected Children in India: Recommendations for Dose Modifications. *Clin Pharmacol Ther* 2017.
20. Ramachandran G, Kumar AK, Bhavani PK, et al. Pharmacokinetics of first-line antituberculosis drugs in HIV-infected children with tuberculosis treated with intermittent regimens in India. *Antimicrob Agents Chemother* 2015;59:1162-7.
21. Ramachandran G, Hemanth Kumar AK, Bhavani PK, et al. Age, nutritional status and INH acetylator status affect pharmacokinetics of anti-tuberculosis drugs in children. *Int J Tuberc Lung Dis* 2013;17:800-6.
22. Thee S, Seddon JA, Donald PR, et al. Pharmacokinetics of isoniazid, rifampin, and pyrazinamide in children younger than two years of age with tuberculosis: evidence for implementation of revised World Health Organization recommendations. *Antimicrob Agents Chemother* 2011;55:5560-7.
23. Schaaf HS, Willemsse M, Cilliers K, et al. Rifampin pharmacokinetics in children, with and without human immunodeficiency virus infection, hospitalized for the management of severe forms of tuberculosis. *BMC Med* 2009;7:19.
24. Mlotha R, Waterhouse D, Dzinjalama F, et al. Pharmacokinetics of anti-TB drugs in Malawian children: reconsidering the role of ethambutol. *J Antimicrob Chemother* 2015;70:1798-803.
25. Justine M, Yeconia A, Nicodemu I, et al. Pharmacokinetics of First-Line Drugs Among Children With Tuberculosis in Rural Tanzania. *J Pediatric Infect Dis Soc* 2020;9:14-20.

26. Arya A, Roy V, Lomash A, Kapoor S, Khanna A, Rangari G. Rifampicin pharmacokinetics in children under the Revised National Tuberculosis Control Programme, India, 2009. *Int J Tuberc Lung Dis* 2015;19:440-5.
27. Garcia-Prats A. Optimising rifampicin exposure in children towards treatment shortening and treatment of severe disease: OptiRif Kids trial. Union World Conference 2019. Hyderabad, India 2019.
28. World Health Organization. Rapid Advice: Treatment of tuberculosis in children. Geneva, Switzerland: WHO Press; 2010.
29. McIlleron H, Willemse M, Werely CJ, et al. Isoniazid plasma concentrations in a cohort of South African children with tuberculosis: implications for international pediatric dosing guidelines. *Clin Infect Dis* 2009;48:1547-53.
30. Donald PR, Maritz JS, Diacon AH. The pharmacokinetics and pharmacodynamics of rifampicin in adults and children in relation to the dosage recommended for children. *Tuberculosis (Edinb)* 2011;91:196-207.
31. Svensson EM, Yngman G, Denti P, McIlleron H, Kjellsson MC, Karlsson MO. Evidence-Based Design of Fixed-Dose Combinations: Principles and Application to Pediatric Anti-Tuberculosis Therapy. *Clin Pharmacokinet* 2018;57:591-9.
32. Hattis D, Ginsberg G, Sonawane B, et al. Differences in pharmacokinetics between children and adults--II. Children's variability in drug elimination half-lives and in some parameters needed for physiologically-based pharmacokinetic modeling. *Risk Anal* 2003;23:117-42.
33. Bekker A, Schaaf HS, Draper HR, et al. Pharmacokinetics of Rifampin, Isoniazid, Pyrazinamide, and Ethambutol in Infants Dosed According to Revised WHO-Recommended Treatment Guidelines. *Antimicrob Agents Chemother* 2016;60:2171-9.
34. Hibma JE, Radtke KK, Dorman SE, et al. Rifapentine Population Pharmacokinetics and Dosing Recommendations for Latent Tuberculosis Infection. *Am J Respir Crit Care Med* 2020.



35. Imperial MZ, Nahid P, Phillips PPJ, et al. A patient-level pooled analysis of treatment-shortening regimens for drug-susceptible pulmonary tuberculosis. *Nat Med* 2018;24:1708-15.
36. Hoglund RM, Workman L, Edstein MD, et al. Population Pharmacokinetic Properties of Piperaquine in *Falciparum* Malaria: An Individual Participant Data Meta-Analysis. *PLoS Med* 2017;14:e1002212.

## Chapter 3. Alternative dosing regimens to improve outcomes for children with tuberculosis \*

### Abstract

#### Background

Malnourished and young children are particularly vulnerable to severe forms of tuberculosis and poor treatment response. Current World Health Organization (WHO) dosing guidelines are only based on weight, which may lead to systematic underdosing and worse outcomes in these vulnerable children. We evaluate and quantify the population impact of current WHO guidelines for drug-susceptible tuberculosis in children in the 20 countries with highest disease burden.

#### Methods

Using an integrated model which links country-specific individual-level demographic data to pharmacokinetic, outcome, and epidemiological models, we assessed tuberculosis treatment outcomes in children under five years of age following the current WHO guidelines and two alternative dosing strategies: a simple algorithm that utilizes age, weight, and available formulations, and an individualized algorithm without dose limitations.

#### Findings

We estimated that 57,234/133,302 (43%) treated cases would be underdosed with WHO dosing and only 47% would reach the rifampicin exposure target. Underdosing and subtherapeutic

---

\* Modified from the publication: Radtke KK, Dooley KE, Dodd PJ, Garcia-Prats AJ, McKenna L, Hesselring AC, Savic RM (2019). Alternative dosing guidelines to improve outcomes for childhood tuberculosis: a mathematical modeling study. *Lancet Child and Adolescent Health*. 3(9):636-645. PMID: 31324596.

exposures were more common among malnourished children. The simple proposed dosing approach improved estimated rifampicin target exposure attainment to 62% and equalized outcomes by nutritional status. An estimated one-third of unfavorable treatment outcomes might be resolved with this dosing strategy, saving a minimum of 2423 children in these countries annually. With individualized dosing approaches, almost all children could achieve adequate exposure for cure.

### Interpretation

This work demonstrates that a simple change in dosing procedure to include age and nutritional status, requiring no additional measurements or new drug formulations, is one approach to improve tuberculosis treatment outcomes in children, especially malnourished children who are at high risk of mortality.

### **Background**

Childhood tuberculosis is among the top 10 killers of children under five years of age.<sup>1</sup> Although global reports on leading causes of child mortality historically had omitted tuberculosis, recent estimates suggest that 191,000 children younger than five years died of tuberculosis in 2015.<sup>1</sup> Late or missed diagnosis of tuberculosis is a primary driver of mortality among children, but evidence from clinical studies also show that even when diagnosed and treated, tuberculosis outcomes are still far from ideal in countries with high incidence.<sup>2,3</sup> Narrowing the treatment-response gap for children with tuberculosis will be a pivotal step toward curbing childhood mortality and will help move us towards the goal of Zero Deaths from childhood tuberculosis.<sup>4</sup>

Tuberculosis disease severity, compromised immune response, and suboptimal treatment all contribute to morbidity and mortality from childhood tuberculosis. Young children are vulnerable

to severe forms of tuberculosis including disseminated disease (e.g., tuberculosis meningitis and miliary tuberculosis), which is more difficult to cure.<sup>5</sup> Likewise, comorbidities that impair immune function (e.g., HIV infection, malnutrition) have been linked with lower survival.<sup>6,7</sup> Early and accurate disease detection as well as initiation of appropriate supportive therapy (e.g., anti-retroviral therapy in HIV co-infection and nutritional support in undernourished) are important for proper tuberculosis disease management. Further, adequate drug exposure of anti-tuberculosis treatment is essential for optimal disease outcomes and preventing the development of drug-resistant tuberculosis, which has substantially worse outcomes.<sup>8,9</sup> While many factors certainly contribute to tuberculosis disease outcome, the precise impact of each factor has not been quantified. Optimizing treatment dosing for children is one known and established intervention that can be easily controlled and is an attractive, simple, and efficient strategy for tuberculosis policy change that could immediately benefit children's lives.

Pediatric dosing guidelines, including the WHO guidelines for child tuberculosis,<sup>10</sup> are historically derived based on weight and may leave young and malnourished children vulnerable to underdosing. Flat weight-based dosing (e.g., mg/kg for all ages) assumes a linear relationship between dose requirement and weight, neglecting basic principles of developmental pharmacology.<sup>11</sup> In general, weight is a good indicator of a child's capacity to distribute, metabolize, and eliminate drug if the child is well-nourished and school-aged or older. However, young children undergo dynamic changes in metabolic capacity and body composition during growth that alter drug pharmacokinetics.<sup>11</sup> These changes are often correlated to weight using  $\frac{3}{4}$  power laws, which forms the basis for weight-based dosing where higher mg/kg doses are required in very young children. Further, weight and metabolic rate do not correlate well in malnourished children who have the same metabolic potential as healthy children of equal age. The current tuberculosis dosing guidelines do not consider allometry, age, or malnutrition, which is likely to result with systematic underexposure of young and malnourished children. For

example, in the case of children one year of age, a child with a normal weight of 9 kg receives twice as much drug as a malnourished child who weighs 6 kg with WHO weight band dosing,<sup>12</sup> but both children would be expected to eliminate the drug at similar rates. Correcting systematically low drug exposures in the most vulnerable children by modifying drug dosing is an unrecognized and simple area of intervention that could greatly improve outcomes in all of pediatric medicine.

We conducted a modeling study to estimate the prevalence of potential underdosing of first-line anti-tuberculosis drugs and the consequent impact on drug exposures and population outcomes (including mortality) in the 20 countries with the highest burden of childhood tuberculosis. We used a novel, integrative modeling design which used real, individual-level child demographic data along with relevant population pharmacokinetic, exposure-response, and epidemiological models to minimize assumptions and to establish an environment representative of true conditions. To our knowledge, this is the first time a model such as this has been used. With this design, we estimated the impact of a revised dosing method which incorporates age and nutritional status, simply measured, on treatment outcomes compared to the current standard.

## **Methods**

The integrated model was created by linking individual child demographic data obtained from country-specific population health surveys with pharmacokinetic, pharmacodynamic (outcome), and epidemiological models (**Figure 3.1**).

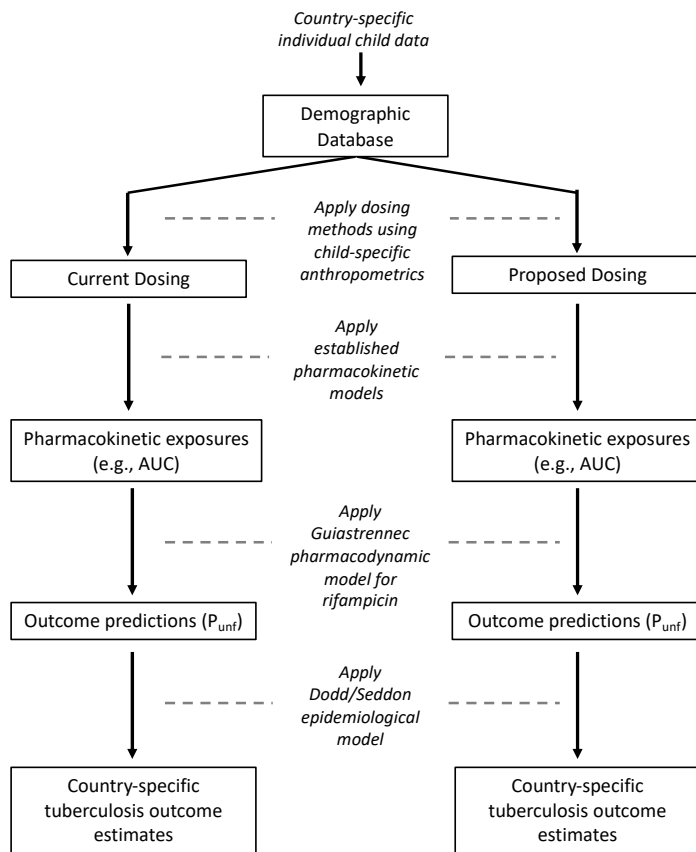


**Figure 3.1** Integrative model schematic.  
 AUC = area under-the-curve.  $P_{unf}$  = Probability of unfavorable outcome.

### Demographic Database

We created a database of nationally-representative child populations under five years of age from publicly accessible survey data for the 20 countries with the highest total tuberculosis incidence (**Table 3.1**). These countries account for 82% of total estimated under-5 tuberculosis incidence.<sup>13</sup> The Demographic and Health Surveys (DHS) Program, a standardized international survey that collects accurate and representative data on health and nutrition for more than 90 countries with large sample sizes, was used as the primary data source.<sup>14</sup> For eight out of the

20 countries analyzed in this study, child anthropometric data were either unavailable or incomplete in the DHS. Instead, the Joint Child Malnutrition Estimates were used to locate other sources for standardized, government-administered survey data for the remaining countries.<sup>15</sup> The most recent survey with the greatest number of children and publicly accessible individual anthropometric data was selected. Longitudinal data, if available, was accepted to increase population sample size (e.g., China); data prior to 2006 was excluded. Likewise, data from children over the age of five years from non-DHS data sources (if available) were excluded for consistency across data sources. No publicly accessible data source was available for the Democratic People's Republic of Korea; instead, Zambia was included to complete the list of top 20 countries with highest tuberculosis burden. Further, the database was complemented with child demographic data from the authors' observational and clinical studies.<sup>16-20</sup> Ethical approval and subject consent were obtained by the survey or clinical study providing the data.

Child-specific anthropometrics, gender, age, and nutritional status markers (height-for-age z-score [HAZ], weight-for-age z-score [WAZ], weight-for-height z-score [WHZ], and body mass index-for-age z-score [BAZ]) were extracted from each database. When unavailable from the database, nutritional markers were calculated in R 3.4.2 (R Core Team; Vienna, Austria) using the WHO's Anthro software.<sup>21</sup> Exclusion criteria were weight or expected weight below 4 kg, consistent with the lower bound of weight band dosing,<sup>12</sup> and implausible nutritional z-scores per WHO child growth standards (WAZ <-6 or >5, HAZ <-6 or >6, WHZ <-5 or >5, or BAZ <-5 or >5).<sup>21</sup> Z-scores were calculated using WHO Anthro software or obtained directly from the survey source. The general formula for Z-score calculation is: (measured value – mean value of reference population) / (standard deviation of reference population), where the reference population is specific for age and gender.

**Table 3.1** Study Population.

Country	N	Nutritional Status, n (%)			Survey, Year(s) <sup>Reference</sup>
		Underweight	Stunted	Wasted	
Angola	6135	1139 (19)	2309 (38)	305 (5)	DHS, 2015 <sup>22</sup>
< 1 year	1310	202 (15)	275 (21)	93 (7)	
1-3 years	2528	518 (20)	1149 (45)	136 (5)	
3-5 years	2297	419 (18)	885 (39)	76 (3)	
Bangladesh	6857	2225 (32)	2522 (37)	972 (14)	DHS, 2011 <sup>23</sup>
< 1 year	1236	216 (17)	203 (16)	202 (16)	
1-3 years	2862	974 (34)	1162 (41)	405 (14)	
3-5 years	2759	1035 (38)	1157 (42)	365 (13)	
Brazil	4288	81 (2)	311 (7)	62 (1)	PNDS, 2006 <sup>24</sup>
< 1 year	801	15 (2)	35 (4)	24 (3)	
1-3 years	1721	29 (2)	149 (9)	21 (1)	
3-5 years	1766	37 (2)	127 (7)	17 (1)	
China	1729	74 (4)	220 (13)	76 (4)	CHNS, 2006 <sup>25</sup>
< 1 year	233	7 (3)	35 (15)	13 (6)	
1-3 years	708	28 (4)	95 (13)	32 (5)	
3-5 years	788	39 (5)	90 (11)	31 (4)	
DRC	7913	1835 (23)	3515 (44)	613 (8)	DHS, 2013 <sup>26</sup>
< 1 year	1608	213 (13)	303 (19)	181 (11)	
1-3 years	3275	725 (22)	1513 (46)	268 (8)	
3-5 years	3030	897 (30)	1699 (56)	164 (5)	
Ethiopia	9482	2850 (30)	4043 (43)	1095 (12)	DHS, 2011 <sup>27</sup>
< 1 year	1839	289 (16)	243 (13)	307 (17)	
1-3 years	3654	1253 (34)	1816 (50)	461 (13)	
3-5 years	3989	1308 (33)	1984 (50)	327 (8)	
India	221,113	75,869 (34)	85,069 (38)	44,323 (20)	DHS, 2015 <sup>28</sup>
< 1 year	37,970	9541 (25)	8018 (21)	9968 (26)	Clinical Studies <sup>17, 16</sup>
1-3 years	90,396	31,759 (35)	38,196 (42)	18,274 (20)	
3-5 years	92,747	34,569 (37)	38,855 (42)	16,081 (17)	
Indonesia	4398	850 (19)	1582 (36)	411 (9)	IFLS, 2006, 2007 <sup>29</sup>
< 1 year	767	100 (13)	206 (27)	92 (12)	
1-3 years	1805	366 (20)	729 (40)	182 (10)	
3-5 years	1826	384 (21)	647 (35)	137 (8)	
Kenya	18,424	2427 (13)	4995 (27)	989 (5)	DHS, 2014 <sup>30</sup>
< 1 year	3478	233 (7)	437 (13)	192 (6)	
1-3 years	7639	1102 (14)	2522 (33)	407 (5)	
3-5 years	7307	1092 (15)	2036 (28)	390 (5)	
Mozambique	9142	1178 (13)	3604 (39)	450 (5)	DHS, 2011 <sup>31</sup>
< 1 year	1873	228 (12)	463 (25)	133 (7)	
1-3 years	3893	545 (14)	1770 (45)	237 (6)	
3-5 years	3376	405 (12)	1371 (41)	80 (2)	
Myanmar	4138	763 (18)	1268 (31)	263 (6)	DHS, 2015 <sup>32</sup>
< 1 year	786	67 (9)	73 (9)	60 (8)	
1-3 years	1661	319 (19)	574 (35)	114 (7)	
3-5 years	1691	377 (22)	621 (37)	89 (5)	
Nigeria	24,076	6444 (27)	8720 (36)	3936 (16)	DHS, 2013 <sup>33</sup>
< 1 year	4893	1027 (21)	921 (19)	1171 (24)	
1-3 years	9631	2880 (30)	3930 (41)	1698 (18)	
3-5 years	9552	2537 (27)	3869 (41)	1067 (11)	
Pakistan	3011	787 (26)	1350 (45)	304 (10)	DHS, 2012 <sup>34</sup>
< 1 year	520	110 (21)	115 (22)	73 (14)	
1-3 years	1203	344 (29)	603 (50)	139 (12)	
3-5 years	1288	333 (26)	632 (49)	92 (7)	



**Table 3.1 (continued)**

Country	N	Nutritional Status, n (%)			Survey, Year(s) <sup>Reference</sup>
		Underweight	Stunted	Wasted	
Philippines	15,922	3510 (22)	5506 (35)	1043 (7)	FNRI-NNS,
< 1 year	2593	322 (12)	343 (13)	246 (9)	2015 <sup>35</sup>
1-3 years	6089	1379 (23)	2322 (38)	451 (7)	
3-5 years	7240	1809 (25)	2841 (39)	346 (5)	
Russia	9665	282 (3)	919 (10)	828 (9)	RLMS-HSE,
< 1 year	1803	87 (5)	208 (12)	142 (8)	2006-
1-3 years	4020	76 (2)	395 (10)	272 (7)	2015 <sup>36</sup>
3-5 years	3842	119 (3)	316 (8)	414 (11)	
South Africa	9691	671 (7)	2573 (27)	406 (4)	NIDS,
< 1 year	859	65 (8)	171 (20)	80 (9)	2008-2014 <sup>37-40</sup>
1-3 years	4012	265 (7)	1310 (33)	158 (4)	Clinical Studies <sup>20,18</sup>
3-5 years	4820	341 (7)	1092 (23)	168 (3)	
Tanzania	8735	1177 (13)	2961 (34)	400 (5)	DHS,
< 1 year	1773	169 (10)	310 (17)	128 (7)	2015 <sup>41</sup>
1-3 years	3808	569 (15)	1525 (40)	170 (4)	
3-5 years	3154	439 (14)	1126 (36)	102 (3)	
Thailand	8688	593 (7)	1187 (14)	516 (6)	MICS,
< 1 year	987	67 (7)	140 (14)	84 (9)	2012 <sup>42</sup>
1-3 years	3722	223 (6)	559 (15)	177 (5)	
3-5 years	3979	303 (8)	488 (12)	255 (6)	
Vietnam	3515	379 (11)	758 (22)	135 (4)	MICS,
< 1 year	592	26 (4)	44 (7)	32 (5)	2010 <sup>43</sup>
1-3 years	1500	157 (10)	353 (24)	48 (3)	
3-5 years	1423	196 (14)	361 (25)	55 (4)	
Zambia	11,287	1687 (15)	4493 (40)	693 (6)	DHS,
< 1 year	2103	220 (10)	480 (23)	175 (8)	2014 <sup>44</sup>
1-3 years	4669	782 (17)	2269 (49)	284 (6)	
3-5 years	4515	685 (15)	1744 (39)	234 (5)	

Underweight = weight-for-age Z-score (WAZ) < -2; Stunted = height-for-age Z-score (HAZ) < -2; Wasted = weight-for-height Z-score (WHZ) < -2. CHNS = Chinese Health and Nutrition Surveys; DHS = Demographic and Health Surveys Program; DRC = Democratic Republic of the Congo; FNRI-NNS = Food and Nutrition Research Institute-National Nutrition Survey; IFLS = Indonesia Family Life Survey; MICS = Multiple Indicator Cluster Surveys; NIDS = National Income Dynamics Study; PNDS = Pesquisa Nacional de Demografia e Saude; RLMS = Russia Longitudinal Monitoring Survey- Higher School of Economics.

## Dosing Methods

All children were sampled from the above-mentioned database as a potential child with drug-susceptible tuberculosis disease. The WHO-recommended fixed-dose combination (FDC) formulation for intensive phase treatment (75 mg rifampicin, 50 mg isoniazid, 150 mg pyrazinamide) was used.<sup>12</sup> Tuberculosis treatment was simulated for each child with two different dosing methods: the current standard, and a proposed simple algorithm to account for the effects of malnutrition (**Figure 3.2**). A third, individualized dose for each child was also explored.

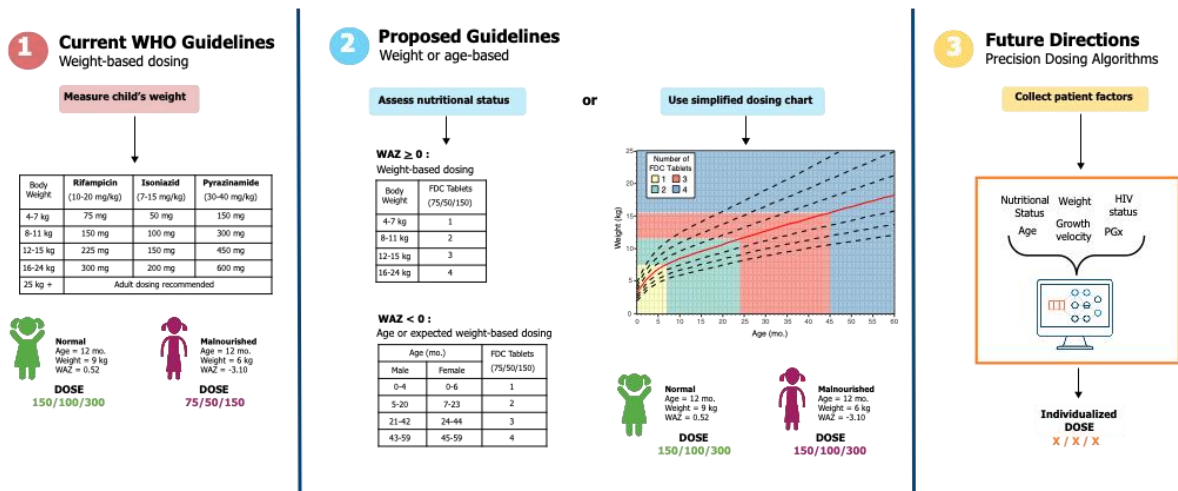


**Figure 3.2** Childhood tuberculosis dosing schematic.

For the proposed guidelines, dosing is stratified by nutritional status (WAZ > 0, use weight-based dosing; WAZ < 0, use age or expected weight dosing). Alternatively, a simplified dosing chart can be used to determine dose. WAZ = weight-for-age z-score. PGx = pharmacogenomics. FDC = fixed dose combination.

The current dosing procedure followed the most recent WHO childhood tuberculosis guidelines.<sup>10</sup> In this method, children are dosed by weight bands (4-7 kg, 8-11 kg, 12-15 kg, 16-24 kg, 25+) corresponding to incremental FDC tablet quantity and flat mg/kg dose range.<sup>12</sup>

For the new proposed dosing procedure, we chose a simple method where underweight children would receive equal drug doses as normal weight children of the same. This method was derived by evaluating what dose a child would receive if they were of normal weight (**Table 3.2**). In this proposed method, children with good nutritional status ( $WAZ \geq 0$ ) received weight-based dosing according to the WHO recommendations while children with poor nutritional status ( $WAZ < 0$ ) received age-based (i.e., expected weight-based) dosing resulting in higher doses than would be received with the current method. A schematic is shown in **Figure 3.2**. This method utilizes the WHO-recommended FDC formulation for children, is simple to implement in resource-limited clinical settings and minimizes the need for additional measurements. Furthermore, to facilitate using WAZ for dose determination, a simplified dosing chart resembling a child growth chart was constructed to eliminate any calculation requirements (**Figure 3.3**, boys; **Figure 3.4**, girls).

**Table 3.2** Age or expected weight-based dosing for underweight children.

Age (month)	Expected Weight (kg)		FDC quantity		Age (month)	Expected Weight (kg)		FDC quantity	
	Male	Female	Male	Female		Male	Female	Male	Female
0	3.3	3.2	1	1	30	13.3	12.7	3	3
1	4.5	4.2	1	1	31	13.5	12.9	3	3
2	5.6	5.1	1	1	32	13.7	13.1	3	3
3	6.4	5.8	1	1	33	13.8	13.3	3	3
4	7.0	6.4	1	1	34	14.0	13.5	3	3
5	7.5	6.9	2	1	35	14.2	13.7	3	3
6	7.9	7.3	2	1	36	14.3	13.9	3	3
7	8.3	7.6	2	2	37	14.5	14.0	3	3
8	8.6	7.9	2	2	38	14.7	14.2	3	3
9	8.9	8.2	2	2	39	14.8	14.4	3	3
10	9.2	8.5	2	2	40	15.0	14.6	3	3
11	9.4	8.7	2	2	41	15.2	14.8	3	3
12	9.6	8.9	2	2	42	15.3	15.0	3	3
13	9.9	9.2	2	2	43	15.5	15.2	4	3
14	10.1	9.4	2	2	44	15.7	15.3	4	3
15	10.3	9.6	2	2	45	15.8	15.5	4	4
16	10.5	9.8	2	2	46	16.0	15.7	4	4
17	10.7	10.0	2	2	47	16.2	15.9	4	4
18	10.9	10.2	2	2	48	16.3	16.1	4	4
19	11.1	10.4	2	2	49	16.5	16.3	4	4
20	11.3	10.6	2	2	50	16.7	16.4	4	4
21	11.5	10.9	3	2	51	16.8	16.6	4	4
22	11.8	11.1	3	2	52	17.0	16.8	4	4
23	12.0	11.3	3	2	53	17.2	17.0	4	4
24	12.2	11.5	3	3	54	17.3	17.2	4	4
25	12.4	11.7	3	3	55	17.5	17.3	4	4
26	12.5	11.9	3	3	56	17.7	17.5	4	4
27	12.7	12.1	3	3	57	17.8	17.7	4	4
28	12.9	12.3	3	3	58	18.0	17.9	4	4
29	13.1	12.5	3	3	59	18.2	18.0	4	4

Expected weight is defined as the global median weight for age and gender as reported in the WHO 2006 child growth standards. Colors correspond to those in Figures 3.3 and 3.4.

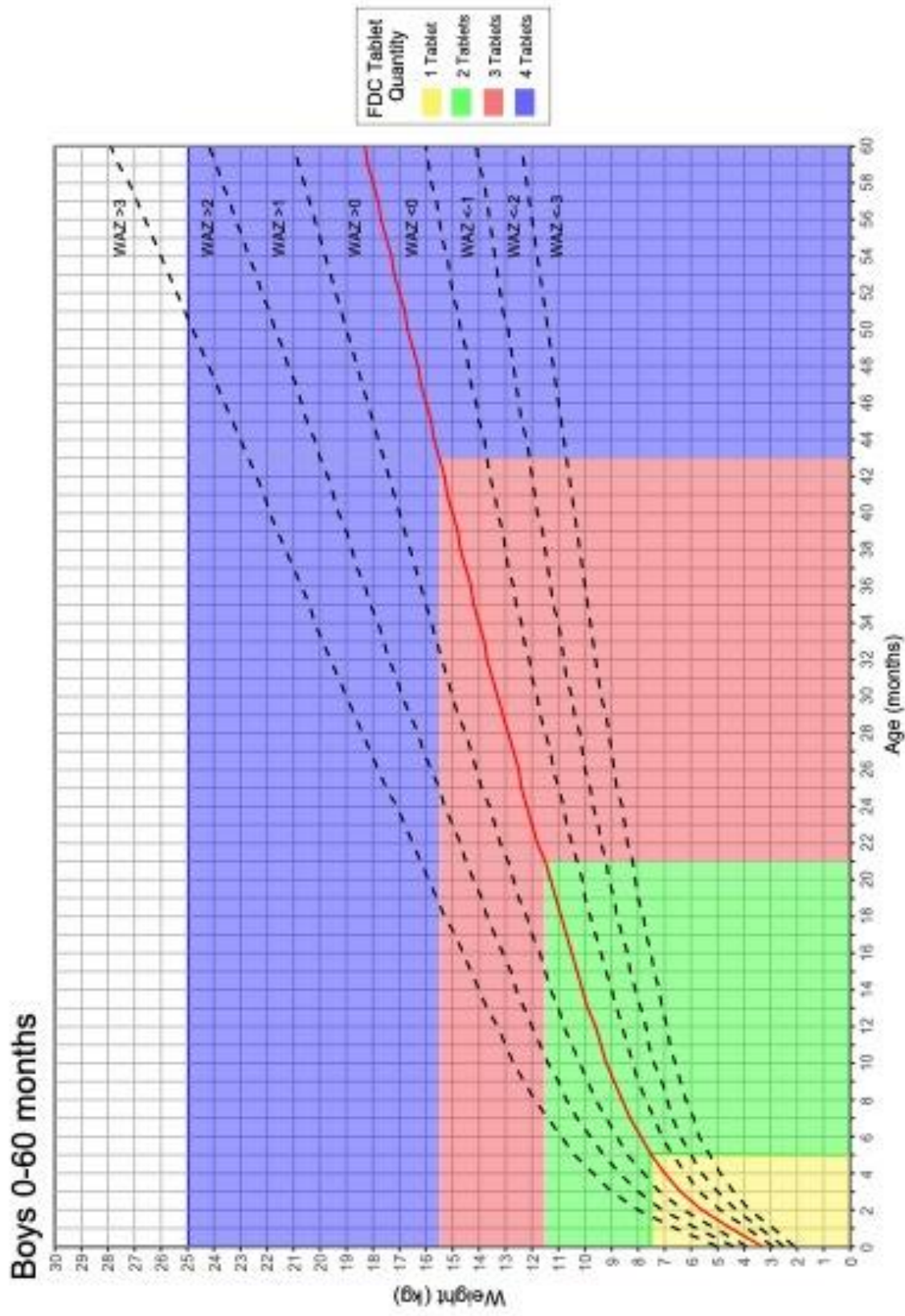


**Figure 3.3** Proposed dosing chart for boys.  
WAZ = weight for age z-score. FDC = fixed-dose combination

### Girls 0-60 months

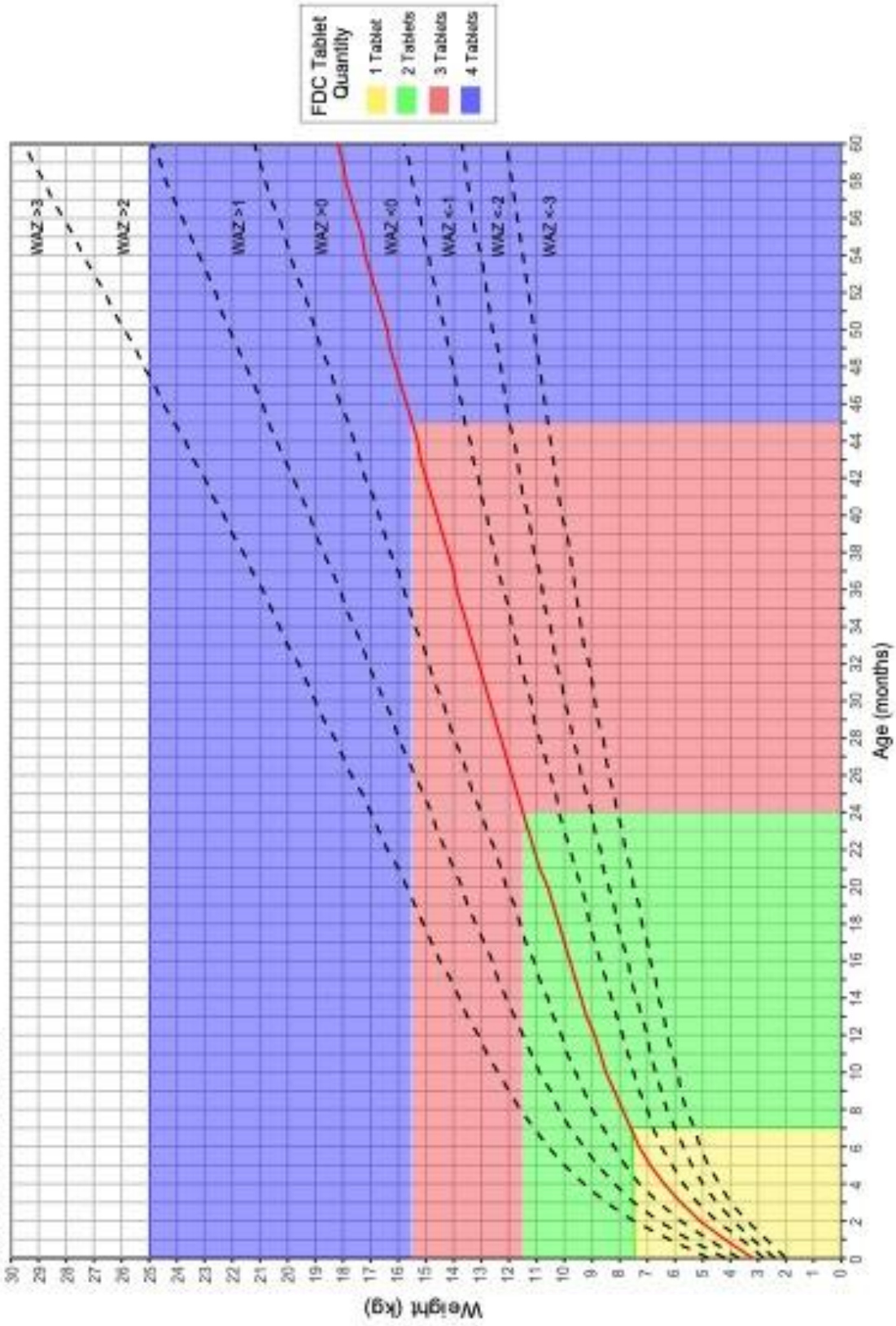


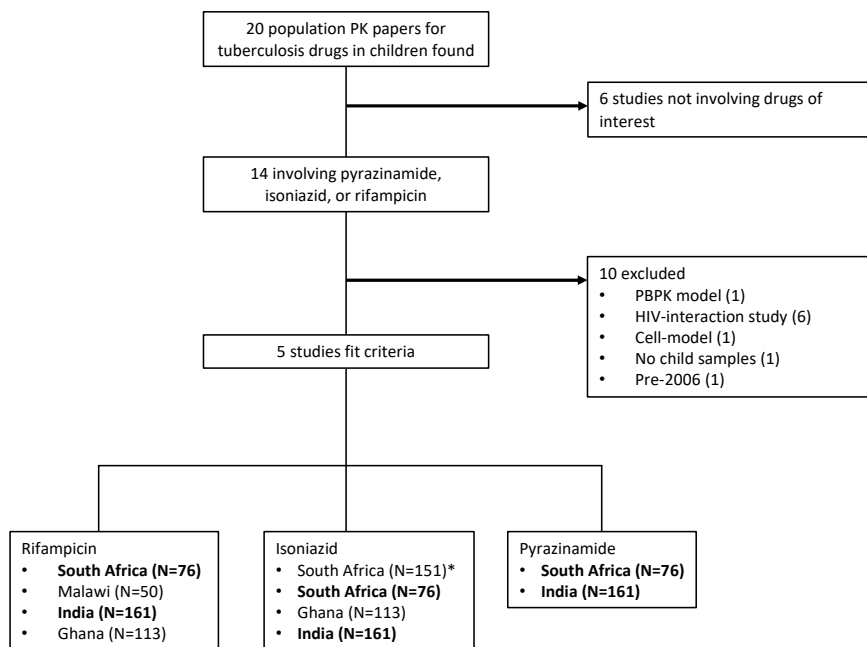
**Figure 3.4** Proposed dosing chart for girls.  
WAZ = weight for age z-score. FDC = fixed-dose combination

An individualized dosing scheme was also tested which utilized a developmental pharmacology-driven approach to define the optimal dose. Here individual drug doses ( $Dose_{ind}$ ) were determined using drug-specific target steady state AUC over 24 hours ( $AUC_{ss}$ ) of 30.7 mg\*h/L for rifampicin, 23.4 mg\*h/L for isoniazid, and 427 mg\*h/L for pyrazinamide and predicted individual clearance ( $CL/F$ ) and relative bioavailability ( $F_{rel}$ ), without constraint to available formulations or rounding (Equation 3.1). This method focused on ensuring that each child reached the target exposure for each drug. With these individualized doses, we explored optimized fixed-dose formulations and dose ratios that may be required for implementing this method.

**Eq. 3.1**       $Dose_{ind} = AUC_{ss,target} * \frac{CL/F}{F_{rel}}$

### Identification of Pharmacokinetic Models

A literature search was conducted using PubMed to identify published population pharmacokinetic models for simulating rifampicin, isoniazid, and pyrazinamide exposure in our database population. The model selection flow is outlined in **Figure 3.5**. Only models based on pediatric data collected since the publication of the first WHO childhood tuberculosis treatment guidelines (i.e., 2006 or later) were considered. Two population pharmacokinetic models (one from South Africa<sup>45</sup> and one from India<sup>46</sup>) were chosen for each drug based on sample size, population ethnicity, and inclusion of children under five years of age. The model structures and parameter estimates are extracted from the original publications and provided in Supplemental Tables 3.1 and 3.2.



**Bolded** studies represent the models chosen for the analysis based on mutually represented study population  
 \* Not chosen as preferred model because 1) only children under 2 years, and 2) did not use FDC formulation

**Figure 3.5** Pharmacokinetic model selection flowchart.

## Exposure Simulations

Drug exposures were predicted for rifampicin, isoniazid, and pyrazinamide based on the selected models.<sup>45,46</sup> Individual child pharmacokinetic parameters were sampled from the established population distribution, defined with median values and between-child variability. Pharmacokinetic profiles were simulated in R using Monte Carlo for each drug and dosing method assuming once-daily oral administration with full adherence to represent the most promising scenario (i.e., treatment completion). For isoniazid, pharmacokinetic profiles for both slow and fast acetylators were simulated. To account for potentially different pharmacokinetic properties exhibited by different populations, the Indian-based model was used for children from Asian countries, and the South African-based model was used for African countries. The weight



distribution of children from Brazil and Russia paralleled that of the South African children, and thus, the South African model was used for these children. Pharmacokinetic profiles were summarized as area under the curve at steady state over a 24-hour period ( $AUC_{ss}$ ) and average daily concentration at steady state ( $C_{ave}$ ).

### **Definition of Target Exposure and Outcome Predictions**

The simulated pharmacokinetic profiles were linked to drug exposure targets to predict tuberculosis treatment outcome. Target exposures for children are typically based on adult reference concentrations, so the  $AUC_{ss}$  targets of 23.4 mg\*h/L for isoniazid and 427 mg\*h/L for pyrazinamide over 24 hours were used.<sup>45</sup> For rifampicin, a child-specific target defined from an exposure-response model was used, where the relationship between rifampicin  $AUC_{ss}$  over one week ( $AUC_{ss,wk}$ ) is related to the probability of unfavorable event ( $P_{unf}$ ), defined as death or treatment failure, aligning with the fact that rifampicin is the most important drug in the regimen.<sup>46</sup> Using this model, we defined the rifampicin exposure target as  $AUC_{ss,wk} \geq 222$  mg\*h/L (i.e.,  $AUC_{ss} \geq 31.7$  mg\*h/L for a 24-hour period), which results in a  $P_{unf} \leq 5\%$ . Using this pharmacokinetic-pharmacodynamic model, we predicted the  $P_{unf}$  for each child.

### **Linkage to Epidemiological Models**

The epidemiologic model described by Dodd and colleagues was used to predict age-disaggregated tuberculosis incidence in children under five years.<sup>47</sup> The model describes the probability of disease progression by age category (0-1, 1-2, 2-5 years) based on disease progression risks from a review of pre-chemotherapy era literature by Marais and colleagues.<sup>5</sup> In the present paper, the disease progression risks were adjusted for age group width so the sum of the probabilities was equal to 1 (**Table 3.3**). The probability of disease progression by age category was used to weight an assumed uniformly distributed underlying age distribution to age-disaggregate the WHO tuberculosis notification and estimated incidence data<sup>13</sup> for

children 0-5 years. Notified cases were assumed to represent treated cases. Total estimated incidence was used as a sensitivity analysis as an unknown proportion of unnotified (unregistered) tuberculosis cases are treated (e.g., in the private sector or at other health facilities). Age-disaggregated epidemiologic estimates were linked to the pharmacodynamic model to predict the number of unfavorable events over one year with each dosing algorithm. The median probability of unfavorable outcome for each age category (0-1, 1-2, 2-5) were calculated and applied to the corresponding predicted tuberculosis incidence of that age group.

**Table 3.3** Probability of disease progression.

Age group (year)	Probability of disease progression <sup>1</sup>	Probability of disease being in a given age group, adjusted for width of age-group <sup>2</sup>
0 to <1	0.5	0.556
1 to <2	0.25	0.278
2 to <5	0.05	0.167

<sup>1</sup> The median probability of disease progression as described by Dodd et al. 2014.  
<sup>2</sup> Estimates were scaled by the width of the age group, and then normalized so the sum of the probabilities was equal to 1.

## Analysis

All data manipulation, nutritional marker calculations, summary statistics, model simulations, and visualizations were performed in R. Children were considered underweight if WAZ < -2, stunted if HAZ < -2, and wasted if WHZ < -2. Malnutrition severity was defined based on z-score: normal ( $z \geq 0$ ), mildly malnourished ( $-2 \leq z < 0$ ), moderately malnourished ( $-3 \leq z < -2$ ), or severely malnourished ( $z < -3$ ). Children were considered underdosed by current guidelines if the WHO-recommended dose was lower than the dose that child would have received with the proposed guidelines (i.e., if the weight-based dosing resulted in lower dose than the expected

weight-based dosing for an underweight child). Underexposure was defined as  $AUC_{ss}$  below the defined exposure target.

## Results

### Population Characteristics

Our database included individual-level anthropometric data from 388,209 children under five years of age from 20 high-burden tuberculosis countries. Overall, 27% of children were underweight, 36% were stunted, and 15% were wasted. Stunting was prevalent in most countries (>30% in 13 countries; **Table 3.1**). Bangladesh, India, and Ethiopia had high proportions of underweight children (>30%) and wasting was critically (>15%) or seriously (10-15%) high in five countries.

Of note, some of the survey data used to construct this database were old (>10 years). It is possible that the demographics of our child database do not represent the most current populations demographics for each country. Despite this limitation, we utilized the most recent publicly accessible data according to the Joint Malnutrition Estimates.<sup>15</sup> Further, data was limited for some countries and may not provide an accurate demographic representation of child tuberculosis incidence. For example, only 1729 child observations were available for China where total estimated under-5 incidence is 54,000. Other countries, like India, had adequate representation, with 221,113 children in our database compared with an estimated 118,000 under-5 cases.

### Underdosing Prevalence

We estimated that 43% of children or 57,234 of 133,302 treated under-5 tuberculosis cases would be underdosed following current guidelines, based on predicted underdosing by country

(Figure 3.6). Among underweight children only, the prevalence of underdosing was consistently high (>70%) across all countries. Following the current dosing method, the average dose was 16.0 mg/kg for rifampicin, 10.7 mg/kg for isoniazid, and 32.0 mg/kg for pyrazinamide. With the proposed dosing, average doses were 19.6 mg/kg for rifampicin, 13.1 mg/kg for isoniazid, and 39.2 mg/kg for pyrazinamide. This dosing gap was consistent across age groups.

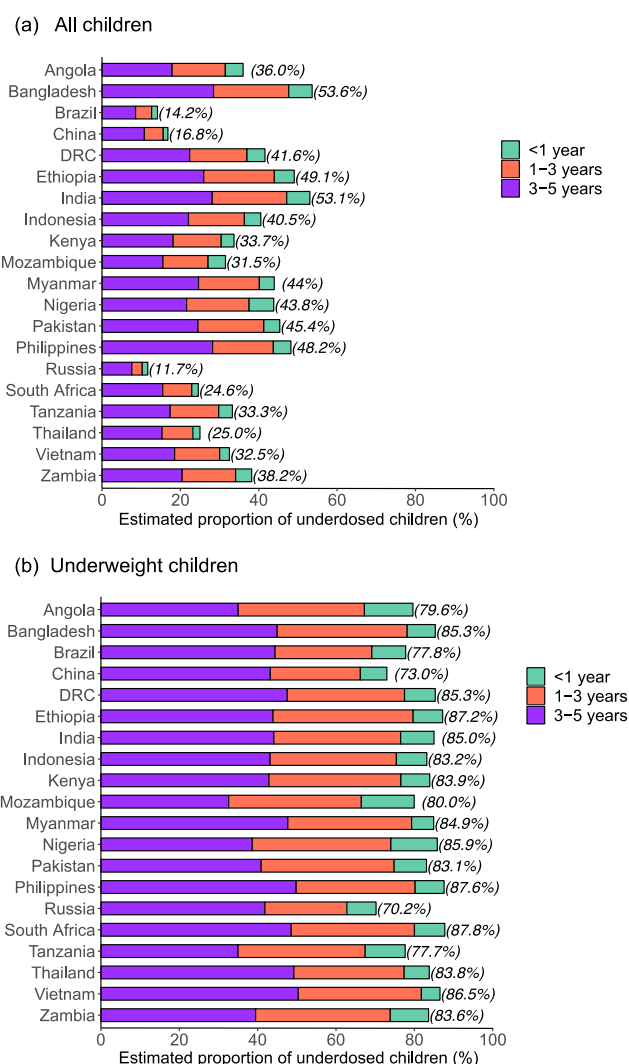


**Figure 3.6** Underdosing prevalence with current WHO treatment guidelines. Bar segments represent the contribution of each age group to the overall underdosing prevalence in all (a) or underweight (b) children. DRC = Democratic Republic of the Congo.

## Drug exposure profiles of first-line tuberculosis therapy

Underweight children (WAZ <-2) had consistently low  $AUC_{ss}$  with the current dosing method for all drugs (**Figure 3.7**). These modeled drug concentrations were more uniform across age and nutritional status with the proposed dosing method.  $AUC_{ss}$  for individualized dosing mimicked the adult exposures. Average daily concentration ( $C_{ave}$ ) was above the minimum inhibitory concentration (MIC) for rifampicin and isoniazid, but not pyrazinamide (**Figure 3.8**).

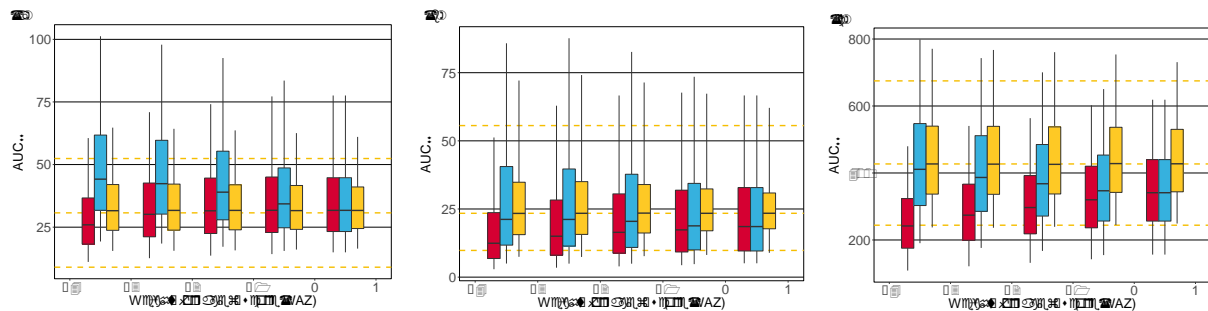


**Figure 3.7** Simulated  $AUC_{ss}$  of rifampicin (a), isoniazid (b), and pyrazinamide (c) for current (red), proposed (blue), and individualized (yellow) dosing algorithms. Dashed lines (yellow) represent 5<sup>th</sup> (lower), median (middle), and 95<sup>th</sup> (upper) percentile of adult exposure.<sup>45</sup>  $AUC_{ss}$  expressed as mg·h/L over 24 hours.

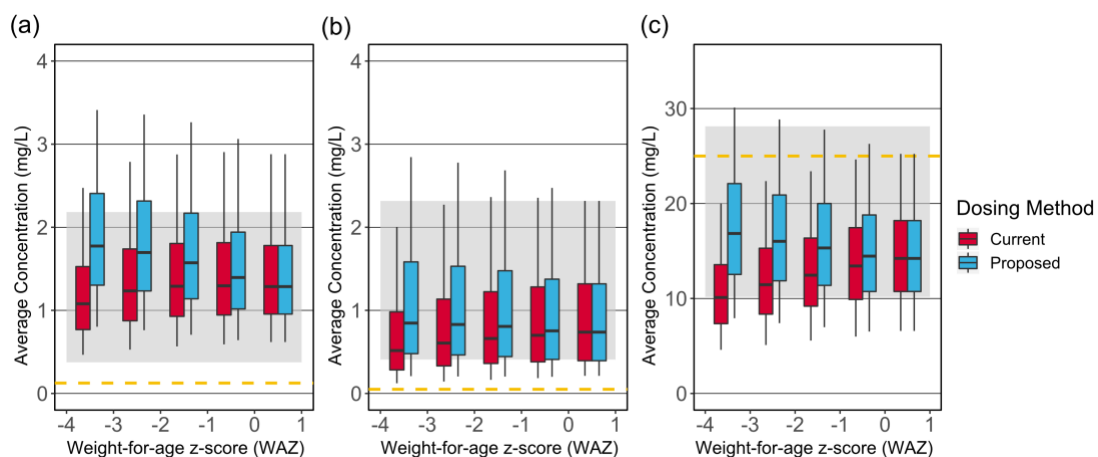


**Figure 3.8** Simulated average daily concentration of rifampicin (a), isoniazid (b), and pyrazinamide (c) versus minimum inhibitory concentration (MIC; yellow dashed line). Median MIC was 0.125 mg/L for rifampicin, 0.05 mg/L for isoniazid, 25 mg/L for pyrazinamide.<sup>48</sup> Shaded grey area indicates the 95% prediction interval of adult  $C_{ave}$ .<sup>45</sup>

### Malnutrition Effects on Target Exposure Outcomes

With current dosing guidelines, only 47% of all children were predicted to reach the defined rifampicin target exposure (**Figure 3.9**). Most cases of target attainment (>75%) occurred in children of adequate weight ( $WAZ \geq -2$ ). Rifampicin target exposure attainment following current dosing guidelines was lower among malnourished children and lessened with increasing malnutrition severity. The proposed dosing method improved outcomes not only for all children but also for those with poor nutritional status and equalized target outcomes across different measures of malnutrition and severity. This trend of improved exposure target outcomes with the proposed method was consistent in all 20 high burden countries (**Figure 3.10**). Target exposure trends for isoniazid and pyrazinamide are shown in **Figure 3.11** and **Figure 3.12**, respectively. Like rifampicin, malnourished children had lower target attainment compared to well-nourished children.

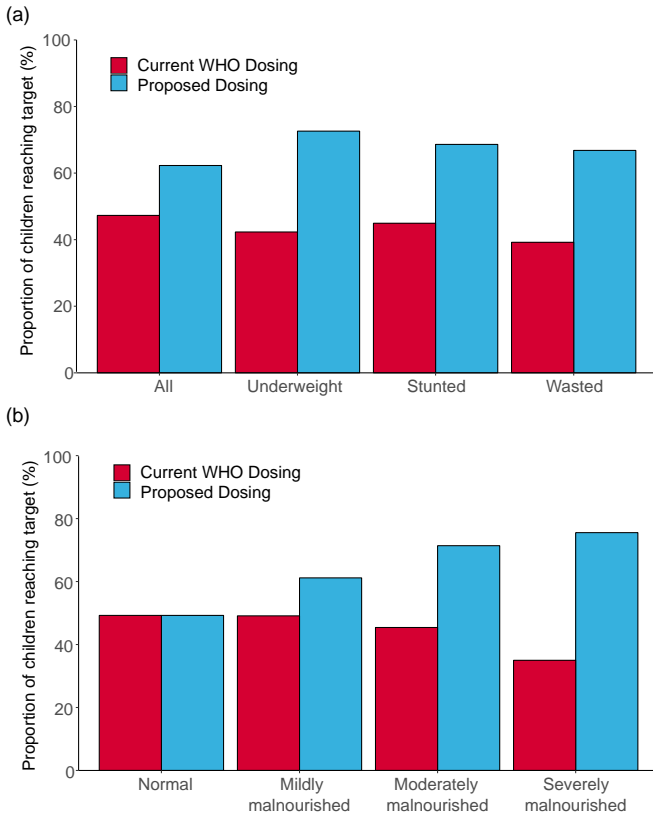


**Figure 3.9** Impact of malnutrition on rifampicin exposure target outcomes. Target outcomes are shown with respect to different measures of nutritional status (a) and severity of malnourishment, determined by weight-for-age z-score (b).

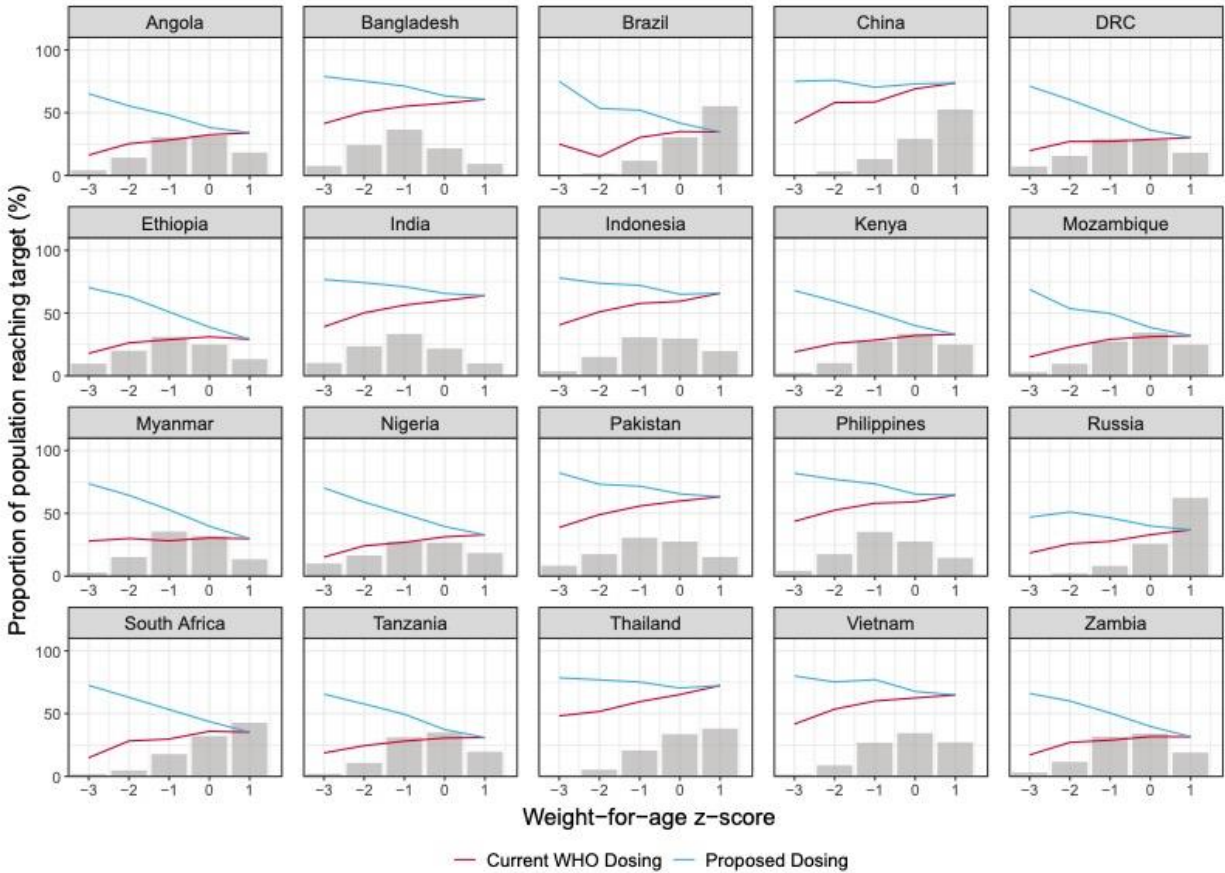
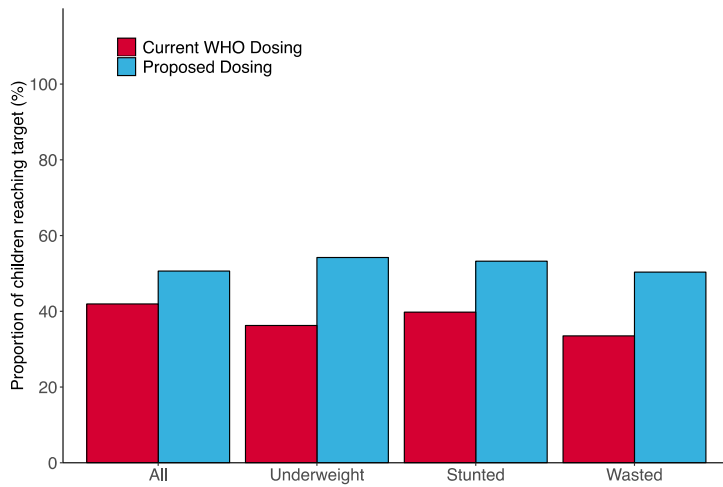


**Figure 3.10** Rifampicin target exposure outcomes in high-burden tuberculosis countries. The proportion of children reaching the rifampicin exposure target across weight-for-age z-score (WAZ) is shown for each dosing scheme. Histogram shows the population distribution. DRC = Democratic Republic of the Congo.



(a) Nutritional status type



(b) Malnutrition severity

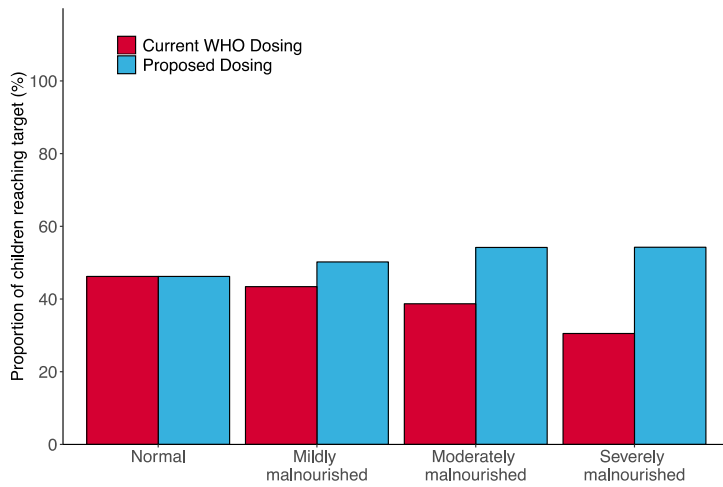
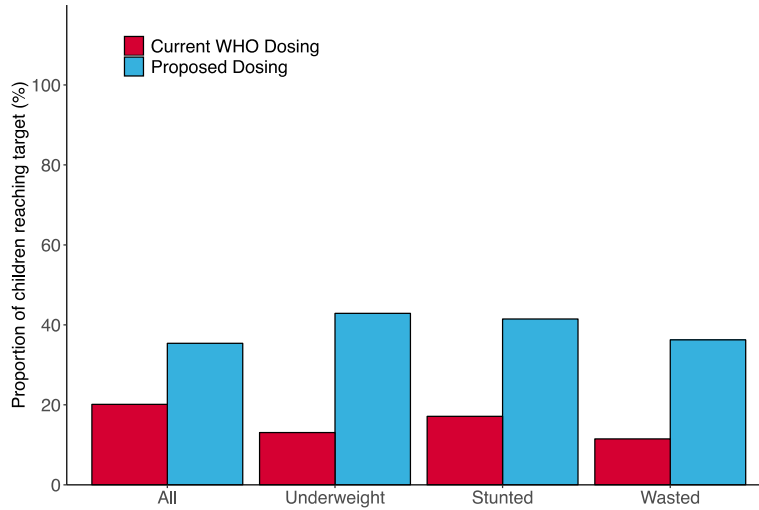


**Figure 3.11** Impact of malnutrition on isoniazid exposure target outcomes. Target outcomes are shown with respect to different measures of nutritional status (A) and malnutrition severity (B) based on weight-for-age z-score (WAZ). Isoniazid target exposure was defined as AUC > 23.4 mg\*h/L.

(a) Nutritional status type



(b) Malnutrition severity

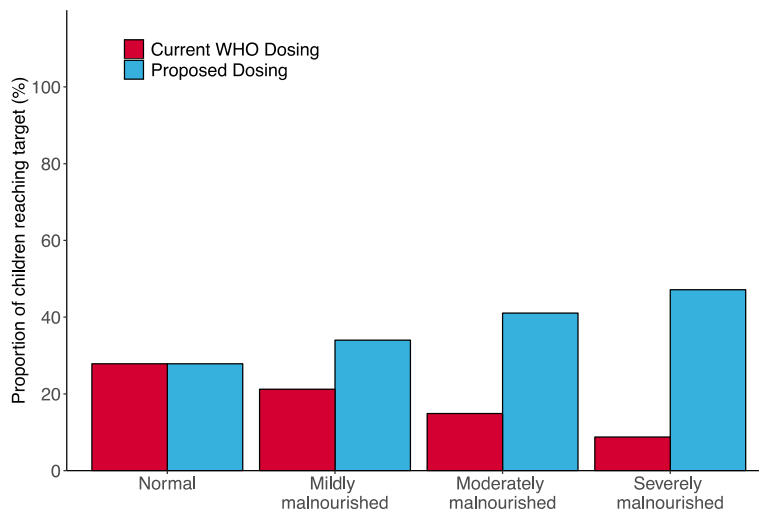


**Figure 3.12** Impact of malnutrition on pyrazinamide exposure target outcomes. Target outcomes are shown with respect to different measures of nutritional status (A) and malnutrition severity (B) based on weight-for-age z-score (WAZ). Pyrazinamide target exposure was defined as AUC > 427 mg\*h/L.

### Population Estimate of Unfavorable Outcome

The median  $P_{\text{unf}}$  for the study population following the current dosing regimen was 3.3%. Notably, very young (median  $P_{\text{unf}} = 7.7\%$ ) or underweight (median  $P_{\text{unf}} = 4.0\%$ ) children were predicted to be particularly vulnerable to poor treatment outcomes with current guidelines. The proposed dosing method improved treatment outcomes for all children (median  $P_{\text{unf}} = 1.8\%$ ), with the best improvement seen in the very young (median  $P_{\text{unf}} = 4.7\%$ ) and underweight (median  $P_{\text{unf}} = 1\%$ ). Estimated  $P_{\text{unf}}$  was more equal with the proposed and individualized dosing across varying WAZ (**Figure 3.13**).

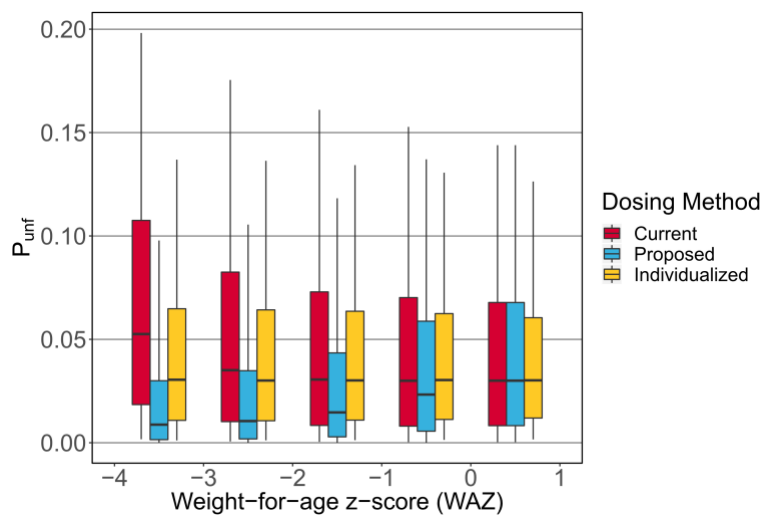


**Figure 3.13** Predicted probability of unfavorable outcome ( $P_{\text{unf}}$ ) for each dosing method.

Linking the exposure-response model to tuberculosis case notification data, we found that the number of treatment failures or deaths in children under five years decreased for all 20 high-burden countries with the proposed dosing method (**Table 3.5**). Considering only treatment of notified cases, which represents 30% of the total estimated under-5 incidence in these

countries,<sup>13</sup> the proposed method would prevent treatment failure or death from tuberculosis in at least one-third of children predicted to have unfavorable outcome with current dosing practices (equivalent to 2423 actual cases saved per year, at minimum). This impact could be as high as 7844 children saved if all estimated cases are considered.

**Table 3.4** Estimated number of treatment failures or deaths from tuberculosis per year in children under five years of age.

Country	Notified 'treated' cases *				All estimated cases **			
	Tuberculosis cases	Treatment failures/death with current dosing	Treatment failures/death with proposed dosing	Estimated number saved from treatment failure or death	Tuberculosis cases	Treatment failures/death with current dosing	Treatment failures/death with proposed dosing	Estimated number saved from treatment failure or death
Angola <sup>†</sup>	102	7	5	2	6300	430	317	113
Bangladesh	957	51	27	24	17,800	948	507	441
Brazil	888	54	48	6	4300	260	231	28
China	261	9	8	1	54,000	1763	1577	186
DRC	5607	398	283	114	18,500	1312	935	377
Ethiopia	3452	244	161	83	10,900	771	510	261
India	26,063	1442	799	643	118,000	6527	3616	2911
Indonesia	22,203	970	676	294	20,600	900	627	273
Kenya	3903	253	195	57	11,800	764	590	174
Mozambique	3841	257	186	71	12,700	849	614	235
Myanmar	13,176	880	626	254	12,200	815	579	236
Nigeria	2517	184	116	68	33,000	2407	1519	888
Pakistan	16,880	846	558	288	31,000	1553	1025	528
Philippines	16,573	836	529	307	38,000	1916	1212	704
Russia	1025	62	56	6	1060	64	58	6
South Africa	9254	563	456	107	20,100	1222	990	232
Tanzania	4899	327	252	75	4900	327	252	75
Thailand	318	14	10	3	4200	179	134	45
Vietnam	589	22	18	5	5200	199	155	44
Zambia	794	55	39	15	4400	304	218	86
<b>Total</b>	<b>133,302</b>	<b>7470</b>	<b>5047</b>	<b>2423</b>	<b>428,960</b>	<b>23,510</b>	<b>15,666</b>	<b>7844</b>

Predictions were calculated using median probability of unfavorable outcome ( $P_{unf}$ ) and number of notified under-five tuberculosis cases to WHO in 2019 (\*) or total estimated tuberculosis incidence in 2019 (\*\*), disaggregated by age. <sup>†</sup> 2016 notification data was used.

## Discussion

In this study, we introduce a novel, integrative modeling approach which links pharmacologic with epidemiologic models to predict population-level outcomes for childhood tuberculosis. This is the first time that individual child demographic data, representative of true global populations, are used in this context. We included individual-level data from more than 300,000 children under five years of age from 20 high-burden tuberculosis countries, enabling true representation of malnourished children and populations at the highest risk of tuberculosis and severe disease. We compare the current WHO-recommended dosing guidelines with alternative dosing methods to show that simple modifications to dosing practices can improve anti-tuberculosis drug exposure and consequently, population outcomes for children with tuberculosis.

Effective anti-tuberculosis therapy has drastically decreased child mortality from tuberculosis disease in recent decades.<sup>49</sup> However, treatment failures and mortality rates are still high in many endemic areas, especially among children who are very young, malnourished, HIV infected, or have severe disease.<sup>2,3,50</sup> Adequate treatment exposure is essential in these children for successful disease outcomes. Our model predicted that less than half of children under five years of age would reach the rifampicin exposure target, a key drug for tuberculosis cure, with the current guidelines. Malnourished children had lower drug exposures and higher probabilities of unfavorable outcome. These findings support trends shown in clinical studies and reflect the inadequacy of current weight-based dosing recommendations that do not consider age or nutritional status.

With high malnutrition prevalence in tuberculosis-endemic countries, it is important to consider the treatment needs of malnourished children separately. Currently, the way malnourished children are distinguished from their well-nourished peers of the same age is by receiving less

drug for the same disease, as evidenced by the percentage of potentially underdosed children in our model. In addition to receiving less drug, pathophysiological changes in the poor nutritional state such as malabsorption, decreased glomerular filtration rate, and altered protein-binding capacity can further lead to variable and sub/supra-therapeutic drug exposures in malnourished children.<sup>16,51</sup> These factors demonstrate that malnourished children cannot be expected to absorb, distribute, metabolize, and eliminate drugs in the same manner as well-nourished children.

The simple dosing method proposed here shows that accounting for malnutrition could improve tuberculosis treatment outcomes in underweight children by delivering adequate drug exposure. With the proposed dosing method, more children reached target exposures compared to the current guidelines in all 20 countries evaluated, even those with low malnutrition prevalence. This method is a simple change from current guidelines that can be readily implemented in clinical practice. It would be easy-to-use by tuberculosis clinicians, even in remote settings, as it requires only the measurement of weight, age, gender, and estimation of nutritional status (i.e., WAZ for which a simple dosing chart could be used).

When considering dose increases, the risk of toxicity must also be assessed. These drugs have high therapeutic margins and are well-tolerated in children even at higher doses, as routinely prescribed in tuberculosis meningitis.<sup>3,52,53</sup> Furthermore, no studies have reported decreased clearance of rifampicin, isoniazid, or pyrazinamide in malnourished children. Therefore, any concerns regarding administering higher doses to underweight children are likely unjustified. Without established upper limits of exposure associated with toxicity, the benefit of higher dosages will likely outweigh any potential risk. Regardless, the risk/benefit ratio should be considered for malnourished children who are extremely vulnerable to death.

Even with the proposed dosing method, treatment success was still far below desired targets (~90%). Further, drug exposure outcomes in normal weight children were suboptimal with both dosing methods. The proposed method is based on the minimum change required to make a sizeable impact. We constrained dosing to WHO-recommended dose ranges and FDC formulations, which may not be appropriate for all individuals. Precision dosing algorithms, which account for additional patient and/or disease factors that impact exposure (e.g., HIV infection, *SLCO1B1* genotype, and NAT2 acetylator status), will likely be needed to achieve WHO targets with current therapeutics.<sup>16,17,50,54,55</sup> Optimized FDC formulations were explored based on the individualized doses, but drug doses and dose ratios varied by pharmacokinetic model and isoniazid metabolizing capacity. Our work along with others<sup>46,56</sup> suggests that higher anti-tuberculosis doses and new FDC formulations are needed to ensure optimal outcomes. However, it remains unclear from current pediatric pharmacologic data whether a single global FDC formulation can meet the needs of all children. One simple intermediate solution would be to develop a stand-alone, child-friendly rifampicin formulation to supplement current FDC tablets when higher dosages are necessary.

Drug exposures were simulated using two pharmacokinetic models from distinct populations (India and South Africa) and applied in regionally and demographically similar populations. Outcomes were predicted for all children with a pharmacodynamic model representative of an Indian population alone. These assumptions were made due to the lack of country-specific pharmacologic models and are a limitation of the study. Still, these models represent the only pediatric pharmacokinetic and pharmacodynamic models in the countries of interest and are of the highest quality. The two pharmacokinetic models differed slightly. Genetic diversity or other differences in patient demographics may explain the slight inequality we observed. However, whether the pharmacology truly does differ by region remains unclear as these questions were either not considered in the original trial design or lacked sufficient power to detect differences.



It is imperative that future multi-regional studies are conducted and data sharing between countries is improved in order to fully understand dose-concentration-response relationships in children across the globe.

Our study focused on evaluating tuberculosis treatment and obtaining adequate exposure for cure. The effects of non-pharmacological interventions for malnutrition, HIV co-infection, and extrapulmonary disease, independent of drug exposure, were not included in our model. These children at high risk of poor outcomes may require even higher doses and/or additional interventions to overcome a poor immune response or severe disease to have an equal chance of cure. Future pediatric studies should be designed to include these high-risk cohorts to establish drug efficacy targets for vulnerable populations and efficacy of additional pharmacological and non-pharmacological interventions if we hope to cure tuberculosis in all.

Our epidemiological model accounted for age-related differences in disease risk, but malnutrition and HIV infection, both known to impact disease progression, were not included. Malnutrition impacts the immune system, increasing a child's risk of progression to active tuberculosis, and the disease further exacerbates the child's nutritional state.<sup>57</sup> While the relationship between tuberculosis and malnutrition is well-known, the relative risk of disease progression in malnourished children has not been quantified. We assumed that the malnutrition prevalence among tuberculosis cases in our model matched the prevalence in our demographic database. In tuberculosis disease, we would expect more malnourished children than the general population, implying that our population-level estimates with the proposed dosing algorithm are conservative. Further, HIV status information was sparse in the demographic datasets, limiting our analysis to an HIV uninfected population. While we cannot make unique dose recommendations or predict outcomes for HIV co-infected children from this study, we

would expect that the proposed dosing would improve exposure outcomes in HIV co-infected children, as these children are often malnourished.

Less than half of the estimated one million child tuberculosis cases per year are represented in WHO notification data.<sup>13</sup> Case detection is extremely low in children under five years of age due to diagnostic challenges and under-reporting.<sup>47</sup> Clearly, finding and diagnosing children with tuberculosis is the highest priority for decreasing disease burden. However, this work shows that even with access to the correct treatment, an impact can be made by optimizing dosing. The minimum impact of implementing the proposed dosing strategy is 2423 fewer treatment failures or deaths annually in children under five years in these 20 high-burden countries, based on notified cases. Unfavorable outcomes could be reduced from 23,510 to 15,666 per year if we assume all estimated under-5 tuberculosis cases in these countries are diagnosed and treated. While the proposed dosing method improves outcomes, treatment failures and deaths still occur. Future studies that evaluate the impact of all key factors such as treatment, malnutrition, HIV status, etc. are imperative. Only by carefully studying and understanding the quantitative impact of all factors and unbiased efficacy predictions of targeted interventions can we move closer to achieving zero childhood deaths from tuberculosis. Acting on discoveries that could lead to simple adjustments in how we treat the most vulnerable of children is an important first step.

**Supplemental Table 3.1 Pharmacokinetic models from literature.**

	Guiastrennec et al. model <sup>46</sup>	Zvada et al. model <sup>45</sup>
Population	Indian Children	South African Children
<u>Rifampicin model</u>		
Clearance	$CL/F = \theta_{CL} * MF * \left(\frac{WT}{WT_{med}}\right)^{0.75} * e^{\eta}$	$CL/F = \theta_{CL} * MF * \left(\frac{WT}{WT_{med}}\right)^{0.75} * e^{\eta}$
Volume	$V/F = \theta_V * \left(\frac{WT}{WT_{med}}\right) * e^{\eta}$	$V/F = \theta_V * \left(\frac{WT}{WT_{med}}\right) * e^{\eta}$
Relative bioavailability	$F_{rel} = \left(\frac{WT}{WT_{med}}\right)^{pwr}$	$F_{rel} = 1$
<u>Isoniazid model</u>		
Clearance	$CL/F = \theta_{CL} * MF * ACE_{CL} * \left(\frac{WT}{WT_{med}}\right)^{0.75} * e^{\eta}$	$CL/F = \theta_{CL} * MF * \left(\frac{WT}{WT_{med}}\right)^{0.75} * e^{\eta}$
Volume	$V/F = \theta_V * \left(\frac{WT}{WT_{med}}\right) * e^{\eta}$	$V/F = \theta_V * \left(\frac{WT}{WT_{med}}\right)$
Peripheral volume	$VP/F = \theta_{VP} * \left(\frac{WT}{WT_{med}}\right)$	$VP/F = \theta_{VP}$
Inter-compartment clearance	$Q/F = \theta_Q * \left(\frac{WT}{WT_{med}}\right)^{0.75}$	$Q/F = \theta_Q$
Relative bioavailability	$F_{rel} = ACE_F * \left(\frac{WT}{WT_{med}}\right)^{pwr}$	$F_{rel} = ACE_F$
<u>Pyrazinamide model</u>		
Clearance	$CL/F = \theta_{CL} * \left(\frac{WT}{WT_{med}}\right)^{0.75} * e^{\eta}$	$CL/F = \theta_{CL} * \left(\frac{WT}{WT_{med}}\right)^{0.75} * e^{\eta}$
Volume	$V/F = \theta_V * \left(\frac{WT}{WT_{med}}\right) * e^{\eta}$	$V/F = \theta_V * \left(\frac{WT}{WT_{med}}\right)$
Relative bioavailability	$F_{rel} = \left(\frac{WT}{WT_{med}}\right)^{pwr}$	$F_{rel} = 1$

Table adapted from Guiastrennec et al. (2018) and Zvada et al. (2014). MF = Maturation function, expressed as  $1/[1+(PMA/TM_{50})^{-Hill}]$ ;  $TM_{50}$  = post-menstrual age in weeks at 50% of adult clearance; PMA = post-menstrual age, calculated as age in weeks + 36; Hill = steepness of maturation function;  $\theta$  = typical parameter estimate;  $\eta$  = between-subject variability; pwr = exponential scaling factor; WT = child weight (kg);  $WT_{med}$  = median weight of study population (17.8 kg for Guiastrennec model; 12.5 kg for Zvada model);  $F_{rel}$  = relative bioavailability;  $CL/F$  = apparent clearance (L/h);  $V/F$  = apparent volume of distribution (L);  $Q/F$  = apparent inter-compartment clearance (L/h);  $VP/F$  = apparent peripheral volume of distribution (L); ACE = relative effect of isoniazid acetylator status.

**Supplemental Table 3.2 Pharmacokinetic parameter estimates from literature.**

Population	Guiastrennec et al. model <sup>46</sup>		Zvada et al. model <sup>45</sup>	
	Estimate (RSE%)	BSV (RSE%)	Estimate (RSE%)	BSV (RSE%)
<b>Rifampicin</b>				
$\theta_{CL}$ (L/h)	5.72 (5.9)	45.4 (9.5)	8.15 (9.0)	32.6 (37.7)
$\theta_V$ (L)	23.8 (5.3)	37.3 (12)	16.2 (10.2)	43.4 (19.8)
TM <sub>50</sub> (weeks)	58.2 fixed <sup>a</sup>	-	58.2 (9.0)	-
Hill	2.21 fixed <sup>a</sup>	-	2.21 (11.7)	-
pwr	0.467 (25)	-	-	-
<b>Isoniazid</b>				
$\theta_{CL}$ (L/h)	4.41 (13)	74.2 (13)	-	-
$\theta_{CL}$ (L/h) - slow	-	-	4.44 (11.6)	25.1 (12.3)
$\theta_{CL}$ (L/h) - int	-	-	8.94 (13.1)	25.1 (12.3)
$\theta_{CL}$ (L/h) - fast	-	-	11.3 (14.8)	25.1 (12.3)
$\theta_V$ (L)	19.9 (11)	44.9 (13)	11.0 (10.2)	-
TM <sub>50</sub> (weeks)	49.0 fixed <sup>a</sup>	-	49.0 (13.5)	-
Hill	2.19 fixed <sup>a</sup>	-	2.19 (46.1)	-
pwr	0.711 (20)	-	-	-
ACE <sub>CL</sub> - slow	1 fixed	-	-	-
ACE <sub>CL</sub> - fast	1.944 (20)	-	-	-
ACE <sub>F</sub> - slow	1 fixed	-	1 fixed	-
ACE <sub>F</sub> - fast	0.786 (32)	-	0.772 (30.3)	-
$\theta_{VP}$ (L)	459 (68)	-	5.03 (33.1)	-
$\theta_Q$ (L/h)	1.61 (21)	-	2.0 (26.3)	-
<b>Pyrazinamide</b>				
$\theta_{CL}$ (L/h)	1.55 (6.0)	37.4 (22)	1.08 (5.6)	27.1 (16.3)
$\theta_V$ (L)	13.2 (5.0)	34.4 (15)	9.64 (2.6)	-
pwr	0.315 (31)	-	-	-

Table adapted from Guiastrennec et al. (2018) and Zvada et al. (2014). <sup>a</sup> Maturation function parameters were fixed to values derived by Zvada et al. model. BSV = between-subject variability, expressed as % coefficient of variation. RSE = relative standard error. TM<sub>50</sub> = post-menstrual age in weeks at 50% of adult clearance. Hill = steepness of maturation function.  $\theta_{CL}$  = typical value of apparent clearance.  $\theta_V$  = typical value of apparent volume.  $\theta_{VP}$  = typical value of apparent peripheral volume.  $\theta_Q$  = typical value of apparent peripheral clearance. pwr = exponential scaling factor, applied to relative bioavailability. ACE<sub>CL</sub> = relative effect of isoniazid acetylator status on clearance. ACE<sub>F</sub> = relative effect of isoniazid acetylator status on relative bioavailability.

## References

1. Dodd PJ, Yuen CM, Sismanidis C, Seddon JA, Jenkins HE. The global burden of tuberculosis mortality in children: a mathematical modelling study. *Lancet Glob Health* 2017;5:e898-e906.
2. Bekker A, Schaaf HS, Draper HR, et al. Pharmacokinetics of Rifampin, Isoniazid, Pyrazinamide, and Ethambutol in Infants Dosed According to Revised WHO-Recommended Treatment Guidelines. *Antimicrob Agents Chemother* 2016;60:2171-9.
3. Nansumba M, Kumbakumba E, Orikiriza P, et al. Treatment outcomes and tolerability of the revised WHO anti-tuberculosis drug dosages for children. *Int J Tuberc Lung Dis* 2018;22:151-7.
4. Roadmap towards ending TB in children and adolescents, second edition. World Health Organization, 2018. (Accessed November 7, 2018, at <http://apps.who.int/iris/bitstream/handle/10665/275422/9789241514798-eng.pdf?ua=1>.)
5. Marais BJ, Gie RP, Schaaf HS, et al. The natural history of childhood intra-thoracic tuberculosis: a critical review of literature from the pre-chemotherapy era. *Int J Tuberc Lung Dis* 2004;8:392-402.
6. Drobac PC, Shin SS, Huamani P, et al. Risk Factors for In-Hospital Mortality Among Children With Tuberculosis: The 25-Year Experience in Peru. *Pediatrics* 2012;130:e373-e9.
7. Russell GK, Merle CS, Cooke GS, Casas EC, Silveira da Fonseca M, du Cros P. Towards the WHO target of zero childhood tuberculosis deaths: an analysis of mortality in 13 locations in Africa and Asia. *Int J Tuberc Lung Dis* 2013;17:1518-23.
8. Pasipanodya JG, McIlleron H, Burger A, Wash PA, Smith P, Gumbo T. Serum drug concentrations predictive of pulmonary tuberculosis outcomes. *J Infect Dis* 2013;208:1464-73.

9. Swaminathan S, Pasipanodya JG, Ramachandran G, et al. Drug Concentration Thresholds Predictive of Therapy Failure and Death in Children With Tuberculosis: Bread Crumb Trails in Random Forests. *Clin Infect Dis* 2016;63:S63-S74.
10. WHO. Guidance for National Tuberculosis Programmes on the Management of Tuberculosis in Children. 2nd ed. Geneva 2014.
11. Kearns GL, Abdel-Rahman SM, Alander SW, Blowey DL, Leeder JS, Kauffman RE. Developmental pharmacology--drug disposition, action, and therapy in infants and children. *N Engl J Med* 2003;349:1157-67.
12. New fixed-dose combinations for the treatment of TB in children. World Health Organization, 2016. (Accessed July 25, 2018, at <http://www.who.int/tb/areas-of-work/children/en/>.)
13. WHO. Global Tuberculosis Report 2018. Geneva: World Health Organization; 2018.
14. The DHS Program. 2018. (Accessed December 20, 2018, at <https://dhsprogram.com/Data/>.)
15. Joint child malnutrition estimates - levels and trends. 2018. (Accessed 22 August, 2018, at <http://www.who.int/nutgrowthdb/estimates/en/>.)
16. Ramachandran G, Hemanth Kumar AK, Bhavani PK, et al. Age, nutritional status and INH acetylator status affect pharmacokinetics of anti-tuberculosis drugs in children. *Int J Tuberc Lung Dis* 2013;17:800-6.
17. Ramachandran G, Kumar AK, Bhavani PK, et al. Pharmacokinetics of first-line antituberculosis drugs in HIV-infected children with tuberculosis treated with intermittent regimens in India. *Antimicrob Agents Chemother* 2015;59:1162-7.
18. McIlleron H, Hundt H, Smythe W, et al. Bioavailability of two licensed paediatric rifampicin suspensions: implications for quality control programmes. *Int J Tuberc Lung Dis* 2016;20:915-9.

19. McIlleron H, Willemse M, Werely CJ, et al. Isoniazid plasma concentrations in a cohort of South African children with tuberculosis: implications for international pediatric dosing guidelines. *Clin Infect Dis* 2009;48:1547-53.
20. Thee S, Seddon JA, Donald PR, et al. Pharmacokinetics of isoniazid, rifampin, and pyrazinamide in children younger than two years of age with tuberculosis: evidence for implementation of revised World Health Organization recommendations. *Antimicrob Agents Chemother* 2011;55:5560-7.
21. WHO Multicentre Growth Reference Study Group. WHO Child Growth Standards: Length/height-for-age, weight-for-age, weight-for-length, weight-for-height and body mass index-for-age: Methods and development. Geneva: World Health Organization; 2006.
22. Instituto Nacional de Estatística (INE) and ICF. Angola Demographic and Health Survey 2015. . In: INE and ICF, ed. Rockville, Maryland: ICF; 2018.
23. National Institute of Population Research and Training (NIPORT) and Mitra and Associates of Dhaka and ICF. Bangladesh Demographic and Health Survey 2011. In: NIPORT and Mitra and Associates of Dhaka and ICF, ed. Rockville, Maryland: ICF; 2018.
24. Brazilian Center for Analysis and Planning (CEBRAP) BloPOaSI, Ministry of Health (Brazil),. Brazil National Demographic and Health Survey of Children and Women 2006-2007. In: Ministry of Health (Brazil), ed. Rio de Janeiro, Brazil: Ministry of Health (Brazil),; 2018.
25. National Institute of Nutrition and Food Safety CCfDCaP, Carolina Population Center at the University of North Carolina (UNC) at Chapel Hill,. China Health and Nutrition Survey 1989-2011. In: China Center for Disease Control and Prevention, ed. Chapel Hill, North Carolina: UNC,; 2016.
26. Ministry of Planning and ICF. Democratic Republic of the Congo Demographic and Health Survey 2013. In: Ministry of Planning al, ed. Rockville, Maryland: ICF,; 2018.
27. Central Statistical Agency (CSA) and ICF. Ethiopia Demographic and Health Survey 2011 In: CSA and ICF, ed. Rockville, Maryland: ICF,; 2018.

28. International Institute for Population Sciences Mal. India Demographic and Health Survey 2015. In: International Institute for Population Sciences and ICF, ed. Rockville, Maryland: ICF,; 2018.
29. Strauss J, F. Witoelar, B. Sikoki and A.M. Wattie,. The Fourth Wave of the Indonesian Family Life Survey (IFLS4). 2009.
30. Kenya National Bureau of Statistics and ICF. Kenya Demographic and Health Survey 2014. In: Kenya National Bureau of Statistics and ICF, ed. Rockville, Maryland: ICF,; 2018.
31. Instituto Nacional de Estatística (INE) and ICF. Mozambique Demographic and Health Survey 2011 In: Instituto Nacional de Estatística (INE) and ICF, ed. Rockville, Maryland: ICF,; 2018.
32. The Department of Health Planning under the Ministry of Health and ICF. Myanmar Demographic and Health Survey 2015. In: The Department of Health Planning under the Ministry of Health and ICF, ed. Rockville, Maryland: ICF,; 2018.
33. National Population Commission (NPC) and ICF. Nigeria Demographic and Health Survey 2013 In: National Population Commission (NPC) and ICF, ed. Rockville, Maryland: ICF,; 2018.
34. National Institute of Population Studies (NIPS) and ICF. Pakistan Demographic and Health Survey 2012 In: National Institute of Population Studies (NIPS) and ICF, ed. Rockville, Maryland: ICF,; 2018.
35. Department of Science and Technology - Food and Nutrition Research Institute (DOST-FNRI). 2015 Updating of Nutritional Status of Filipino Children and Other Population Groups. In: DOST-FNRI, ed. Manila, Philippines: DOST-FNRI; 2018.
36. Russia Longitudinal Monitoring survey R-H, conducted by Higher School of Economics and ZAO "Demoscope" together with Carolina Population Center, University of North Carolina (UNC) at Chapel Hill and the Institute of Sociology RAS,. RLMS-HSE Longitudinal Data 1994-2015. In: HSE, ed. Chapel Hill, North Carolina: UNC,; 2016.



37. Southern Africa Labour and Development Research Unit. National Income Dynamics Study 2014-2015, Wave 4. In: Southern Africa Labour and Development Research Unit ed. Cape Town, South Africa: DataFirst,; 2016.
38. Southern Africa Labour and Development Research Unit. National Income Dynamics Study 2012, Wave 3. In: Southern Africa Labour and Development Research Unit ed. Cape Town, South Africa: DataFirst,; 2016.
39. Southern Africa Labour and Development Research Unit. National Income Dynamics Study 2010-2011, Wave 2 In: Southern Africa Labour and Development Research Unit ed. Cape Town, South Africa: DataFirst,; 2016.
40. Southern Africa Labour and Development Research Unit. National Income Dynamics Study 2008, Wave 1 In: Southern Africa Labour and Development Research Unit ed. Cape Town, South Africa: DataFirst,; 2016.
41. National Bureau of Statistics (NBS) and ICF. Tanzania Demographic and Health Survey 2015 In: National Bureau of Statistics (NBS) and ICF, ed. Rockville, Maryland: ICF,; 2018.
42. Thailand National Statistical Office. Thailand Multiple Indicator Cluster Survey 2012 In: Office NS, ed. Bangkok, Thailand: UNICEF; 2012.
43. General Statistical Of ce (GSO). Viet Nam Multiple Indicator Cluster Survey 2011. In: GSO, ed. Ha Noi, Viet Nam: UNICEF; 2011.
44. National Bureau of Statistics (NBS) and ICF. Zambia Demographic and Health Survey 2014 In: National Bureau of Statistics (NBS) and ICF, ed. Rockville, Maryland: ICF,; 2018.
45. Zvada SP, Denti P, Donald PR, et al. Population pharmacokinetics of rifampicin, pyrazinamide and isoniazid in children with tuberculosis: in silico evaluation of currently recommended doses. *J Antimicrob Chemother* 2014;69:1339-49.
46. Guiastrennec B, Ramachandran G, Karlsson MO, et al. Suboptimal Antituberculosis Drug Concentrations and Outcomes in Small and HIV-Coinfected Children in India: Recommendations for Dose Modifications. *Clin Pharmacol Ther* 2017.

47. Dodd PJ, Gardiner E, Coghlan R, Seddon JA. Burden of childhood tuberculosis in 22 high-burden countries: a mathematical modelling study. *Lancet Glob Health* 2014;2:e453-9.
48. Chigutsa E, Pasipanodya JG, Visser ME, et al. Impact of nonlinear interactions of pharmacokinetics and MICs on sputum bacillary kill rates as a marker of sterilizing effect in tuberculosis. *Antimicrob Agents Chemother* 2015;59:38-45.
49. Jenkins HE, Yuen CM, Rodriguez CA, et al. Mortality in children diagnosed with tuberculosis: a systematic review and meta-analysis. *Lancet Infect Dis* 2017;17:285-95.
50. Mukherjee A, Velpandian T, Singla M, Kanhiya K, Kabra SK, Lodha R. Pharmacokinetics of isoniazid, rifampicin, pyrazinamide and ethambutol in Indian children. *BMC Infect Dis* 2015;15:126.
51. Oshikoya KA, Senbanjo IO. Pathophysiological changes that affect drug disposition in protein-energy malnourished children. *Nutr Metab (Lond)* 2009;6:50.
52. Donald PR. Antituberculosis drug-induced hepatotoxicity in children. *Pediatr Rep* 2011;3:e16.
53. van Well GT, Paes BF, Terwee CB, et al. Twenty years of pediatric tuberculous meningitis: a retrospective cohort study in the western cape of South Africa. *Pediatrics* 2009;123:e1-8.
54. Yang H, Enimil A, Gillani FS, et al. Evaluation of the Adequacy of the 2010 Revised World Health Organization Recommended Dosages of the First-line Antituberculosis Drugs for Children: Adequacy of Revised Dosages of TB Drugs for Children. *Pediatr Infect Dis J* 2018;37:43-51.
55. Chigutsa E, Visser ME, Swart EC, et al. The SLCO1B1 rs4149032 polymorphism is highly prevalent in South Africans and is associated with reduced rifampin concentrations: dosing implications. *Antimicrob Agents Chemother* 2011;55:4122-7.

56. Svensson EM, Yngman G, Denti P, McIleron H, Kjellsson MC, Karlsson MO. Evidence-Based Design of Fixed-Dose Combinations: Principles and Application to Pediatric Anti-Tuberculosis Therapy. *Clin Pharmacokinet* 2018;57:591-9.
57. Jaganath D, Mupere E. Childhood tuberculosis and malnutrition. *J Infect Dis* 2012;206:1809-15.

## Chapter 4. Moxifloxacin pharmacokinetics, cardiac safety, and dosing for the treatment of rifampicin-resistant tuberculosis in children \*

### Abstract

*Background:* Moxifloxacin is a recommended drug for rifampin-resistant tuberculosis (RR-TB) treatment, but there is limited pediatric pharmacokinetic and safety data, especially in young children. We characterize moxifloxacin population pharmacokinetics, QT-interval prolongation and evaluate optimal dosing in children with RR-TB.

*Methods:* Pharmacokinetic data were pooled from two observational studies in South African children 0-17 years of age with RR-TB routinely treated with oral moxifloxacin once daily. The population pharmacokinetics and Fridericia-corrected QT (QTcF)-interval prolongation were characterized in NONMEM. Pharmacokinetic simulations were performed to predict expected exposure and optimal weight-banded dosing.

*Results:* Eighty-five children contributed pharmacokinetic data (median [range] age of 4.6 [0.8-15] years); 16 (19%) were <2 years of age, and 8 (9%) were HIV-positive. The median (range) moxifloxacin dose on sampling days was 11 mg/kg (6.1 to 17). Apparent clearance was 6.95 L/h for a typical 16 kg child. Stunting and HIV infection increased apparent clearance. Crushed or suspended tablets had faster absorption. The median (range) maximum change in QTcF after

---

\* adapted from a manuscript under review: Radtke KK, Hesselring AC, Winckler JL, Draper HR, Solans BP, Thee S, Wiesner L, van der Laan LE, Fourie B, Nielsen J, Schaaf HS, Savic RM, Garcia-Prats AJ. Moxifloxacin pharmacokinetics, cardiac safety, and dosing for the treatment of rifampicin-resistant tuberculosis in children.

moxifloxacin administration was 16.3 (-27.7 to 61.3) ms. No child had QTcF  $\geq$  500 ms. The concentration-QTcF relationship was nonlinear, with a maximum drug effect ( $E_{max}$ ) of 8.80 ms (inter-individual variability = 9.75 ms). Clofazimine use increased  $E_{max}$  by 3.3-fold. Model-based simulations of moxifloxacin pharmacokinetics predicted that current dosing recommendations are too low in children.

*Conclusions:* Moxifloxacin doses above 10-15 mg/kg are likely required in young children to match exposures in adults receiving 400 mg but require further safety assessment, especially when co-administered with other QT-prolonging agents.

## **Introduction**

Moxifloxacin is a high-priority drug for rifampicin-resistant tuberculosis (RR-TB) treatment.<sup>1</sup> It is recommended by the World Health Organization (WHO) for use in both short (9-11 month) and longer ( $\geq$ 18 months) regimens.<sup>1</sup> Moxifloxacin has higher potency and better penetration into and activity in lesions than levofloxacin.<sup>2-5</sup> It has demonstrated clinical efficacy in a phase 3 clinical trial of RR-TB and was associated with better drug-resistant TB outcomes in a large individual participant data meta-analysis.<sup>6,7</sup> Recently, moxifloxacin was a key component in the first shortened treatment regimen for drug-susceptible TB, which was non-inferior to the standard 6-month regimen, further establishing its importance for TB treatment.<sup>8</sup>

Despite its proven efficacy in adults, pediatric use of moxifloxacin has been limited, in part due to lack of pharmacokinetic and safety data, especially in young children and children with TB. Moxifloxacin is eliminated partly through metabolism (52%) by glucuronidation and sulfate conjugation with a half-life of 10-14 hours.<sup>9</sup> It has good bioavailability, and food minimally affects

its absorption.<sup>9,10</sup> One safety concern is prolongation of the QT interval.<sup>9</sup> Two pharmacokinetic and safety studies have been completed in children: one in South African children 7-15 years of age with RR-TB,<sup>11</sup> and one in children 0.25-14 years of age from the United States with non-TB infections after a single intravenous dose.<sup>12</sup> These studies were small (<35 children), but neither identified significant safety concerns.

Poor palatability and the lack of a child-friendly formulation has also limited moxifloxacin use in children with TB, which requires long treatment durations.<sup>13</sup> Until recently, oral moxifloxacin was only available as a 400 mg film-coated tablet, which does not support dosing for younger children. A new 100 mg dispersible tablet is becoming more widely available but has not been studied in children. Crushing or preparing an extemporaneous solution of the 400 mg tablet may facilitate its use, if tolerable, but requires pharmacokinetic assessment.

Moxifloxacin efficacy and the risk of QT interval prolongation are concentration-dependent.<sup>14-16</sup> Characterizing moxifloxacin pharmacokinetics and the concentration-QT relationship in children with TB is critical to support its safe and effective use. The aim of this analysis was to describe moxifloxacin population pharmacokinetics, QT interval prolongation, and optimal dosing in a cohort of children 0-<18 years of age routinely treated for RR-TB.

## **Methods**

### **Study Design, Patients and Treatment**

The data were collected from two prospective observational pharmacokinetic studies (MDR-PK1, MDR-PK2) in Cape Town, South Africa, that have been previously described in detail.<sup>17,18</sup> MDR-PK1 enrolled HIV-positive and -negative children 0 to <15 years of age routinely treated

for probable or confirmed RR-TB from 2011-2015. MDR-PK2 enrolled HIV-positive and -negative children 0 to <18 years of age routinely treated for RR-TB from 2016-2020, during which treatment guidelines recommended treatment with moxifloxacin ( $\geq 8$  years of age) or levofloxacin (<8 years of age) and at least three additional drugs for 9-18 months.<sup>19,20</sup> In MDR-PK2, all children received both levofloxacin and moxifloxacin, separately, with at least 3 days of treatment before pharmacokinetic sampling (**Figure 4.1**). All children with moxifloxacin concentration data in MDR-PK1 and MDR-PK2 were included in this analysis.

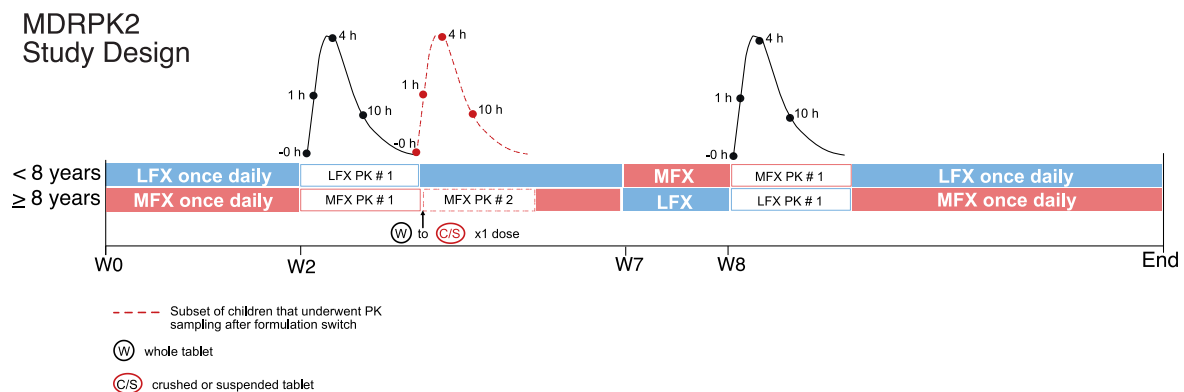


**Figure 4.1** MDR-PK2 Study Design.

Children <8 years were started on levofloxacin (LFX) and children  $\geq 8$  years were started on moxifloxacin (MFX). Pharmacokinetic (PK) sampling and ECG sampling occurred at the same time points. A subset of children  $\geq 8$  years switched formulations and received one additional sampling event as part of a bioequivalence sub-study. 'W' refers to week of treatment.

Children received approximately 7.5-15 mg/kg (max = 400 mg) of moxifloxacin (Dr Reddy's Laboratories Ltd, Hyderabad, India) once daily. On the sampling day, exactly 10 mg/kg was administered in MDR-PK1 by cutting and weighing the tablets as previously described<sup>11</sup>; in

MDR-PK2, a weight-banded dosing approach was used (**Supplemental Table 4.1**).

Medications were given on an empty stomach after an overnight fast as whole tablets (400 mg), if possible, or as an extemporaneously prepared suspension,<sup>21</sup> or as crushed tablets mixed in water. In MDR-PK2, older children able to swallow whole tablets had additional pharmacokinetic sampling after receiving crushed or suspended tablets to assess bioequivalence (**Figure 4.1**). Administration by nasogastric tube was done on sampling days if a child was unable to swallow. All HIV-positive children were established on antiretroviral (ARV) treatment at study enrollment per standard of care and continued ARV treatment throughout RR-TB treatment. ARV medications were administered one hour after moxifloxacin on the sampling day.

### **Pharmacokinetic Sampling and Analysis**

Pharmacokinetic sampling was performed after at least 4 daily doses (i.e., steady state). Blood was drawn pre-dose and 1, 2, 4, 8, and either 6 or 10 hours after the observed dose (MDR-PK1) or pre-dose and 1, 4, and 10 hours after the observed dose (MDR-PK2). Moxifloxacin plasma concentrations were determined with a validated liquid chromatography tandem mass spectrometry assay developed at the University of Cape Town, as previously described.<sup>11</sup>

Moxifloxacin concentration data were pooled and analyzed using non-linear mixed effects modeling. Population pharmacokinetic parameters were estimated with first-order conditional estimation with interaction. Inter-individual and inter-occasion variability were modeled exponentially assuming a log-normal distribution. One and two compartment disposition models were evaluated with first-order absorption or absorption delay. Model building was guided by goodness-of-fit plots, objective function value, and simulation-based diagnostics. Stepwise covariate modeling ( $p < 0.05$  forward selection;  $p < 0.01$  backward deletion) was performed to identify predictors of volume, clearance, bioavailability, and absorption including body size (total body weight, fat-free mass<sup>22</sup>, ideal body weight), formulation, administration route, age,



nutritional status (weight-for-age, height-for-age, BMI-for-age Z-scores)<sup>23,24</sup> HIV status, ARV regimen, gender, and study. Selection was informed by statistical and clinical significance and physiological plausibility.

### **QT interval prolongation and safety assessment**

A 12-lead electrocardiogram (ECG) was performed in triplicate during pharmacokinetic sampling pre-dose and 1, 4, and 10 hours after dose (MDR-PK-2) or pre-dose and 2 hours after dose (MDR-PK1). QT intervals were corrected by Fridericia formula (QTcF). For descriptive analysis, triplicate mean was used. For modelling, all observations were used.

The moxifloxacin concentration-QTcF relationship was modelled sequentially with individual pharmacokinetic parameters estimated from the final pharmacokinetic model. QTcF measures prior to TB treatment initiation were not available. Instead, the population baseline QTcF and inter-individual variability were estimated using pre-dose QTcF measures from MDR-PK2 children during levofloxacin therapy since pre-dose levofloxacin concentrations were near or below the lower limit of quantification (n=51 subjects; n=252 measures) (**Figure 4.1**). Baseline values were fixed, and the moxifloxacin drug effect was estimated in the moxifloxacin treatment dataset. Age, gender, use of concomitant QT-prolonging agents, and study were tested as covariates on baseline and drug-effect parameters.

### **Simulations**

Model-informed optimal doses were derived based on the target exposure in adults receiving 400 mg once-daily (median 24-hour AUC at steady state [AUC<sub>24</sub>] of 40 mg/L)<sup>25,26</sup>, pre-specified WHO weight bands, and available formulations. Steady state pharmacokinetics were simulated 500 times in a representative population of children with TB (demographics of the simulated

population are shown in **Supplemental Table 4.2**) under current WHO dosing guidance<sup>1</sup> and the model-informed optimal dosing.

### **Statistics and Software**

NONMEM 7.41 (ICON Development Solutions, Elliott City, Maryland) and Perl-speaks-NONMEM (version 4.7.0) were used for all modelling and simulation. R (version 3.4.2) was used for data management, statistical analyses, and graphical visualization. Xpose (version 0.4.4) and vpc (version 1.0.1) were used for visual diagnostics.

### **Ethics**

Written informed consent was provided by the parent/s or legal guardians, and written informed assent by participants  $\geq 7$  years of age. Ethics approval for the study was provided by the Health Research Ethics Committee of Stellenbosch University (N11/03/059 for MDR-PK1 and N15/02/012 for MDR-PK2).

## **Results**

### **Patients and sampling**

Pharmacokinetic data were collected from 33 children ( $n=198$  samples) in MDR-PK1 and 52 children ( $n=242$  samples) in MDR-PK2. Thirteen children had two sampling occasions. Nine samples below the lower limit of quantification (0.0628 mg/L) were excluded. The patient characteristics are summarized in **Table 4.1**. Children in MDR-PK2 were younger and fewer received a whole tablet. There were 16 children  $< 2$  years and 1 child  $< 1$  year of age.

**Table 4.1.** Demographic and clinical characteristics of children treated for rifampicin-resistant tuberculosis in the MDR-PK1 and MDR-PK2 studies.

Description	MDR-PK1 (n=33)	MDR-PK2 (n=52)	Combined (n=85)	p-value <sup>d</sup>
<b>Male</b> , n (%)	13 (39.4)	24 (46.2)	37 (43.5)	0.540
<b>Age (year)</b> , median (IQR) [min, max]	9.6 (4.6 to 12.3) [1.0, 15.0]	3.0 (2.1 to 6.0) [0.90, 14.6]	4.6 (2.5 to 9.9) [0.90, 15.0]	<0.001
<b>Weight (kg)</b> , median (IQR) [min, max]	25.1 (16.0 to 36.3) [10.7, 66]	12.8 (10.9 to 18.1) [7.66, 46.6]	16.0 (11.4 to 27.9) [7.66, 66.0]	<0.001
<b>Height (cm)</b> , median (IQR) [min, max]	130 (103 to 144) [76.0, 172]	90.0 (81.6 to 112) [71.4, 158]	102 (84.0 to 132) [71.4, 172]	<0.001
<b>HIV positive</b> , n (%)	7 (21.2)	1 (1.9)	8 (9.4)	0.005
<b>Antiretroviral therapy<sup>a</sup></b> , n (%)				
EFV-based	3 (43)	1 (100)	4 (50)	
LPV/r-based	4 (57)	0 (0)	4 (50)	1.000
<b>WAZ<sup>b</sup></b> , mean (SD) [min, max]	-0.358 (0.924) [-2.28, 1.53]	-0.95 (1.22) [-4.08, 1.37]	-0.777 (1.16) [-4.08, 1.53]	0.062
<b>HAZ</b> , mean (SD) [min, max]	-0.905 (1.20) [-3.76, 1.43]	-1.26 (1.23) [-4.02, 1.79]	-1.12 (1.22) [-4.02, 1.79]	0.189
<b>BAZ</b> , mean (SD) [min, max]	-0.009 (1.21) [-2.41, 2.89]	-0.236 (1.24) [-3.98, 1.88]	-0.148 (1.23) [-3.98, 2.89]	0.411
<b>Route of administration<sup>c</sup></b> , n (%)				
Oral	25 (75.8)	46 (88.5)	71 (83.5)	
Nasogastric tube	8 (24.2)	6 (11.5)	14 (16.5)	0.124
<b>Moxifloxacin dose (mg/kg)<sup>c</sup></b> , median (IQR) [min, max]	9.99 (9.88 to 10.0) [6.06, 14.9]	12.4 (11.3 to 14.2) [8.58, 19.1]	10.9 (10.0 to 13.1) [6.06, 19.1]	<0.001
<b>Formulation administered<sup>c</sup></b> , n (%)				
Whole tablet	20 (60.6)	8 (15.4)	28 (32.9)	
Crushed tablet	7 (21.2)	2 (3.8)	9 (10.6)	
Extemporaneous suspension	6 (18.2)	42 (80.8)	48 (56.5)	<0.001

<sup>a</sup> percentage reflects percent of children living with HIV

<sup>b</sup> children < 10 years only, [n=19] for MDR-PK1 and [n=46] for MDR-PK2

<sup>c</sup> values are based on the first pharmacokinetic sampling occasion

<sup>d</sup> medians were compared for continuous variables not normally distributed using the Wilcoxon rank-sum test, and means were compared using t-tests for variables normally distributed. Proportions were compared using Chi-squared or Fisher Exact test (n<5) as appropriate for categorical variables.

HAZ: height for age z-score; WAZ: weight for age z-score; EFV: efavirenz; LPV/r: lopinavir/ritonavir; IQR: interquartile range; SD: standard deviation.

## Moxifloxacin pharmacokinetics and population model

Moxifloxacin pharmacokinetic profiles were similar between studies (**Figure 4.2**). The population pharmacokinetics were best described with two compartment distribution and transit compartment (N=1) absorption.<sup>27</sup>

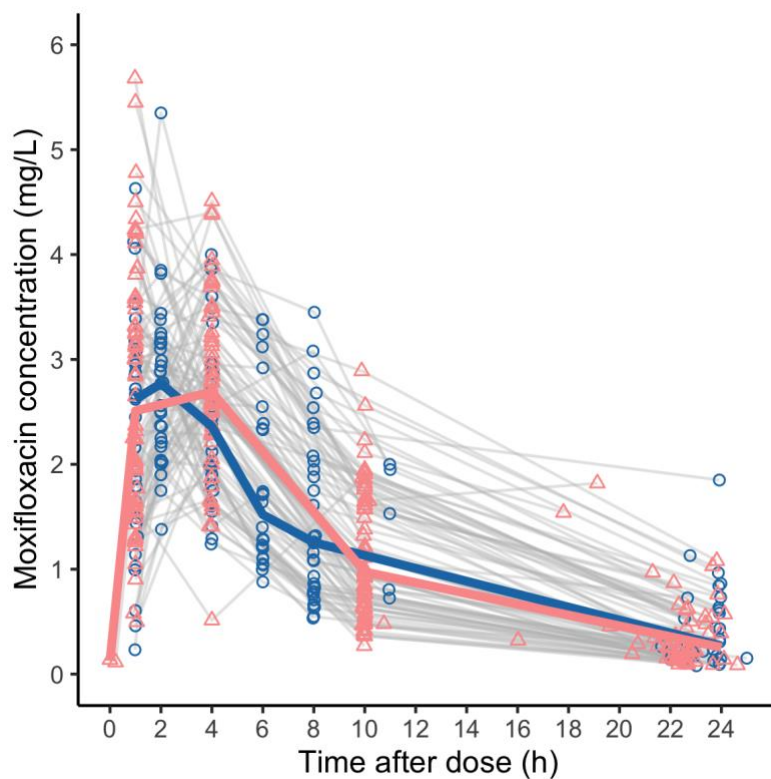


**Figure 4.2** Moxifloxacin pharmacokinetic profiles in children treated for rifampicin-resistant tuberculosis.

Gray lines connect individual observed concentrations (circle = MDR-PK1; triangle = MDR-PK2) over time at unique sampling occasions. Mean concentrations over time are shown in bold lines (blue = MDR-PK1; pink = MDR-PK2). Trough concentrations are shown as the actual time after the previous recorded dose.

Allometric scaling (fixed exponent: 0.75 for clearance and 1 for volume) by fat-free mass resulted in a similar fit to body weight; thus, body weight was chosen. HIV-positive children had 44% higher clearance (CL/F). Low height-for-age z-score (HAZ) increased CL/F by 9.8% per unit decrease in HAZ (**Table 4.2**). These effects remained whether fat-free mass or total body weight was used for allometric scaling. Crushing or suspending the moxifloxacin tablet resulted in faster absorption. No difference was observed in relative bioavailability by formulation in the bioequivalence group (n=8, MDR-PK2) (**Figure 4.3**).

Maturation of CL/F with age was not supported. Conversely, a statistically significant decrease in CL/F with age was observed after adjusting for weight. This effect (-2.5% per year of age) was driven by children older than 12 years (n=14). Given the small effect size and no physiological explanation, it was excluded from the final model.

The final population pharmacokinetic model predicted the observed data well (**Figure 4.4**).

**Table 4.2** shows the final parameter estimates. The median (2.5<sup>th</sup>, 97.5<sup>th</sup> percentiles) individual Bayesian estimates of maximum concentration ( $C_{max}$ ) were 3.05 (1.81, 4.43) mg/L and of  $AUC_{24}$  were 25.9 (13.6, 51.5) mg\*h/L. Children who were stunted (HAZ < -2) or of low weight had lower dose-adjusted  $AUC_{24}$  and higher weight-adjusted CL/F (**Figure 4.5**).

**Table 4.2.** Population pharmacokinetic and QTcF parameter estimates in children treated for moxifloxacin for rifampicin-resistant tuberculosis.

	Population Estimate (RSE, %)	Interindividual Variability, %CV <sup>e</sup> (RSE, %)
<b>Pharmacokinetic model</b>		
CL/F <sup>a,b</sup> (L/h)	6.95 (3.59)	29.1 (7.92)
V/F <sup>a</sup> (L)	40.7 (9.54)	-
MTT (h) <sup>c</sup>	1.44 (12.7)	51.5 (8.2)
Q/F <sup>a</sup> (L/h)	1.98 (50.0)	-
VP/F <sup>a</sup> (L)	24.1 (68.0)	-
Effect of HIV on CL/F (%)	+ 44.0 (32.3)	
Effect of HAZ on CL/F (% per HAZ)	- 9.83 (56.8)	
Effect of formulation on MTT (%)		
Whole tablet	<i>Reference</i>	
Crushed tablet	- 39.6 (44.2)	
Extemporaneous suspension	- 22.5 (41.8)	
ε, proportional (%)	20.4 (12.1)	-
ε, additive (mg/L)	0.0455 (43.4)	-
<b>QTcF model<sup>d</sup></b>		
Baseline (ms) <sup>f</sup>		26.5 (12.6)
MDR-PK1	381 (1.01)	
MDR-PK2	354 (32.1)	
E <sub>max</sub> (ms)		9.75 (31.3) <sup>g</sup>
MFX alone	8.80 (64.3)	
MFX+CFZ	28.4 (91.6)	
EC <sub>50</sub> (mg/L)	0.293 (55.4)	-
Effect of age ≤ 2.6 years on baseline (% per year)	7.05 (17.6)	
Effect of age > 2.6 years on baseline (% per year)	0 *	
ε, additive (ms)	17.8 (5.20)	-
<sup>a</sup> allometrically scaled to median weight of population (16 kg) with exponent of 0.75 for CL/F and Q/F and 1 for V/F and VP/F. <sup>b</sup> $CL/F = \theta_{pop} \cdot (WT/16)^{0.75} \cdot (1 + \theta_{HIV}) \cdot (1 + \theta_{HAZ} \cdot (HAZ + 1.06))$ <sup>c</sup> $MTT = \theta_{pop} \cdot (1 + \theta_{form})$ <sup>d</sup> $QTcF = Baseline \cdot (1 + \theta_{age} \cdot (age - 2.6 \text{ years})) + E_{max} \cdot C_p / (EC_{50} + C_p) + \varepsilon$ <sup>e</sup> Inter-individual variability was modelled exponentially for pharmacokinetic parameters and additively for QTcF parameters. <sup>f</sup> Baseline was modeled based on pre-dose QTcF data from MDR-PK2 during levofloxacin treatment. The estimate was adjusted for MDR-PK1 children. <sup>g</sup> Modeled as intra-individual variability. * Estimate was approximately 0 and therefore fixed.		
CL/F: apparent clearance; Q/F: apparent intercompartmental clearance; V/F: apparent volume of distribution; VP/F: apparent peripheral volume of distribution; MTT: mean transit time; $\theta_{pop}$ : population estimate; $\theta_{HIV}$ : effect of HIV positive status on CL/F; $\theta_{HAZ}$ : effect of height for age z-score (HAZ) on CL/F, centered at the population median HAZ of -1.06; $\theta_{form}$ : effect of formulation (crushed or suspended tablet) on MTT; E <sub>max</sub> : maximum drug effect; EC <sub>50</sub> : concentration at 50% maximum effect; $\theta_{MDRPK1}$ : effect of MDRPK1 study on baseline QTcF; $\theta_{age}$ : effect of age on baseline QTcF, centered at the population median of 2.6 years; C <sub>p</sub> : concentration of moxifloxacin in plasma; WT: body weight (kg); QTcF: QT-interval corrected by Fridericia formula; RSE: relative standard error; ε: residual unexplained error; MFX: moxifloxacin; MFX+CFZ: moxifloxacin and clofazimine.		

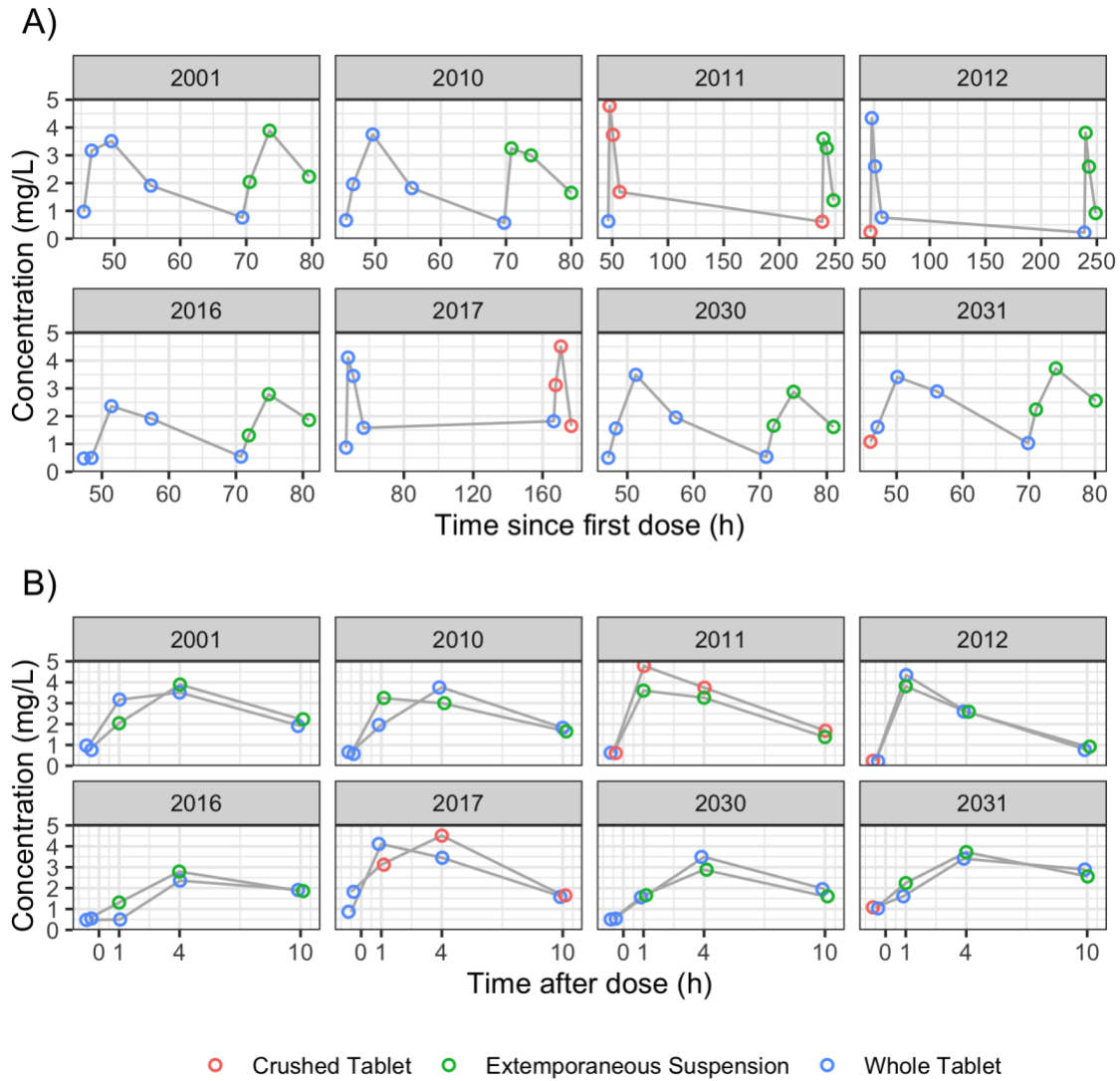


**Figure 4.3** Pharmacokinetic profiles in 8 subjects that received two formulations in MDRPK2. Panel (A) shows the data as time since first dose. Panel (B) shows the data as time after dose, where lines connect unique sampling dates and pre-dose values are shown at -0.5 h.

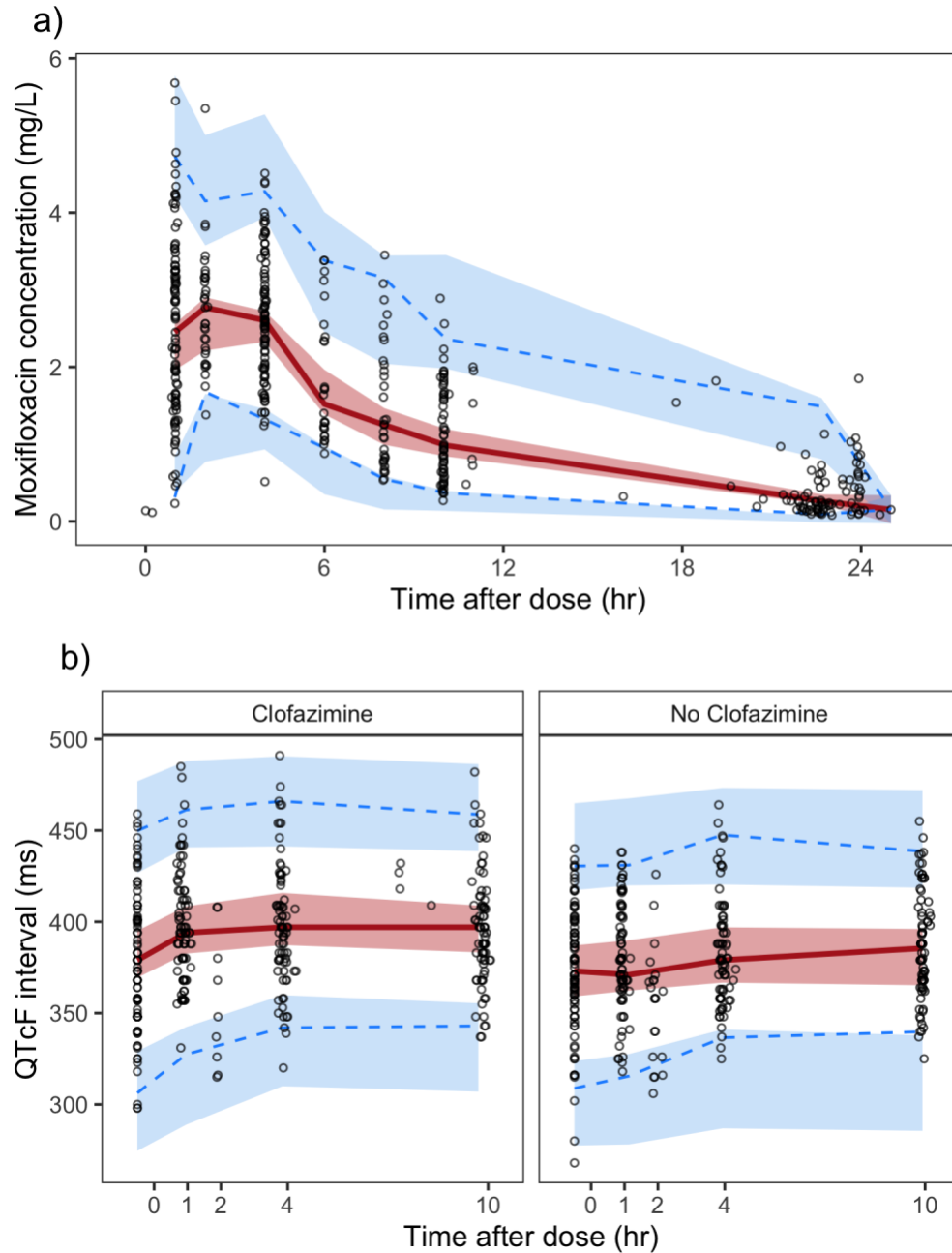


**Figure 4.4** Visual predictive check of the final (a) pharmacokinetic model and (b) pharmacokinetic-QTcF model. Dots represent observed data. Lines correspond to 5<sup>th</sup> (dashed), 50<sup>th</sup> (solid), 95<sup>th</sup> (dashed) percentiles of observed data. Shaded areas are the model-predicted 95% confidence intervals for the 5<sup>th</sup>, 50<sup>th</sup>, and 95<sup>th</sup> percentiles obtained from 1000 simulated datasets.



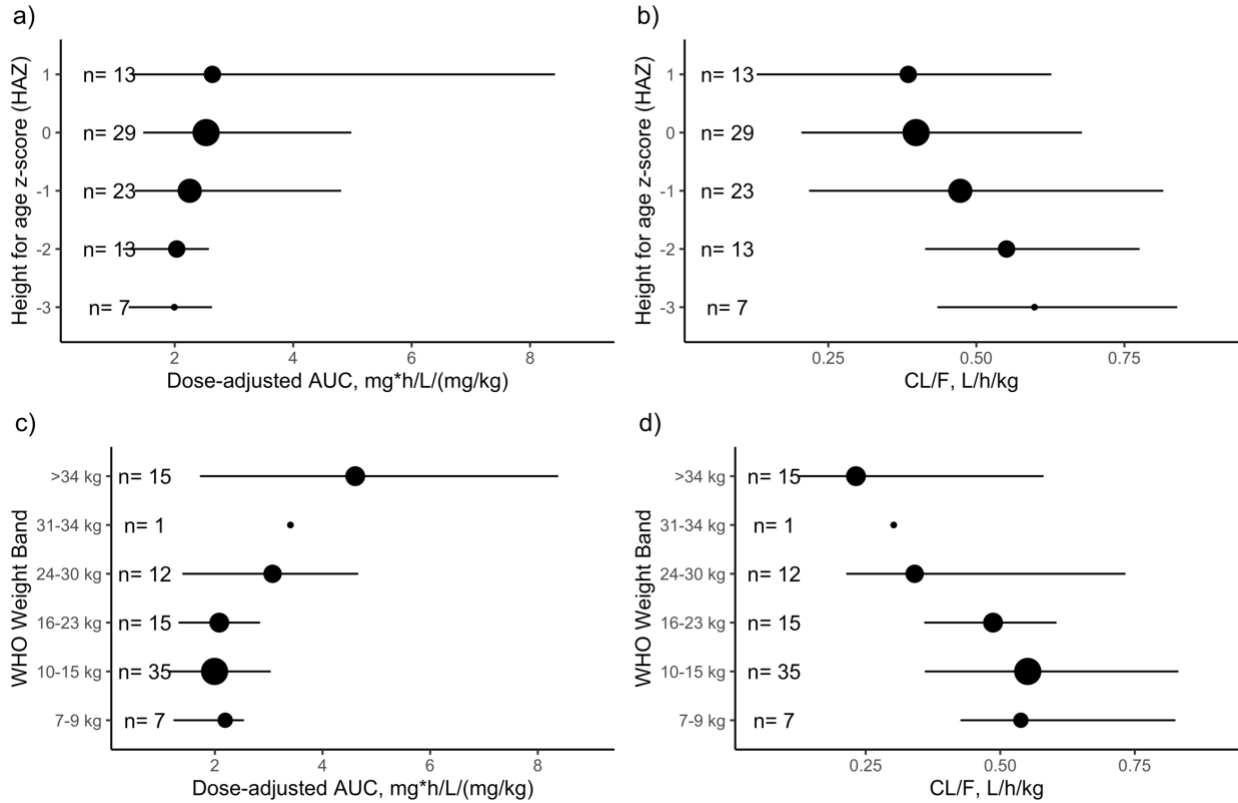


**Figure 4.5** Moxifloxacin AUC<sub>24</sub> (a,c) and apparent clearance (b,d) by nutritional status and body weight.

Nutritional status is shown by height-for-age z-score (HAZ) and body weight by World Health Organization (WHO) weight band. AUC<sub>24</sub> is adjusted for the mg/kg dose. CL/F is adjusted for body weight. The sample size (n) of each group is displayed in text and the size of the center point represents the relative sample size. Center points represent the median. Lines represent the 2.5th to 97.5th percentile range.

### Cardiac safety

There were 57 children (n=45 younger than 7 years) who contributed ECG data (n=711 measurements) after repeated oral dosing of moxifloxacin. Ten children contributed data on 2 occasions (n=67 total occasions). Clofazimine was the major concomitantly used QT-prolonging anti-TB agent: clofazimine (n=3 MDR-PK1; n=26 MDR-PK2), delamanid (n=1), bedaquiline (n=0). The median (range) maximum QTcF interval was 409 (325 to 491) ms and time of peak QTcF was 1.88 (0-10) hours. High intra-individual variability was observed among triplicate

QTcF measures at the same time point and occasion (mean +/- SD absolute difference, 20.2 +/- 15.8 ms). No child had a QTcF interval > 500 ms or clinical cardiac adverse event (i.e., arrhythmia). There were 3 (4.5%) out of 67 occasions with QTcF  $\geq$ 450 to <480 ms, and 2 (2.9%)  $\geq$ 480 to <500 ms; 4 of 5 occasions with QTcF  $\geq$ 450 ms occurred in children receiving clofazimine. The median (range) maximum change in QTcF ( $\Delta$ QTcF) was 16.3 (-27.7, 61.3) ms: 13.7 (-27.7 to 47.0) ms in children not receiving clofazimine and 23.3 (-11.8 to 61.3) ms in children receiving clofazimine (**Figure 4.6**). There were 11 (19%) children with maximum  $\Delta$ QTcF  $\geq$ 30 to <60 ms, and 1 (1.7%) of  $\Delta$ QTcF  $\geq$  60 ms.

### **Moxifloxacin concentration-QTcF relationship**

The pharmacokinetic-QTcF model estimates are shown in **Table 4.2**. Moxifloxacin-induced QTcF prolongation was best characterized with a direct concentration-response model and maximum effect ( $E_{max}$ ) relationship. An effect compartment model (time delay) was evaluated to explain sustained QTcF prolongation after 4 hours post-dose (i.e., time of moxifloxacin  $C_{max}$ ). The models had similar fit, so the direct model (simplest) was chosen. Younger children had lower baseline QTcF, which increased linearly up to age 2.6 years with no effect thereafter. Clofazimine use increased  $E_{max}$  from 8.8 ms to 28 ms but did not increase baseline QTcF. Visual diagnostics show that QTcF interval data were well predicted by the model (**Figure 4.5**).

### **Optimal dosing and simulations**

Model-informed optimized doses were 10-50% higher than current WHO recommendations for children < 24 kg (**Table 4.3**). In children > 30 kg, doses above 400 mg were required to match the AUC target, but the dose was limited to 400 mg. Model simulations predict low target attainment among children 5-15 kg, which improved with model-informed dosing (**Figure 4.7**).

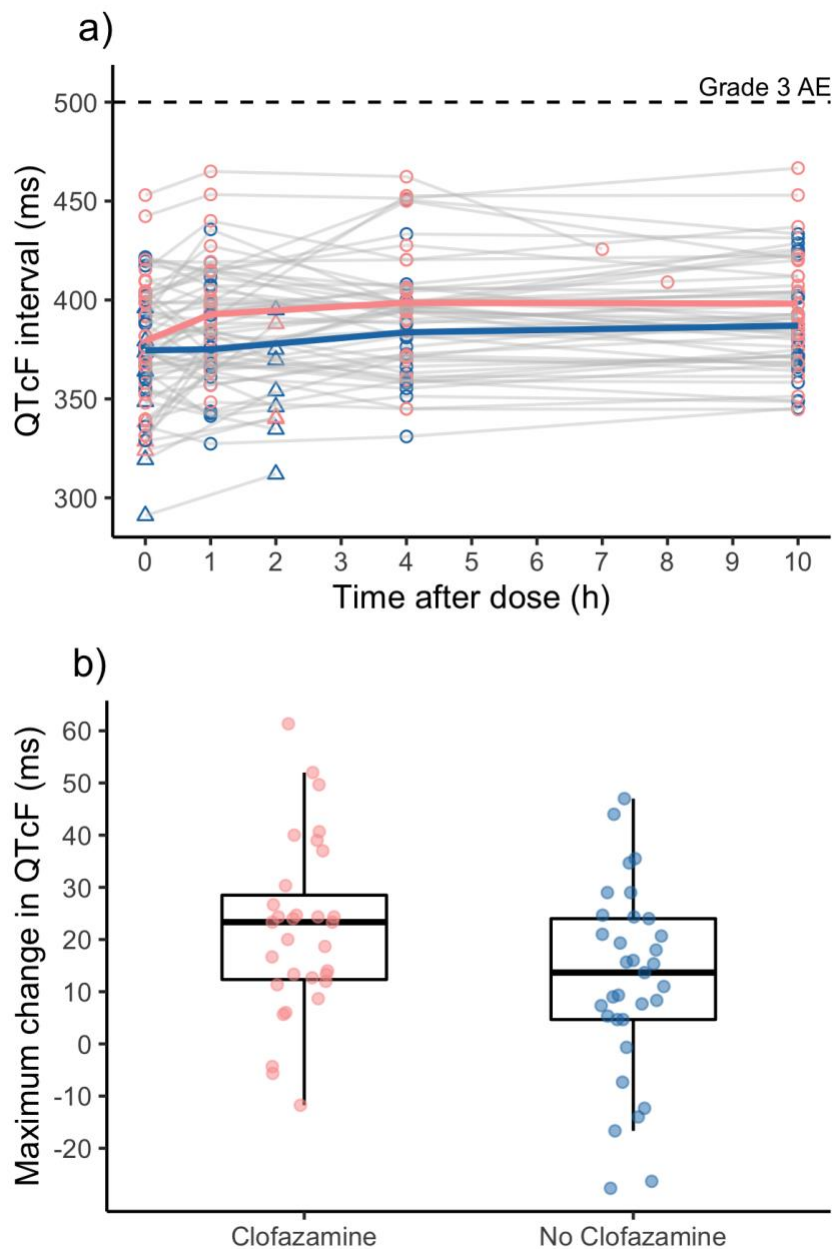


**Figure 4.6** QTcF profiles in children treated with moxifloxacin for rifampicin-resistant tuberculosis as (a) QTcF interval over time and (b) maximum change in QTcF during the dosing interval in children receiving clofazimine (n= 29) and not (n=27). (a) Gray lines represent distinct children and sampling occasions with individual observations as triangles (MDR-PK1) or circles (MDR-PK2). The bold line (pink = clofazimine group; blue= no clofazimine group) is the population mean. (b) Boxplots represent the median, interquartile range, and whiskers show 95th and 5th percentile. QTcF = Fridericia-corrected QT interval. AE = adverse event.

**Table 4.3.** Currently recommended and optimized pediatric weight band dosing for moxifloxacin.

	Current WHO Dosing				Model-informed Optimized Dosing			
	100 mg dt		400 mg tab		100 mg dt		400 mg tab	
Weight band	Tabs	Dose	Tabs	Dose	Tabs	Dose	Tabs	Dose
5-6 kg	0.8	80 mg	2 mL*	80 mg	1.5	150 mg	4 mL*	160 mg
7-9 kg	1.5	150 mg	3 mL*	120 mg	2	200 mg	5 mL*	200 mg
10-15 kg	2	200 mg	5 mL*	200 mg	3	300 mg	7 mL*	280 mg
16-23 kg	3	300 mg	0.5	200 mg	4	400 mg	1	400 mg
24-30 kg	4	400 mg	4	400 mg	4	400 mg	1	400 mg
31-34 kg	4	400 mg	4	400 mg	4	400 mg	1	400 mg
>34 kg	4	400 mg	4	400 mg	4	400 mg	1	400 mg

\*400 mg tab dissolved in 10 mL water (40 mg/mL). dt = dispersible tablet.

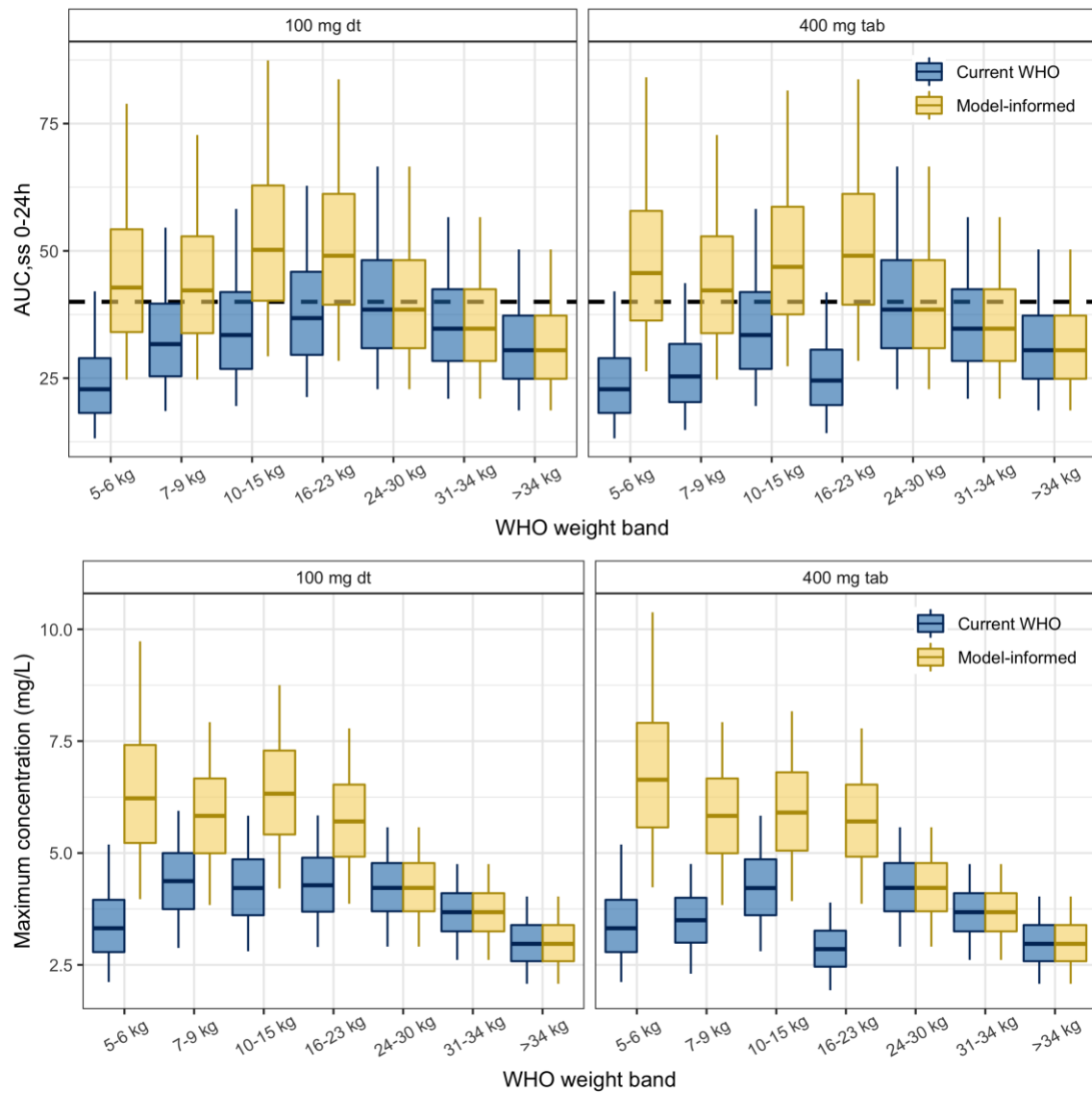


**Figure 4.7** Simulated moxifloxacin (a) AUC<sub>24</sub> and (b) maximum concentration at steady state with weight band dosing according to current WHO recommendations (blue) and model-informed optimized doses (yellow). Data are based on 500 simulations. Weight band doses are shown in Table 4.3. Dashed line in (a) represents the target AUC. dt = dispersible tablet.

## Discussion

This is the first report of moxifloxacin population pharmacokinetics and cardiac safety in young children with TB. We show that moxifloxacin did not prolong the QTcF interval to  $\geq 500$  ms with 10-15 mg/kg once daily in children, including those cotreated with clofazimine. However, moxifloxacin concentrations were below adult target concentrations at the doses evaluated. Suboptimal exposures are predicted in all weight bands with current WHO dosing recommendations.<sup>1</sup> The model-informed optimized doses proposed here ensure adequate exposures in children of all weights, align with WHO weight bands, and can be practically implemented with available oral formulations.

We observed comparatively higher moxifloxacin CL/F in our pediatric population. In adults with TB, moxifloxacin CL/F was 6.66-8.50 L/h, which scales to 2-3 L/h compared to our estimate of 6.95 L/h in a typical 16 kg child.<sup>26,28,29</sup> This difference may be explained, in part, by our observation of decreased CL/F in children older than 12 years, after applied allometric scaling, suggesting CL/F changes minimally with weight after childhood. In a pediatric study, CL/F was 5.48 L/h (median weight, 16.5 kg)<sup>12</sup>, adjusting for 90% oral bioavailability.<sup>9</sup> A population pharmacokinetic analysis of children 3 months to 17 years estimated 0.45 L/h/kg<sup>0.75</sup>, similar to our estimate (0.43 L/h/kg<sup>0.75</sup>).<sup>30</sup> Clearance maturation was not supported with our data, which agrees with Willmann *et al.*, suggesting adult activity is reached early in childhood.<sup>30</sup> However, few children aged <1 year were included in either study. Moxifloxacin is eliminated unchanged through glomerular filtration and biliary excretion (45%) and through phase II metabolism via Sulfotransferase 2A1 (38%) and UDP-glucuronosyltransferase 1A1 (14%) in adults.<sup>9</sup> Ontogeny of these enzymes is not well understood, but it is reasonable to conclude that at least 80% of adult activity is reached by one year post-natal age.<sup>31-33</sup> Pharmacokinetic data in children <1

year and adolescents 12-18 years are needed to characterize moxifloxacin pharmacokinetics from infancy to adulthood.

Children with low HAZ had higher moxifloxacin clearance and lower AUC compared to children of normal HAZ. Low HAZ (ie, stunting) typically represents chronic undernutrition. We did not find an association with weight-for-age or BMI-for-age with moxifloxacin pharmacokinetics. HAZ or stunting has been associated with low exposures of first-line TB drugs in children.<sup>34,35</sup> Higher CL/F in children with low HAZ may reflect under-prediction of CL/F by total body weight alone. Interestingly, this effect persisted when estimated fat-free mass was used in place of body weight. While total body weight is lower, liver size may not differ in malnourished children.<sup>36</sup> Further, malnutrition may compromise drug absorption thereby increasing the apparent CL/F.<sup>37</sup> Given the prevalence of stunting in TB-endemic countries, it is important to consider the pharmacokinetics and dosing needs in representative populations.<sup>38</sup>

Efavirenz induces UDP-glucuronosyltransferase activity.<sup>39</sup> Naidoo and colleagues reported 42% higher moxifloxacin clearance in TB/HIV co-infected adults receiving efavirenz, similar to the 44% increase we observed in HIV-positive children.<sup>40</sup> Distinguishing HIV from efavirenz was not possible since only four (50%) HIV-positive children received efavirenz. More data in HIV/TB co-infected children receiving efavirenz is required to understand if dose adjustments are needed.

The median maximum  $\Delta$ QTcF observed in the children in our study was similar to adults receiving 400 mg of moxifloxacin; however, we estimated a weaker concentration response.<sup>16,41-</sup>  
<sup>44</sup> In healthy adults, reported  $E_{\max}$  was 34 ms and concentration at 50%  $E_{\max}$  ( $EC_{50}$ ) was 3.9 mg/L compared to 8.4 ms ( $E_{\max}$ ) and 0.28 mg/L ( $EC_{50}$ ) in our study.<sup>43</sup> Other adult studies report 2.3-4.1 ms increase in QTcF per mg/L of moxifloxacin.<sup>16,41,44</sup> We observed high intra-individual variability in QTcF measures, potentially limiting estimation of a strong moxifloxacin effect.

Therefore, our model cannot confidently predict QTcF intervals at higher doses. Nonetheless, simulated  $C_{\max}$  with the optimized doses do not exceed  $C_{\max}$  observed after intravenous infusion (up to 10 mg/L), which was safe from severe QTcF prolongation.<sup>9,12</sup> Future QTcF studies in children should ideally include pre-drug ECGs collected under the same conditions and time of day as during pharmacokinetic sampling to improve estimation of concentration-QTcF response.

At the population level, QTcF prolongation appeared sustained after the time of moxifloxacin  $C_{\max}$ . However, at the individual level, QTcF profiles were highly heterogeneous. The sustained effect was equally described with direct and delayed drug-effect models. Sustained QT interval prolongation with moxifloxacin has been described previously.<sup>42</sup> Without a control arm, we were unable to account for normal fluctuations in QTcF, so the simplest model was most appropriate. In our study, the majority of QTcF sampling times were near the bounds of predicted moxifloxacin  $C_{\max}$  (1.5 to 4 hours after dose). Additional QTcF measures 2-3 hours after dose, along with true baseline measures, might be helpful in future studies to fully understand if a delayed effect on QTcF prolongation occurs in children.

Current WHO guidelines for drug-resistant TB recommend treatment with clofazimine and fluoroquinolones, potentially also in combination with bedaquiline.<sup>1</sup>  $E_{\max}$  was 3.3-fold higher with concomitant clofazimine use compared to moxifloxacin alone, likely reflecting additional QT-prolongation from clofazimine. While clofazimine has known QT-prolonging risk<sup>45,46</sup>, no significant QT prolongation occurred in 27 children treated with clofazimine for *Mycobacterium abscessus* infection.<sup>47</sup> In our study, two children had  $\Delta\text{QTcF} > 50$  ms and were taking clofazimine. No child experienced QTcF  $> 500$  ms or clinical cardiac event. Therefore, concomitant use of moxifloxacin and clofazimine was safe from severe QT prolongation at the studied doses.



The model-informed doses proposed here align with WHO weight bands and available formulations and ensure target exposure attainment in all weight bands where the maximum daily dose was not reached. This has important implications for RR-TB treatment as fluoroquinolones have higher bactericidal activity than other second-line anti-TB medications <sup>45</sup>. Although most children treated for RR-TB have good outcomes, children living with HIV, poor nutritional status, and severe TB, including adolescents, have worse outcomes <sup>48</sup>. These populations all had suboptimal moxifloxacin exposure in this study. Proposed doses for children <10 kg should be interpreted with caution as few data were available in these groups. Targeted pharmacokinetic studies in these vulnerable populations are essential to ensure RR-TB dosing is optimized for all.

Furthermore, moxifloxacin is a component of multiple shortened regimens for RR-TB currently under evaluation. Recently, a 4-month regimen with moxifloxacin demonstrated non-inferiority to the standard 6-month regimen without moxifloxacin in adults with drug-susceptible TB <sup>8</sup>. Ensuring appropriate dosing may be even more important for efficacy of novel regimens containing fewer drugs and/or shortened durations. Our findings now have broader relevance for pediatric TB treatment, as many more children develop drug-susceptible TB each year (1.19 million) compared to rifampicin-resistant TB (~26-30,000) <sup>49</sup>.

In conclusion, up to 15 mg/kg of moxifloxacin was safe in children with RR-TB. Higher than currently recommended doses are needed to match adult exposures. Further investigation of QTcF interval prolongation with higher doses and concomitant use with other QT-prolonging agents is urgently needed.

**Supplemental Table 4.1. Moxifloxacin weight banded dosing used in MDR-PK2**

<b>Targeted adult dose:</b> 400 mg once daily		
<b>Available formulations:</b> 400 mg tablet; 20 mg/mL extemporaneously prepared suspension		
	<b>Moxifloxacin dose (mg)</b>	<b>Number of tabs OR mL suspension</b>
2 to <3	40	1.5 mL
3 to <5	60	3 mL
5 to <10	100	5 mL
10 to <15	160	8 mL
15 to <20	200	1/2 tab
20 to <30	300	3/4 tab
30 to <40	400	1 tab

**Supplemental Table 4.2. Demographics of child population with TB used for pharmacokinetic simulations.**

<b>Weight band</b>	<b>Number of children</b>	<b>Height for age z-score (HAZ)</b> Median (2.5 <sup>th</sup> to 97.5 <sup>th</sup> percentile)	<b>Age (year)</b> Median (2.5 <sup>th</sup> to 97.5 <sup>th</sup> percentile)
5-6 kg	48	-1.92 (-5.74 to 5.33)	0.5 (0.2 to 1.9)
7-9 kg	93	-2.21 (-5.44 to 1.73)	1.2 (0.2 to 3)
10-15 kg	153	-1.63 (-5.61 to 2.65)	2.6 (0.8 to 8.3)
16-23 kg	76	-1.47 (-5.95 to 1.1)	6.6 (3.2 to 11.6)
24-30 kg	21	-1.09 (-3.96 to 2.21)	9.9 (6.7 to 14.2)
31-34 kg	13	-0.82 (-2.69 to 0.33)	12.6 (10.6 to 15.3)
>34 kg	19	-0.28 (-1.79 to 1.84)	13.8 (10.6 to 15.3)

## References

1. WHO consolidated guidelines on tuberculosis treatment. Module 4: Treatment - Drug-resistant tuberculosis treatment. WHO, 2020. (Accessed November 1, 2020, at <https://www.who.int/publications/i/item/9789240007048>.)
2. Sarathy J, Blanc L, Alvarez-Cabrera N, et al. Fluoroquinolone efficacy against tuberculosis is driven by penetration into lesions and activity against resident bacterial populations. *Antimicrob Agents Chemother* 2019;63:e02516-18.
3. Gosling RD, Uiso LO, Sam NE, et al. The bactericidal activity of moxifloxacin in patients with pulmonary tuberculosis. *Am J Respir Crit Care Med* 2003;168:1342-5.
4. Strydom N, Gupta SV, Fox WS, et al. Tuberculosis drugs' distribution and emergence of resistance in patient's lung lesions: A mechanistic model and tool for regimen and dose optimization. *PLoS Med* 2019;16:e1002773.
5. Pienaar E, Sarathy J, Prideaux B, et al. Comparing efficacies of moxifloxacin, levofloxacin and gatifloxacin in tuberculosis granulomas using a multi-scale systems pharmacology approach. *PLoS Comput Biol* 2017;13:e1005650.
6. Nunn AJ, Phillips PPJ, Meredith SK, et al. A trial of a shorter regimen for rifampin-resistant tuberculosis. *N Engl J Med* 2019;380:1201-13.
7. Collaborative Group for the Meta-Analysis of Individual Patient Data in MDR-TB treatment, Ahmad N, Ahuja SD, et al. Treatment correlates of successful outcomes in pulmonary multidrug-resistant tuberculosis: an individual patient data meta-analysis. *Lancet* 2018;392:821-34.
8. Dorman S. [Abstract SP-10] The design and primary efficacy results of Study 31/A5349. 51st Union World Lung Health Conference. Sevilla, Spain2020.

9. Avelox (moxifloxacin hydrochloride). 1990. (Accessed Feb 16, 2021, 2021, at [https://www.accessdata.fda.gov/drugsatfda\\_docs/label/2016/021085s063lbl.pdf](https://www.accessdata.fda.gov/drugsatfda_docs/label/2016/021085s063lbl.pdf).)
10. Lettieri J, Vargas R, Agarwal V, Liu P. Effect of food on the pharmacokinetics of a single oral dose of moxifloxacin 400mg in healthy male volunteers. *Clin Pharmacokinet* 2001;40 Suppl 1:19-25.
11. Thee S, Garcia-Prats AJ, Draper HR, et al. Pharmacokinetics and safety of moxifloxacin in children with multidrug-resistant tuberculosis. *Clin Infect Dis* 2015;60:549-56.
12. Stass H, Lettieri J, Vanevski KM, et al. Pharmacokinetics, safety, and tolerability of single-dose intravenous moxifloxacin in pediatric patients: dose optimization in a phase 1 study. *J Clin Pharmacol* 2019;59:654-67.
13. Winckler JL, Draper HR, Schaaf HS, van der Laan LE, Hesselning AC, Garcia-Prats AJ. Acceptability of levofloxacin, moxifloxacin and linezolid among children and adolescents treated for TB. *Int J Tuberc Lung Dis* 2020;24:1316-8.
14. Klugman KP, Capper T. Concentration-dependent killing of antibiotic-resistant pneumococci by the methoxyquinolone moxifloxacin. *J Antimicrob Chemother* 1997;40:797-802.
15. Johnson JL, Hadad DJ, Boom WH, et al. Early and extended early bactericidal activity of levofloxacin, gatifloxacin and moxifloxacin in pulmonary tuberculosis. *Int J Tuberc Lung Dis* 2006;10:605-12.
16. Panicker GK, Karnad DR, Kadam P, Badilini F, Damle A, Kothari S. Detecting moxifloxacin-induced QTc prolongation in thorough QT and early clinical phase studies using a highly automated ECG analysis approach. *Br J Pharmacol* 2016;173:1373-80.
17. Garcia-Prats AJ, Schaaf HS, Draper HR, et al. Pharmacokinetics, optimal dosing, and safety of linezolid in children with multidrug-resistant tuberculosis: Combined data from two prospective observational studies. *PLoS Med* 2019;16:e1002789.

18. Denti P, Garcia-Prats AJ, Draper HR, et al. Levofloxacin population pharmacokinetics in South African children treated for multidrug-resistant tuberculosis. *Antimicrob Agents Chemother* 2018;62:e01521-17.
19. Guidelines for the programmatic management of drug-resistant tuberculosis—2011 update. 2011. (Accessed Feb 16, 2021, 2021, at [www.who.int/tb/challenges/mdr/programmatic\\_guidelines\\_for\\_mdrtb/en/](http://www.who.int/tb/challenges/mdr/programmatic_guidelines_for_mdrtb/en/).)
20. WHO Treatment guidelines for drug-resistant tuberculosis: 2016 update. 2016. (Accessed Feb 16, 2021, 2021, at <https://apps.who.int/iris/bitstream/handle/10665/250125/9789241549639eng.pdf;jsessionid=9614E58676BC0CF78A458229C6205E67?sequence=1>.)
21. Hutchinson DJ, Johnson CE, Klein KC. Stability of extemporaneously prepared moxifloxacin oral suspensions. *Am J Health Syst Pharm* 2009;66:665-7.
22. Al-Sallami HS, Goulding A, Grant A, Taylor R, Holford N, Duffull SB. Prediction of fat-free mass in children. *Clin Pharmacokinet* 2015;54:1169-78.
23. Growth reference data for 5-19 years. (Accessed May 1, 2020, 2020, at <https://www.who.int/tools/growth-reference-data-for-5to19-years>.)
24. Child growth standards. (Accessed May 1, 2020, 2020, at <https://www.who.int/tools/child-growth-standards>.)
25. Zvada SP, Denti P, Geldenhuys H, et al. Moxifloxacin population pharmacokinetics in patients with pulmonary tuberculosis and the effect of intermittent high-dose rifapentine. *Antimicrob Agents Chemother* 2012;56:4471-3.
26. Chang MJ, Jin B, Chae JW, et al. Population pharmacokinetics of moxifloxacin, cycloserine, p-aminosalicylic acid and kanamycin for the treatment of multi-drug-resistant tuberculosis. *Int J Antimicrob Agents* 2017;49:677-87.

27. Savic RM, Jonker DM, Kerbusch T, Karlsson MO. Implementation of a transit compartment model for describing drug absorption in pharmacokinetic studies. *J Pharmacokinet Pharmacodyn* 2007;34:711-26.
28. Zvada SP, Denti P, Sirgel FA, et al. Moxifloxacin population pharmacokinetics and model-based comparison of efficacy between moxifloxacin and ofloxacin in African patients. *Antimicrob Agents Chemother* 2014;58:503-10.
29. Peloquin CA, Hadad DJ, Molino LP, et al. Population pharmacokinetics of levofloxacin, gatifloxacin, and moxifloxacin in adults with pulmonary tuberculosis. *Antimicrob Agents Chemother* 2008;52:852-7.
30. Willmann S, Frei M, Sutter G, et al. Application of physiologically-based and population pharmacokinetic modeling for dose finding and confirmation during the pediatric development of moxifloxacin. *CPT Pharmacometrics Syst Pharmacol* 2019;8:654-63.
31. Ladumor MK, Bhatt DK, Gaedigk A, et al. Ontogeny of Hepatic Sulfotransferases and Prediction of Age-Dependent Fractional Contribution of Sulfation in Acetaminophen Metabolism. *Drug Metab Dispos* 2019;47:818-31.
32. Bhatt DK, Mehrotra A, Gaedigk A, et al. Age- and Genotype-Dependent Variability in the Protein Abundance and Activity of Six Major Uridine Diphosphate-Glucuronosyltransferases in Human Liver. *Clin Pharmacol Ther* 2019;105:131-41.
33. Kearns GL, Abdel-Rahman SM, Alander SW, Blowey DL, Leeder JS, Kauffman RE. Developmental pharmacology--drug disposition, action, and therapy in infants and children. *N Engl J Med* 2003;349:1157-67.
34. Seneadza NAH, Antwi S, Yang H, et al. Effect of malnutrition on the pharmacokinetics of anti-TB drugs in Ghanaian children. *Int J Tuberc Lung Dis* 2021;25:36-42.
35. Ramachandran G, Kumar AK, Kannan T, et al. Low Serum Concentrations of Rifampicin and Pyrazinamide Associated with Poor Treatment Outcomes in Children with Tuberculosis Related to HIV Status. *Pediatr Infect Dis J* 2016;35:530-4.

36. Brown RE. Organ weight in malnutrition with special reference to brain weight. *Dev Med Child Neurol* 1966;8:512-22.
37. Oshikoya KA, Senbanjo IO. Pathophysiological changes that affect drug disposition in protein-energy malnourished children. *Nutr Metab (Lond)* 2009;6:50.
38. Radtke KK, Dooley KE, Dodd PJ, et al. Alternative dosing guidelines to improve outcomes in childhood tuberculosis: a mathematical modelling study. *Lancet Child Adolesc Health* 2019;3:636-45.
39. Ji HY, Lee H, Lim SR, Kim JH, Lee HS. Effect of efavirenz on UDP-glucuronosyltransferase 1A1, 1A4, 1A6, and 1A9 activities in human liver microsomes. *Molecules* 2012;17:851-60.
40. Naidoo A, Chirehwa M, McIlleron H, et al. Effect of rifampicin and efavirenz on moxifloxacin concentrations when co-administered in patients with drug-susceptible TB. *J Antimicrob Chemother* 2017;72:1441-9.
41. Xu FY, Huang JH, He YC, et al. Population pharmacokinetics of moxifloxacin and its concentration-QT interval relationship modeling in Chinese healthy volunteers. *Acta Pharmacol Sin* 2017;38:1580-8.
42. Taubel J, Ferber G, Fernandes S, Camm AJ. Diurnal profile of the QTc interval following moxifloxacin administration. *J Clin Pharmacol* 2019;59:35-44.
43. Hong T, Han S, Lee J, et al. Pharmacokinetic-pharmacodynamic analysis to evaluate the effect of moxifloxacin on QT interval prolongation in healthy Korean male subjects. *Drug Des Devel Ther* 2015;9:1233-45.
44. Florian JA, Tornoe CW, Brundage R, Parekh A, Garnett CE. Population pharmacokinetic and concentration--QTc models for moxifloxacin: pooled analysis of 20 thorough QT studies. *J Clin Pharmacol* 2011;51:1152-62.

45. Diacon AH, Dawson R, von Groote-Bidlingmaier F, et al. Bactericidal activity of pyrazinamide and clofazimine alone and in combinations with pretomanid and bedaquiline. *Am J Respir Crit Care Med* 2015;191:943-53.
46. Lamprene (clofazimine). 1986. (Accessed Feb 16, 2021, 2021, at [https://www.accessdata.fda.gov/drugsatfda\\_docs/label/2019/019500s014lbl.pdf](https://www.accessdata.fda.gov/drugsatfda_docs/label/2019/019500s014lbl.pdf).)
47. Adler-Shohet FC, Singh J, Nieves D, et al. Safety and Tolerability of Clofazimine in a Cohort of Children With Odontogenic Mycobacterium abscessus Infection. *J Pediatric Infect Dis Soc* 2020;9:483-5.
48. Harausz EP, Garcia-Prats AJ, Law S, et al. Treatment and outcomes in children with multidrug-resistant tuberculosis: A systematic review and individual patient data meta-analysis. *PLoS Med* 2018;15:e1002591.
49. Global Tuberculosis Report. WHO, 2020. (Accessed February 25, 2021, 2021, at <https://www.who.int/publications/i/item/9789240013131>.)



## Chapter 5. Rifapentine population pharmacokinetics and dosing recommendations for latent tuberculosis infection \*

### Abstract

*Rationale:* Rifapentine has been investigated at various doses, frequencies, and dosing algorithms but clarity on the optimal dosing approach is lacking.

*Objectives:* In this individual participant data meta-analysis of rifapentine pharmacokinetics, we characterize rifapentine population pharmacokinetics, including autoinduction, and determine optimal dosing strategies for short-course rifapentine-based regimens for latent tuberculosis infection.

*Methods:* Rifapentine pharmacokinetic studies were identified through a systematic review of literature. Individual plasma concentrations were pooled, and non-linear mixed effects modeling was performed. A subset of data was reserved for external validation. Simulations were performed under various dosing conditions including current weight-based methods and alternative methods driven by identified covariates.

*Measurements and Main Results:* We identified nine clinical studies with a total of 863 participants with pharmacokinetic data (n=4301 plasma samples). Rifapentine population pharmacokinetics were described successfully with a one-compartment distribution model.

---

\* Modified from the publication: Hibma JE and Radtke KK, Dorman SE, Jindani A, Dooley KE, Weiner M, McIlleron HM, Savic RM (2020). Rifapentine Population Pharmacokinetics and Dosing Recommendations for Latent Tuberculosis Infection. *Am J Respir Crit Care Med.* 202(6):866-877. PMID: 32412342.

Autoinduction of clearance was driven by rifapentine plasma concentration. The maximum effect was a 72% increase in clearance and was reached after 21 days. Drug bioavailability decreased by 27% with HIV infection, decreased by 28% with fasting, and increased by 49% with a high-fat meal. Body weight was not a clinically relevant predictor of clearance. Pharmacokinetic simulations showed that current weight-based dosing leads to lower exposures in low weight individuals, which can be overcome with flat dosing. In HIV-positive patients, 30% higher doses are required to match drug exposure in HIV-negative patients.

*Conclusions:* Weight-based dosing of rifapentine should be removed from clinical guidelines and higher doses for HIV-positive patients should be considered to provide equivalent efficacy.

## **Introduction**

The World Health Organization (WHO) estimates that 23% of the world's population has latent tuberculosis infection (LTBI) and is at risk of developing active disease.<sup>1</sup> Standard treatment for LTBI has historically been nine months of daily isoniazid, for which patient compliance is poor and hepatotoxicity is a concern.<sup>2,3</sup> Recently, novel rifapentine-based regimens have demonstrated efficacy in preventing tuberculosis disease with much shorter treatment durations.<sup>4,5</sup> Additionally, these regimens have shown equal to better safety profiles and higher patient compliance. The first regimen was three months of once-weekly rifapentine plus isoniazid (3HP);<sup>4</sup> it received FDA approval in 2014 and is now recommended by the Centers for Disease Control and the WHO for individuals with LTBI.<sup>6-8</sup> An ultra-short-course regimen, one month of daily isoniazid-rifapentine (1HP), has also shown efficacy, safety, and improved compliance in HIV-infected patients at high risk of developing tuberculosis disease;<sup>5</sup> 1HP inclusion into WHO guidelines is under review.<sup>9</sup>

Rifapentine has high anti-mycobacterial activity and a long elimination half-life of 15 hours that makes it an attractive candidate for treatment shortening regimens.<sup>6,10,11</sup> However, unlike in LTBI, it is still unknown if rifapentine will be effective in short-course regimens for active drug-sensitive tuberculosis disease (DS-TB). The only completed Phase 3 clinical trial (Rifaquin) failed to demonstrate non-inferiority of intermittent rifapentine regimens in DS-TB patients compared to the 6-month standard of care.<sup>12</sup>

Robust characterization of rifapentine pharmacokinetics is required to determine optimal dosing strategies for new short-course regimens and for special populations. Current rifapentine-based regimens for LTBI use weight band dosing.<sup>6,8</sup> However, these recommendations are not based on pharmacokinetic evidence; rather, they are drawn from the historical mg/kg doses used in rifampin-based therapy. The influence of body weight on rifapentine clearance remains inconclusive as current studies report conflicting findings.<sup>13,14</sup> Meal-type, dose amount, HIV status, race, and age may also impact rifapentine concentration.<sup>14-18</sup> Additionally, repeated dosing of twice weekly and daily administration results in lower rifapentine exposures over time, suggesting that rifapentine induces its own metabolism.<sup>19,20</sup>

Several pharmacokinetic studies have been conducted with varying rifapentine doses (up to 20 mg/kg daily), frequencies (once weekly to twice daily), and methods (weight-based or flat dose).<sup>19-22</sup> Our aim here was to perform an individual participant data meta-analysis and pool individual pharmacokinetic data from all relevant clinical studies in various populations (healthy volunteers and LTBI and DS-TB patients with and without HIV infection). The goals are (i) to characterize rifapentine population pharmacokinetics, including the time course of autoinduction and relevant covariates that may have a significant clinical impact on rifapentine exposures and

clinical efficacy, and (ii) to derive dosing recommendations to inform optimal current and future use of rifapentine in tuberculosis infection and disease.

## **Methods**

### **Clinical Studies**

Rifapentine pharmacokinetic studies were identified through a literature search in PubMed with the terms 'rifapentine' AND ('study' OR 'trial') from 1 January 1980 to 31 December 2015 according to PRISMA guidelines.<sup>23</sup> Additional studies were identified through author collaborations. Corresponding authors of the study were invited to contribute data if the studies were prospective and multiple dose, pharmacokinetic measurements were available and validated, and covariates of interest were documented (e.g., HIV status, meal-type, and weight). All studies included in the analysis received ethical approval by their local ethical review boards.

### **Population Pharmacokinetic Analysis**

Identified studies were split into an analysis cohort for structural model development and a validation cohort for external validation. We sought to conserve 1/3 of drug concentration data for the validation cohort and to match dosing schedules and covariates (e.g., HIV) between cohorts when possible. Rifapentine plasma concentrations were natural log-transformed and analyzed using non-linear mixed effects modeling with NONMEM 7.41 (ICON Development Solutions, Elliott City, Maryland). Pharmacokinetic parameter estimation was performed with the first-order conditional method. Inter-individual variability was modeled exponentially assuming a log-normal distribution. The residual error was described by an additive error on the individually

predicted logarithmic concentrations (i.e., equivalent to an exponential error on non-logarithmic concentrations). Pharmacokinetic data without an associated dosing record were excluded.

Population pharmacokinetic model building followed standard procedures by first characterizing the base structural model.<sup>24</sup> One and two compartment disposition models were evaluated with first-order absorption to describe rifapentine pharmacokinetics. Drug absorption delays were further evaluated with the addition of a lag time or a more flexible chain of transit compartments. Since only oral data were available, the relative bioavailability was fixed to 1. Inter-individual variability was tested on absorption parameters (i.e., bioavailability and mean transit time), drug clearance, and volume of distribution. Once a stable model was established, previously identified and well-established covariates (i.e., dose, meal-type, and HIV status) were incorporated into the base structural model followed by formal statistical assessment. Next, rifapentine autoinduction was described by employing a semi-mechanistic enzyme turnover model.<sup>25</sup>

Following model evaluation, pharmacokinetic parameters were re-estimated with all data (analysis and validation datasets), and covariate analysis was performed to further explore factors that explain inter-individual variability in clearance and/or bioavailability. Additional candidate covariates included weight, age, race, BMI and sex. Covariates were identified using stepwise covariate modeling (SCM) approach: covariates were added one at a time and then removed one at a time in a stepwise manner and evaluated using the likelihood ratio test. A significance level of  $p < 0.05$  was used for forward selection, and  $p < 0.01$  was used for backward elimination. Final inclusion of identified covariates considered statistical significance, clinical relevance, and scientific plausibility. The threshold for clinical relevance was a 20% change in the parameter estimate.<sup>26</sup>

Model development was guided by graphical assessment of goodness-of-fit plots, condition number, and the likelihood ratio test. Simulation-based diagnostics, or visual predictive checks (VPCs), were used for model validation. Due to large variability in the dose for the combined dataset, the observed and simulated concentrations were normalized based on the typical population predictions.<sup>27</sup> VPCs were based on 500 simulations using fixed and random effect parameter estimates, including dosing information and demographic information for each subject. The precision of all final parameters was evaluated using a nonparametric bootstrap approach with 1,000 resampled datasets. The predictive performance of the model was evaluated through an external model validation: 500 simulations of rifapentine concentration were performed with the validation cohort using the base structural model and parameter estimates from the analysis cohort alone. Simulated concentrations were compared to observed concentrations through VPC.

### **Rifapentine metabolite modelling procedures**

To complete the model, 25-desacetyl-rifapentine concentration data were added and modeled. All the included studies except Riomar and Rifaquin had metabolite data to contribute. All parameters from the parent drug model were fixed except residual variability. Then, the metabolite clearance ( $CL_m$ ) and volume of distribution ( $V_d$ ) were estimated. One and two compartment distribution models were tested, along with nonlinear elimination, and dose-dependent fraction metabolized ( $f_m$ ) in accordance with previously published models.<sup>14,15,17</sup> Stepwise covariate modeling was also performed; weight, HIV status, and sex were tested on metabolite parameters. Those with statistically significant effects and clinically relevant effect sizes were included in the model.

## Software

R software (version 3.4.2) was used for all data management, analyses, and graphical visualization. The `xpose` (version 0.4.4) and `vpc` (version 1.0.1) packages were used for visual diagnostics. Nonparametric bootstrap and covariate modeling were performed with `Perl-speaks-NONMEM` (version 4.7.0).

## Dosing simulations

Simulations were performed with the final model to (i) predict the autoinduction process with different doses and dosing schedules, (ii) assess the impact of clinically relevant patient factors (e.g., HIV, weight) on rifapentine exposure, and (iii) to propose pragmatic dosing for rifapentine-containing LTBI regimens. Pharmacokinetic profiles were evaluated by different drivers of pharmacodynamics, including time above minimum inhibitory concentration (MIC), area under the concentration-time curve (AUC), AUC/MIC, maximum concentration ( $C_{max}$ ), and  $C_{max}/MIC$ , with MIC set to 0.06 mg/L.<sup>28</sup> For 1HP and 3HP simulations, we predicted rifapentine exposure following current weight band dosing (1HP: 300 mg [ $<35$  kg], 450 mg [ $35-45$  kg], or 600 mg [ $>45$  kg] daily; 3HP: 750 mg [ $<50$  kg] and 900 mg [ $\geq 50$  kg] once weekly).<sup>4,5</sup> Alternative dosing methods were explored based on identified covariates. All simulations were performed under low-fat meal conditions (the referent, where relative bioavailability =1) given label recommendations.

## Univariate analysis of month 2 culture conversion

Microbiological outcome data (i.e., liquid and solid culture data) was acquired from two Phase II clinical studies: TBTC-29 and TBTC-29x.<sup>22,29</sup> Participant body weight and rifapentine AUC were evaluated as predictors of month 2 culture conversion by logistic regression. Body weight was categorized as  $< 50$  kg or  $\geq 50$  kg, consistent with the weight band dosing strategy used in these studies. AUC was categorized at the median AUC.

## Results

### Clinical Studies

We identified nine clinical studies with rifapentine pharmacokinetic data for the pooled analysis (**Figure 5.1**), including Phase 3 (n=2), Phase 2 (n=4), and Phase 1 (n=3) studies.<sup>12,14,19-21,29-32</sup>

Overall, 863 subjects were included: 84 healthy volunteers, 702 patients with DS-TB, and 77 persons treated for LTBI. The analysis cohort included 360 subjects (n=3273 samples) from five studies. The validation cohort included 503 subjects (n=1115 samples) from four studies.

Participant and trial characteristics are shown in **Table 5.1**. The analysis and validation cohorts were similar in design and participant characteristics. Overall, the median age was 34 years, the median weight was 59 kg, 31% were men, and 9% of patients were HIV-positive. There was a wide range of rifapentine doses, dosing frequencies, and diets that were tested across studies (**Table 5.1**).



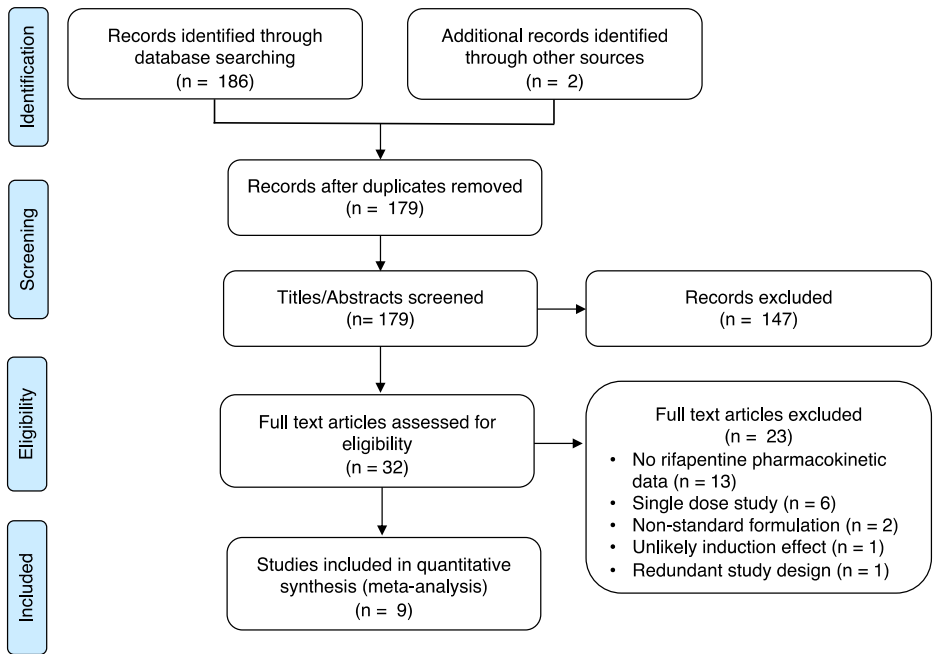


**Figure 5.1** PRISMA Flow Diagram.

**Table 5.1** Baseline characteristics of the study participants in the pooled datasets

Trial* (Ref)	Rifapentine Regimen	N Individuals, (N samples)	Age, yr	Weight, kg	Female sex	HIV-positive
<b>Analysis cohort</b>						
06-0050 <sup>19</sup> Phase 1 HV PM	900 mg thrice weekly with low fat meal	14, (269)	41 (24-64)	76 (50-97)	3 (21.4)	-
Rifaquin <sup>12</sup> Phase 3 DS-TB PM	900 mg twice weekly or 1200 mg once weekly with high-fat meal	241, (846)	32 (18-80)	56 (38-78)	88 (36.5)	46 (19.1)
TBTC-29B <sup>14</sup> Phase 1 HV P[Mdz]	5 - 20 mg/kg once daily with low-fat meal	26, (504)	47 (24-60)	82 (60-99)	5 (19.2)	-
TBTC-25 <sup>30</sup> Phase 2 DS-TB PH	600, 900, or 1200 mg once weekly on empty stomach	35, (357)	44 (18-68)	65 (46-110)	12 (34.3)	-
ACTG-A5311 <sup>21</sup> Phase 1 HV P	10 mg/kg twice daily or 15 or 20 mg/kg once daily with low- or high-fat meal	44, (1210)	35 (20-59)	82 (60-99)	12 (27.3)	-
<b>Validation cohort</b>						
TBTC-29X <sup>29</sup> Phase 2 DS-TB PHZE	10, 15, or 20 mg/kg once daily with high-fat meal	225, (713)	30 (18-70)	55 (40-83)	66 (29.3)	19 (8.4)
TBTC-26 <sup>31</sup> Phase 3 LTBI PH	900 mg once weekly with food	77, (77)	40 (19-63)	81 (49-169)	37 (48.1)	-
TBTC-29 <sup>22</sup> Phase 2 DS-TB PHZE	10 mg/kg 5 days per week on empty stomach	158, (158)	36 (18-86)	60 (40-101)	46 (29.1)	16 (10.1)
RioMar <sup>32</sup> Phase 2 DS-TB PHMZ	7.5 mg/kg once daily with food	43, (167)	-	58 (45-83)	NR	-

Data are expressed as median (range) or number (percentage).

\* A description of each trial is below including study phase, population, and drug regimen.

*Definition of abbreviations:* NR = not recorded; HV= healthy volunteers; DS-TB = drug-sensitive tuberculosis; LTBI = latent tuberculosis infection; P = rifapentine; H = isoniazid. M = moxifloxacin; [Mdz] = midazolam, only administered in some of the study participants; Z = pyrazinamide; E = ethambutol.

## Pharmacokinetic-enzyme model

The final rifapentine pharmacokinetic-enzyme model is shown in **Figure 5.2**, and final parameter estimates are in **Table 5.2**. All pharmacokinetic parameters were well estimated with low relative standard errors. Rifapentine apparent clearance was estimated to be 1.11 L/h in the typical adult and increased up to 1.92 L/h (173%) over time as a result of autoinduction. The induction process was described using an indirect response semi-mechanistic enzyme turnover model (**Figure 5.2**). The full compartmental model for rifapentine pharmacokinetics with incorporated autoinduction can be represented with equations (Eq) 5.1-5.3, where Eq 5.1 represents the amount of drug in the absorption compartment ( $A_a$ ) with a series of  $n$  transit compartments,<sup>33</sup> Eq 5.2 represents the amount of drug in the central compartment ( $A_c$ ), and Eq 5.3 is the amount of enzyme (ENZ), initially equal to 1 and increased as a result of the drug effect (EFF):

$$\text{Eq 5.1} \quad \frac{dA_a}{dt} = F \cdot \text{Dose} \cdot k_{tr} \cdot \frac{(k_{tr} \cdot t)^n \cdot e^{-k_{tr} \cdot t}}{\sqrt{2\pi} \cdot n^{n+0.5} \cdot e^{-n}} - k_a \cdot A_a$$

$$\text{Eq 5.2} \quad \frac{dA_c}{dt} = k_a \cdot A_a - \text{CL}/V \cdot A_c \cdot \text{ENZ}$$

$$\text{Eq 5.3} \quad \frac{d\text{ENZ}}{dt} = k_{\text{ENZ}} \cdot (1 + \text{EFF}) - k_{\text{ENZ}} \cdot \text{ENZ}$$

$$\text{Eq 5.4} \quad \text{EFF} = \left( \frac{E_{\text{max}} \cdot C_p^\gamma}{\text{EC}_{50}^\gamma + C_p^\gamma} \right)$$

In the above equations,  $k_{tr}$  is the transit rate constant,  $F$  is relative bioavailability,  $k_a$  is the absorption rate constant,  $\text{CL}$  is the clearance,  $V$  is the volume of distribution, and  $k_{\text{ENZ}}$  is the enzyme turnover rate. Linear and nonlinear drug effect (EFF) relationships were evaluated as a function of rifapentine concentration in plasma ( $C_p$ ); the sigmoid maximum effect ( $E_{\text{max}}$ ) model

was the best (Eq. 5.4), with an estimated concentration at 50% maximum effect ( $EC_{50}$ ) of 4.27 mg/L and steepness factor ( $\gamma$ ) of 10. Maximum autoinduction is expected at the steady state concentrations achieved with daily doses of 300 mg or more, and clearance stabilizes by day 21 of therapy, assuming 5 half-lives to steady state (**Figure 5.3**).

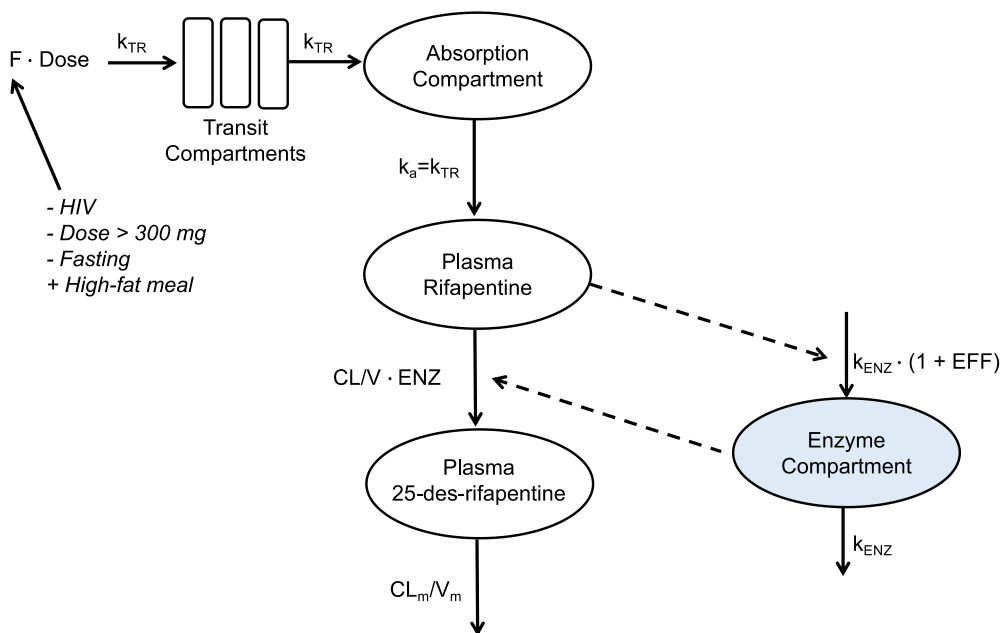


**Figure 5.2** Final rifapentine pharmacokinetic-enzyme model.

The number of transit compartments (NN) was estimated using the relationship of  $k_{TR} = (NN+1)/\text{MTT}$ , where MTT is the mean transit time and  $k_{TR}$  is the transit rate constant. The absorption rate constant ( $k_a$ ) was assumed equal to  $k_{TR}$ . Rifapentine autoinduction was modeled with an enzyme turnover model, where the effect (EFF) of rifapentine concentration in the central compartment increased the enzyme production rate ( $k_{ENZ}$ ), thereby increasing the enzyme pool (ENZ). Rifapentine clearance (CL) increased as a result of increased ENZ. V is the apparent volume of distribution. The fraction of the drug absorbed (F; relative bioavailability) increased (+) or decreased (-) as indicated.

**Table 5.2.** Final parameter estimates for the rifapentine population pharmacokinetic model

Parameter	Population Estimate		Inter-individual variability	
	Value [%RSE]	95% CI <sup>†</sup>	%CV [%RSE]	95% CI <sup>†</sup>
CL/F (L/h)	1.11 [1.92]	0.952 - 1.48	24.3 [9.34]	12.8 - 28.0
V/F (L)	36.7 [1.99]	28.5 - 40.9	17.6 [17.7]	10.5 - 24.0
MTT (h)	1.94 [2.97]	1.83 - 2.04	-	-
NN	2.15 [5.44]	1.66 - 2.70	-	-
Bioavailability	100 <i>fixed</i>	-	29.8 [10.8]	21.5 - 34.6
Fixed effects on bioavailability <sup>‡</sup>				
Dose	0.0167 [5.30]	0.00343 - 0.0287	-	-
HIV infection	0.729 [6.26]	0.584 - 0.815	-	-
High-fat meal	1.49 [3.05]	1.37 - 1.64	-	-
Fasting	0.731 [5.51]	0.546 - 0.776	-	-
k <sub>ENZ</sub> (h <sup>-1</sup> ) <sup>* , ††</sup>	0.00587 [32.1]	0.00291 - 0.0135	-	-
E <sub>max</sub> (%) <sup>*</sup>	73.0 [25.2]	51.0 - 116	-	-
EC <sub>50</sub> (mg/L) <sup>*</sup>	4.27 [39.8]	1.80 - 6.57	-	-
γ	10 <i>fixed</i>	-	-	-
Residual error of rifapentine	0.577 [4.13]	0.573 - 0.699	-	-
CL <sub>m</sub> /f <sub>m</sub> (L/h)	3.11 [12.2]	1.89-6.26	40.0 [6.69]	34.2-44.6
V <sub>m</sub> /f <sub>m</sub> (L)	2.15 [7.07]	1.67-3.15	-	-
f <sub>m, dose</sub> <sup>**</sup>	0.0185 [3.56]	0.0004 -0.0266	-	-
HIV effect on CL <sub>m</sub>	1.36 [9.85]	-	-	-
Residual error of metabolite	0.631 [5.59]	0.560-0.695	-	-

<sup>\*</sup> autoinduction parameters were estimated based on the analysis dataset alone.

<sup>†</sup> Confidence intervals were based on 926 (out of 1000) successful bootstrap runs for rifapentine model and 999 (out of 1000) successful bootstrap runs for metabolite model.

<sup>‡</sup> Fixed effects on bioavailability (F) were relative to HIV-negative individuals taking 300 mg of rifapentine with a low-fat meal, where F=1 for each reference condition. Relative bioavailability is calculated as:  $F = F_{\text{dose}} * F_{\text{HIV}} * F_{\text{high-fat}} * F_{\text{fasting}}$ , where  $F_{\text{dose}}$  is the relative reduction in bioavailability per 100 mg above 300 mg (equal to  $1 - \text{estimate} * (\text{dose}/100 \text{ mg})$ ),  $F_{\text{HIV}}$  is the relative bioavailability in HIV-positive individuals,  $F_{\text{high-fat}}$  is the relative bioavailability with a high-fat meal (vs. low-fat meal), and  $F_{\text{fasting}}$  is the relative bioavailability with fasting (vs. low-fat meal).

<sup>††</sup> Translates to an enzyme turnover half-life of 118 hours.

<sup>\*\*</sup> Fraction metabolized is a function of dose, where  $f_m = 1 - f_{m, \text{dose}} * (\text{dose}/100 \text{ mg})$ .

*Definition of abbreviations:* RSE=relative standard error; CI=confidence interval; CV=coefficient of variation; CL/F=apparent clearance; V/F=apparent volume of distribution; MTT=mean transit time; NN=number of transit compartments; k<sub>ENZ</sub>=enzyme production rate; EC<sub>50</sub>=concentration where effect is 50% of maximum; E<sub>max</sub>=maximum effect; γ =steepness for E<sub>max</sub> equation; CL<sub>m</sub>/f<sub>m</sub> =metabolite clearance; V<sub>m</sub>/f<sub>m</sub> =metabolite volume of distribution; f<sub>m, dose</sub>= dose-dependent reduction in fraction metabolized.

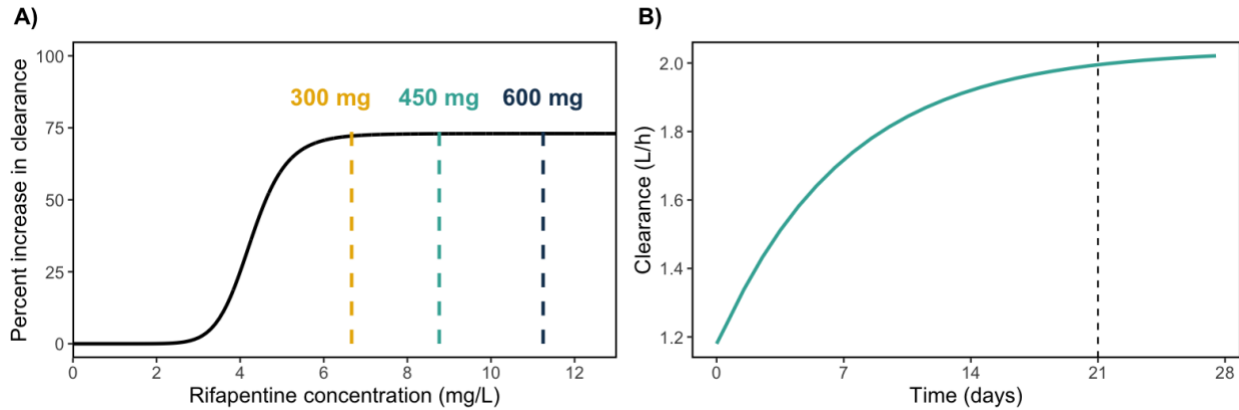


**Figure 5.3** Rifapentine autoinduction profile.

(A) The sigmoid relationship between rifapentine concentration and autoinduction is shown in the black line. Dashed lines represent the average concentration at steady state of daily therapy with 300 mg (yellow), 450 mg (green), and 600 mg (navy) of rifapentine in a typical HIV-negative individual. (B) Rifapentine induction over time following daily administration of 600 mg. Black dashed line represents the time at which the induction process reaches steady state.

### Rifapentine model evaluation and validation

The VPC of the basic structural model (built with analysis cohort data alone) shows that the model predicted the analysis cohort raw data well: the median, 5<sup>th</sup>, and 95<sup>th</sup> percentiles of raw data fell within or near the percentiles of model-predicted concentrations for all time points (**Figure 5.4A**). Further, we show that model-predicted concentrations matched the raw data of an external dataset (i.e., the validation cohort, which was not used in model development; **Figure 5.4B**). After model validation, data from both cohorts were pooled and parameters re-estimated. The final model predicted rifapentine concentrations well for all studies (**Figure 5.5**).

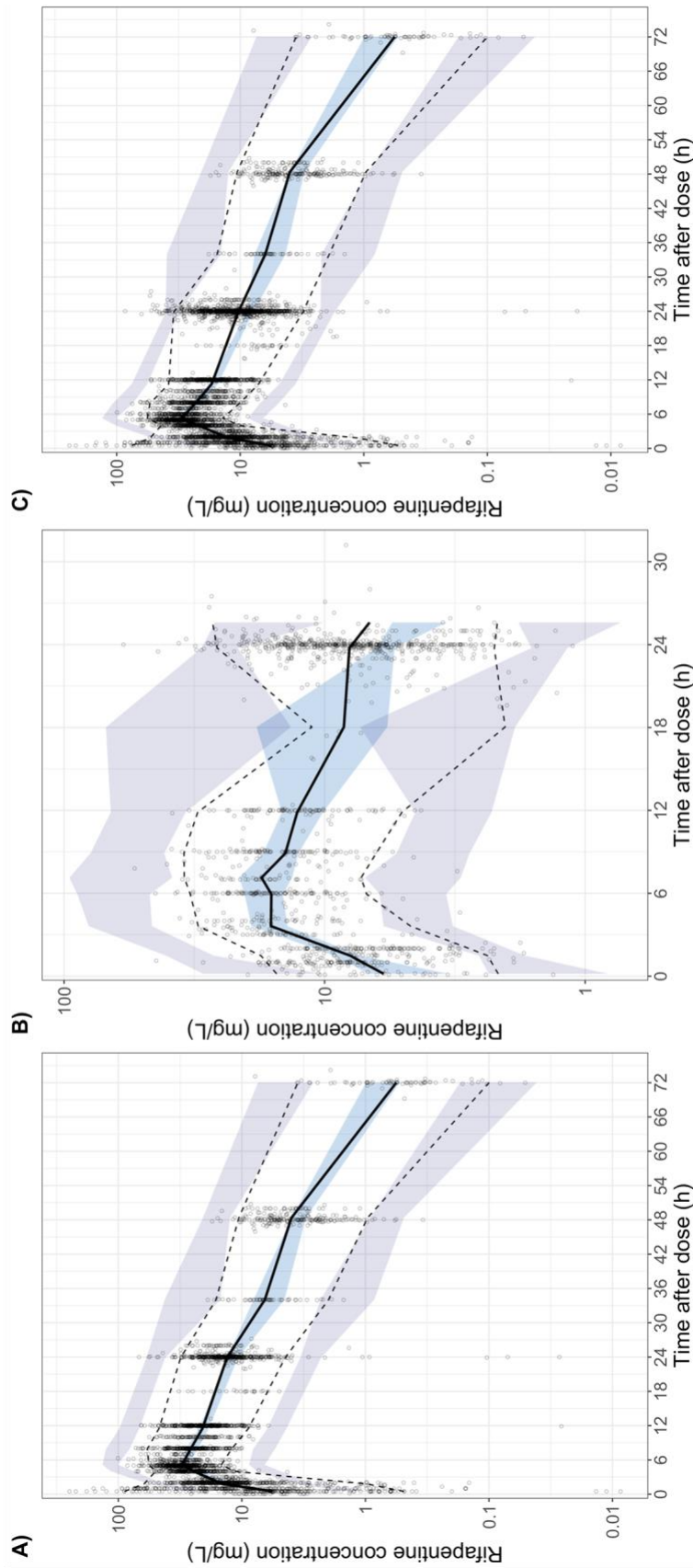


**Figure 5.4.** Validation of the structural rifampentine population pharmacokinetic model. Prediction-corrected visual predictive check (VPC) of base model with (A) analysis dataset, (B) validation dataset, and (C) combined dataset. Figures show the model predictions (shaded areas) compared to observed/raw rifampentine concentrations (dots). Model predictions were based on the base structural model, built from the analysis dataset alone. The 5<sup>th</sup> (dashed line), 50<sup>th</sup> (solid line), 95<sup>th</sup> (dashed line) percentiles of the observed raw data are overlaid onto the 95% confidence intervals of model-predicted concentrations at the 50<sup>th</sup> (light blue), and 5<sup>th</sup> and 95<sup>th</sup> (dark blue) percentiles, obtained from 500 simulations of each respective dataset.

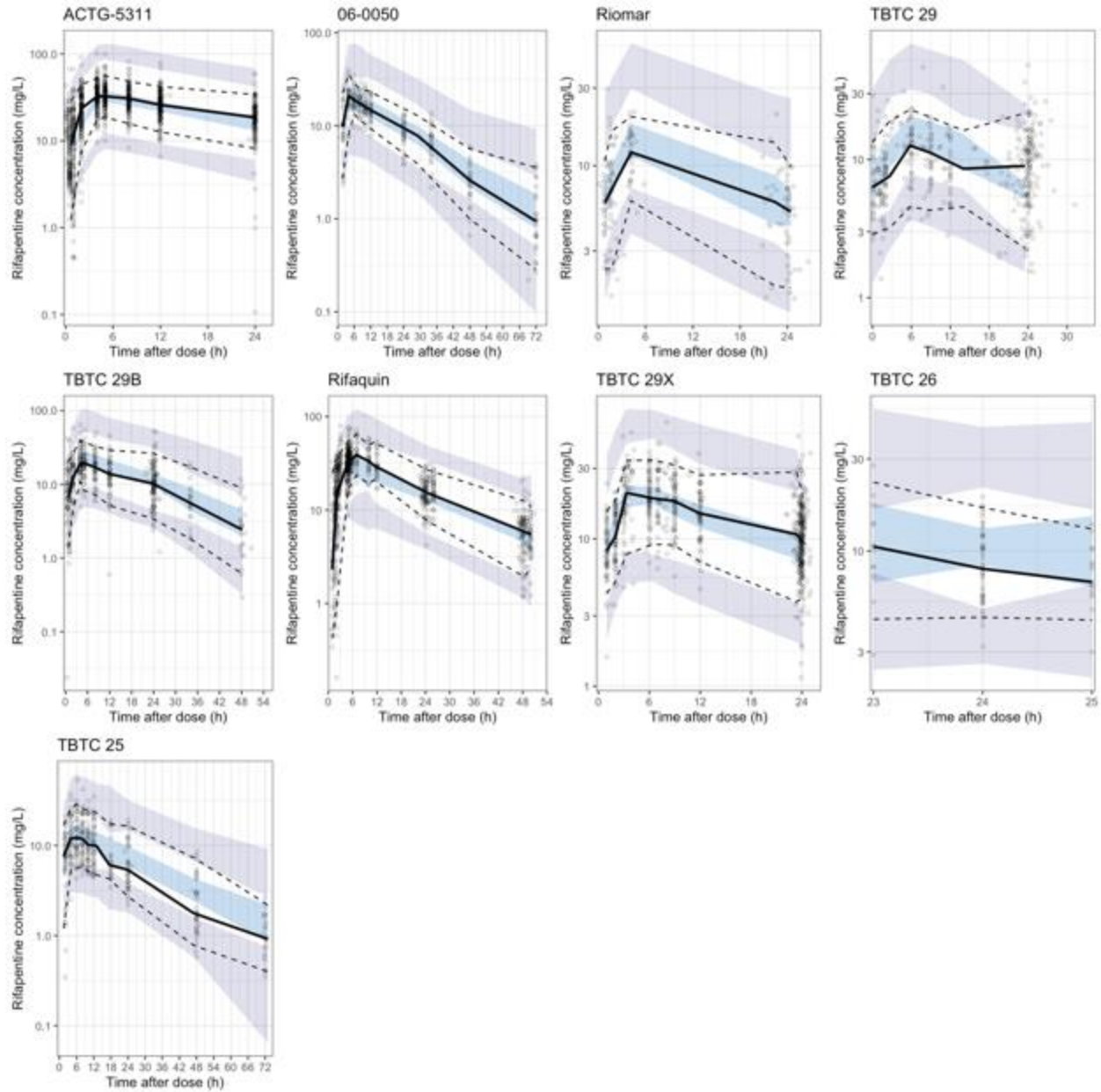


**Figure 5.5** Final visual predictive check (VPC) of full rifapentine population pharmacokinetic model, stratified by study.

Dots represent observed rifapentine concentrations. Lines correspond to 5<sup>th</sup> (dashed), 50<sup>th</sup> (solid), 95<sup>th</sup> (dashed) percentiles of observed data. Shaded areas are the model-predicted 95% confidence intervals for the median (light blue), and 5<sup>th</sup> and 95<sup>th</sup> (dark blue) percentiles obtained from 500 simulated datasets.



## Rifapentine metabolite model results

The pharmacokinetics of 25-desacetyl-rifapentine were best described with a one compartment distribution model with first order elimination and dose-dependent fraction metabolized. The typical  $CL_m$  was 3.11 L/h and  $V_m$  was 2.15 L. HIV infection was found to be a strong predictor ( $p < 0.001$ ) of  $CL_m$ , such that HIV-positive individuals had 35% higher  $CL_m$ . Model evaluation through VPC (**Figure 5.6**) demonstrated that the model predicted the metabolite concentrations well.

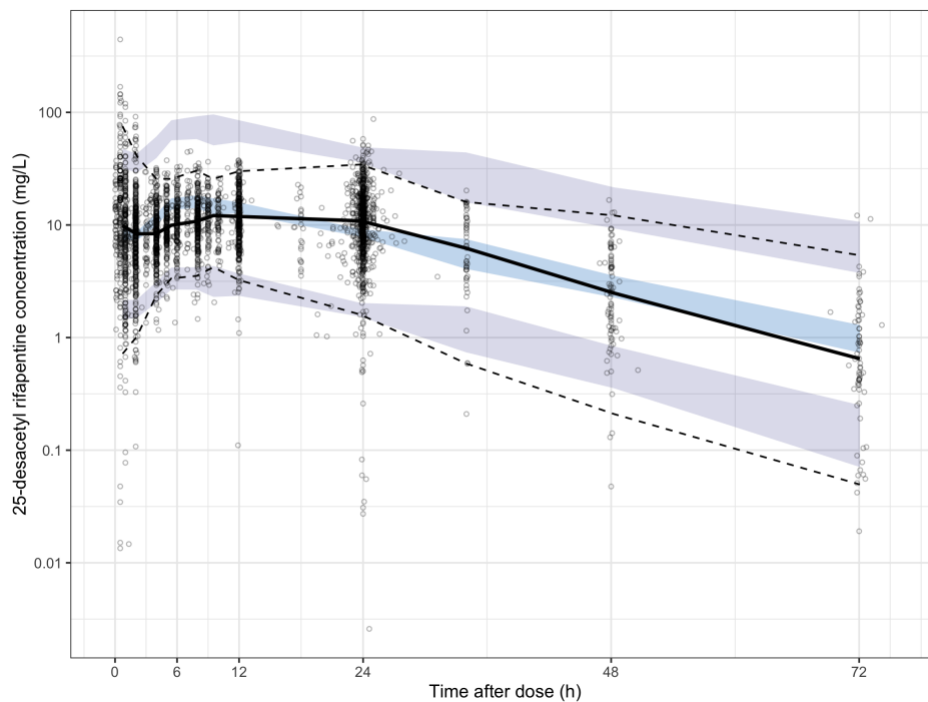


**Figure 5.6** Visual predictive check (VPC) of 25-desacetyl-rifapentine (i.e., metabolite) pharmacokinetic model.

Dots represent observed 25-desacetyl-rifapentine concentrations. Lines correspond to 5<sup>th</sup> (dashed), 50<sup>th</sup> (solid), 95<sup>th</sup> (dashed) percentiles of observed data. Shaded areas are the model-predicted 95% confidence intervals for the median (light blue), and 5<sup>th</sup> and 95<sup>th</sup> (dark blue) percentiles obtained from 500 simulated datasets. The dependent variable was prediction corrected.<sup>27</sup>

## Impact of covariates on rifapentine pharmacokinetics

Rifapentine bioavailability was strongly ( $p < 0.001$ ) influenced by HIV status, food, and dose with clinically relevant effect sizes. The relative effects on bioavailability of HIV-positive status (vs. HIV-negative), high-fat meal or fasting condition (vs. low-fat meal), and dose per 100 mg above 300 mg (the referent) are shown in **Table 5.2**. Body weight was related to rifapentine clearance ( $p < 0.001$ ) with a 0.1 L/h (9%) increase in clearance per 10 kg increase in weight (**Figure 5.7**). However, weight explained only 2.9% of the inter-individual variability in clearance, and the effect size did not meet our criteria for clinical relevance. Further, the majority of statistical significance was from a few influential individuals over 90 kg in weight (**Figure 5.8**). Allometrically scaling clearance did not provide any additional improvement over the linear relationship, and the functions were nearly identical at relevant weight ranges (40-100 kg). Therefore, the only covariates included in the final model were HIV, food, and dose.

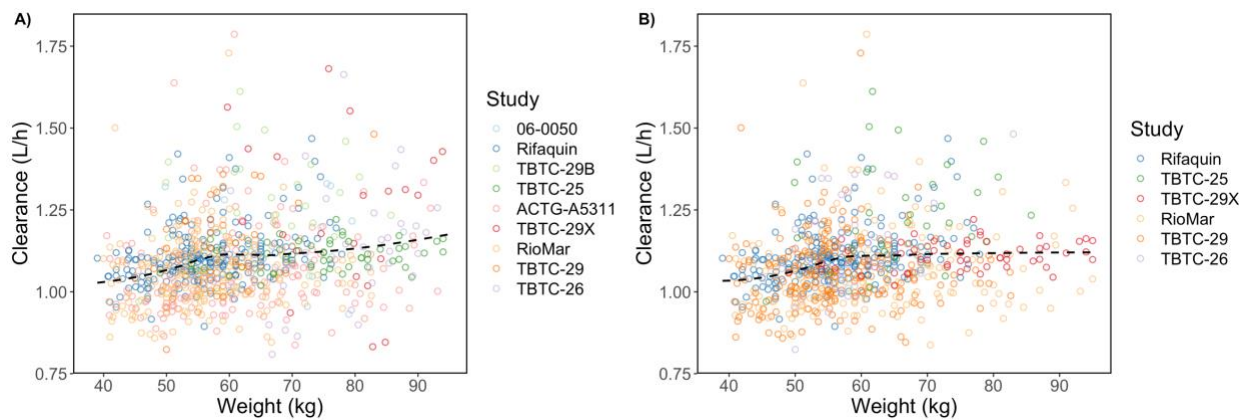


**Figure 5.7** Relationship between weight and rifapentine clearance. The relationship was assessed for (A) all subjects and (B) only DS-TB and LTBI patients with final model parameter estimates. Dashed line represents loess regression curve.

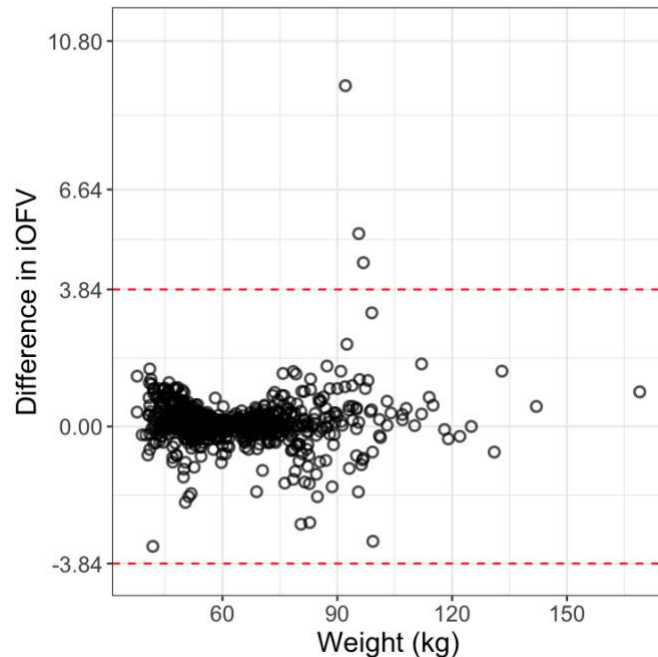


**Figure 5.8** Individuals influencing the relationship between weight and clearance. Each circle represents one individual. Influential individuals are those with change in iOFV > |3.84|. Red dashed lines represent the statistical significance threshold ( $p=0.05$ ) per likelihood ratio test. iOFV = individual objective function.

### Rifapentine simulations of different dosing schedules

The effect of dose and dosing frequency on rifapentine pharmacokinetics is shown in **Figure 5.9**. With intermittent dosing, autoinduction was minimal to moderate and clearance increased slightly with larger doses (**Table 5.5**). With daily dosing, maximum induction was achieved with doses of 300 mg or more. All dosing schedules were able to maintain concentrations above MIC during the dosing interval except once weekly in which concentrations fall below MIC just prior to the next dose.  $C_{max}/MIC$  and  $AUC/MIC$  were highest with daily dosing, due to drug accumulation, and increased with increasing dose (**Table 5.4**).

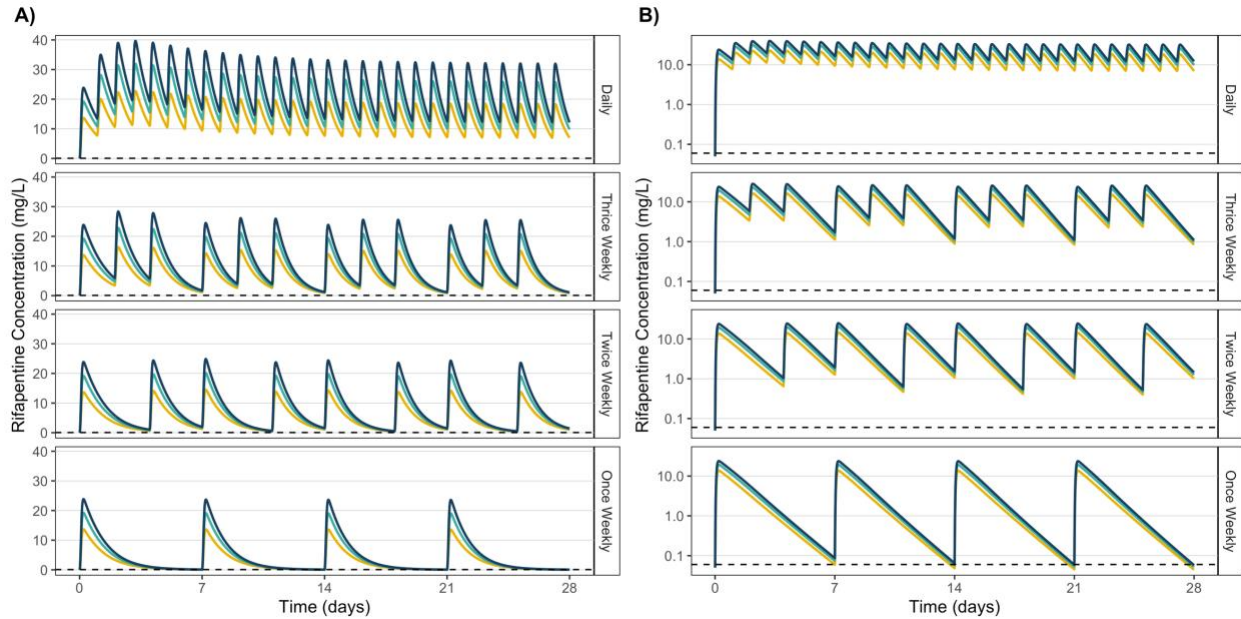


**Figure 5.9** Effect of dose and dosing frequency on rifapentine exposure. (A) Rifapentine concentration over time, and (B) concentration over time in log-scale, in a typical HIV-uninfected individual following once daily, thrice weekly, twice weekly, and once weekly administration of 600 mg (yellow), 900 mg (green), or 1200 mg (dark blue). Black dashed line = minimum inhibitory concentration (MIC; equal to 0.06 mg/L)

**Table 5.3** Change in rifapentine clearance by dose and dosing frequency. Values reflect the percent change from first dose to last dose of a one-month treatment course.

	Increase in clearance			
	Once Weekly	Twice Weekly	Thrice Weekly	Daily
<b>600 mg</b>	16%	29%	44%	72%
<b>900 mg</b>	20%	35%	52%	72%
<b>1200 mg</b>	26%	39%	56%	72%

**Table 5.4.** Pharmacokinetic-pharmacodynamic indices by rifapentine dose and dosing frequency.

	<b>AUC/MIC</b>	<b>Free AUC/MIC</b>	<b>C<sub>max</sub>/MIC</b>	<b>Free C<sub>max</sub>/MIC</b>
600 mg once weekly	3936	78.7	226.4	4.5
600 mg twice weekly	4011	80.2	236.8	4.7
600 mg thrice weekly	3846	76.9	232.1	4.6
600 mg daily	4928	98.6	308.6	6.2
900 mg once weekly	5481	109.6	317	6.3
900 mg twice weekly	5500	110	328.5	6.6
900 mg thrice weekly	5248	105	321.2	6.4
900 mg daily	6921	138.4	433.2	8.7
1200 mg once weekly	6773	135.5	393.1	7.9
1200 mg twice weekly	6733	134.7	405.1	8.1
1200 mg thrice weekly	6415	128.3	395.8	7.9
1200 mg daily	8600	172	538.1	10.8

Values reflect a typical HIV-negative individual. AUC was integrated over 24 hours on day 21 of therapy, and thus, reflects steady state AUC for daily dosing. Free AUC and C<sub>max</sub> assume a fraction unbound of 0.02. MIC (minimum inhibitory concentration) was set to 0.06 mg/L. AUC = area under the concentration time curve. C<sub>max</sub> = maximum concentration.

### Rifapentine simulations for 1HP and 3HP therapy

We simulated rifapentine drug concentrations under the 1HP and 3HP regimens for LTBI in both HIV-positive and HIV-negative adults. The typical HIV-positive patient had lower drug concentrations than the typical HIV-negative patient when given the same dose due to decreased rifapentine bioavailability (**Figure 5.10**). Lower drug concentrations are also predicted in low weight individuals with the current weight band dosing. Removing weight bands and administering the same flat dose to all individuals would result in equal exposures across weights; however, it did not equalize exposures by HIV status (**Figure 5.11**). With a stratified regimen, where HIV-positive individuals receive ~30% higher doses, similar exposures are expected by HIV status and weight for both 1HP and 3HP (**Figure 5.11**).

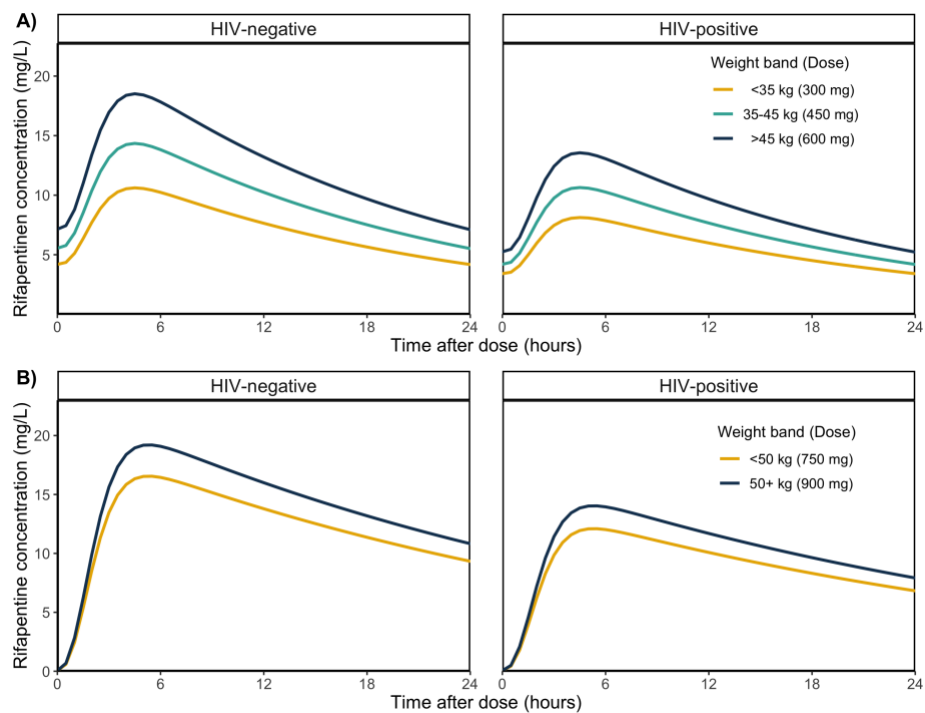


**Figure 5.10** Pharmacokinetic profiles of rifapentine following (A) 1HP and (B) 3HP regimens. Concentration-time profiles over 24 hours are shown for the typical adult by HIV status on (A) day 21 of therapy, to reflect steady state concentrations, and (B) after first dose since no accumulation occurs with weekly dosing.

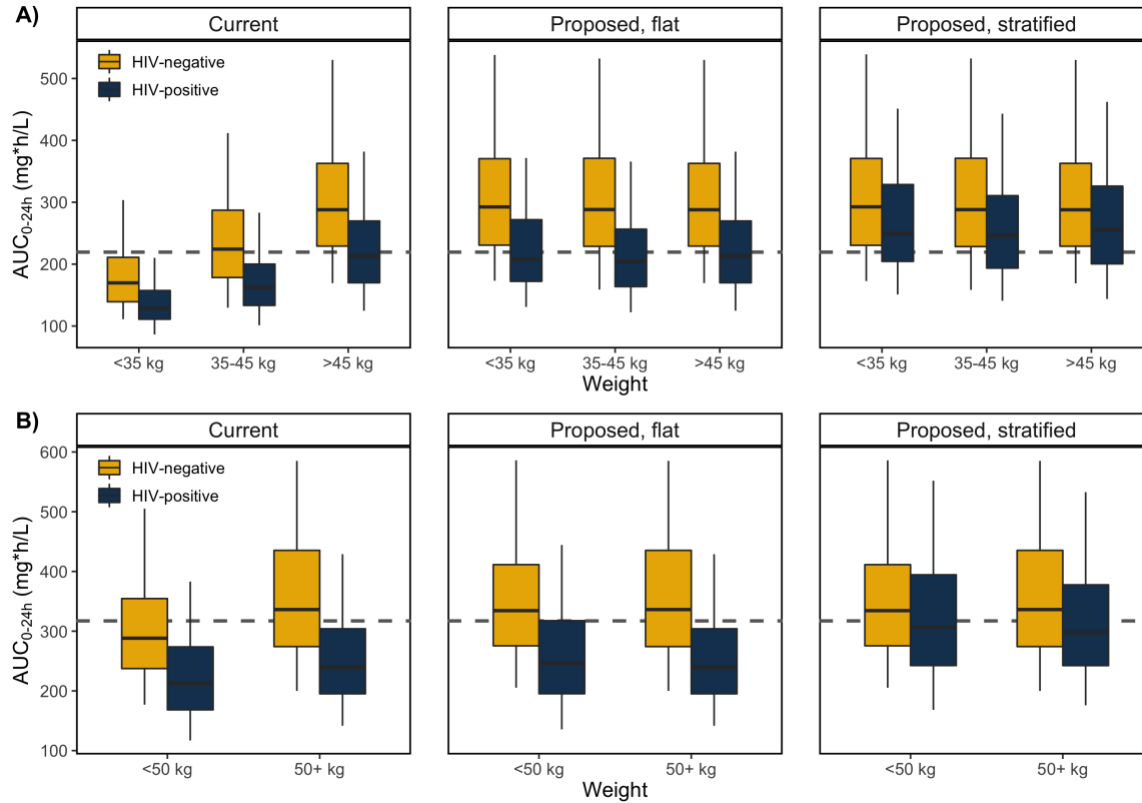


**Figure 5.11** Predicted rifapentine exposures with different dosing methods for (A) 1HP and (B) 3HP regimens.

Drug exposure over 24 hours ( $AUC_{0-24h}$ ) profiles are based on 500 simulations. (A) 1HP predictions reflect steady state exposures to account for autoinduction. ‘Weight band’ rifapentine doses were 300 mg for < 35 kg, 450 mg for 35-45 kg, and 600 mg for >45 kg, as currently recommended for 1HP. The ‘Flat’ approach prescribed 600 mg to all individuals, and ‘HIV stratified’ increased dose in HIV-positive to 750 mg. (B) 3HP doses were 750 mg for <50 kg and 900 mg for 50+ kg for the ‘weight band’ approach, as currently recommended. The ‘Flat’ approach prescribed 900 mg to all individuals, and ‘HIV stratified’ increased dose in HIV-positive to 1200 mg. Gray dashed lines represent (B) the median  $AUC_{0-24h}$  (=317 mg\*h/L) observed in patients treated with 3HP in the PREVENT-TB trial (i.e., TBTC-26) and (A) the median predicted  $AUC_{0-24h}$  in HIV-positive patients with 600 mg daily (=219 mg\*h/L).

## Univariate analysis of month 2 culture conversion

A total of 363 individuals treated with 10 mg/kg rifapentine had Phase II microbiological data available. Univariate logistic regression results for month 2 culture conversion of liquid media are shown in **Figure 5.12**. Month 2 culture conversion was less likely in individuals who had lower rifapentine AUC (Odds ratio = 0.49) and in those who weighed less than 50 kg (Odds ratio = 0.60).

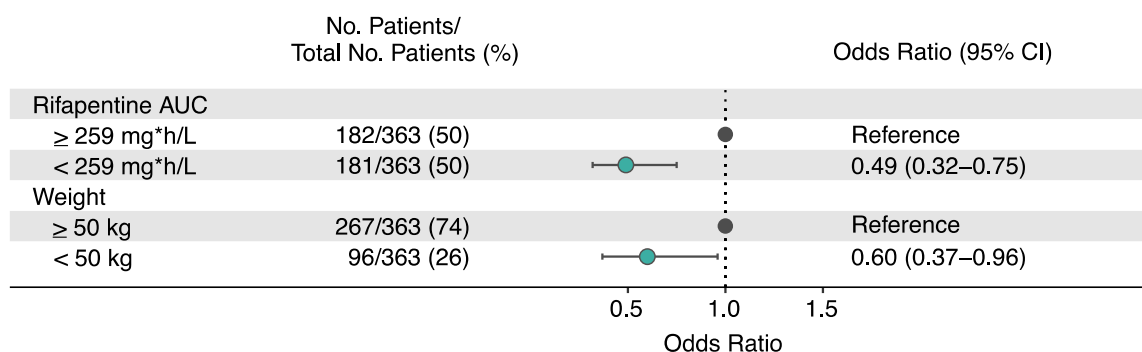


**Figure 5.12** Predictors of month 2 culture conversion.

Data were acquired from two Phase II clinical studies (TBTC29, TBTC29x) where participants received 10 mg/kg rifapentine daily. Odds ratios are from univariate analysis.

## Discussion

In this study, we used a pooled individual-data approach with an external validation to describe rifapentine population pharmacokinetics in a large cohort of subjects. This analysis included nine clinical studies with a wide range of rifapentine doses and scheduling frequencies, allowing for successful characterization of rifapentine autoinduction with respect to drug concentration. It represents the largest analysis of rifapentine population pharmacokinetics to date. Our results



establish several findings that may help guide rifapentine dosing strategies: (i) pharmacokinetic data do not support dosing rifapentine by body weight; (ii) HIV-positive individuals require at least 30% higher doses to achieve equal drug exposures to HIV-negative persons; (iii) rifapentine autoinduction is strongly influenced by dosing frequency rather than dose amount.

Since rifapentine's approval, several studies have shown evidence of rifapentine inducing its own elimination but none have characterized autoinduction with respect to rifapentine concentration.<sup>14,16,17,19,20</sup> Previously published models have described rifapentine autoinduction empirically with time-varying clearance model<sup>14,17</sup> or reduced bioavailability.<sup>16</sup> While these approaches are adequate for describing data, they have limited utility in clinical settings and for dose determination in new clinical trials. In our analysis, we used a semi-mechanistic turnover model where rifapentine concentration was the driver of autoinduction.<sup>25</sup> This method is advantageous in that it allows for predicting the magnitude of autoinduction with different rifapentine regimens of various doses and frequencies, including those which have not yet been tested in a clinical trial.

Rifapentine autoinduction is strongly influenced by dosing frequency. Simulated pharmacokinetic profiles showed increasing  $C_{max}$  and AUC in the first week of therapy with daily dosing due to drug accumulation but decreased thereafter as a result of clearance induction. This effect was most prominent with daily dosing, moderate with thrice weekly dosing, and minimal with less frequent dosing. These findings are in agreement with previous reports from non-compartmental analyses.<sup>20,31,34</sup> Dose amount had little effect on the magnitude of autoinduction (~10% higher clearance with 1200 mg vs. 600 mg), regardless of dosing frequency. A dose effect on rifapentine autoinduction has been described previously.<sup>17,19</sup> In our model, nonproportional increases in drug exposure with increasing dose were described through a reduction in bioavailability, consistent with saturable absorption.<sup>14</sup> Still, as the

induction process is a function of rifapentine plasma concentration in our model, any additional dose effects on clearance would be captured. While full autoinduction is predicted with daily dosing, drug accumulation was also high, leading to superior  $C_{max}/MIC$  and  $AUC/MIC$  compared to less frequent dosing. This confirms that daily dosing has the highest potential for concentration-dependent killing of *M. tuberculosis*. Further, this work is an important contribution to the understanding of the rifapentine dose-exposure relationship, especially in the context of DS-TB where daily dosing is likely required.<sup>15</sup>

Currently, body weight is the only dose determining factor for rifapentine, which was not supported in our analysis. In three previously described population pharmacokinetic models, weight did not influence rifapentine pharmacokinetics.<sup>15 14,17</sup> Furthermore, Savic and colleagues supported flat dosing of rifapentine, which was later implemented in a Phase 3 clinical trial for DS-TB (Study 31, Clinicaltrials.gov NCT02410772).<sup>15</sup> Contrarily, Langdon and colleagues report a change in rifapentine clearance by 0.5 L/h per 10 kg of body weight in a small cohort of 46 patients.<sup>13</sup> However, their model did not incorporate dose-dependent absorption (i.e., reduced bioavailability with increased dose), which likely would reduce the estimated weight effect on clearance since the study dosed by weight, and clearance and bioavailability are indirectly linked with oral dosing.<sup>13</sup> Francis et al. allometrically scaled clearance by fat-free mass.<sup>16</sup> The model's application to rifapentine dosing, which is based on total body weight, was not described. Our study is the largest population pharmacokinetic study to-date with over 800 patients and healthy volunteers. While a small weight effect was observed (<10% change in clearance per 10 kg in body weight), it does not justify a 150 mg (~30%) change in dose as currently recommended in LTBI dosing guidelines. Weight and patient population appeared correlated in our dataset (i.e., DS-TB patients weighed less on average); therefore, we investigated the weight effect in healthy volunteers, individuals with LTBI, and DS-TB patients separately. The weight effect was comparable and remained clinically irrelevant. We conclude

that weight is not a clinically relevant predictor of rifapentine clearance and that weight-based dosing should not be recommended.

Simulations of the 1HP and 3HP regimens showed lower rifapentine exposures in low weight individuals who receive lower doses with current weight band dosing. This ultimately puts the smallest, most vulnerable individuals at risk of underexposure and consequently, treatment failure.<sup>35,36</sup> A univariate analysis of Phase 2 culture data from two DS-TB studies showed month 2 culture conversion was less likely in low weight individuals and those with low rifapentine exposure. While the pharmacokinetic-pharmacodynamic relationships in LTBI have not been established, rifamycins show concentration-dependent killing of *M. tuberculosis* and rifapentine AUC is a strong predictor of month 2 culture conversion.<sup>15,37</sup> Flat dosing of rifapentine (e.g., prescribing the same dose to all adults) ensures equal rifapentine exposure in adult patients of all sizes and thus, equal chance of successful outcome. Moreover, flat dosing simplifies the regimen in adults and encourages coformulation of rifapentine and isoniazid into a fixed-dose combination tablet, reducing pill burden and simplifying the regimen even further.

Dose discrimination may be warranted by HIV status. HIV-positive persons have 27% lower rifapentine bioavailability, resulting in lower exposures than HIV-negative adults. Reduced bioavailability of rifamycins with HIV infection has been reported previously<sup>15,17</sup> and has been attributed to malabsorption.<sup>38-40</sup> While antiretroviral drugs may also explain decreases in rifamycin concentration, the HIV-positive participants in our analysis did not receive antiretroviral therapy.<sup>12,22,29</sup> Given rifapentine's main metabolite has activity against *M. tuberculosis*, we also looked at metabolite concentrations by HIV status. It appeared that HIV-positive individuals had lower exposures of both rifapentine and its metabolite, confirming need for higher doses in HIV+ patients. Increasing the 3HP dose to 1200 mg once weekly in HIV-positive patients results in similar exposures to 900 mg once weekly in HIV-negative patients. Likewise, 750 mg daily in

HIV-positive adults is similar to 600 mg daily in HIV-negative adults for the 1HP regimen. While 1HP at 600 mg daily was effective in preventing tuberculosis disease in HIV-positive individuals<sup>5</sup>, this may reflect the minimum effective dose and higher doses may provide better protection.

The proposed dosing recommendations are limited by the lack of established pharmacokinetic targets in LTBI. We proposed doses that would match median exposures following the standard doses tested in clinical trials with demonstrated efficacy. Given the development of tuberculosis was rare in those studies, these pharmacokinetic targets are reasonable, and we would expect the proposed doses to result in similar efficacy to that observed in clinical trial. The pharmacokinetic target for 1HP regimen reflects the median predicted exposure in a typical HIV-positive adult receiving 600 mg daily and may be on the low end. Pharmacokinetic data from BRIEF-TB and future trials are urgently needed to confirm pharmacokinetic thresholds for 1HP. Additionally, one study showed higher rifapentine bioavailability in Asians compared to Africans, which could impact dose requirement.<sup>15</sup> This finding could not be confirmed in our study because TBTC 29X was the only study contributing substantial Asian population. Further investigation of race effects on rifapentine pharmacokinetics is required.

Our systematic review included all relevant studies published prior to 2016. Only one pharmacokinetic study was identified in more recent literature and would not have met our inclusion criteria due to non-standardized meal administration.<sup>16</sup> Thus, our model represents the most up-to-date analysis of rifapentine pharmacokinetics. Of note, the analysis includes only one study in LTBI participants. To-date, these remain the only pharmacokinetic data in this population. Further, there is no evidence to suggest pharmacokinetics would differ by disease state, so we do not expect this to impact the generalizability of our work to LTBI treatment.

In conclusion, rifapentine exhibits autoinduction which is strongly influenced by dosing frequency. Weight was not a clinically relevant predictor of rifapentine clearance; thus, dosing should not be based on an individual's weight. In fact, weight-based dosing results in substantially lower drug concentrations that could ultimately compromise treatment efficacy. If stratified dosing is to be implemented, it should be done on the basis of HIV status to ensure that HIV-positive individuals are adequately exposed to drug. Lastly, as rifapentine use becomes more widespread in tuberculosis treatment and prevention, this model can serve as a useful tool in clinical practice and in clinical trial design for dose determination and exposure prediction.

## References

1. WHO. Global Tuberculosis Report 2018. Geneva: World Health Organization; 2018.
2. American Thoracic Society, Centers for Disease Control and Prevention. Targeted tuberculin testing and treatment of latent tuberculosis infection. *Am J Respir Crit Care Med* 2000;161:S221-47.
3. Horsburgh CR, Jr., Goldberg S, Bethel J, et al. Latent TB infection treatment acceptance and completion in the United States and Canada. *Chest* 2010;137:401-9.
4. Sterling TR, Villarino ME, Borisov AS, et al. Three months of rifapentine and isoniazid for latent tuberculosis infection. *N Engl J Med* 2011;365:2155-66.
5. Swindells S, Ramchandani R, Gupta A, et al. One Month of Rifapentine plus Isoniazid to Prevent HIV-Related Tuberculosis. *N Engl J Med* 2019;380:1001-11.
6. Prifitin (rifapentine) Product Label. 1998. at [https://www.accessdata.fda.gov/drugsatfda\\_docs/label/2014/021024s011lbl.pdf](https://www.accessdata.fda.gov/drugsatfda_docs/label/2014/021024s011lbl.pdf).)
7. Treatment Regimens for Latent TB Infection (LTBI). 2016. (Accessed September 11, 2019, at <https://www.cdc.gov/tb/topic/treatment/ltbi.htm>.)
8. World Health Organization. Guidelines for treatment of tuberculosis. fourth ed. Geneva, Switzerland: WHO Press; 2010.
9. WHO Global TB Programme. Latent tuberculosis infection: Updated and consolidated guidelines for programmatic management. Background document on the 2019 revision.2019.
10. Heifets LB, Lindholm-Levy PJ, Flory MA. Bactericidal activity in vitro of various rifamycins against *Mycobacterium avium* and *Mycobacterium tuberculosis*. *Am Rev Respir Dis* 1990;141:626-30.

11. Sirgel FA, Fourie PB, Donald PR, et al. The early bactericidal activities of rifampin and rifapentine in pulmonary tuberculosis. *Am J Respir Crit Care Med* 2005;172:128-35.
12. Jindani A, Harrison TS, Nunn AJ, et al. High-dose rifapentine with moxifloxacin for pulmonary tuberculosis. *N Engl J Med* 2014;371:1599-608.
13. Langdon G, Wilkins J, McFadyen L, McIlleron H, Smith P, Simonsson US. Population pharmacokinetics of rifapentine and its primary desacetyl metabolite in South African tuberculosis patients. *Antimicrob Agents Chemother* 2005;49:4429-36.
14. Savic RM, Lu Y, Bliven-Sizemore E, et al. Population pharmacokinetics of rifapentine and desacetyl rifapentine in healthy volunteers: nonlinearities in clearance and bioavailability. *Antimicrob Agents Chemother* 2014;58:3035-42.
15. Savic RM, Weiner M, MacKenzie WR, et al. Defining the optimal dose of rifapentine for pulmonary tuberculosis: Exposure-response relations from two phase II clinical trials. *Clin Pharmacol Ther* 2017;102:321-31.
16. Francis J, Zvada SP, Denti P, et al. A Population Pharmacokinetic Analysis Shows that Arylacetamide Deacetylase (AADAC) Gene Polymorphism and HIV Infection Affect the Exposure of Rifapentine. *Antimicrob Agents Chemother* 2019;63.
17. Zvada SP, Van Der Walt JS, Smith PJ, et al. Effects of four different meal types on the population pharmacokinetics of single-dose rifapentine in healthy male volunteers. *Antimicrob Agents Chemother* 2010;54:3390-4.
18. Keung AC, Owens RC, Jr., Eller MG, Weir SJ, Nicolau DP, Nightingale CH. Pharmacokinetics of rifapentine in subjects seropositive for the human immunodeficiency virus: a phase I study. *Antimicrob Agents Chemother* 1999;43:1230-3.
19. Dooley K, Flexner C, Hackman J, et al. Repeated administration of high-dose intermittent rifapentine reduces rifapentine and moxifloxacin plasma concentrations. *Antimicrob Agents Chemother* 2008;52:4037-42.

20. Dooley KE, Bliven-Sizemore EE, Weiner M, et al. Safety and pharmacokinetics of escalating daily doses of the antituberculosis drug rifapentine in healthy volunteers. *Clin Pharmacol Ther* 2012;91:881-8.
21. Dooley KE, Savic RM, Park JG, et al. Novel dosing strategies increase exposures of the potent antituberculosis drug rifapentine but are poorly tolerated in healthy volunteers. *Antimicrob Agents Chemother* 2015;59:3399-405.
22. Dorman SE, Goldberg S, Stout JE, et al. Substitution of rifapentine for rifampin during intensive phase treatment of pulmonary tuberculosis: study 29 of the tuberculosis trials consortium. *J Infect Dis* 2012;206:1030-40.
23. Moher D, Liberati A, Tetzlaff J, Altman DG, Group P. Preferred reporting items for systematic reviews and meta-analyses: the PRISMA statement. *Ann Intern Med* 2009;151:264-9, W64.
24. Byon W, Smith MK, Chan P, et al. Establishing best practices and guidance in population modeling: an experience with an internal population pharmacokinetic analysis guidance. *CPT Pharmacometrics Syst Pharmacol* 2013;2:e51.
25. Smythe W, Khandelwal A, Merle C, et al. A semimechanistic pharmacokinetic-enzyme turnover model for rifampin autoinduction in adult tuberculosis patients. *Antimicrob Agents Chemother* 2012;56:2091-8.
26. Mould DR, Upton RN. Basic concepts in population modeling, simulation, and model-based drug development-part 2: introduction to pharmacokinetic modeling methods. *CPT Pharmacometrics Syst Pharmacol* 2013;2:e38.
27. Bergstrand M, Hooker AC, Wallin JE, Karlsson MO. Prediction-corrected visual predictive checks for diagnosing nonlinear mixed-effects models. *AAPS J* 2011;13:143-51.
28. Alfarisi O, Alghamdi WA, Al-Shaer MH, Dooley KE, Peloquin CA. Rifampin vs. rifapentine: what is the preferred rifamycin for tuberculosis? *Expert Rev Clin Pharmacol* 2017;10:1027-36.



29. Dorman SE, Savic RM, Goldberg S, et al. Daily rifapentine for treatment of pulmonary tuberculosis. A randomized, dose-ranging trial. *Am J Respir Crit Care Med* 2015;191:333-43.
30. Weiner M, Bock N, Peloquin CA, et al. Pharmacokinetics of rifapentine at 600, 900, and 1,200 mg during once-weekly tuberculosis therapy. *Am J Respir Crit Care Med* 2004;169:1191-7.
31. Weiner M, Savic RM, Kenzie WR, et al. Rifapentine Pharmacokinetics and Tolerability in Children and Adults Treated Once Weekly With Rifapentine and Isoniazid for Latent Tuberculosis Infection. *J Pediatric Infect Dis Soc* 2014;3:132-45.
32. Conde MB, Mello FC, Duarte RS, et al. A Phase 2 Randomized Trial of a Rifapentine plus Moxifloxacin-Based Regimen for Treatment of Pulmonary Tuberculosis. *PLoS One* 2016;11:e0154778.
33. Savic RM, Jonker DM, Kerbusch T, Karlsson MO. Implementation of a transit compartment model for describing drug absorption in pharmacokinetic studies. *J Pharmacokinetic Pharmacodyn* 2007;34:711-26.
34. Keung A, Reith K, Eller MG, McKenzie KA, Cheng L, Weir SJ. Enzyme induction observed in healthy volunteers after repeated administration of rifapentine and its lack of effect on steady-state rifapentine pharmacokinetics: part I. *Int J Tuberc Lung Dis* 1999;3:426-36.
35. Pasipanodya JG, McIlleron H, Burger A, Wash PA, Smith P, Gumbo T. Serum drug concentrations predictive of pulmonary tuberculosis outcomes. *J Infect Dis* 2013;208:1464-73.
36. Weiner M, Benator D, Burman W, et al. Association between acquired rifamycin resistance and the pharmacokinetics of rifabutin and isoniazid among patients with HIV and tuberculosis. *Clin Infect Dis* 2005;40:1481-91.
37. Gumbo T, Louie A, Deziel MR, et al. Concentration-dependent Mycobacterium tuberculosis killing and prevention of resistance by rifampin. *Antimicrob Agents Chemother* 2007;51:3781-8.

38. Gengiah TN, Botha JH, Soowamber D, Naidoo K, Abdool Karim SS. Low rifampicin concentrations in tuberculosis patients with HIV infection. *J Infect Dev Ctries* 2014;8:987-93.
39. Gurumurthy P, Ramachandran G, Hemanth Kumar AK, et al. Malabsorption of rifampin and isoniazid in HIV-infected patients with and without tuberculosis. *Clin Infect Dis* 2004;38:280-3.
40. Jeremiah K, Denti P, Chigutsa E, et al. Nutritional supplementation increases rifampin exposure among tuberculosis patients coinfecting with HIV. *Antimicrob Agents Chemother* 2014;58:3468-74.

## **Chapter 6. Pragmatic global dosing recommendations for the 3-month, once-weekly rifapentine and isoniazid preventive TB regimen in children\***

### **Introduction**

The End TB Strategy, proposed by the World Health Organization (WHO) in 2014, calls for a 90% reduction in tuberculosis (TB)-related deaths and an 80% reduction in the TB incidence by 2030.<sup>1</sup> TB remains a leading cause of death in children under five years of age,<sup>2</sup> and interventions to eliminate preventable child deaths from TB are urgently needed. Additional and effective TB prevention measures are crucial for the End TB Strategy goals to be met.<sup>3</sup>

Children have a high risk of progressing to TB disease following *Mycobacterium tuberculosis* infection, especially if young (<5 years of age) or HIV-infected.<sup>4</sup> Since 2014, the WHO has placed an increased emphasis on TB prevention with multiple guidelines promoting household contact investigation and management to identify children at the greatest risk of TB disease.<sup>5,6</sup> The updated 2019 WHO guidelines for latent TB infection recommend TB preventive therapy in at-risk children, including all children living with HIV and children under 5 years of age with a household TB source case.<sup>6</sup>

---

\* Modified from the publication: Radtke KK, Hibma JE, Hesselning AC, Savic RM (2020). Pragmatic global dosing recommendations for the 3-month, once-weekly rifapentine and isoniazid preventive TB regimen in children. *Eur Respir J.* 57(1):2001756. PMID: 32703775.

A 3-month regimen of once-weekly rifapentine and isoniazid (3HP) has demonstrated efficacy and improved safety and tolerability in preventing TB disease in adults and children (>2 years).<sup>7,8</sup> However, these drugs are not co-formulated, and rifapentine is not available in a child-friendly formulation. Based on existing pediatric pharmacokinetic data, rifapentine dosing follows a weight band algorithm.<sup>6,9</sup> In contrast, isoniazid is dosed in mg/kg, which differs in young children versus adolescents and adults.<sup>6</sup> This requires healthcare workers to calculate and round isoniazid doses to determine the appropriate tablet count for children. Dosing complexity is a major barrier to children receiving this effective, short-course preventive regimen in the field.

To address these shortcomings, we performed pharmacokinetic modelling and simulations to devise a synchronized, simple and pragmatic dosing strategy for 3HP in children that utilizes currently available formulations based on request from the WHO PK-PD Task Force. This work will provide interim guidance on the optimal dosing with existing formulations (rifapentine 150 mg; isoniazid 100 mg), while informing the development of child-friendly rifapentine formulations for young children.

## **Methods**

We performed dosing simulations with pediatric population pharmacokinetic models for isoniazid<sup>10</sup> and rifapentine<sup>9</sup> to predict concentrations using the current once-weekly 3HP dosing recommendations and adult formulations: rifapentine 300 mg (10-14 kg), 450 mg (14.1-25 kg), 600 mg (25.1-32 kg), or 750 mg (32.1-50 kg) and isoniazid 25 mg/kg (age 2-11 years) or 15 mg/kg (age  $\geq$  12 years).<sup>6</sup> With predicted drug exposures, unified weight band doses were determined for each drug and aligned with WHO pre-specified weight bands for TB treatment in children and current formulations. Dosing simulations were performed for adults using drug-

specific population pharmacokinetic models and recommended dosing: 900 mg rifapentine and 600 mg (< 50 kg) or 900 mg (50+ kg) isoniazid.<sup>11,12</sup>

Demographic data (i.e., gender, weight, age) representative of actual pediatric global populations acquired from national surveys (e.g., Demographic and Health Surveys Program) were used in simulations of children 2-4 years.<sup>13</sup> Child demographics from the randomized controlled trial on 3HP (PREVENT-TB) were used for children 5-14 years.<sup>9</sup> Children <10 kg were excluded due to the lack of rifapentine pharmacokinetic data in this group.

## Results

The revised weight bands matched WHO pre-specified weight bands for anti-TB drug dosing in children (Table 1). These weight band breakpoints differ from those currently in the rifapentine product label by 1-2 kg. Isoniazid doses for each weight band in the revised recommendations are clearly defined and match available formulations (**Table 6.1**). Under this revised dosing method, median (interquartile range) rifapentine exposures were 725 (549-952) mg\*h/L in children 10-15 kg, 888 (670-1177) mg\*h/L in children 16-23 kg, 955 (724-1272) mg\*h/L in children 24-30 kg, and 909 (679-1189) mg\*h/L in children >30 kg compared to 660 (509-839) mg\*h/L in adults. Median (interquartile range) isoniazid exposures were 66 (38-113) mg\*h/L in children 10-15 kg, 84 (47-148) mg\*h/L in children 16-23 kg, 64 (37-115) mg\*h/L in children 24-30 kg, and 52 (30-90) mg\*h/L in children >30 kg compared to 55 (41-90) mg\*h/L in adults, assuming 1:1 ratio of slow:fast acetylator.

**Table 6.1.** Revised dosing recommendations for 3-month, once-weekly rifapentine and isoniazid (3HP) preventive treatment regimen

Weight band	Rifapentine (P)		Isoniazid (H)	
	Dose	Tablets	Dose	Tablets
<b>Children<sup>1</sup></b>				
10-15 kg	300 mg	2	300 mg	3
16-23 kg	450 mg	3	500 mg	5
24-30 kg	600 mg	4	600 mg	6
≥ 31 kg	750 mg	5	600 mg	6
<b>Adults<sup>2</sup></b>				
< 50 kg	900 mg	6	600 mg	2
≥ 50 kg	900 mg	6	900 mg	3

<sup>1</sup> Child tablet sizes are 150 mg (P) and 100 mg (H)

<sup>2</sup> Adult tablet sizes are 150 mg (P) and 300 mg (H)

## Discussion

We propose a revised pragmatic dosing table for the 3HP regimen that (1) simplifies isoniazid dosing into weight bands, (2) aligns with pre-specified WHO weight bands for pediatric TB dosing, and (3) utilizes the available and registered formulations in the field. We demonstrate adequate rifapentine and isoniazid exposure in children 2-14 years with these revised doses, and therefore expect equal efficacy to current dosing practices.

Our field-friendly dosing table is readily accessible to healthcare workers in TB services and clearly defines rifapentine and isoniazid doses by weight band. This new dosing strategy is a substantial improvement to current guidelines that require calculations and rounding for isoniazid that may potentiate dosing errors and add complexity to regimen implementation, especially high TB burden regions where human resources for TB services are typically limited. Aligning weight bands with other TB drugs simplifies pediatric dose determination across TB

disease states and is an important next step towards co-formulation of this important TB prevention regimen.

These dosing recommendations are based on data from normal weight children and cannot be confidently applied to overweight or obese children as no pharmacokinetic data currently exist in this population. Given the growing global issue of childhood obesity, pharmacokinetic studies are urgently needed in obese children to establish optimal dosing approaches and avoid sub- or supra-therapeutic exposures.

Despite FDA approval for pediatric use in 2014, no child-friendly rifapentine formulation is licensed or routinely available; such formulations are currently limited to pediatric phase I/II trials. A novel child-friendly rifapentine formulation is urgently needed to support safe and effective 3HP dosing in all children, including those <2 years of age who have the highest risk of TB disease progression and disseminated TB, and as new data emerge from very young children (i.e., Study 35: [clinicaltrials.gov NCT03730181](https://clinicaltrials.gov/ct2/show/study/NCT03730181)). Our work demonstrates adequate rifapentine exposure with a 150 mg tablet, supporting development of a dispersible formulation at this strength. The dispersible tablet should be scored to allow for accurate dosing in small children and be palatable. This will allow for evaluation and potential programmatic use in novel ultrashort regimens (e.g., 28 days of daily rifapentine/isoniazid) and potentially TB disease as data emerge (Study 31; [clinicaltrials.gov NCT02410772](https://clinicaltrials.gov/ct2/show/study/NCT02410772)). The time between drug approval and pediatric dosing and formulation development has historically been long in TB. The WHO has established the Global Accelerator for Paediatric Formulations (GAP-f), which will hopefully accelerate child formulation development and uptake across diseases.

Implementing safe and effective shorter TB prevention therapy in children needs to be scaled up worldwide, especially in the context of HIV and novel pandemics like SARS-CoV-2 given the

dramatic impact such diseases may have on TB burden. It is essential that TB services, including testing, prevention, and treatment, are maintained as a small decline in TB services may dramatically increase TB incidence and mortality.<sup>14</sup> Simple, pragmatic dosing and short-course TB prevention therapy will aid efforts to significantly prevent morbidity and death due to TB in children.



## References

1. WHO End TB Strategy: Global strategy and targets for tuberculosis prevention, care and control after 2015. (Accessed March 1, 2020, at [https://www.who.int/tb/post2015\\_strategy/en/](https://www.who.int/tb/post2015_strategy/en/).)
2. Dodd PJ, Yuen CM, Sismanidis C, Seddon JA, Jenkins HE. The global burden of tuberculosis mortality in children: a mathematical modelling study. *Lancet Glob Health* 2017;5:e898-e906.
3. Hamada Y, Glaziou P, Sismanidis C, Getahun H. Prevention of tuberculosis in household members: estimates of children eligible for treatment. *Bull World Health Organ* 2019;97:534-47D.
4. Marais BJ, Gie RP, Schaaf HS, et al. The natural history of childhood intra-thoracic tuberculosis: a critical review of literature from the pre-chemotherapy era. *Int J Tuberc Lung Dis* 2004;8:392-402.
5. Recommendations for investigating contacts of persons with infectious tuberculosis in low and middle-income countries. (Accessed May 4, 2020, at [https://www.who.int/tb/publications/2012/contact\\_investigation2012/en/](https://www.who.int/tb/publications/2012/contact_investigation2012/en/).)
6. Latent TB Infection : Updated and consolidated guidelines for programmatic management. (Accessed March 1, 2020, at <https://www.who.int/tb/publications/2018/latent-tuberculosis-infection/en/>.)
7. Sterling TR, Villarino ME, Borisov AS, et al. Three months of rifapentine and isoniazid for latent tuberculosis infection. *N Engl J Med* 2011;365:2155-66.
8. Villarino ME, Scott NA, Weis SE, et al. Treatment for preventing tuberculosis in children and adolescents: a randomized clinical trial of a 3-month, 12-dose regimen of a combination of rifapentine and isoniazid. *JAMA Pediatr* 2015;169:247-55.

9. Weiner M, Savic RM, Kenzie WR, et al. Rifapentine Pharmacokinetics and Tolerability in Children and Adults Treated Once Weekly With Rifapentine and Isoniazid for Latent Tuberculosis Infection. *J Pediatric Infect Dis Soc* 2014;3:132-45.
10. Guiastrenec B, Ramachandran G, Karlsson MO, et al. Suboptimal antituberculosis drug concentrations and outcomes in small and HIV-coinfected children in India: recommendations for dose modifications. *Clin Pharmacol Ther* 2018;104:733-41.
11. Hibma JE, Radtke KK, Dorman SE, et al. Rifapentine Population Pharmacokinetics and Dosing Recommendations for Latent Tuberculosis Infection. *Am J Respir Crit Care Med* 2020;202:866-77.
12. Wilkins JJ, Langdon G, McIleron H, Pillai G, Smith PJ, Simonsson US. Variability in the population pharmacokinetics of isoniazid in South African tuberculosis patients. *Br J Clin Pharmacol* 2011;72:51-62.
13. Radtke KK, Dooley KE, Dodd PJ, et al. Alternative dosing guidelines to improve outcomes in childhood tuberculosis: a mathematical modelling study. *Lancet Child Adolesc Health* 2019;3:636-45.
14. COVID-19: Considerations for tuberculosis (TB) care. (Accessed May 12, 2020, at [https://www.who.int/tb/COVID\\_19considerations\\_tuberculosis\\_services.pdf](https://www.who.int/tb/COVID_19considerations_tuberculosis_services.pdf).)

## **Chapter 7. Prediction of optimal opening doses of rifapentine-based tuberculosis preventive therapy for evaluation in novel pediatric clinical trials**

### **Introduction**

Prevention of tuberculosis (TB) in children through post-exposure preventive pharmacotherapy is an important public health strategy to reduce the TB burden amongst children.<sup>1</sup> This is especially important for children under the age of 5 years, who have a high risk of disease progression and developing severe forms of TB following exposure to and infection with *Mycobacterium tuberculosis*. Anti-TB medications are effective at preventing the progression of TB disease among individuals with latent TB infection or household contacts of active cases. However, adherence to preventive TB therapy is particularly poor in children, especially in high-burden settings, partly due to long therapy durations (e.g., 6-9 months of isoniazid daily).<sup>2,3</sup> This greatly limits the effectiveness in the field.

Novel short-course and ultra-short-course prevention regimens have the potential to improve patient compliance and thus, efficacy. Three months of once weekly rifapentine and isoniazid (3HP) was non-inferior to 9 months of isoniazid and improved treatment completion (82% versus 69%).<sup>4</sup> Similar results were found in 905 children and adolescents 2 years and older, where treatment completion was 88% with 3HP versus 81% with isoniazid alone ( $p=0.003$ ).<sup>5</sup> Emerging data from the field confirm high completion rates with 3HP in children.<sup>6,7</sup> The newer and shorter one-month regimen of daily rifapentine and isoniazid (1HP) was also non-inferior to nine months of isoniazid, and 97% of participants completed treatment in a randomized clinical

trial.<sup>8</sup> Notably, these individuals were all HIV-positive and at risk of TB but did not necessarily have confirmed TB infection.

The 3HP is the shortest TB preventive regimen approved for use in children but only for children 2 years and older due to the lack of rifapentine pharmacokinetic (PK) and safety data in younger children.<sup>9</sup> As such, TB preventive therapy in children under 2 years of age is limited to 4 months of daily rifampicin or 6-9 months of daily isoniazid. Two pediatric PK and safety studies will be performed to support the approval and programmatic use of shorter, rifapentine-based regimens for TB prevention. These include Tuberculosis Trials Consortium (TBTC) Study 35, evaluating 3HP in HIV-positive and -negative children 0-12 years, and International Maternal Pediatric Adolescent AIDS Clinical Trials Network (IMPAACT) 2024, evaluating 1HP in HIV-positive and -negative children 0-15 years. We perform model-informed dose selection to support opening pediatric doses of 3HP and 1HP in the corresponding Phase I/II dose-finding studies.

## **Methods**

### **Rifapentine PK model**

Two separate rifapentine population PK models were used to predict apparent clearance ( $CL/F_{pred}$ ) for (a) children 2 years and older and (b) children under 2 years of age, in which the maturation function ( $f_{mat}$ ) and typical value of apparent clearance (TVCL) varied (equation 7.1). The rationale behind separate models is that rifapentine PK are unknown in children under 2 years of age. Therefore, in this population, an adult population PK model<sup>10</sup> (TVCL = 1.11 L/h) was allometrically scaled by body weight and a rifampicin maturation function ( $f_{mat}$ ) was applied (equation 7.2a),<sup>11</sup> where 50% maturation occurs at 54 weeks post-menstrual age (PMA). An adjustment factor of 1.55 was applied to  $f_{mat}$  in equation 7.2-a based on emerging rifampicin

data that showed faster apparent clearance maturation.<sup>12</sup> In children 2 years and older, rifapentine pharmacokinetics have been described.<sup>13</sup> In this model, the TVCL was 1.65 L/h when rifapentine was administered with a low-fat meal, and the  $f_{\text{mat}}$  followed an exponential decay function with a half-life of 1.49 years (equation 7.2b). The resulting combined rifapentine clearance function is shown in **Figure 7.1**.

Equation 7.1 
$$CL/F_{\text{pred}} = \text{TVCL} \cdot \left(\frac{\text{Weight}}{70 \text{ kg}}\right)^{0.75} \cdot f_{\text{mat}}$$

Equation 7.2a 
$$f_{\text{mat}} = \frac{\text{PMA}^{-3.22}}{54^{-3.22} + \text{PMA}^{-3.22}} \cdot 1.55$$

Equation 7.2b 
$$f_{\text{mat}} = \left(1 - 0.22 + 0.22 \cdot e\left[-(\text{Age} - 2 \text{ years}) \cdot \frac{\ln(2)}{1.49}\right]\right)$$

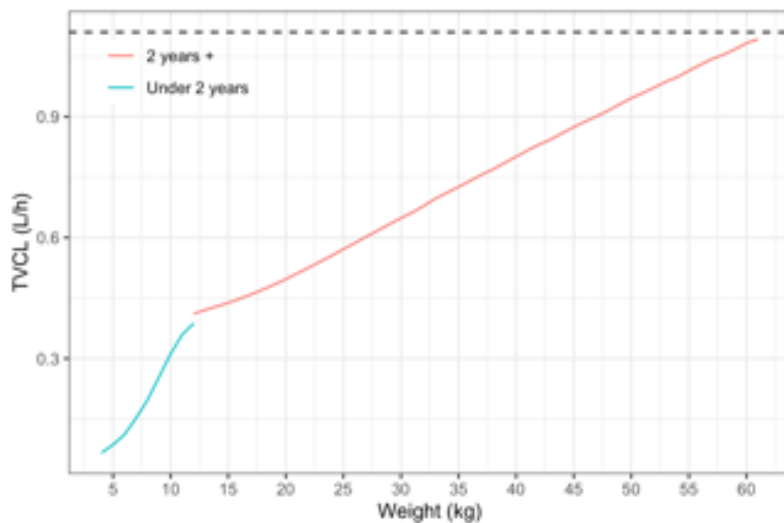


**Figure 7.1** Typical value of rifapentine clearance (TVCL) in children 0-15 years based on assumed functions. Median weight for age per WHO and CDC growth standards was used for age-weight inputs. Dashed line represents the adult TVCL, 1.11 L/h.

## PK targets

PK targets were based on the typical area under the concentration-time curve (AUC) in adults receiving standard doses (equation 7.3). Based on the standard doses of 900 mg for 3HP and 600 mg for 1HP and population estimates of TVCL and relative bioavailability (F),<sup>10</sup> the 3HP  $AUC_{\text{target}}$  was 688 mg\*h/L and the 1HP  $AUC_{\text{target}}$  was 486 mg\*h/L.

Equation 7.3 
$$AUC_{\text{target}} = \frac{F \cdot \text{Dose}}{TVCL}$$

## Rifapentine formulations and administration

The available rifapentine formulations for 3HP dosing were 20 mg rifapentine dispersible tablet (experimental), 100 mg rifapentine dispersible tablet (experimental), 150/150 mg rifapentine/isoniazid dispersible combination tablet (experimental), and 100 mg isoniazid dispersible tablet. The available formulations for 1HP dosing were 150 mg rifapentine film-coated tablet (commercial) and 100 mg isoniazid dispersible tablet (commercial).

## Opening dose predictions

3HP is FDA-approved in children 2 years and older. Therefore, 3HP dose predictions were only performed for children under 2 years of age. Isoniazid doses were chosen based on WHO mg/kg dose recommendations: up to 25 mg/kg for 3HP and 7-15 mg/kg for 1HP, based on daily isoniazid recommendations.<sup>9</sup> Rifapentine doses were predicted using equation 7.4, where  $AUC_{\text{target}}$  is determined by equation 7.3 and  $CL/F_{\text{pred}}$  is determined by equation 7.1. Real world anthropometric data from national/international surveys in TB-endemic countries and pediatric clinical trials were used for age and weight inputs, as previously described.<sup>14</sup> Opening doses were summarized (median, interquartile range) in body weight increments of 1 kg and the appropriate weight band cutoffs determined for each regimen considering formulation and

pragmatic use. For the smallest children, ¼ or ½ tablets were allowed for tailored dosing. Since dispersible rifapentine tablets were not available for the 1HP trial, doses were predicted under different assumptions of a tablet crushing effect on bioavailability (a 26% reduction was determined in a previous trial but was based on sparse data).<sup>13</sup> Given the good safety profile of rifapentine,<sup>13</sup> higher doses were allowed to prevent potential underdosing. Finally, simulations were performed with inter-individual variability to confirm target attainment and exposure distribution. All analyses were performed in RStudio © (version 1.2.5019).

Equation 7.4             $\text{Dose}_{\text{pred}} = \text{AUC}_{\text{target}} \cdot \text{CL}/\text{F}_{\text{pred}}$

## Results

### Opening doses of 3HP

The predicted optimal doses of isoniazid and rifapentine in the 3HP regimen for children under 2 years of age are shown in **Table 7.1**. The rifapentine dose ranged from 16 to 36 mg/kg depending on weight. All weight bands required use of the FDC plus a standalone rifapentine formulation to supplement higher rifapentine dose requirements. Rifapentine PK simulations predicted good target attainment (**Figure 7.2**).

**Table 7.1** Opening doses for 3HP in children under 2 years of age

Weight band (kg)	RPT dosing		INH dosing		Formulation, number of tablets	
	RPT Dose	RPT mg/kg	INH Dose	INH mg/kg	RPT/INH 150/150 FDC	RPT 100
3.0-3.9	62.5 mg	16-21	37.5 mg	10-13	0.25	0.25
4.0-4.9	87.5 mg	18-22	37.5 mg	8-9	0.25	0.5
5.0-6.9	125 mg	18-25	75 mg	11-15	0.5	0.5
7.0-8.9	250 mg	28-36	150mg	17-21	1	1
9.0-12.9	300 mg	23-33	150 mg	12-17	1	1.5
13.0-15.9	350 mg	22–27	300 mg	19-23	2	0.5

RPT/INH 150/150 FDC: 150 mg RPT, 150 mg INH, fixed dose combination, dispersible, not scored

RPT 100: 100 mg RPT not scored, dispersible

RPT=Rifapentine, INH=Isoniazid

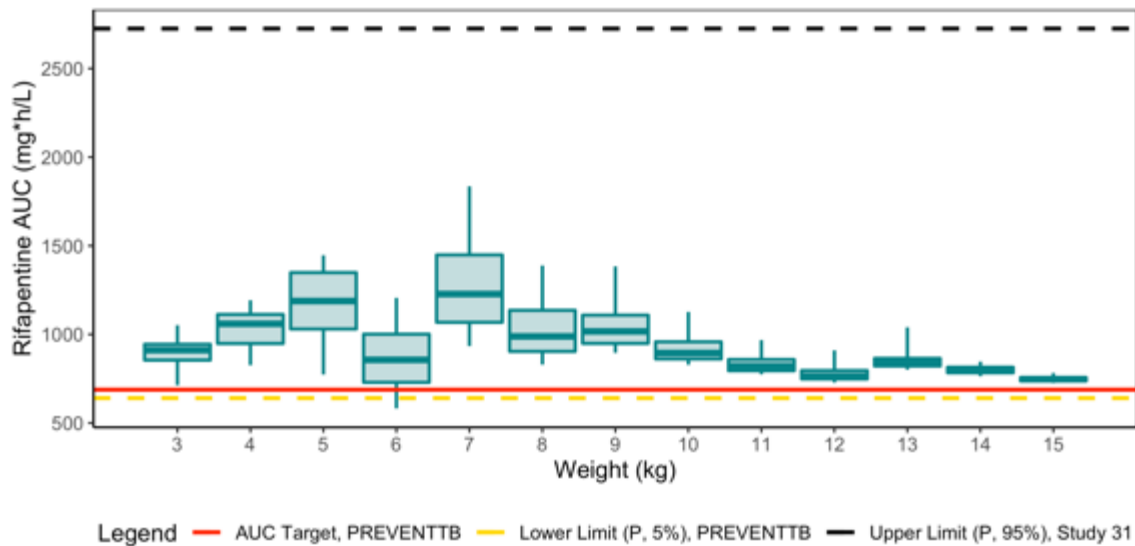


**Figure 7.2** Simulated rifapentine AUC with opening 3HP doses in children under 2 years. Horizontal lines represent the AUC target (red, solid), lower bound (yellow, dashed; based on 5<sup>th</sup> percentile from PREVENTTB (900 mg rifapentine weekly)), and upper bound (black, dashed; based on 95<sup>th</sup> percentile from Tuberculosis Trials Consortium Study 31 (1200 mg rifapentine daily)).



### Opening doses of 1HP

The predicted optimal doses of isoniazid and rifapentine in the 1HP regimen for children 0-15 years of age are shown in **Table 7.2**. Rifapentine doses ranged from 13 to 30 mg/kg with higher mg/kg doses in children < 15 kg. Absolute rifapentine dose approached the adult recommended dose (600 mg) with increasing child body weight; however, higher than adult doses were required for crushed tablets: up to 1050 mg was required in children 31 kg or more under the extreme assumption (50% reduction in relative bioavailability (F)). Rifapentine PK simulations predicted good target attainment in all weight bands and tablet crushing assumptions (**Figure 7.3**). Given the large variability in exposures, especially in young children, upper and lower AUC limits were utilized for comparison based on adult exposures with 1200 mg and 600 mg daily, respectively.

**Table 7.2** Opening doses for 1HP in children 0-15 years of age

Weight band	RPT dose, number of tablets (mg)					INH dose, number of tablets (mg)				
	mg/kg	-0% F	-20% F	-30% F	-40% F	-50% F	mg/kg	-	-	-
3-4 kg		0.5 (75)	0.5 (75)	1 (150)	0.5 (150)	0.5 (150)				0.5 (50)
5-6 kg	18-30	1 (150)	1 (150)	1 (150)	1 (150)	1 (225)				1 (100)
7-9 kg		1 (150)	2 (300)	2 (300)	1 (300)	1 (450)				1 (100)
10-15 kg		2 (300)	2 (300)	2 (300)	2 (450)	2 (450)			7-15	1.5 (150)
16-23 kg		2 (300)	3 (450)	3 (450)	2 (450)	2 (600)				2 (200)
24-30 kg	13-19	3 (450)	3 (450)	4 (600)	3 (750)	3 (750)				2.5 (250)
>=31 kg		4 (600)	4 (600)	5 (750)	4 (900)	4 (1050)				3 (300)

RPT doses are shown for different assumptions of the reduction in relative bioavailability with tablet crushing (F), from -0 to -50%.  
RPT: rifapentine, 150 mg film-coated formulation. INH: isoniazid, 100 mg scored dispersible tablet formulation.

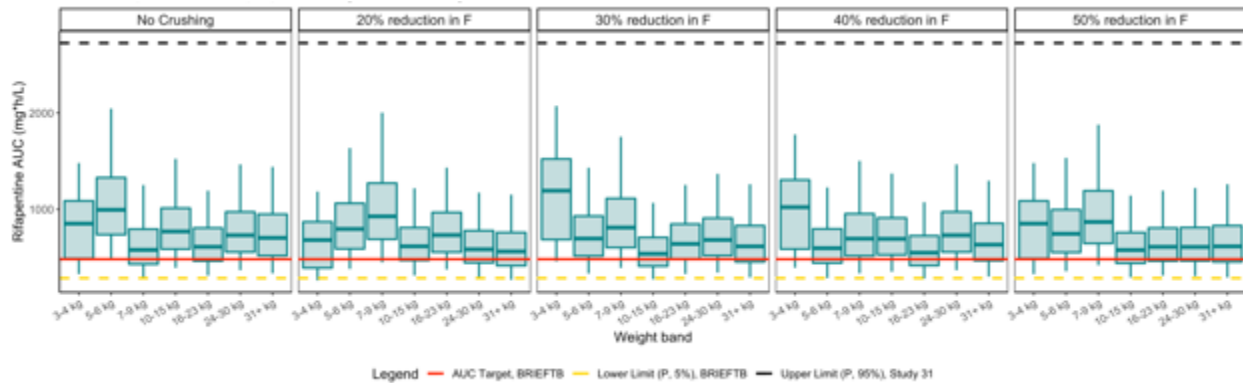


**Figure 7.3** Simulated rifapentine AUC with opening 1HP doses. Panels represent different dosing schemes according to -0%, -20%, -30%, -40%, and -50% F (left to right) in Table 3.3.2. Horizontal lines represent the AUC target (red, solid), lower bound (yellow, dashed; based on 5<sup>th</sup> percentile from BRIEF-TB (600 mg rifapentine daily)), and upper bound (black, dashed; based on 95<sup>th</sup> percentile from Tuberculosis Trials Consortium Study 31 (1200 mg rifapentine daily)).

## Discussion

This work proposes opening doses for rifapentine and isoniazid as part of two short-course combination regimens for TB preventive treatment to be evaluated in novel pediatric clinical trials: TBTC-35 and IMPAACT 2024. We predict that these doses will result in efficacious and safe drug exposures in children treated with rifapentine and isoniazid daily for 1 month or weekly for 3 months.

TB preventive therapy is a major component of the End TB strategy.<sup>15</sup> There is an estimated 1.7 billion individuals with latent TB infection globally, of which 97 million are children under the age of 15 years.<sup>16</sup> The COVID-19 pandemic threatens to reverse much of the progress made in TB control.<sup>17</sup> While physical distancing may help perturb TB spread and disease development, the disruptions in TB services in major high-burden countries is expected to have a major impact.<sup>18</sup>

TB burden could increase by 3 to 10% or more from 2020-2025 depending on shutdown and recovery times in high-burden countries.<sup>19</sup> This is devastating considering the TB burden has decreased by 9% from 2015.<sup>17</sup> As such, TB preventive therapy, especially if short, effective, and safe, is perhaps more crucial than ever before.

For short rifapentine-based regimens to be widely utilized in pediatric populations, a child-friendly rifapentine formulation needs to be developed. The optimal dose predictions for both TBTC-35 and IMPAACT 2024 clearly demonstrate this need. A scored, 150 mg rifapentine tablet or an unscored, 75 mg rifapentine tablet would serve weekly and daily rifapentine-based regimens well. Dose increments of 75 mg were advantageous for small children, in whom the drug exposures are sensitive to small differences in dose. A dispersible formulation would prevent potential drug loss from tablet crushing, which could increase dose requirements by up to 50%. Further, our analysis does not support a fixed-dose combination of rifapentine-isoniazid in a 1:1 ratio; children required greater rifapentine doses compared to isoniazid. Therefore, a standalone rifapentine formulation that is palatable and dispersible would be the most pragmatic and beneficial for development at this stage. This formulation could also be used in the treatment of drug-susceptible TB disease as part of the novel TBTC-31 regimen that recently demonstrated efficacy in adults.<sup>20</sup>

This work leverages PK modeling and simulation to generate model-informed pediatric doses. Given no rifapentine PK data are available in children under 2 years of age, some assumptions were made. Rifapentine PK were assumed to fit an allometrically scaled adult model with a rifampicin maturation function. Rifapentine and rifampicin are both metabolized by esterases to form 25-desacetyl compounds as the major metabolite.<sup>21,22</sup> Therefore, our assumption is reasonable. Further, the formulations for the 1HP regimen were limited to those commercially available. Therefore, tablet crushing will be required for young children who are unable to

swallow a whole tablet. The effect of tablet crushing on rifapentine bioavailability is unknown. We evaluated assumptions of 0 to 50% reduction in bioavailability and proposed doses for each assumption. Modeling from the PREVENT-TB study estimated a 26% reduction in rifapentine bioavailability with tablet crushing.<sup>13</sup> However, this data was based on single drug concentrations from 80 children, of whom 55 (69%) received crushed tablets, and no child was under the age of 2 years. Therefore, there was low confidence in the -26% estimate, and a range of effect sizes were considered.

In conclusion, the proposed opening trial doses of rifapentine and isoniazid for TBTC-35 and IMPAACT 2024 are expected to deliver safe and effective drug exposures with available trial formulations. While final recommendations will need to wait until these trials have been completed, a dispersible rifapentine formulation should be developed now so children across the globe can take advantage of this highly effective therapy.

## References

1. Marais BJ, Gie RP, Schaaf HS, et al. The natural history of childhood intra-thoracic tuberculosis: a critical review of literature from the pre-chemotherapy era. *Int J Tuberc Lung Dis* 2004;8:392-402.
2. Van Wyk SS HH, Hesselning AC, Beyers N, Enarson DA, Mandalakas AM. Recording isoniazid preventive therapy delivery to children: operational challenges. *Int J Tuberc Lung Dis* 2010;14:650-3.
3. Van Zyl S, Marais BJ, Hesselning AC, Gie RP, Beyers N, Schaaf HS. Adherence to anti-tuberculosis chemoprophylaxis and treatment in children. *Int J Tuberc Lung Dis* 2006;10:13-8.
4. Sterling TR, Villarino ME, Borisov AS, et al. Three months of rifapentine and isoniazid for latent tuberculosis infection. *N Engl J Med* 2011;365:2155-66.
5. Villarino ME, Scott NA, Weis SE, et al. Treatment for preventing tuberculosis in children and adolescents: a randomized clinical trial of a 3-month, 12-dose regimen of a combination of rifapentine and isoniazid. *JAMA Pediatr* 2015;169:247-55.
6. Sandul AL, Nwana N, Holcombe JM, et al. High Rate of Treatment Completion in Program Settings With 12-Dose Weekly Isoniazid and Rifapentine for Latent Mycobacterium tuberculosis Infection. *Clin Infect Dis* 2017;65:1085-93.
7. Cruz AT, Starke JR. Completion Rate and Safety of Tuberculosis Infection Treatment With Shorter Regimens. *Pediatrics* 2018;141.
8. Swindells S, Ramchandani R, Gupta A, et al. One Month of Rifapentine plus Isoniazid to Prevent HIV-Related Tuberculosis. *N Engl J Med* 2019;380:1001-11.
9. WHO operational handbook on tuberculosis. Module 1: Prevention- tuberculosis preventive treatment. 2020.

10. Hibma JE, Radtke KK, Dorman S, et al. Rifapentine population pharmacokinetics and dosing recommendations for latent tuberculosis infection. *American Journal of Respiratory and Critical Care Medicine* 2020;accepted.
11. Zvada SP, Denti P, Donald PR, et al. Population pharmacokinetics of rifampicin, pyrazinamide and isoniazid in children with tuberculosis: in silico evaluation of currently recommended doses. *J Antimicrob Chemother* 2014;69:1339-49.
12. R. Wasmann PD, E. Svensson, C. Gonzales,, J. Winckler AB, H. Rabie, H. Zar, A. van Rie, H. McIlleron. Population pharmacokinetics and potential new optimized fixed-dose combinations of rifampicin, isoniazid, and pyrazinamide in paediatric patients with tuberculosis [Abstract OA-41-752-24]. 51st Union World Conference on Lung Health. Sevilla, Spain2020.
13. Weiner M, Savic RM, Kenzie WR, et al. Rifapentine Pharmacokinetics and Tolerability in Children and Adults Treated Once Weekly With Rifapentine and Isoniazid for Latent Tuberculosis Infection. *J Pediatric Infect Dis Soc* 2014;3:132-45.
14. Radtke KK, Hibma JE, Hesselning AC, Savic RM. Pragmatic global dosing recommendations for the 3-month, once-weekly rifapentine and isoniazid preventive TB regimen in children. *Eur Respir J* 2020.
15. WHO End TB Strategy: Global strategy and targets for tuberculosis prevention, care and control after 2015. (Accessed March 1, 2020, at [https://www.who.int/tb/post2015\\_strategy/en/](https://www.who.int/tb/post2015_strategy/en/).)
16. Houben RM, Dodd PJ. The Global Burden of Latent Tuberculosis Infection: A Re-estimation Using Mathematical Modelling. *PLoS Med* 2016;13:e1002152.
17. Global Tuberculosis Report. WHO, 2020. (Accessed February 25, 2021, 2021, at <https://www.who.int/publications/i/item/9789240013131>.)
18. McQuaid CF, McCreesh N, Read JM, et al. The potential impact of COVID-19-related disruption on tuberculosis burden. *Eur Respir J* 2020;56.
19. The potential impact of the COVID-19 response on tuberculosis in high-burden countries: a modelling analysis. Geneva: Stop TB Partnership in collaboration with Imperial

College, Avenir Health, Johns Hopkins University and USAID. 2020. (Accessed May 25, 2021, at

[http://stoptb.org/assets/documents/news/Modeling%20Report\\_1%20May%202020\\_FINAL.pdf](http://stoptb.org/assets/documents/news/Modeling%20Report_1%20May%202020_FINAL.pdf).)

20. Dorman S. [Abstract SP-10] The design and primary efficacy results of Study 31/A5349. 51st Union World Lung Health Conference. Sevilla, Spain2020.
21. Reith K, Keung A, Toren PC, Cheng L, Eller MG, Weir SJ. Disposition and metabolism of 14C-rifapentine in healthy volunteers. *Drug Metab Dispos* 1998;26:732-8.
22. Jamis-Dow CA, Katki AG, Collins JM, Klecker RW. Rifampin and rifabutin and their metabolism by human liver esterases. *Xenobiotica* 1997;27:1015-24.



## **Chapter 8. Stochastic simulation and estimation to support pediatric clinical design: a case study with rifapentine for preventive tuberculosis treatment**

### **Introduction**

Pediatric therapeutics do not require the standard drug development pipeline of pre-clinical to phase 3 studies for pediatric labelling. When it is reasonable to assume that children have similar disease progression and response to an intervention as adults, extrapolation of efficacy can be employed according to United States Food and Drug Administration (FDA) guidance.<sup>1</sup> In such cases, pharmacokinetic (PK) and safety studies are considered sufficient for drug approval in lieu of a formal efficacy trial. This has facilitated increased FDA approval of new pediatric indications, which is preferred over off-label use.<sup>2</sup>

Pediatric clinical trial design is challenging for several reasons. Parental/guardian consent rates of vulnerable children are low, making recruitment of phase 3-level sample sizes incredibly challenging.<sup>3</sup> Ethically, it is important to ensure trials will be safe and appropriate. Children cannot tolerate traditional PK study blood draws (10+ samples of 3 mL each) due to lower blood volumes. Therefore, semi-intensive or sparse sampling is often required. This combined with typically high PK variability and developing physiology that is difficult to predict creates statistical challenges for parameter estimation and covariate identification.<sup>3,4</sup> Approximately 20% of pediatric trials fail due to inappropriate study design, suboptimal experiment planning, or inadequate participant enrollment.<sup>5,6</sup> Therefore, it is imperative for pediatric studies to undergo

thoughtful design and leverage prior data and developmental pharmacology principles as much as possible.

Pharmacokinetic/Pharmacodynamic modelling and simulation can play an important role in pediatric study design and mitigate several of these challenges.<sup>3,7,8</sup> Non-linear mixed effects modelling facilitates the analysis of sparse data and non-standardized sampling time points between individuals. These models can also incorporate the complex and dynamic physiological processes that occur in children with age and weight as well as other important factors. Employing this approach through clinical trial simulations can inform dose selection, trial sample size, and optimal sampling design.<sup>2,3</sup>

The aim of this work was to determine the effect of the sampling design, sample size, and inter-individual variability on the success of a pediatric PK study. Specifically, a case study was performed with rifapentine as the drug of interest, an anti-tuberculosis agent with minimal pediatric data, applied to a trial currently in development: International Maternal Pediatric Adolescent AIDS Clinical Trials Network (IMPAACT) 2024 (<https://www.impaactnetwork.org/studies/impaact2024>).

## **Methods**

### **Clinical trial objectives and design overview**

IMPAACT 2024 is a phase I/II dose finding, safety and tolerability study of daily rifapentine combined with isoniazid (1HP) for tuberculosis prevention in infants, children, and adolescents.

The drug regimen is daily rifapentine and isoniazid for 28 days. The primary study objectives are (1) to evaluate the relative bioavailability of rifapentine film-coated tablet when administered as a crushed or whole tablet, (2) to determine weight band-based dosing of rifapentine as part of the 1HP regimen in children 0-15 years with and without HIV, and (3) to evaluate the safety and tolerability of the 1HP regimen. The secondary objectives include evaluating the effect of rifapentine on dolutegravir and efavirenz PK and efavirenz on rifapentine PK in children with HIV, rifapentine induction effects, and the effect of covariates (e.g., age, gestational age, weight, sex, ethnicity, nutritional status, and HIV-1 infection) on the rifapentine PK when given daily.

To enable assessment of primary and secondary objectives, study enrollment will be by age and HIV status: age 0-<3 years, age 3-<6 years, and age 6-<15 years. Age cutoffs were chosen to enrich for young age. HIV-negative and HIV-positive children will be enrolled in each age group. Given the transition from efavirenz- to dolutegravir-based antiretroviral therapy, there will be two HIV-positive arms: efavirenz-based therapy (3 years and older only) and dolutegravir-based therapy.

### **Pharmacokinetic models and assumptions**

The true rifapentine PK model was assumed to follow an adult model, allometrically scaled by total body weight, with an applied rifampicin maturation function.<sup>9,10</sup> The chosen adult model represents the highest quality rifapentine model available in literature, utilizing PK data from 863 adults treated at various dose levels and dosing frequencies.<sup>11</sup> Rifapentine clearance autoinduction is characterized through a dynamic function involving rifapentine concentration, with a maximum induction of 173%. The effect of efavirenz was assumed to be 30-50%, based on emerging data from a recent clinical trial evaluating rifapentine PK in adults with HIV treated with efavirenz.<sup>12</sup> Inter-individual variability was applied exponentially to clearance and volume parameters with coefficients of variation (CV) ranging from 20 to 50%. Alternative models for

power assessment included: no enzyme maturation (i.e., 100% maturity at birth), no effect of weight, no effect of efavirenz, and no enzyme induction. For simplicity and faster run times, enzyme induction was implemented as a step function.

### Evaluation of different study designs

Stochastic simulation and estimation (SSE) was performed in NONMEM (version 7.41) and Perl Speaks NONMEM (version 4.9) to evaluate parameter precision, estimate bias, and the power ( $1-\beta$  error) to detect important factors influencing rifapentine PK parameters. An overview of the SSE procedure is shown in **Figure 8.1**. The estimation method used was first order conditional estimation with interaction.

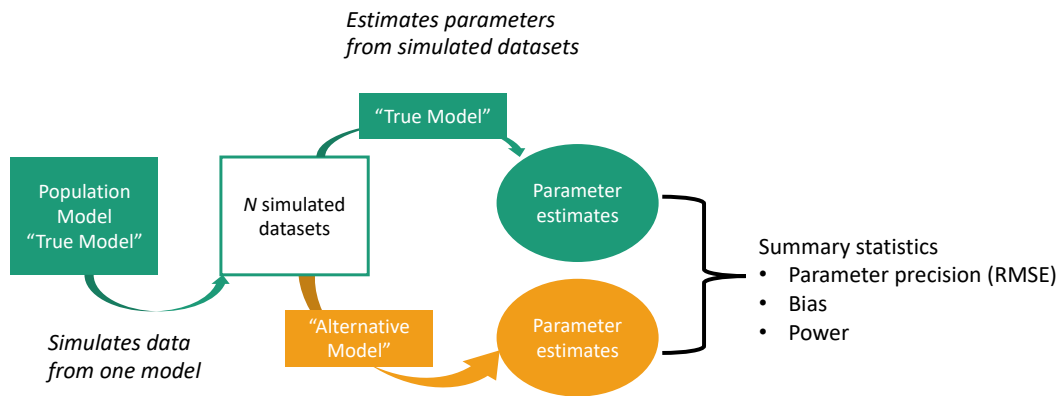


**Figure 8.1** Stochastic simulation and estimation schematic.

SSE was performed under different sampling designs (**Table 8.1**), study sample sizes (20-100 total children), and assumptions of inter-individual variability (IIV) in volume and clearance (20-50% coefficient of variation (CV)). Study populations were sampled from true populations of children with TB and TB/HIV coinfection from available in-house data, enriching for young children (**Figure 8.2**).<sup>10,13</sup>

**Table 8.1** Overview of tested sampling designs

	<b>N</b>	<b>Details</b>
<b>Occasions:</b>	1	Day 1
	3	Day 1, 14, 28
<b>Time Points:</b>	1	Trough
	3	Trough, C <sub>max</sub> , post-C <sub>max</sub>
	5	Trough, pre-C <sub>max</sub> , pre-C <sub>max</sub> , C <sub>max</sub> , post-C <sub>max</sub>

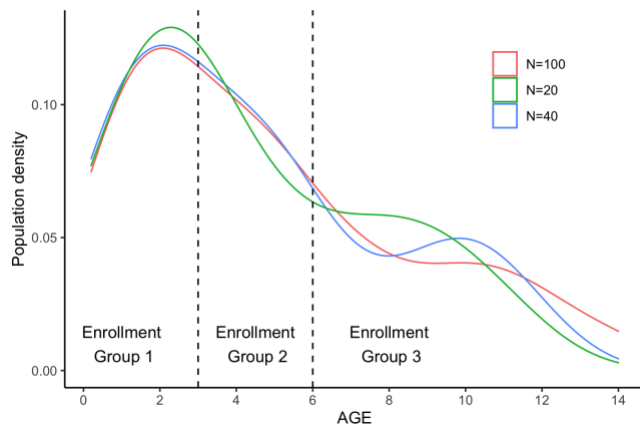


**Figure 8.2** Distribution of age in each simulated clinical trial population.

One-hundred simulated datasets were generated for each trial condition based on the assumed 'true' model. The PK parameters were estimated with the 'true' model and alternative models (e.g., no effect of age). Relative precision (rRMSE; equation 8.1) and bias (rBias; equation 8.2) were determined through comparison of the mean estimates from SSE ( $est_i$ ) and the true estimates ( $true_i$ ) in the 'true' model for  $N$  datasets. Acceptable limits were 10% rBias, 20% rRMSE, and 80% power.

$$\text{Equation 8.1} \quad rRMSE = 100\% \cdot \sqrt{\frac{1}{N} \sum \frac{(est_i - true_i)^2}{true_i^2}}$$

$$\text{Equation 8.2} \quad rBias = 100\% \cdot \frac{1}{N} \sum \frac{(est_i - true_i)}{true_i}$$

## Results

### rRMSE and rBias of rifapentine clearance

The reliability of clearance estimation was evaluated by rRMSE and rBias for various study designs. rBias was lowest with 20% IIV and increased with increasing IIV (**Figure 8.3**). At 20% IIV, the simplest design of one PK occasions with 5 samples (5/0/0) resulted in acceptable rBias for a sample size of 40 or more children. With 40-50% IIV, a design with multiple sampling occasions and 100 children were required. There was little difference in rBias between 3 or 5 samples collected at multiple occasions with 100 children in the study. rRMSE was large for most study designs tested (**Figure 8.3**). Our target threshold of 20% or lower rRMSE was only met with multiple occasion designs of 100 children with 20% IIV in clearance. These findings assume constant rifapentine clearance over time (i.e., no induction). With an autoinduction

effect (57% and 73% increase in clearance at occasion 2 and 3, respectively), the rBias was greater with N=20 but similar (<5% difference) with greater sample sizes at 40% IIV. The best designs were those with 3 or 5 samples on occasions 2 and 3.

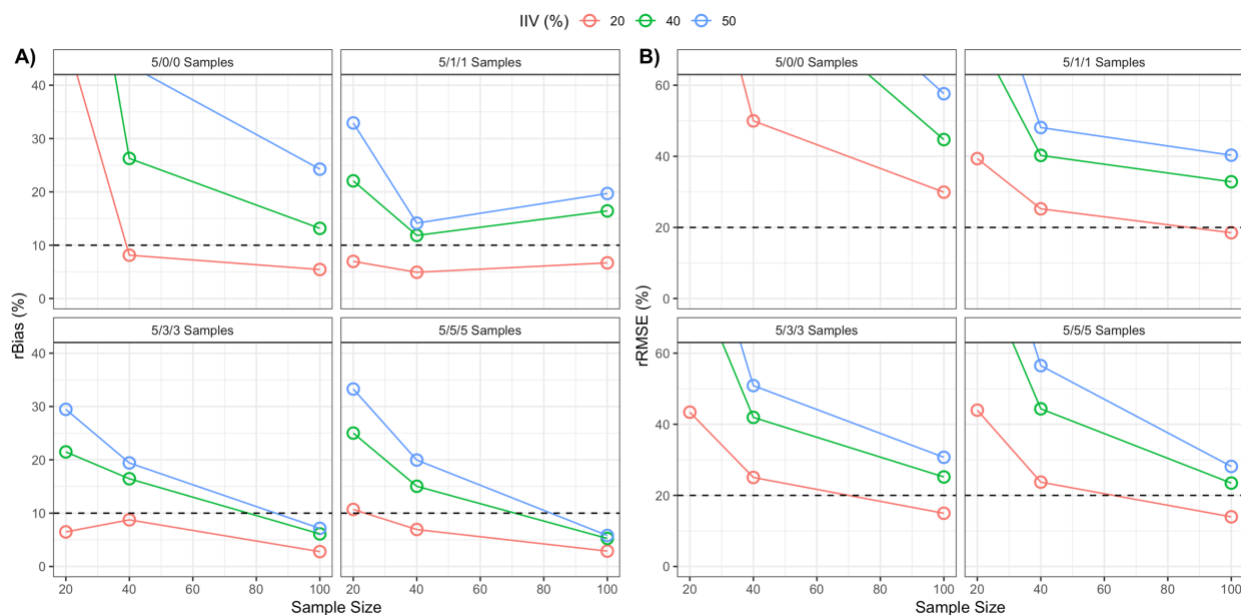


**Figure 8.3** Relative bias (A) and RMSE (B) of rifapentine clearance under different study designs. Each panel displays the number of pharmacokinetic samples taken on occasions 1, 2, and 3. The dashed line shows the acceptable limit. IIV: interindividual variability expressed as % coefficient of variation.

## rRMSE and rBias of rifapentine volume of distribution

All designs resulted in acceptable rBias (**Figure 8.4**) for volume of distribution estimation. Unlike clearance, some designs resulted in negative rBias, where the estimate from clinical trial simulations was lower than the true value. All designs resulted in acceptable rRMSE except those with N=20 and 50% IIV in volume ( **Figure 8.4**). rBias and rRMSE were higher with larger IIV, but the difference was small at sample sizes of 40 more. Similarly, 3 versus 5 samples on occasions 2 and 3 had little impact on rRMSE or rBias.

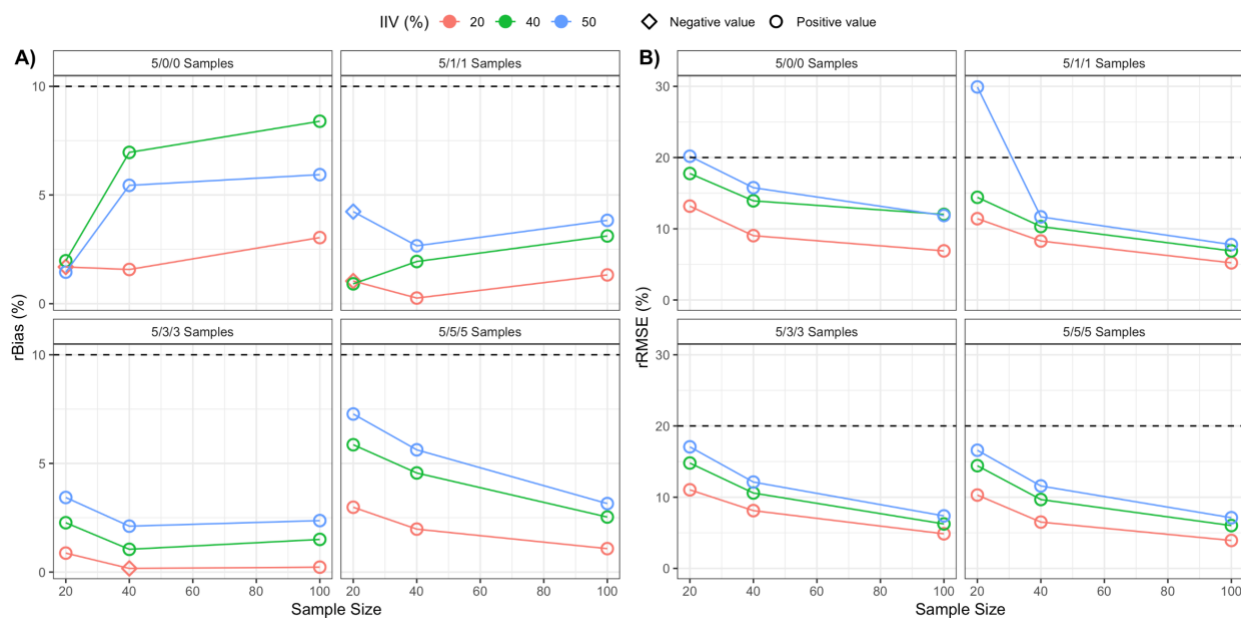


**Figure 8.4** Relative bias (A) and RMSE (B) of rifapentine volume of distribution under different study designs.

Each panel displays the number of pharmacokinetic samples taken on occasions 1, 2, and 3. The dashed line shows the acceptable limit. IIV: interindividual variability expressed as % coefficient of variation.



### **Statistical power to detect pediatric covariates**

The power to identify body weight allometry, age maturation, clearance induction, and a drug-drug interaction effect was tested separately. The results for an assumed IIV of 40% are shown in **Figure 8.5**. There was more than 80% power to detect a significant effect ( $p=0.05$ ) of body weight, age, and enzyme autoinduction with sample sizes of 40 or more when more than one sampling occasion was performed. The induction effect could not be assessed for a single sampling occasion since there was only one time point. To detect a 50% increase in rifapentine clearance with coadministration of efavirenz, a study size of 100 children was required. For a 30% effect size, the power for a study of 100 children was 64%.

### **Formulation and PK estimation**

The effect of tablet crushing on rifapentine bioavailability (25% reduction) was assessed separately to determine the sample size required to maintain unbiased and precise parameter estimation. We assumed 90% of children <3 years, 75% of children 3 to <6 years, and 25% of children 6 to <15 years would require crushed tablets due to their inability to swallow whole tablets. A minimum sample size of 154 children was required, which resulted in an rRMSE of 21% (clearance) and 27% (volume of distribution), rBias of -1.2% (clearance) and 25% (volume of distribution) with 5 samples collected on occasion 1 and 3 samples collected on occasions 2 and 3 (i.e., 5/3/3 design). There was > 80% power to detect a 25% decrease in bioavailability with tablet crushing as well as age, weight, and efavirenz effects assuming 50% IIV.

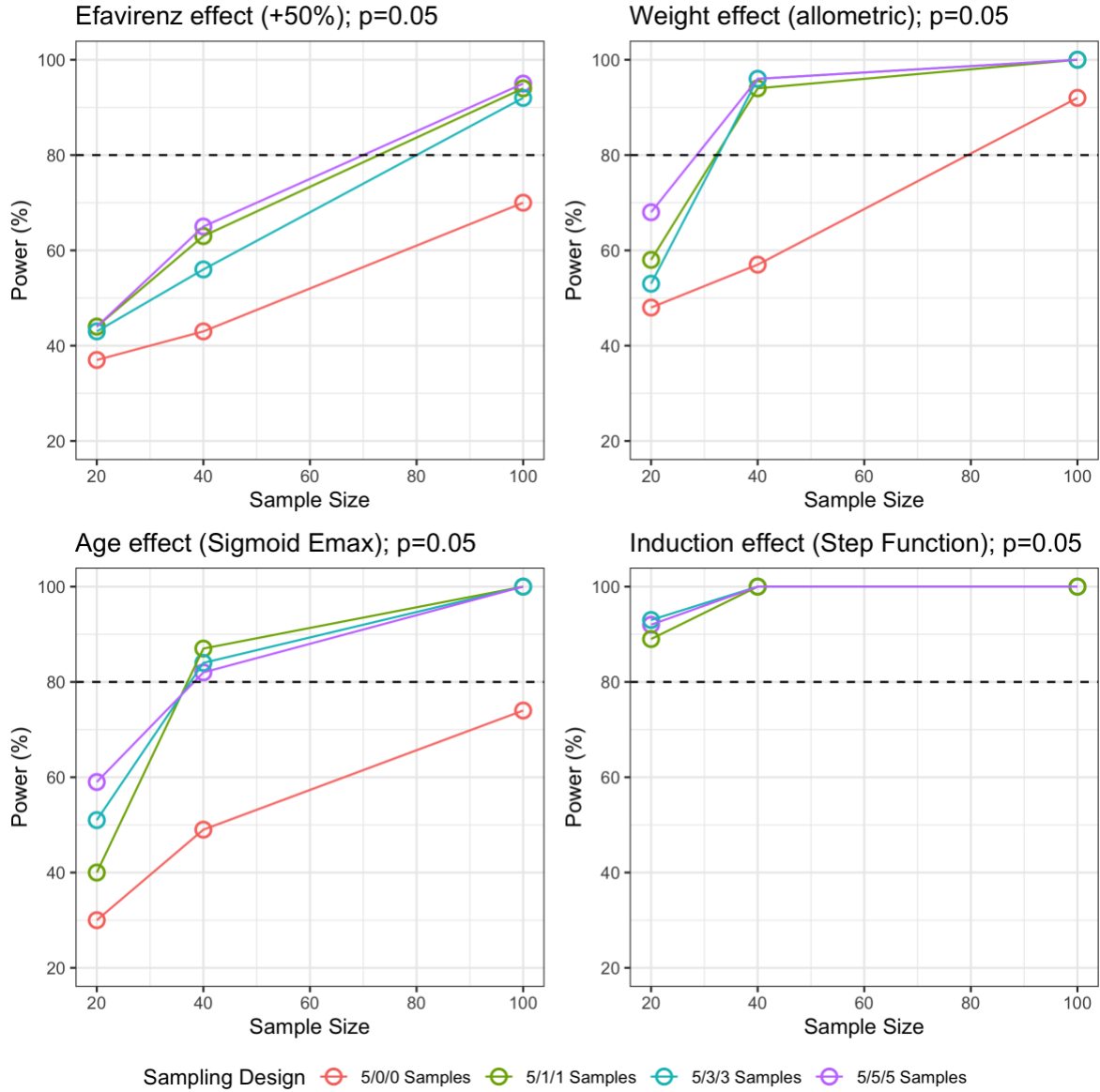


**Figure 8.5** Power to detect relevant factors influencing rifapentine clearance with 40% interindividual variability. Point and line colors represent the sampling design, labeled with number of pharmacokinetic samples taken on occasions 1, 2, and 3.

## Discussion

To our knowledge, this is the first study to assess the statistical power and PK parameter estimation precision of pediatric PK studies utilizing a nonlinear mixed effects modelling approach. Using rifapentine administered daily for tuberculosis preventive therapy as a case study, we determined that a study sample size of 100 children (0-15 years) and a design with three sampling occasions were required to be successful under our criteria. This clinical trial design provided reliable PK parameter estimation and statistical power to detect the dynamic and complex factors affecting pediatric PK.

The primary goal of IMPAACT 2024, as well as many pediatric PK and safety studies, is to determine pediatric drug dosing. As rifapentine efficacy is likely driven by AUC,<sup>14,15</sup> accurate and precise estimation of rifapentine clearance is most important. Our analysis shows that multiple PK occasions and sample sizes of at least 100 children were required for less than 10% rBias and 20% rRMSE. Conversely, precise and accurate volume estimation was achieved with simpler designs and less children. The likely explanation for this difference is the elimination half-life, which is 22 hours in a typical adult, making clearance estimation difficult with only one sampling occasion over the first 24 hours. Adding sampling occasions at steady state concentrations inform on the accumulation ratio, and thus, clearance. These findings suggest that the previously published rifapentine clearance estimates by Weiner and colleagues are likely biased as they are based on one PK sample, taken 24 hours after dose, from 80 children.<sup>16</sup> If multiple PK occasions are not feasible and no induction is expected, adding PK samples at 2-3 half-lives after dose could be another approach to improve clearance estimation and accurately inform on the optimal pediatric dose.

Due to challenges in recruitment, parental consent, and ethical considerations, pediatric PK studies often do not enroll sufficient sample sizes to capture all the complexity and variability in PK.<sup>17,18</sup> For example, only 3 of the 14 recent rifampicin PK studies (presented in **Table 2.1**) recruited 100 children or more with a typical age range of 0-15 years. In our analysis, smaller sample sizes resulted in biased clearance, which could lead to dosing recommendations that are too low to match adult exposures in larger populations. Bias and RMSE were correlated with statistical power—designs that did not have enough statistical power to detect all existing covariate relationships resulted in inaccurate estimates. For example, bias in clearance was above our threshold at a sample size of 40 likely because there was insufficient power to identify efavirenz induction effects. As such, the population estimate was biased toward higher rifapentine clearance. Pediatric clinical trials must be powered to detect age and weight effects at minimum as these will undoubtedly affect the PK of all drugs. When other effects are anticipated that could impact dosing needs, investigators should consider powering studies to capture these effects as well to avoid biased estimates.

A greater study sample size was required to detect a drug-drug interaction effect with efavirenz than for weight or age maturation effects. This is likely due to fewer children receiving efavirenz. Children under 3 years of age were not eligible for efavirenz therapy in accordance with guideline recommendations.<sup>19</sup> Enrollment was further split by HIV status and anti-retroviral treatment, leaving only 1/3 of the enrollment groups with efavirenz co-treatment. These enrollment criteria limited the number of children receiving efavirenz, thereby increasing the total number of children required to have at least 80% power. In contrast, all children enrolled contributed to estimating age and weight effects. Therefore, when designing pediatric clinical trials, it is important to consider not only the total sample size but also, the expected sample size (or proportion of the total sample size) with the covariate of interest. If there is not sufficient

power to reject the null hypothesis, the typical value estimates will likely be biased and, as a result, so will the predicted doses required to reach a PK target.

Our analysis applies nonlinear mixed effects modelling to pediatric PK data. This approach is becoming more widely utilized in pediatric research and has several advantages.<sup>3,17,18</sup> Most relevant to this work is the ability to leverage sparse sampling, which can spare participants blood volume and missed school time, and to characterize within-subject and between-subject variability and patient-specific factors that explain variability. If, instead, traditional pharmacokinetic modeling, such as non-compartmental analysis, were performed, more samples and more children would likely be needed to accurately inform PK and dosing.<sup>18</sup> Furthermore, as population PK modelling can account for diverse populations, dosing schemes and sampling times, it can be applied to pooled data from several smaller studies to enhance PK characterization.

In conclusion, multiple PK occasions, enriching young (<3 years) children, and sample sizes of at least 100 children were required to characterize rifapentine population PK precisely and accurately and, in turn, properly inform dose selection in children. This work demonstrates how SSE methods can serve as valuable tools to inform pediatric clinical trial design.

## References

1. Draft Guidance for Industry: General Clinical Pharmacology Considerations for Pediatric Studies for Drugs and Biological Products. (Accessed June 1, 2021, at <http://www.fda.gov/downloads/Drugs/GuidanceComplianceRegulatoryInformation/Guidances/UCM425885.pdf>.)
2. Mulugeta Y, Barrett JS, Nelson R, et al. Exposure Matching for Extrapolation of Efficacy in Pediatric Drug Development. *J Clin Pharmacol* 2016;56:1326-34.
3. Laughon MM, Benjamin DK, Jr., Capparelli EV, et al. Innovative clinical trial design for pediatric therapeutics. *Expert Rev Clin Pharmacol* 2011;4:643-52.
4. Kearns GL, Abdel-Rahman SM, Alander SW, Blowey DL, Leeder JS, Kauffman RE. Developmental pharmacology--drug disposition, action, and therapy in infants and children. *N Engl J Med* 2003;349:1157-67.
5. Abdel-Rahman SM, Reed MD, Wells TG, Kearns GL. Considerations in the rational design and conduct of phase I/II pediatric clinical trials: avoiding the problems and pitfalls. *Clin Pharmacol Ther* 2007;81:483-94.
6. Pica N, Bourgeois F. Discontinuation and Nonpublication of Randomized Clinical Trials Conducted in Children. *Pediatrics* 2016;138.
7. Germovsek E, Barker CIS, Sharland M, Standing JF. Pharmacokinetic-Pharmacodynamic Modeling in Pediatric Drug Development, and the Importance of Standardized Scaling of Clearance. *Clin Pharmacokinet* 2019;58:39-52.
8. Anderson BJ, Allegaert K, Holford NHG. Population clinical pharmacology of children: general principles. *European Journal of Pediatrics* 2006;165:741-6.

9. Hibma JE, Radtke KK, Dorman S, et al. Rifapentine population pharmacokinetics and dosing recommendations for latent tuberculosis infection. *American Journal of Respiratory and Critical Care Medicine* 2020;accepted.
10. Zvada SP, Denti P, Donald PR, et al. Population pharmacokinetics of rifampicin, pyrazinamide and isoniazid in children with tuberculosis: in silico evaluation of currently recommended doses. *J Antimicrob Chemother* 2014;69:1339-49.
11. Hibma JE, Radtke KK, Dorman SE, et al. Rifapentine Population Pharmacokinetics and Dosing Recommendations for Latent Tuberculosis Infection. *Am J Respir Crit Care Med* 2020.
12. Jyoti S. Mathad, Radojka M. Savic, Paula Britto, et al. Rifapentine pharmacokinetics and safety in pregnant women with and without HIV on 3HP [Abstract 144]. Conference on Retroviruses and Opportunistic Infections. Boston, MA2020.
13. Guiastrin B, Ramachandran G, Karlsson MO, et al. Suboptimal antituberculosis drug concentrations and outcomes in small and HIV-coinfected children in India: recommendations for dose modifications. *Clin Pharmacol Ther* 2018;104:733-41.
14. Gumbo T, Louie A, Deziel MR, et al. Concentration-dependent Mycobacterium tuberculosis killing and prevention of resistance by rifampin. *Antimicrob Agents Chemother* 2007;51:3781-8.
15. Savic RM, Weiner M, MacKenzie WR, et al. Defining the optimal dose of rifapentine for pulmonary tuberculosis: Exposure-response relations from two phase II clinical trials. *Clin Pharmacol Ther* 2017;102:321-31.
16. Weiner M, Savic RM, Kenzie WR, et al. Rifapentine Pharmacokinetics and Tolerability in Children and Adults Treated Once Weekly With Rifapentine and Isoniazid for Latent Tuberculosis Infection. *J Pediatric Infect Dis Soc* 2014;3:132-45.
17. Barker CIS, Standing JF, Kelly LE, et al. Pharmacokinetic studies in children: recommendations for practice and research. *Arch Dis Child* 2018;103:695-702.

18. Kern SE. Challenges in conducting clinical trials in children: approaches for improving performance. *Expert Rev Clin Pharmacol* 2009;2:609-17.

19. Guidelines for the Use of Antiretroviral Agents in Pediatric HIV Infection. 2021.

(Accessed June 4, 2021, at <https://clinicalinfo.hiv.gov/en/guidelines/pediatric-arv/whats-new-guidelines>.)



## **Chapter 9. Conclusions and future directions**

The work presented in this dissertation significantly contributes to the understanding of pharmacokinetics and optimal dosing of key anti-tuberculosis (TB) drugs in children.

Quantitative, model-based approaches were applied to propose dosing algorithms that ensure target exposure attainment. The research also prioritized identifying child populations at risk of subtherapeutic drug exposure. The proposed dosing algorithms were pragmatic in that formulation availability and ease of clinical implementation were considered. Several of these works have already contributed to TB policy while others have important policy implications, which will be highlighted below.

In Chapter 2, a systematic review and meta-analysis of rifampicin pharmacokinetics was performed. This work was initiated by the World Health Organization (WHO) as a result of evidence presented at the 2020 Pediatric Anti-TB Drug Optimization (PADO-TB) group meeting, which suggested rifampicin concentrations in children were subtherapeutic. Part of the supporting evidence included the analyses and results presented in Chapter 3 of this dissertation, which highlights underdosing of first-line TB drugs in malnourished children and the potential impact on TB outcomes. Based on the evidence presented in Chapters 2 and 3, the following conclusions can be drawn: (i) rifampicin dosing is not optimized for pharmacokinetic targets in all children; (ii) stratified dosing algorithms, such as that proposed for malnourished children in Chapter 3, can be pragmatic and may improve outcomes; (iii) there is high heterogeneity in pediatric pharmacokinetic studies and the study sample sizes are generally small ( $n < 100$ ), greatly limiting our ability to understand key drivers of subtherapeutic drug exposures in children.

The obvious next step for optimizing rifampicin and other first-line TB drug dosing in children is to apply robust, quantitative methods with pooled data such as an individual participant data meta-analysis (IPD-MA). Ideally, these analyses would include both pharmacokinetic and clinical outcome data, which would further inform on the exposure-response relationships in all children but also, key high-risk groups (e.g., children with HIV, undernutrition or young age). With this approach, there will be sufficient sample sizes to understand the factors influencing the pharmacokinetics and pharmacodynamics of first-line TB medicines in children. These results can then be used to inform on optimal formulation strengths and strength ratios for fixed-dose combination tablets, dosing algorithms, and dose amounts.

Moxifloxacin is a high-priority drug for rifampicin-resistant TB treatment and now a key component for treatment shortening of drug-susceptible TB.<sup>1,2</sup> In Chapter 4, moxifloxacin pharmacokinetics in young children with rifampicin-resistant TB is described for the first time along with the impact on QT interval prolongation. The modeling work found that currently recommended weight band dosing of moxifloxacin in children produced drug exposures below those expected in adults and that up to 50% higher doses are needed. However, there are many unknowns that require further investigation, including (i) the lack of quality data in very young children (<1 year of age) and in adolescents 12-18 years of age limiting reliable estimation of oral clearance, (ii) nonlinearities and/or delays in QTcF response, and (iii) cardiac safety with the proposed higher mg/kg doses and (iv) cardiac safety of moxifloxacin at all doses when administered with other QT-prolonging second-line TB agents like bedaquiline, clofazimine, and delamanid. Despite these uncertainties, this research generated key insights that will inform moxifloxacin use in children with rifampicin-resistant TB and likely also drug-susceptible TB.

Chapters 5-8 focus on optimization of rifapentine use in children and adults with latent TB infection. Rifapentine population pharmacokinetics were first characterized in an adult population with pooled data from several clinical trials. This analysis concluded that weight-based dosing was not required in adults, and simple flat dose regimens could be recommended. Further, rifapentine's autoinduction is mostly influenced by dosing frequency, such that intermittent frequencies have little induction but daily dosing, even with small dose amounts, results in maximal autoinduction. A revision of weight band doses for the 3-month once-weekly rifapentine and isoniazid (3HP) regimen in children was pursued in a subsequent analysis. This revision aligned rifapentine and isoniazid weight bands and proposed doses based on available formulations that would ensure pharmacokinetic target attainment. The two pieces of work (Chapter 5, Chapter 6) directly influenced WHO guidelines for TB preventive treatment, which were updated in 2020.<sup>3</sup>

Tuberculosis Trials Consortium study 35 (TBTC-35) and International Maternal Pediatric Adolescent AIDS Clinical Trials Network (IMPAACT) study 2024 are two pediatric clinical trials evaluating the pharmacokinetics and safety of rifapentine for TB prevention in children. TBTC-35 and IMPAACT 2024 are expected to inform rifapentine use in children with two major FDA label extensions: approval in children < 2 years of age, and approval for one month of daily use in combination with isoniazid (i.e., 1HP regimen). The analyses and results presented in Chapter 7 and Chapter 8 informed the design and implementation of these two clinical trials. The main conclusions were that (i) a child-friendly rifapentine formulation is urgently needed given the difficulty for young children to swallow large tablets and also, the potential variability and impact of tablet crushing on drug exposure, (ii) a scored, 150 mg dispersible rifapentine tablet would offer the most flexibility in use, and (iii) rifapentine pharmacokinetic studies need to include at least 100 children with multiple sampling occasions to precisely and accurately inform optimal rifapentine dosing.

In September 2020, the Pediatric Anti-tuberculosis Drug Optimization (PADO-TB) group convened to discuss top priorities for pediatric formulations of TB drugs.<sup>4</sup> This forum provides an opportunity for clinicians, researchers, and other key stakeholders to work together to ensure that priority pediatric formulations are investigated and developed. The priority list includes rifapentine (150 mg, scored dispersible tablet) and rifampicin; a taste-masked moxifloxacin formulation is on the watch list.<sup>5</sup> The research presented in this dissertation supported the PADO-TB discussions and resulting priorities. Future investigations (such as the mentioned IPD-MA of rifampicin pharmacokinetics) will be needed to determine the optimal strength of a standalone top-up rifampicin formulation for drug-susceptible TB treatment in children, but its necessity is no longer in question. Rifapentine and moxifloxacin together with isoniazid and pyrazinamide have recently demonstrated efficacy for drug-susceptible TB treatment in adults, shortening treatment to four months compared to the standard six months.<sup>1</sup> A follow-up study in children is already being planned by TBTC. Therefore, accessible, useful, palatable, and child-friendly formulations of rifapentine and moxifloxacin are more important than ever.

In summary, we used quantitative, model-based approaches to optimize treatment of drug-susceptible TB, drug-resistant TB, and latent TB infection in children. The presented work contributed to TB policy and initiatives that will save many children's lives worldwide.

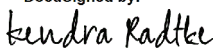
## References

1. Dorman SE, Nahid P, Kurbatova EV, et al. Four-Month Rifapentine Regimens with or without Moxifloxacin for Tuberculosis. *N Engl J Med* 2021;384:1705-18.
2. WHO consolidated guidelines on tuberculosis treatment. Module 4: Treatment - Drug-resistant tuberculosis treatment. WHO, 2020. (Accessed November 1, 2020, at <https://www.who.int/publications/i/item/9789240007048>.)
3. WHO operational handbook on tuberculosis. Module 1: Prevention- tuberculosis preventive treatment. 2020.
4. Report of the meeting to review the Paediatric Antituberculosis Drug Optimization priority list. 2021. (Accessed July 1, 2021, at <https://www.who.int/publications/i/item/9789240022157>.)
5. GAP-f Portfolio: Tuberculosis. 2021. (Accessed July 20, 2021, at <https://www.who.int/initiatives/gap-f/our-portfolio/tuberculosis>.)

## Publishing Agreement

It is the policy of the University to encourage open access and broad distribution of all theses, dissertations, and manuscripts. The Graduate Division will facilitate the distribution of UCSF theses, dissertations, and manuscripts to the UCSF Library for open access and distribution. UCSF will make such theses, dissertations, and manuscripts accessible to the public and will take reasonable steps to preserve these works in perpetuity.

I hereby grant the non-exclusive, perpetual right to The Regents of the University of California to reproduce, publicly display, distribute, preserve, and publish copies of my thesis, dissertation, or manuscript in any form or media, now existing or later derived, including access online for teaching, research, and public service purposes.

DocuSigned by:  
  
C0E11A99C44A493... \_\_\_\_\_  
Author Signature

8/12/2021  
Date